**UNIVERSIDAD NACIONAL AUTÓNOMA DE MÉXICO**
DOCTORADO EN CIENCIAS BIOMÉDICAS
FACULTAD DE MÉDICINA

# EFECTO DEL TRATAMIENTO COMBINADO DE CALCITRIOL CON AGENTES ANTI-ANGIOGÉNICOS SOBRE EL MIMETISMO VASCULAR EN CÁNCER DE MAMA TRIPLE NEGATIVO

**TESIS**

QUE PARA OPTAR POR EL GRADO DE DOCTORA EN CIENCIAS BIOMÉDICAS

**PRESENTA**

M. EN C. SILVIA GABRIELA MORALES GUADARRAMA

**DIRECTORA DE TESIS:**

DRA. LORENZA DÍAZ NIETO
FACULTAD DE MEDICINA

**COMITÉ TUTOR:**

DRA. ROCÍO GARCÍA BECERRA
INSTITUTO DE INVESTIGACIONES BIOMÉDICAS
DR. ALEJANDRO ZENTELLA DEHESA
INSTITUTO DE INVESTIGACIONES BIOMÉDICAS

CIUDAD DE MÉXICO, MAYO 2023

PDCB/FM/013/2023.

**Lic. Diana González Nieto**
Directora de Certificación y Control Documental
Dirección General de Administración Escolar, UNAM
**P r e s e n t e.**

Nos permitimos informar que con base al Artículo 31 del RGEP el Comité Académico de **DOCTORADO EN CIENCIAS BIOMÉDICAS** en su reunión 527 del 08 de febrero del 2023, designó el siguiente jurado para examen de grado de **DOCTORA EN CIENCIAS** de **SILVIA GABRIELA MORALES GUADARRAMA** con número de cuenta **307108735** con la tesis titulada **"Efecto del tratamiento combinado de calcitriol con agentes anti-angiogénicos sobre el mimetismo vascular en cáncer de mama triple negativo",** dirigida por la Dra. Lorenza Díaz Nieto.

| | |
|---|---|
| Presidente: | Dra. Leticia Rocha Zavaleta. |
| Secretario: | Dra. Lorenza Díaz Nieto. |
| Vocal: | Dr. Alfonso León del Río. |
| Vocal: | Dr. Ezequiel Moisés Fuentes Panana. |
| Vocal: | Dr. Miguel Ángel Velázquez Flores. |

Sin otro particular, aprovecho la ocasión para enviarle un cordial saludo.

A t e n t e m e n t e
***"Por mi raza hablará el espíritu"***
Ciudad Universitaria, Cd. de Mx., a 10 de febrero de 2023.

**DRA. YOLANDA IRASEMA CHIRINO LÓPEZ**
**COORDINADORA DEL PROGRAMA**

YICL/ALP/evb

# SOBRE ESTA TESIS

Esta tesis constituye el trabajo realizado del año 2018 al presente año en el Departamento de Biología de la Reproducción del Instituto Nacional de Ciencias Médicas y Nutrición Salvador Zubirán. Está diseñada en 4 partes que albergan 6 capítulos. En el primer capítulo se encuentra la introducción a las generalidades de la vascularización tumoral y sus mecanismos asociados, mientras que en el segundo capítulo se desarrolla el planteamiento del problema y los antecedentes teóricos referentes a las alternativas terapéuticas contra el mimetismo vascular y la angiogénesis. Posteriormente, se presentan de manera puntual las preguntas de investigación y los objetivos abordados durante el proyecto de investigación. Así, la primera parte es la introducción y delimitación del proyecto de tesis. En adelante, la segunda, tercera y cuarta parte, se encuentran los resultados obtenidos durante el desarrollo de esta investigación, con el resumen de lo realizado, las estrategias metodológicas desarrolladas, los resultados obtenidos, discusión y conclusiones. Dichos resultados se encuentran en proceso de publicación o han sido publicados en revistas científicas internacionales indexadas, y han sido presentados en el Vitamin D Workshop 2022 (Texas, EUA), el XXXIII Congreso Nacional de Bioquímica (Mérida, Yucatán. México) y en el 1st Cellular Bases for Patient Response to Conventional Cancer Therapies Conference (Berlín, Alemania), así como en la sesión general de investigación, a cargo del Departamento de Biología de la Reproducción, en el Instituto Nacional de Ciencias Médicas y Nutrición Salvador Zubirán.



Durante la realización del presente trabajo se recibieron apoyos por parte de CONACYT, a través de financiamiento proporcionado a la Dra. Lorenza Díaz (A1-S-10749) y por medio del programa de Becas Nacionales del Programa de Posgrados del Padrón de Alta Excelencia del cual fui beneficiaria (CVU: 662170). Por parte de la UNAM, a través de la del Programa de Apoyo a los Estudios de Posgrado (PAEP), recibí apoyó para la presentación del proyecto en la Berlín (Cellular Bases for Patient Response to Conventional Cancer Therapies Conference). Finalmente, recibí apoyo por parte del Patronato del INCMNSZ, a través del estímulo institucional de la Fundación Amigos del INCMNSZ, para la conclusión de mi investigación del doctorado (348).

Z

*"Science is not about being the first to know. It's about asking questions that have never been asked before."*

Aubrey de Grey

# AGRADECIMIENTOS A TÍTULO PERSONAL

Seguir este camino en el posgrado no hubiera sido posible sin una red de apoyo formada por gente que creyó en mí, mi resiliencia y en mi trabajo. Por ello, quiero agradecer a los miembros de mi primer comité en el anterior posgrado, a la **Dra. Norma Bobadilla** que se acercó en uno de mis momentos más vulnerables para contenerme y guiarme de una manera admirable, gracias por ser una figura a seguir y por su calidad humana.

Al **Dr. Alejandro Zentella**, que creyó en mí y me apoyó de todas las formas que un tutor debería hacerlo, que me enseñó a ver más allá de lo aparente, a recordar que más allá del dolor crecemos por la manera en cómo enfrentamos los obstáculos y lo que decidimos hacer con lo aprendido. Me seguiré esforzando por ser ese apoyo que ustedes fueron para mí cuando alguien lo necesite. A mi comité de otras épocas, la **Dra. Rocío García** y la **Dra. Marcela Lizano**, por su entera comprensión, su tiempo y su apoyo a lo largo de este camino. Gracias por sus valiosos comentarios y aportaciones, todo ayudó a que mi trabajo fuera mejor y mucho más completo.

Agradezco a mi jurado revisor, la **Dra. Leticia Rocha**, el **Dr. Ezequiel Fuentes**, el **Dr. Miguel Ángel Velázquez** y el **Dr. Alfonso León del Río** por su tiempo y entendimiento durante la revisión de este trabajo. Gracias por sus palabras y observaciones al escrito. No puedo olvidar mencionar a los auxiliares de cada departamento, por la facultad de medicina: a Evita por su paciencia enorme, apoyo y porras durante estos 4 años. Gracias al programa de Doctorado en Ciencias Biomédicas por brindarme los recursos necesarios para llevar a cabo este proyecto de investigación y por ofrecerme un espacio de aprendizaje enriquecedor para desarrollar mis habilidades científicas.

Quiero expresar mi más sincero agradecimiento a mi directora de tesis la **Dra. Lorenza Díaz Nieto**, por su guía, apoyo y sabiduría en este camino hacia la culminación de mi doctorado. El camino no fue fácil para ninguna de las dos, pero el saber que contaba con ella, contar con su confianza, con su apoyo, con su pasión por aprender y ayudar fue pilar para que yo llegará hasta acá. Gracias por brindarme un lugar seguro para disfrutar la ciencia, donde he aprendido a crecer como estudiante e investigadora.

Siempre estaré agradecida por su paciencia, dedicación y compromiso para ayudarme a alcanzar mis objetivos.

También quiero agradecer a todos los colaboradores que han hecho posible esta investigación. A la **Dra. Janice García**, al **Dr. Euclides Ávila**, a la **Dra. Andrea Olmos,** por sus aportaciones, enseñanzas, amistad y gran corazón. A la **Dra. Mayel Chirino** y al **Dr. Fernando Larrea** por sus valiosas aportaciones y consejos, cada uno de ellos fue un empujón para que nuestra investigación creciera más allá de los límites imaginados.

A **Edgar Armando Méndez**, por todo su en la parte experimental cuando la vida y las manos ya no eran suficientes para hacer experimentos que contestaran a las interminables preguntas que la Dra. Lore y yo nos hacíamos constantemente.

A todos los alumnos que han pasado por el grupo, **Nohemí, Galia, Sam, Rafael,** gracias por su compañía, por su ayuda, por hacer las tardes livianas y los seminarios entretenidos, por sus comentarios y sugerencias que ayudaron a mejorar mi trabajo.

A los programas de **Mentoría de la U.S.-Mexico Leaders Network** por permitirme ser mentora dentro del programa de Mujeres Líderes en la Ciencia, ha sido una de las experiencias más enriquecedoras, **a mi mentorada Annie** por su confianza, y por llevarme a romper mis propios límites para crecer juntas en este camino. Al **British Council e INOVA** por permitirme ser parte de la segunda generación de Mentees de Mujeres en la Ciencia, a mi mentora la **Dra. Ariadna Garza** por su tiempo, sus observaciones y consejos, por ayudarme con el empujoncito final en este camino. Gracias por generar espacios seguros para mujeres científicas, por compartir la parte humana de la ciencia, y la pasión por lo que hacemos.

Finalmente, a mi red de apoyo**, mi familia** por entender las extenuantes rutinas, por nunca dejar de apoyarme y creer en mí siempre. Nada hubiera sido posible sin su inspiración, sin sus porras y sin su amor. A las amistades que la academia me regaló. Gracias **Juls** por siempre tener un rato para escucharme, y recordarme cómo pequeñas acciones pueden tener grandes impactos. Sin ustedes no podría ahora, agradecerme a mí misma por seguir adelante cuando creí que ya no valía la pena: gracias Gaby de 20 añitos por querer cambiar el mundo y no soltar tus sueños, por aferrarte a tus creencias, para la Gaby del futuro que nunca que nos olvidé que "***a veces, tocar fondo es una maravillosa oportunidad para rehacer tu vida***" y este doctorado fue prueba de ello.

De nuevo, **gracias a todos por ser parte de este viaje. Espero que este trabajo pueda contribuir en algo a la ciencia y a la igualdad de género en nuestro campo**.

# Índice

# PARTE 1.

## INTRODUCCIÓN Y DELIMITACIÓN DEL ESTUDIO

# CAPÍTULO 1.

## DE LA ANGIOGÉNESIS AL MIMETISMO VASCULAR

Tanto el crecimiento tumoral como su diseminación a distancia dependen del suministro de oxígeno y nutrientes al interior del tumor, ya sea por vasculogénesis y/o angiogénesis. La vasculogénesis es la formación de nuevos vasos a partir de células endoteliales precursoras. Mientras que la angiogénesis es el proceso de formación de vasos sanguíneos a partir de vasos preexistentes; puede darse por la ramificación de los vasos, o bien, mediante su segmentación por la formación de pilares al interior, este proceso se conoce como intususcepción [1, 2].

Diversos estudios han correlacionado positivamente la densidad microvascular (DMV) con la progresión y agresividad tumoral, entre estas asociaciones, se ha visto que a mayor DMV la incidencia de enfermedad metastásica es mayor [3–5]. Por ello desde inicios de los 70s, se implementó la identificación y uso de estrategias terapéuticas anti-angiogénicas para combatir el cáncer [6,7]. Dentro de las principales opciones anti-angiogénicas están los inhibidores de los receptores de las cinasas de tirosina (RTKs por sus siglas en inglés) y los anticuerpos monoclonales contra los ligandos de dichos receptores [7,8]. En clínica, este tipo de terapias son una opción tangible para tratar tumores hipervascularizados, especialmente en aquellos cuya opción de tratamiento es la quimioterapia.

Desafortunadamente, se han descubierto mecanismos alternos a la angiogénesis que actúan como vías de escape a la terapia anti-angiogénica. Uno de ellos es la cooptación, un proceso en el que el tumor "secuestra" a los vasos provenientes de tejido adyacente al tumor [9]. Por otra parte también se puede dar la transdiferenciación a endotelio, donde se generan células endoteliales derivadas de células troncales de cáncer [10]. Además de ellos, existe un mecanismo estrechamente ligado a la transdiferenciación endotelial: el mimetismo vascular, mediante este, las células tumorales forman una red de canales sanguíneos en ausencia del endotelio, especialmente en las zonas de hipoxia y necrosis donde el endotelio es incapaz de proliferar [11, 12]. Es particularmente en este proceso en el cuál se hablará en posteriores capítulos.

Todos los mecanismos empleados por el tumor para mantener el suministro de nutrientes y vías de diseminación son procesos altamente regulados por el microambiente tumoral, las interacciones entre los diversos componentes celulares (células tumorales y células no neoplásicas) y las modificaciones en la matriz extracelular (MEC) [12,13]. Las vías de

señalización implicadas en esta compleja regulación juegan un papel esencial en el crecimiento tumoral, la invasión y, posteriormente, en la metástasis de tumores altamente agresivos, por lo que su estudio y entendimiento podría ser de gran ayuda para combatir la progresión tumoral y la resistencia a las terapias.

## 1.1. LA DELGADA LÍNEA ENTRE LA ANGIOGÉNESIS Y EL MIMETISMO VASCULAR

A finales del siglo pasado, Maniotis y colaboradores describieron por primera vez un mecanismo de vascularización tumoral presente en tumores tumores uveales metastásicos y de melanoma cutáneo. En muestras de cáncer provenientes de estos tipos de cáncer, altamente agresivos y metastásicos, observaron la presencia de redes interconectadas por canales vasculares ricos en MEC. Estas estructuras se caracterizaban por ser positivas a la tinción con ácido periódico y reactivo de Schiff (PAS) y negativos a marcadores de células endoteliales (EC), como CD31. Además, al interior se observaba la presencia de eritrocitos, lo que sugería una posible función como estructuras transportadoras de sangre, organizadas en un sistema de microcirculación tumoral. Paralelamente, se demostró que las células de melanoma, M619, caracterizadas como altamente invasivas, eran capaces de formar estructuras tubulares tridimensionales que asemejaban a las redes vasculares. A este proceso se le denominó como mimetismo vascular (MV) [14–17].

Los canales vasculares derivados del MV compartes diversas características con la vasculatura endotelial. Sin embargo, existen rasgos distintivos entre la angiogénesis tumoral y el mimetismo vascular. Por una parte, los vasos tumorales formados por angiogénesis están caracterizados por presentar una capa delimitante de células endoteliales, membrana basal y una capa de células murales (pericitos) poco uniforme que vuelve a los vasos tumorales altamente permeables (Diagrama 1, vista transversal izquierda) [13]. En contraste, los canales vasculares son altamente permeables al igual que los vasos tumorales, pero carecen de la membrana basal, no hay células endoteliales delimitando la estructura y tampoco hay células murales. En cambio, se observa a células tumorales que pueden o no tener una morfología similar al endotelio, y la presencia de una capa rica en matriz extracelular (MEC) que por su

riqueza en peptidoglicanos es positiva a la tinción de PAS (Diagrama 1, vista transversal derecha) [12,14].

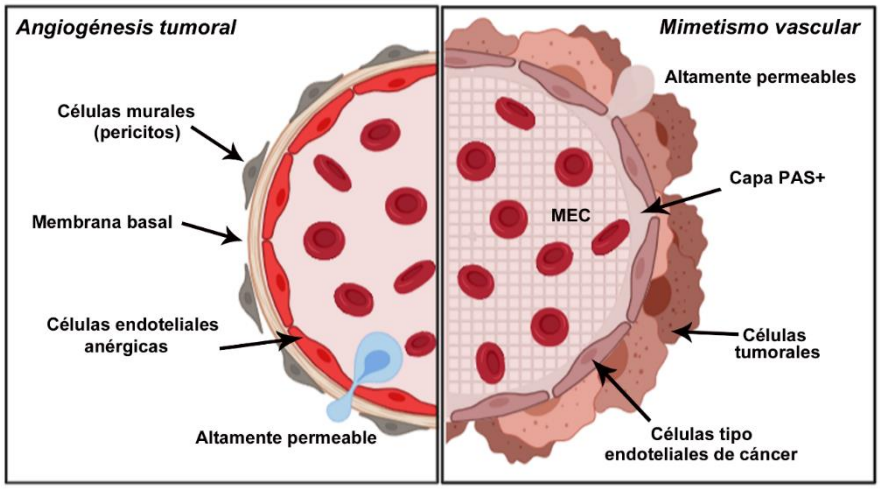


*Diagrama 1. Comparación de las características funcionales entre la angiogénesis tumoral y la angiogénesis vascular.*

A pesar de que al momento no existen marcadores de MV infalibles para la identificación de los canales derivados de MV se han descrito algunas de sus características estructurales, como la presencia de una matriz enriquecida en laminina y peptidoglicanos, así como la expresión de algunos marcadores asociados a estas estructuras (Tabla 1). Por ejemplo, el endotelio expresa la cadherina de endotelio vascular (VE-cadherina), o CD144, que es la principal molécula asociada a las adhesiones célula-célula entre el endotelio. Sin embargo, se ha visto que las células de cáncer, capaces de hacer MV, expresan de manera aberrante la VE-cadherina, sugiriendo la posible participación de esta proteína en la adquisición de la capacidad para formar estructuras tubulares por parte de las células tumorales [18].

Actualmente se han identificado diversos tipos y subtipos de MV, basados en los patrones de la MEC observados en laminillas de tejido tumoral teñido con PAS [28]. Los dos principales tipos son el MV de tipo tubular, y el MV en patrones de matriz [29]. Estos pueden ser observados tanto en cultivos celulares como en tejidos de tumor teñidos con PAS, sin hematoxilina. Del primer tipo se puede identificar la formación de cordones tipo túbulos cuando las células de cáncer se encuentran sobre una matriz delgada in vitro. Por otra parte, el primer tipo se observa como matriz PAS+, dispuesta azarosamente en líneas rectas alargadas, que pueden o no estar interconectadas. En cuanto al segundo tipo, se observa la

formación de arcos con ramificaciones, bucles incompletos con y sin ramificaciones, así como la formación de estos bucles a manera de red. Esta matriz es producida por las células tumorales y en algunos casos, se puede llegar a observar la presencia de células PAS+ con fenotipo similar a endotelio, acomodadas en cordones o delimitando los canales vasculares. El MV de matriz en patrones es característico de los tumores que son sumamente invasivos [28].

| | Mimetismo Vascular | Angiogénesis | Ref. |
|---|---|---|---|
| *Definición* | Formación de canales de sangre a partir de células tumorales y células troncales tumorales | Desarrollo de vasos sanguíneos nuevos a partir de capilares y vasos preexistentes | [8-22] |
| *Tipos* | En patrones de ríos de matriz<br>Tipo tubular (en cordones) | Angiogénesis por ramificación<br>Angiogénesis por intususcepción | [1,14] |
| *Componentes celulares* | Formados por células tumorales (tipo endotelial) y células troncales tumorales | Formados por células endoteliales y células murales. | [18] |
| *VE-cadherina* | Expresión aberrante | Expresión alta, principalmente en membrana. | [20] |
| *PAS/CD31* | PAS positivo, CD31 bajo/negativo | PAS negativo/bajo, CD31+ | [18] |
| *Antígeno asociado a Factor VIII* | Expresión muy baja a negativa | Altamente expresado | [18] |
| *Anti-angiogénicos* | No es afectado por endostatina ni otros factores anti-angiogénicos | Efectivamente inhibida por factores anti-angiogénicos | [20,21] |
| *EphA2, Tie-1, LAMC2* | Sobreexpresados en las células tumorales que hacen MV | Generalmente sin expresión en el endotelio | [22] |
| *Marcadores de troncalidad* | Expresión de CD133, ALDH1 | CD133 positivo en las células precursoras de endotelio | [23-27] |

*Tabla 1. Características distintivas y marcadores del mimetismo vascular y la angiogénesis tumoral.*

## 1.2. MIMETISMO VASCULAR EN EL CÁNCER DE MAMA: PRIMERAS EVIDENCIAS Y ASOCIACIONES CLÍNICO-PATOLÓGICAS

El MV es particularmente frecuente en tumores altamente agresivos, incluido el cáncer de mama. Tan sólo dos años después del primer artículo sobre MV en melanoma, un grupo en Japón identificó la presencia de lagunas de sangre carentes de la típica capa de endotelio que

rodea los vasos sanguíneos, en xenoinjertos hipervascularizados derivados de cultivos primarios de cáncer de mama inflamatorio. Además, estas células eran capaces de hacer tubulogénesis in vitro, mientras que en los modelos in vivo, la presencia de estas estructuras se asoció con la metástasis pulmonar, aportando la primera evidencia científica de MV en el cáncer de mama [30, 31].

Con lo anterior, se estableció la estrecha relación que existe entre la angiogénesis y el MV al interior del tumor. Shirakawa y colaboradores, observaron que la zona hipervascularizados en la periferia del tumor era rico en vasos revestidos por endotelio, con expresión positiva de CD31 murino, esto indicaba el origen angiogénico de los vasos. Sin embargo, en el centro hipóxico del tumor se observaron canales vasculares PAS positivos con expresión baja de la Integrina humana □v□3, además de la ausencia de células endoteliales (EC), siendo esto evidencia de MV. En conjunto, demostraron que algunos tumores pueden desarrollar redes vasculares híbridas que combinan angiogénesis y MV para obtener oxígeno y nutrientes de manera eficiente [32,33].

Otro fenómeno asociado al MV es la presencia de vasos en mosaico, donde un vaso puede estar revestido por EC en algunas partes y por células tumorales en otras, formando estructuras vasculares híbridas que se han asociado con la invasión y diseminación sistémica de las células del tumor [34]. Además, se ha demostrado que el MV puede inducir la metástasis después de un tratamiento anti-angiogénico [35]. Al inducir hipoxia ante la reducción de la DMV, las vías alternativas de vascularización como el MV pueden verse favorecidas y por ende aumentar la incidencia de diseminación a sitios distantes [36,37]. Así como existe una correlación positiva entre la DMV y la metástasis en cáncer de mama [4], se ha visto que el MV se asocia con la diseminación del tumor y peor pronósticos en cuanto a recurrencia, supervivencia, tamaño tumoral y grado de diferenciación de las células del tumor [16, 32, 38, 39], vinculando al MV con un fenotipo de cáncer de mama más maligno y agresivo [32, 98, 39].

Entre los varios estudios que asocian al MV con parámetros clinicopatológicos y pronóstico en pacientes con cáncer de mama, un gran ejemplo es el estudio elaborado por Shirakawa K, et al. [31] donde observaron que de 331 muestras de cáncer de mama extirpadas quirúrgicamente, solo 26 (7,9 %) tuvieron evidencia de MV. Este porcentaje de pacientes tuvo

mayor asociación con la recurrencia hematógena y menor supervivencia global a los 5 años [32]. Sin embargo, en otro estudio de ocho informes clínicos con 1.238 pacientes con cáncer de mama, la tasa de casos con MV fue mayor, al identificarse en el 24% de los tumores evaluados, el MV se asoció con un mayor tamaño tumoral (>2 cm), metástasis en ganglios linfáticos, peor grado de diferenciación (grados 2 y 3) y menor supervivencia general (SG) que aquellos sin MV, reafirmando la asociación del MV con los fenotipos más agresivos [39].

Resulta interesante que a pesar de que la presencia de MV en los tumores de cáncer de mama que se analizan no rebasa el 14%, la mayoría de las muestras positivas a MV se asocian significativamente con características clinicopatológicas negativas como metástasis en los ganglios linfáticos axilares, mayor tamaño del tumoral y mayor grado histológico, así como con un peor pronóstico global [40, 41]. Recientemente, un estudio de meta análisis sobre el papel del MV en la progresión tumoral y su valor pronóstico en diferentes tipos de tumor, demostró que la presencia de MV predice una menor supervivencia en los pacientes con cáncer, corroborando que este tipo de asociaciones está presente en otros tipos de cáncer además del de cáncer de mama [42].

## 1.3. PRINCIPALES MECANISMOS MOLECULARES ASOCIADOS AL MV

Se han descrito diversas vías de regulación del MV, dichas vías suelen estar asociadas a la plasticidad celular, la transición epitelio-mesénquima (EMT) y propiedades troncales en las células de cáncer. Se sabe que en cáncer de mama, la EMT es importante para la adquisición y el mantenimiento de troncalidad, así como con el desarrollo de MV [43]. La presencia de células con dichas características es más frecuente en tumores de cáncer de mama más agresivos, se ha propuesto que el origen del MV reside en las subpoblaciones troncales dentro de dichos tumores [26]. De manera general, los reguladores del MV podrían agruparse en 3 grupos representados en el Diagrama 2; mientras que las principales propiedades fenotípicas, relacionadas con los "*drivers*" del MV en cáncer son:

- **Presencia de subpoblaciones troncales.** Liu y cols. encontraron que la positividad a CD133 en holoclonas de células de cáncer de mama MDA-MB-231, se correlacionaba con la capacidad de MV y el potencial de autorrenovación. Particularmente estas holoclonas también expresaron marcadores endoteliales como VE-cadherina, MMP2 y MMP9, demostrando que las poblaciones troncales de cáncer de mama CD133+

contribuyen con el MV y la adquisición de un fenotipo similar al endotelio [26]. Entre los marcadores de troncalidad mejor asociados con la capacidad de hacer MV están el CD133 y la aldehído deshidrogenasa 1 (ALDH1) [25, 37].

- **Transición epitelio mesénquima (EMT).** Algunos factores derivados del microambiente tumoral se han asociado con la EMT y la inducción de MV, uno de ellos es el factor de crecimiento transformante de citocinas beta (TGFB) y el factor de transcripción TWIST1 [24, 44]. Por ejemplo, en carcinoma hepatocelular, se sabe que TGFB promueve el MV in vitro e in vivo al inducir la expresión de VE-cadherina, MMP2 y LAMC2 [45]. Aunque TGFB no ha sido descrita como un regulador clásico del MV en el cáncer de mama, en xenoinjertos de cáncer de mama, la inducción de hipoxia dependiente de TWIST (blanco de la señalización de TGFB) aumentó la positividad a C133, derivando en la resistencia al tratamiento con sunitinib [24]. Por otra parte, también se ha visto, en hepatocarcinoma, que la EMT que deriva en mimetismo vascular es regulada por la vía de HIF1$\alpha$/AKT [45] mientras que en cáncer de células no pequeñas de pulmón, esta vía incluye río abajo la activación del blanco de la rapamicina en mamíferos, mTOR, [46].
- **Expresión de marcadores endoteliales**. Como se discutió anteriormente, la expresión aberrante de VE-cadherina en los tumores, se ha asociado estrechamente con la formación de MV, y la transdiferenciación a endotelio, donde hay una pérdida de marcadores mesénquimales/epiteliales y la ganancia de endoteliales, como la vimentina y la VE-cadherina, [18, 47].
- **Factores pro-inflamatorios.** La presencia de quimiocinas y citosinas derivadas de la inflamación, como la interleucina 6 (IL-6) han demostrado que participan en la formación de estructuras tipo tubulares in vitro al regular positivamente la expresión de VE-cadherina y la actividad de la MMP-2, entre otros [46]. Particularmente en el cáncer de mama, la IL-8expresa así como sus receptores CXCR1/CXCR2, y se ha demostrado que la internalización de IL-8 aumenta durante la formación del MV [48]. De manera similar, la IL-1$\beta$ estimula la formación de MV en las células de cáncer de mama, y cuando las células son incubadas en presencia de esta quimiocina, las células hacen tubulogénesis y comienzan a expresar la VE-cadherina, así como el receptor 1 de VEGF (VEGFR1), la MMP-2, MMP-9 [49].

- **Hipoxia.** La hipoxia es un estimulador esencial de los procesos de neovascularización, entre las vías de señalización asociadas a la regulación de este mecanismo como inductor del MV se han descrito la participación de EGFR/PI3K/AKT, así como de E-cadherina y vimentina [50, 51]. Así mismo, se ha visto que el MV en glioma es dependiente de FGFR/VEGFR pues la inhibición dual de estos receptores impide la formación de redes tipo tubulares in vitro, especialmente en condiciones de hipoxia [52].

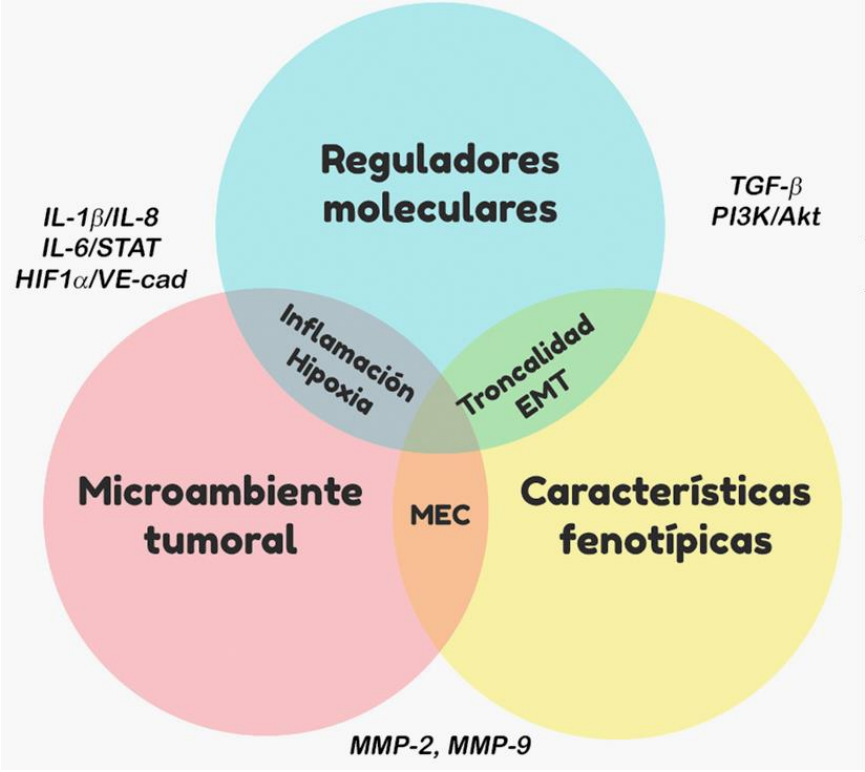


*Diagrama 2. Principales reguladores del mimetismo vascular en cáncer de mama.*

## 1.4. LITERATURA CITADA


1. Kolte, D.; McClung, J.A.; Aronow, W.S. Chapter 6 - Vasculogenesis and Angiogenesis. In Translational Research in Coronary Artery Disease, Aronow, W.S., McClung, J.A., Eds.; *Academic Press: Boston*, **2016**; pp. 49-65.
2. Patan, S.; Munn, L.L.; Jain, R.K. Intussusceptive Microvascular Growth in a Human Colon Adenocarcinoma Xenograft: A Novel Mechanism of Tumor Angiogenesis. *Microvascular Research*, **1996**, 51, 260-272, doi:https://doi.org/10.1006/mvre.1996.0025.
3. Brem, S., R. Cotran, and J. Folkman, Tumor angiogenesis: a quantitative method for histologic grading. *J Natl Cancer Inst*, **1972**. 48(2): p. 347-56.
4. Niu, S., et al., Correlations Among Ultrasound-Guided Diffuse Optical Tomography, Microvessel Density, and Breast Cancer Prognosis. *J Ultrasound Med,* **2018**. 37(4): p. 833-842.
5. Weidner, N., Intratumor microvessel density as a prognostic factor in cancer. *Am J Pathol,* **1995**. 147(1): p. 9-19.
6. Sherwood L. M., Parris E. E., Folkman J. Tumor angiogenesis: therapeutic implications. *NEJM*. **1971**;285(21):1182–1186. doi: 10.1056/nejm197111182852108.
7. Yoo S. Y., Kwon S. M. Angiogenesis and its therapeutic opportunities. *Mediators of Inflammation.* **2013**;2013:11. doi: 10.1155/2013/127170.127170.
8. Schneider B.P, Miller K.D. Angiogenesis of Breast Cancer. *J Clin Oncol*. **2005**; 23:1782-1790. doi: 10.1200/JCO.2005.12.017
9. Kuczynski, E.A.; Vermeulen, P.B.; Pezzella, F.; Kerbel, R.S.; Reynolds, A.R. Vessel co-option in cancer. *Nat. Rev. Clin. Oncol* **2019**, 16, 469-493, doi:10.1038/s41571-019-0181
10. Chen HF, Wu KJ. Endothelial Transdifferentiation of Tumor Cells Triggered by the Twist1-Jagged1-KLF4 Axis: Relationship between Cancer Stemness and Angiogenesis. *Stem Cells Int.* **2016**; 2016:6439864. doi: 10.1155/2016/6439864.
11. Fernández-Cortés M, Delgado-Bellido D, Oliver FJ. Vasculogenic Mimicry: Become an Endothelial Cell "But Not So Much". *Front Oncol*. **2019**, 22; 9:803. doi: 10.3389/fonc.2019.00803
12. Folberg, R.; Hendrix, M.J.; Maniotis, A.J. Vasculogenic mimicry and tumor angiogenesis. *Am. J. Pathol.* **2000,** 156, 361-381, doi:10.1016/s0002-9440(10)64739-6.
13. Bergers, G.; Benjamin, L.E. Tumorigenesis and the angiogenic switch. Nature reviews. *Cancer,* **2003**, 3, 401-410, doi:10.1038/nrc1093.
14. Maniotis, A.J.; Folberg, R.; Hess, A.; Seftor, E.A.; Gardner, L.M.; Pe'er, J.; Trent, J.M.; Meltzer, P.S.; Hendrix, M.J. Vascular channel formation by human melanoma cells in vivo and in vitro: vasculogenic mimicry. *Am. J. Pathol*. **1999**, 155, 739-752, doi:10.1016/S0002-9440(10)65173-5.
15. Folberg, R.; Arbieva, Z.; Moses, J.; Hayee, A.; Sandal, T.; Kadkol, S.; Lin, A.Y.; Valyi-Nagy, K.; Setty, S.; Leach, L.; et al. Tumor cell plasticity in uveal melanoma: microenvironment directed dampening of the invasive and metastatic genotype and phenotype accompanies the generation of vasculogenic mimicry patterns. *Am. J. Pathol*, **2006**, 169, 1376-1389, doi:10.2353/ajpath.2006.060223.

16. Basu, G.D.; Liang, W.S.; Stephan, D.A.; Wegener, L.T.; Conley, C.R.; Pockaj, B.A.; Mukherjee, P. A novel role for cyclooxygenase-2 in regulating vascular channel formation by human breast cancer cells. *BCR*, **2006**, 8, R69, doi:10.1186/bcr1626.
17. Chiao, M.T.; Yang, Y.C.; Cheng, W.Y.; Shen, C.C.; Ko, J.L. CD133+ glioblastoma stem-like cells induce vascular mimicry in vivo. *Curr Neurovasc Res*, **2011**, 8, 210-219, doi:10.2174/156720211796558023.
18. Delgado-Bellido, D.; Serrano-Saenz, S.; Fernández-Cortés, M.; Oliver, F.J. Vasculogenic mimicry signaling revisited: focus on non-vascular VE-cadherin. *Molecular cancer*, **2017**, 16, 65, doi:10.1186/s12943-017-0631-x.
19. Andonegui-Elguera, M.A.; Alfaro-Mora, Y.; Caceres-Gutierrez, R.; Caro-Sanchez, C.H.S.; Herrera, L.A.; Diaz-Chavez, J. An Overview of Vasculogenic Mimicry in Breast Cancer. *Front. Oncol*. **2020**, 10, 220, doi:10.3389/fonc.2020.00220.
20. Breier, G.; Grosser, M.; Rezaei, M. Endothelial cadherins in cancer. *Cell Tissue Res.* **2014**, 355, 523-527, doi:10.1007/s00441-014-1851-7.
21. Hendrix, M.J.; Seftor, E.A.; Hess, A.R.; Seftor, R.E. Vasculogenic mimicry and tumour-cell plasticity: lessons from melanoma. *Nat. Rev. Can.* **2003**, 3, 411-421, doi:10.1038/nrc1092.
22. Van der Schaft DW, Seftor RE, Seftor EA, Hess AR, Gruman LM, Kirschmann DA, Yokoyama Y, Griffioen AW, Hendrix MJ. Effects of angiogenesis inhibitors on vascular network formation by human endothelial and melanoma cells. *J Natl Cancer Inst*. **2004**, 96(19):1473-7. doi: 10.1093/jnci/djh267.
23. Mitra, D.; Bhattacharyya, S.; Alam, N.; Sen, S.; Mitra, S.; Mandal, S.; Vignesh, S.; Majumder, B.; Murmu, N. Phosphorylation of EphA2 receptor and vasculogenic mimicry is an indicator of poor prognosis in invasive carcinoma of the breast. *Breast Cancer Res Treat*. **2020**, 179, 359-370, doi:10.1007/s10549-019-05482-8.
24. Zhang, D.; Sun, B.; Zhao, X.; Ma, Y.; Ji, R.; Gu, Q.; Dong, X.; Li, J.; Liu, F.; Jia, X.; et al. Twist1 expression induced by sunitinib accelerates tumor cell vasculogenic mimicry by increasing the population of CD133+ cells in triple-negative breast cancer. *Molecular cancer*, **2014**, 13, 207, doi:10.1186/1476-4598-13-207.
25. Brugnoli, F.; Grassilli, S.; Al-Qassab, Y.; Capitani, S.; Bertagnolo, V. CD133 in Breast Cancer Cells: More than a Stem Cell Marker. J. Oncol. 2019, 2019, 7512632, doi:10.1155/2019/7512632.
26. Liu, T.J.; Sun, B.C.; Zhao, X.L.; Zhao, X.M.; Sun, T.; Gu, Q.; Yao, Z.; Dong, X.Y.; Zhao, N.; Liu, N. CD133+ cells with cancer stem cell characteristics associates with vasculogenic mimicry in triple-negative breast cancer. Oncogene 2013, 32, 544-553, doi:10.1038/onc.2012.85.
27. Rossi, E.; Poirault-Chassac, S.; Bieche, I.; Chocron, R.; Schnitzler, A.; Lokajczyk, A.; Bourdoncle, P.; Dizier, B.; Bacha, N.C.; Gendron, N.; et al. Human Endothelial Colony Forming Cells Express Intracellular CD133 that Modulates their Vasculogenic Properties. SCRR. 2019, 15, 590-600, doi:10.1007/s12015-019-09881-8.
28. Ribatti, D.; Pezzella, F. Overview on the Different Patterns of Tumor Vascularization. Cells 2021, 10, doi:10.3390/cells10030639.

29. Stålhammar G. Identification of Vasculogenic Mimicry in Histological Samples. Methods Mol Biol. 2022; 2514:121-128. doi: 10.1007/978-1-0716-2403-6_12.
30. Folberg, R.; Maniotis, A.J. Vasculogenic mimicry. APMIS. 2004, 112, 508-525, doi:10.1111/j.1600-0463.2004.apm11207-0810.x.
31. Shirakawa, K.; Tsuda, H.; Heike, Y.; Kato, K.; Asada, R.; Inomata, M.; Sasaki, H.; Kasumi, F.; Yoshimoto, M.; Iwanaga, T.; et al. Absence of endothelial cells, central necrosis, and fibrosis are associated with aggressive inflammatory breast cancer. Canc. Res. 2001, 61, 445-451.
32. Shirakawa, K.; Wakasugi, H.; Heike, Y.; Watanabe, I.; Yamada, S.; Saito, K.; Konishi, F. Vasculogenic mimicry and pseudo-comedo formation in breast cancer. IJC, 2002, 99, 821-828, doi:10.1002/ijc.10423.
33. Shirakawa, K.; Kobayashi, H.; Heike, Y.; Kawamoto, S.; Brechbiel, M.W.; Kasumi, F.; Iwanaga, T.; Konishi, F.; Terada, M.; Wakasugi, H. Hemodynamics in vasculogenic mimicry and angiogenesis of inflammatory breast cancer xenograft. Canc. Res. 2002, 62, 560-566.
34. Silvestri, V.L.; Henriet, E.; Linville, R.M.; Wong, A.D.; Searson, P.C.; Ewald, A.J. A Tissue-Engineered 3D Microvessel Model Reveals the Dynamics of Mosaic Vessel Formation in Breast Cancer. Canc. Res. 2020, 80, 4288-4301, doi:10.1158/0008-5472.can-19-1564.
35. Xu, Y.; Li, Q.; Li, X.Y.; Yang, Q.Y.; Xu, W.W.; Liu, G.L. Short-term anti-vascular endothelial growth factor treatment elicits vasculogenic mimicry formation of tumors to accelerate metastasis. Journal of experimental & clinical cancer research, 2012, 31, 16, doi:10.1186/1756-9966-31-16.
36. Valencia-Cervantes, J.; Huerta-Yepez, S.; Aquino-Jarquín, G.; Rodríguez-Enríquez, S.; Martínez-Fong, D.; Arias-Montaño, J.A.; Dávila-Borja, V.M. Hypoxia increases chemoresistance in human medulloblastoma DAOY cells via hypoxia inducible factor 1α mediated downregulation of the CYP2B6, CYP3A4 and CYP3A5 enzymes and inhibition of cell proliferation. Oncol. Rep. 2019, 41, 178-190, doi:10.3892/or.2018.6790.
37. Weidner, N.; Semple, J.P.; Welch, W.R.; Folkman, J. Tumor angiogenesis and metastasis correlation in invasive breast carcinoma. NEJM, 1991, 324, 1-8, doi:10.1056/nejm199101033240101.
38. Sun, B.; Zhang, S.; Zhang, D.; Du, J.; Guo, H.; Zhao, X.; Zhang, W.; Hao, X. Vasculogenic mimicry is associated with high tumor grade, invasion and metastasis, and short survival in patients with hepatocellular carcinoma. Oncol. Rep. 2006, 16, 693-698.
39. Shen, Y.; Quan, J.; Wang, M.; Li, S.; Yang, J.; Lv, M.; Chen, Z.; Zhang, L.; Zhao, X.; Yang, J. Tumor vasculogenic mimicry formation as an unfavorable prognostic indicator in patients with breast cancer. Oncotarget 2017, 8, 56408-56416, doi:10.18632/oncotarget.16919.
40. Jafarian, A.H.; Kooshkiforooshani, M.; Rasoliostadi, A.; Mohamadian Roshan, N. Vascular Mimicry Expression in Invasive Ductal Carcinoma; A New Technique for Prospect of Aggressiveness. IJP, 2019, 14, 232-235, doi:10.30699/ijp.2019.94997.1939.
41. Liu, T.; Sun, B.; Zhao, X.; Gu, Q.; Dong, X.; Yao, Z.; Zhao, N.; Chi, J.; Liu, N.; Sun, R.; et al. HER2/neu expression correlates with vasculogenic mimicry in invasive breast carcinoma. J Cell Mol Med, 2013, 17, 116-122, doi:10.1111/j.1582-4934.2012.01653.x.

42. Yang, J.P., Liao, Y.D., Mai, D.M. et al. Tumor vasculogenic mimicry predicts poor prognosis in cancer patients: a meta-analysis. Angiogenesis 19, 191–200 (2016). https://doi.org/10.1007/s10456-016-9500-2.
43. Kotiyal, S.; Bhattacharya, S. Epithelial Mesenchymal Transition and Vascular Mimicry in Breast Cancer Stem Cells. Crit. Rev. Eukaryot. Gene Expr. 2015, 25, 269-280, doi:10.1615/critreveukaryotgeneexpr.2015014042
44. Yang, J.; Lu, Y.; Lin, Y.Y.; Zheng, Z.Y.; Fang, J.H.; He, S.; Zhuang, S.M. Vascular mimicry formation is promoted by paracrine TGF-β and SDF1 of cancer-associated fibroblasts and inhibited by miR-101 in hepatocellular carcinoma. Cancer letters 2016, 383, 18-27, doi:10.1016/j.canlet.2016.09.012.
45. Chen Q, Lin W, Yin Z, Zou Y, Liang S, Ruan S, Chen P, Li S, Shu Q, Cheng B, Ling C. Melittin Inhibits Hypoxia-Induced Vasculogenic Mimicry Formation and Epithelial-Mesenchymal Transition through Suppression of HIF-1α/Akt Pathway in Liver Cancer. Evid Based Complement Alternat Med. 2019, 1;2019:9602935. doi: 10.1155/2019/9602935.
46. Jin L, Chen C, Huang L, Bu L, Zhang L, Yang Q. Salvianolic acid A blocks vasculogenic mimicry formation in human non-small cell lung cancer via PI3K/Akt/mTOR signalling. Clin Exp Pharmacol Physiol. 2021, 48(4):508-514. doi: 10.1111/1440-1681.13464.
47. Liu, S.; Ni, C.; Zhang, D.; Sun, H.; Dong, X.; Che, N.; Liang, X.; Chen, C.; Liu, F.; Bai, J.; et al. S1PR1 regulates the switch of two angiogenic modes by VE-cadherin phosphorylation in breast cancer. Cell death & disease 2019, 10, 200, doi:10.1038/s41419-019-1411-x.
48. Fang JH, Zheng ZY, Liu JY, Xie C, Zhang ZJ, Zhuang SM. Regulatory Role of the MicroRNA-29b-IL-6 Signaling in the Formation of Vascular Mimicry. Mol Ther Nucleic Acids. 2017,15;8:90-100. doi: 10.1016/j.omtn.2017.06.009..
49. Aikins AR, Kim M, Raymundo B, Kim CW. Downregulation of transgelin blocks interleukin-8 utilization and suppresses vasculogenic mimicry in breast cancer cells. Exp Biol Med (Maywood). 2017;242(6):573-583. doi: 10.1177/1535370216685435.
50. Nisar MA, Zheng Q, Saleem MZ, Ahmmed B, Ramzan MN, Ud Din SR, Tahir N, Liu S, Yan Q. IL-1β Promotes Vasculogenic Mimicry of Breast Cancer Cells Through p38/MAPK and PI3K/Akt Signaling Pathways. Front Oncol. 2021, 14;11:618839. doi: 10.3389/fonc.2021.618839.
51. Laederich MB, Funes-Duran M, Yen L, Ingalla E, Wu X, Carraway KL 3rd, Sweeney C. The leucine-rich repeat protein LRIG1 is a negative regulator of ErbB family receptor tyrosine kinases. J Biol Chem. 2004 Nov 5;279(45):47050-6. doi: 10.1074/jbc.M409703200.
52. Smith SJ, Ward JH, Tan C, Grundy RG, Rahman R. Endothelial-like malignant glioma cells in dynamic three dimensional culture identifies a role for VEGF and FGFR in a tumor-derived angiogenic response. Oncotarget. 2015, 8;6(26):22191-205. doi: 10.18632/oncotarget.4339. PMID: 26203665; PMCID: PMC4673156.

# CAPÍTULO 2.

## CÁNCER DE MAMA TRIPLE NEGATIVO Y SUS ALTERNATIVAS TERAPÉUTICAS

## 2.1. EL CÁNCER DE MAMA TRIPLE NEGATIVO, UN RETO ACTUAL EN LA CLÍNICA.

Respecto a otros años, en el 2020 el cáncer de mama superó al cáncer de pulmón como el tumor más diagnosticado con un estimado de 2.3 millones de nuevos casos en un año, el 11.7% de todos los casos [1]. En algún momento de su vida, se calcula que 1 de cada 8 mujeres será diagnosticada con cáncer de mama, que además es la segunda causa más común de muerte relacionada con el cáncer en mujeres a nivel mundial [2]. Se ha observado que las mujeres pertenecientes a minorías, especialmente afroamericanas e hispanoamericanas, tienen más probabilidades de ser diagnosticadas con formas agresivas y avanzadas de cáncer de mama, y menor probabilidad de recibir regímenes de tratamiento recomendados [3]. Por ello, la necesidad de identificar tratamientos más eficientes que ayuden a disminuir las muertes por este tipo de cáncer, es una de las prioridades de la salud pública a nivel mundial.

El cáncer de mama se clasifica de diferentes maneras, las más comunes se basan en la expresión de biomarcadores como los receptores hormonales de progesterona (PR) y estrógeno (ER), así como del receptor del factor de crecimiento epidérmico humano (HER2). Además de biomarcadores para la clasificación molecular del cáncer de mama, éstos receptores representan los blancos principales de la terapia dirigida de estos tumores [4]. El subgrupo de cáncer mama triple negativo (CMTN) carece de la expresión de estos receptores y representa del 10 al 20% de los cánceres de mama, además de ser mucho más frecuente en mujeres jóvenes [5–7].

Las pacientes con CMTN suelen tener un peor pronóstico en cuanto a supervivencia global en comparación con las pacientes de los demás subgrupos [8]. Al provenir de células altamente invasivas, los tumores triple negativo son considerados como agresivos pues se asocian con un mayor índice de recurrencia, dentro de los primeros 5 años tras el diagnóstico, así como a un mayor riesgo de metástasis a distancia, siendo las metástasis a cerebro y pulmón las más frecuentes [9, 10].

De acuerdo con el Consenso Mexicano para el Diagnóstico y Tratamiento del Cáncer mamario del 2021 “las pacientes con tumores triple negativos tienen como única opción de tratamiento la quimioterapia, sin que sea posible recomendar en la actualidad un esquema específico”. Desafortunadamente la agresividad biológica de estos tumores, también se asocia

con el desarrollo de quimio-resistencia de origen intrínseco o en etapas mucho más tempranas respecto a los demás subtipos moleculares [11-14].

## 2.2. TERAPIAS ANTI-ANGIOGÉNICAS Y MIMETISMO VASCULAR

Como se mencionó en el Capítulo 1.2, entre las alternativas terapéuticas para tratar tumores altamente agresivos y vascularizados, como los son los tumores triples negativos, están las terapias anti-angiogénicas, entre estas estrategias se encuentran las moléculas sintéticas inhibidoras de RTKs, que actúan al interactuar con el sitio de unión al ATP previniendo la dimerización y fosforilación de los receptores y sus señalizaciones intracelulares [15]. Con el desarrollo de nuevas moléculas específicas dirigidos contra las moléculas mediadoras de la angiogénesis como el factor de crecimiento endotelial (VEGF) y su receptor (VEGFR), o bien del factor de crecimiento de fibroblastos (FGF) y su receptor (FGFR), pues se sabe son cruciales en la angiogénesis, la linfangiogénesis y la remodelación de los vasos sanguíneos [16, 17].

Dos importantes inhibidores de FGFR, en estudios de fase clínica I y II. Por una parte, el dovitinib es una molécula pequeña multiblanco, actúa como un inhibidor selectivo contra FGFR1/2/3, además de VEGFR1/2/3, cKIT y el receptor beta del factor de crecimiento derivado de plaquetas (PDFGR- β), sus potentes efectos anti-proliferativos han sido reportados en modelos tanto *in vitro* como *in vivo* [18,19]. Por otra parte, el AZD4547, es un inhibidor específico cuyos fuertes efectos anti-proliferativos, pro-diferenciantes y anti-angiogénicos en distintos tipos de tumores que sobreexpresan FGFR han sido estudiados y actualmente se encuentra en estudios de fase clínica I y II [20,22]. Cabe destacar que al inicio de este proyecto, el efecto de estos inhibidores sobre la angiogénesis o el mimetismo vascular del cáncer de mama triple negativo se desconocían.

Sin embargo, se ha demostrado que en ocasiones inhibidores similares pueden llegar a aumentar la agresividad y metástasis en modelos murinos [23]. Un estudio *in vivo* en ratones desnudos portadores de tumores xenoinjertados MDA-MB-231 y Hs578T mostró que el tratamiento con sunitinib, un inhibidor de la tirosina quinasa de VEGF, aumenta los canales de mimetismo vasculogénico (VM) y que la interrupción del tratamiento da como resultado un nuevo crecimiento, invasión y un rebrote de vasos dependientes del endotelio mediante mimetismo vasculogénico [24]. Por lo tanto, queríamos abordar algunas de las estrategias alternativas que se ha informado que afectan la VM específicamente en un contexto TNBC y

aquellas que aún no se han explorado pero que podrían resultar en un beneficio para prevenir el desarrollo de VM como mecanismo de resistencia o como un curso para progresión de la metástasis. A pesar de los efectos contundentes de anti-angiogénicos como el sunitinib y el bevacizumab, en CMTN, evidencia reciente ha mostrado que si bien disminuyen la densidad vascular y detienen el crecimiento, la interrupción del tratamiento conduce a recurrencia, permitiendo que el tumor vuelva a crecer empleando el mimetismo vascular como estrategia de vascularización y supervivencia tumoral [23-26].

Ante la necesidad de mejorar la eficiencia de las estrategias terapéuticas actuales, en recientes años la comunidad científica ha invertido grandes esfuerzos en el uso de compuestos de origen natural con efectos anti-tumorales, ya que tienen grandes ventajas por su bajo costo y baja toxicidad. Su potencial uso clínico es interesante y necesario, especialmente para aquellas pacientes, como las del subgrupo triple negativo, que al carecer de estrategias dirigidas u opciones terapéuticas alternativas a las terapias sistémicas, siguen siendo al día de hoy un reto clínico a nivel nacional y mundial.

## 2.3. ALTERNATIVAS TERAPÉUTICAS CONTRA EL MIMETISMO VASCULAR Y LA ANGIOGÉNESIS.

Uno de los graves problemas de las terapias sistémicas, como lo son la radioterapia y la quimioterapia, es que la toxicidad de estos compuestos afecta no sólo a las células del tumor, sino también a las células no neoplásicas del tejido donde se encuentra localizado el cáncer. Debido a que la mayoría de agentes quimioterapéuticos y anti-angiogénicos se asocian a la resistencia a terapia, recurrencia tumoral y efectos adversos, la comunidad científica busca opciones a dichos tratamientos con mejor eficiencia, y con baja o nula toxicidad sistémica, como lo son los compuestos de origen natural, o las moléculas modificadas para transportar los fármacos de manera selectiva a los tumores de cáncer de mama [27].

Al día de hoy diversos compuestos bioactivos, provenientes de especies vegetales u hongos de origen acuático y terrestre son de interés científico por sus potenciales efectos terapéuticos [28]. Evaluar su toxicidad es de gran importancia para descartar efectos adversos asociados a la interacción de hierbas y fármacos, por lo que su efecto combinado debe ser cuidadosamente revisado [29].

Por ello, los efectos benéficos de varios de estos compuestos de origen natural han sido previamente evaluados tanto en modelos *in vitro* como en modelos *in vivo*, así como en la quimioterapia. Dichos compuestos pueden ser empleados en monoterapia o en combinación con otros agentes antitumorales de origen natural, moléculas modificadas o con fármacos sintetizados [30]. Se ha visto que en varios casos, la combinación de compuestos de origen natural con agentes quimioterapéuticos clásicos permite disminuir las dosis empleadas de los compuestos, lo cual conlleva la disminución/prevención de la resistencia a la terapia, mitigación de los efectos secundarios y potenciación o sinergia de los efectos antineoplásicos de los compuestos combinados [31-34].

Lo anterior resulta sumamente prometedor para rediseñar los esquemas de tratamiento y mejorar la eficiencia de las terapias, especialmente en tumores como los CMTN, que al carecer de dianas moleculares para su tratamiento ser altamente angiogénicos y capaces de hacer mimetismo vascular como mecanismo de vascularización alternativo y/o de resistencia. Entre los compuestos con potentes efectos anti-neoplásicos y que ha mostrado tener efectos anti-angiogénicos e inhibitorios sobre el mimetismo vascular, destaca la curcumina.

### 2.3.1. CURCUMINA, EL BOLETO DORADO CONTRA LA VASCULARIZACIÓN TUMORAL

La curcumina, el principal curcuminoide derivado de la cúrcuma (*Curcuma longa*), es un polifenol que se ha propuesto como complemento dietario para prevenir el cáncer y como agente terapéutico por sus potentes efectos sobre la proliferación, la inflamación y el estrés oxidativo, en cáncer [35, 36]. Varios de los efectos de la curcumina son mediados por su papel sobre la apoptosis y su actividad como inhibidor de la actividad de las cinasas de tirosina, por lo que sus efectos anti-neoplásicos involucran la regulación negativa de cascadas de señalización mediadas por fosforilación [37]. Dichos efectos van desde la prevención de la metástasis en el CMTN hasta la sensibilización a la quimioterapia y radioterapia [38, 39]. Sin embargo, también se ha visto que la curcumina puede incidir sobre la regulación de vías involucradas con la regulación negativa de a vascularización tumoral, tanto por medio de la angiogénesis, como por mimetismo vascular (Ilustración 1), [39, 42], lo anterior sugiere que su

uso por sí solo o en combinación con otros agentes anti-neoplasicos podría prevenir el desarrollo de mecanismos de resistencia que involucren dichas vías de señalización.

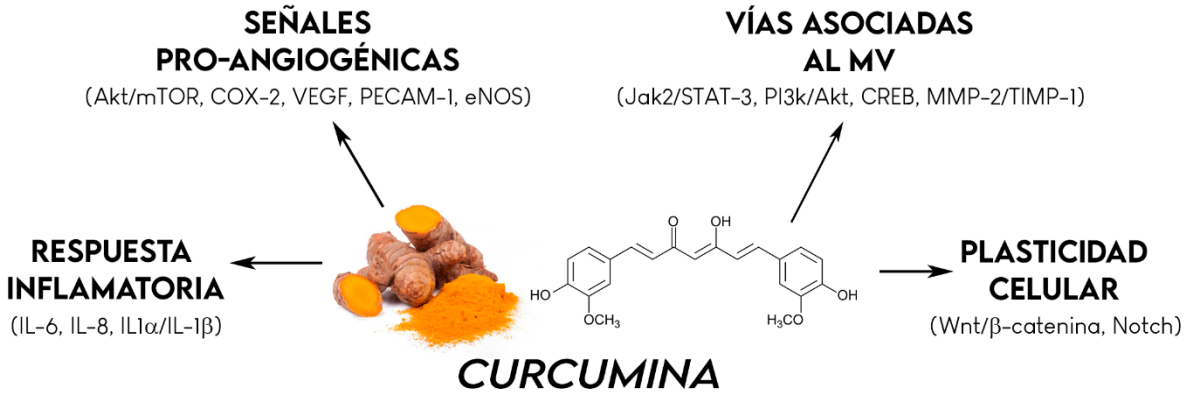


*Ilustración 1. Efectos de la curcumina sobre la vascularización tumoral y procesos asociados.*
*La curcumina es un polifenol derivado de la cúrcuma (Curcuma longa). Se han reportado diferentes efectos de la curcumina sobre señales pro-angiogénicas y vías asociadas con el mimetismo vascular (MV) así como con la respuesta inflamatoria y la plasticidad celular, que como se ha discutido en secciones anteriores son importantes en el desarrollo del MV y la resistencia a las terapias anti-angiogénicas.*

Algunos estudios han sugerido que parte de los efectos quimiopreventivos y anti-tumorales de la curcumina son mediados por su interacción directa con el receptor de la vitamina D, VDR, así como su activación y la regulación de sus funciones genómicas [43,44]. Estudios epidemiológicos han mostrado que existe una asociación inversa entre el riesgo de desarrollar cáncer de mama y una concentración baja de vitamina D; se sabe que mantener niveles de suficiencia de 25-hidroxivtamina D3 (25OHD3) puede disminuir el riesgo de padecer cáncer en mujeres hasta en un 50% (cuando se comparan mujeres con suficiencia vs deficiencia de 25OHD3), esto sugiere que evitar la hipovitaminosis D es una manera segura y económicamente accesible de prevenir esta patología [44,45]. Por ello, diversos grupos han propuesto la suplementación nutricional con fuentes de vitamina D, que aumentan la expresión del VDR, su bioactividad y sus efectos anti-neoplásicos [43-47].

### 2.3.2. CALCITRIOL: OPORTUNIDADES TERAPÉUTICAS EN EL CÁNCER DE MAMA

El calcitriol es un secoesteroide derivado de la vitamina D3, es su principal metabolito activo y en condiciones fisiológicas cumple con la función de mantener la homeostasis de calcio y fósforo para preservar la salud ósea; sus acciones hormonales tienen efecto en riñones, intestino y huesos [48]. En cambio, en el contexto del cáncer, esta forma hormonal de la vitamina D, calcitriol, ejerce potentes efectos anti-proliferativos y pro-diferenciantes, por lo que actúa como un factor antitumoral multiblanco cuando se encuentra en concentraciones adecuadas [49]. Sus funciones son mediadas por su unión al VDR, que actúa como factor de transcripción dependiente de ligando, y regula la expresión de los genes con elementos de respuesta a la vitamina D (VDRE) en su región promotora [50].

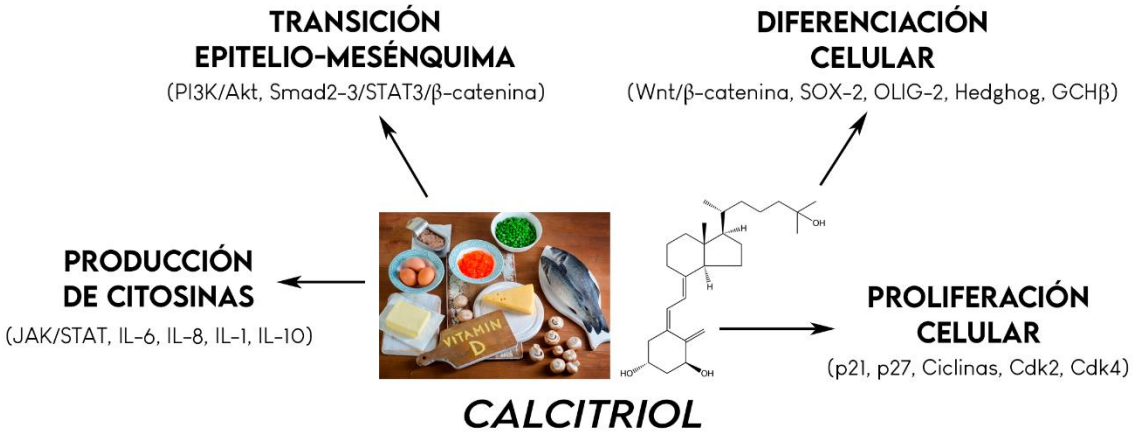


*Ilustración 2. Efectos anti-neoplásicos del calcitriol y principales reguladores moleculares.*
El calcitriol es una hormona secoesteroide derivada de la vitamina D con fuertes efectos pro-diferenciantes y anti-proliferativos en células de cáncer, donde además inhibe la expresión de oncogenes y activa apoptosis. Sin embargo, también se ha visto que regula mecanismos asociados al MV como la producción de citosinas pro-inflamatorias y la EMT.

Como se muestra en la Ilustración 2, el calcitriol tiene una amplia variedad de blancos moleculares que inciden en diversos procesos de importancia para la supervivencia tumoral y su diseminación a distancia. Los efectos anti-tumorales del calcitriol van desde la inhibición de la proliferación celular y la regulación de la diferenciación celular, hasta la inhibición de la EMT y la producción de citosinas, procesos altamente ligados con el desarrollo del mimetismo vascular [51, 55].

Debido a sus efectos multiblanco, diversos grupos de investigación han demostrado el potencial del calcitriol para actuar de manera sinérgica con fármacos antineoplásicos usados comúnmente en la clínica [56]. Entre otras cosas, se ha demostrado que el calcitriol o sus análogos potencian los efectos terapéuticos de taxanos, análogos del platino, agentes alquilantes, inhibidores de RTKs y radiaciones ionizantes [56-62].

De manera interesante, nuestro grupo de investigación, reporto recientemente que en células de CMTN así como en ratones xenoinjertados con dichas células, el tratamiento combinado de calcitriol con curcumina inhibe de manera significativa el crecimiento tumoral al impedir la angiogénesis, disminuyendo significativamente la DMV, el diámetro de los vasos, y la captación de marcadores del endotelio activado [63]. Ambos compuestos interactuaron sinérgicamente inhibiendo la proliferación celular de las células de CMTN de manera significativa, respecto a cada compuesto por separado. A la fecha, los efectos de la combinación de calcitriol con agentes anti-angiogénicos como la curcumina o los inhibidores de FGFR/VEGFR, como AZD4547 o dovitinib, sobre el mimetismo vascular no han sido evaluados por otro grupo de investigación.

### 2.3.3. USO POTENCIAL DEL CALCITRIOL Y LA CURCUMINA EN EL MV

Como se menciona anteriormente, el estudio de compuestos de origen natural con potenciales efectos inhibitorios del mimetismo vascular o sus procesos asociados ha despuntado en los últimos años ante las limitaciones encontradas al usar terapias anti-angiogénicas que lejos de brindar un beneficio a las pacientes, pueden llegar a generar la resistencia mediante el mimetismo vascular, la inestabilidad cromosómica y la plasticidad celular del tumor [23, 24]. Sobre la curcumina, se ha visto que tiene potentes efectos inhibitorios del MV y otros procesos asociados en tumores como el hepatocarcinoma, donde su efecto es mediado por la vía de PI3K/Akt, melanoma coroideo, a través de la regulación negativa de la vía EphA2/PI3K/MMP-2 y el carcinoma de células escamosas de laringe, donde la inhibición del MV se asoció a la inhibición de la vía de JAK-2/STAT3 y la regulación negativa de la expresión de MMP-2 y VEGF [64-66]. A la fecha, su efecto sobre el MV del cáncer de mama, en particular del CMTN no se había reportado.

Por otro lado, el calcitriol, el metabolito más activo de la vitamina D, que posee potentes efectos pro-diferenciadores y anti proliferativos en cáncer de mama [67], ha mostrado que es

capaz de inhibir la EMT al regular negativamente la vía de PI3K/Akt/β-catenina [68]. Además, el calcitriol tiene una potente actividad antiinflamatoria, pues regula negativamente la activación de la vía JAK/STAT y la producción de citoquinas inflamatorias, procesos que se sabe están involucrados en la carcinogénesis y la VM [69, 70]; sin embargo, no se han explorado los efectos del calcitriol sobre el MV.

Al momento de la realización de este proyecto de investigación y mientras el artículo original se encontraba en revisión, Khuloud Bajbouj et al. reportaron que el calcitriol regula diferencialmente las vías relacionadas con MV y la expresión de sus marcadores clásicos en las células de cáncer de mama tratadas con calcitriol, esto se determinó mediante el análisis *in silico* de bases de datos transcriptómicas [71]. El mismo grupo de investigación también demostró que en una concentración muy alta de calcitriol (10 μM) la expresión de inhibidores tisulares de MMP (TIMP) aumenta, mientras que la de MMP disminuye, lo cual se vio reflejado en la inhibición del MV en las células MDA-MB-231 [71]. No obstante, a la fecha de la realización de esta investigación, los efectos de la curcumina, los de las concentraciones nanomolares del calcitriol y los de la combinación de ambos compuestos en cáncer de mama triple negativo, y los mecanismos involucrados en dicha respuesta permanecen desconocidos, esto dio origen a nuestra pregunta de investigación.

Para abordar este asunto, implementamos un modelo que incluye la participación de factores derivados del microambiente tumoral involucrados en la inducción del MV. Desarrollamos un modelo de MV inducido por endotelio in vitro en co-cultivos de células de CMTN co-cultivadas con células endoteliales [ver Capítulo 4.]. Una vez que caracterizamos el proceso de VM en nuestro modelo experimental, probamos los efectos del calcitriol, la curcumina y su combinación en la capacidad de las células tumorales para formar redes de cordones similares a túbulos. Además, para conocer los mecanismos moleculares, exploramos la capacidad de los compuestos naturales para modificar el patrón de fosforilación de varias cinasas que se sabe que están involucradas en la formación del MV [ver Capítulo 5.]. Parte de la novedad de esta investigación reside en el modelo experimental que utilizamos, las concentraciones de calcitriol probadas que se pueden alcanzar de forma segura en los pacientes y el efecto combinatorio de los compuestos sobre la VM.

## 2.4. LITERATURA CITADA


1. Sung H, Ferlay J, Siegel RL, Laversanne M, Soerjomataram I, Jemal A, Bray F. Global Cancer Statistics 2020: GLOBOCAN Estimates of Incidence and Mortality Worldwide for 36 Cancers in 185 Countries. CA Cancer J Clin. 2021 May;71(3):209-249. doi: 10.3322/caac.21660.
2. Strunk MA, Zopf EM, Steck J, Hamacher S, Hallek M and Baumann FT. Effects of Kyusho Jitsu on Physical Activity-levels and Quality of Life in Breast Cancer Patients. In vivo, 2018. 32(4), 819–824. doi: 10.21873/invivo.11313
3. Chen L, Li CI. Racial disparities in breast cancer diagnosis and treatment by hormone receptor and HER2 status. Cancer Epidemiol Biomarkers Prev. 2015, 24(11):1666-72. doi: 10.1158/1055-9965.
4. Dai X, Li T, Bai Z, Yang Y, Liu X, Zhan J, Shi B. Breast cancer intrinsic subtype classification, clinical use and future trends. Am J Cancer Res. 2015 Sep 15;5(10):2929-43
5. Hernández-Álvarez C, Romo-Aguirre C, Ortíz-de Iturbe C. Cáncer de mama triple negativo: frecuencia y características en el hospital Ángeles Pedregal. Acta Médica Grupo Ángeles. 2017. 15(4):269-274.
6. Triple-Negative Breast Cancer. [(consultado el 01 de Agosto del 2022)]. Disponible en línea: https://www.cancer.org/cancer/breast-cancer/about/types-of-breast-cancer/triple-negative.html
7. Li X, Yang J, Peng L, Sahin AA, Huo L, Ward KC, O'Regan R, Torres MA, Meisel JL. Triple-negative breast cancer has worse overall survival and cause-specific survival than non-triple-negative breast cancer. Breast Cancer Res Treat. 2017; 161(2):279-287. doi: 10.1007/s10549-016-4059-6.
8. Dent R, Trudeau M, Pritchard KI, Hanna WM, Kahn HK, Sawka CA, Lickley LA, Rawlinson E, Sun P, Narod SA. Triple-negative breast cancer: clinical features and patterns of recurrence. Clin Cancer Res. 2007 1;13(15 Pt 1):4429-34. doi: 10.1158/1078-0432.CCR-06-3045.
9. Medina MA, Oza G, Sharma A, Arriaga LG, Hernández Hernández JM, Rotello VM, Ramirez JT. Triple-Negative Breast Cancer: A Review of Conventional and Advanced Therapeutic Strategies. Int J Environ Res Public Health. 2020 20;17(6):2078. doi: 10.3390/ijerph17062078.
10. Ferrari P, Scatena C, Ghilli M, Bargagna I, Lorenzini G, Nicolini A. Molecular Mechanisms, Biomarkers and Emerging Therapies for Chemotherapy Resistant TNBC. Int J Mol Sci. 2022 31;23(3):1665. doi: 10.3390/ijms23031665.
11. Clinical Practice Guidelines in Oncology (NCCN guidelines). Breast Cancer version 1.2017. Disponible en: www.nccn.org. Acceso el 01/03/2021.
12. Cardoso F, Paluch-Shimon S, Senkus E, Curigliano G, et al. 5th ESO-ESMO International Consensus. Guidelines for Advanced Breast Cancer (ABC 5) Ann Oncol. 2020. doi: 10.1016. Publicado en línea el 23 September, 2020.

13. Clinical Practice Guidelines in Oncology (NCCN guidelines). Breast Cancer version 3.2018. Disponible en: www.nccn.org. Acceso el 10/03/2021.
14. Consenso Mexicano sobre diagnóstico y tratamiento del cáncer mamario (Novena revisión). 2021. Disponible en http://consensocancermamario.com/
15. Takeuchi K, Ito F. Receptor tyrosine kinases and targeted cancer therapeutics. Biol Pharm Bull. 2011;34(12):1774-80. doi: 10.1248/bpb.34.1774.
16. Lee, S.H., et al. 2015. Pivotal role of vascular endothelial growth factor pathway in tumor angiogenesis. Ann Surg Treat Res, 89, 1-8.
17. Lieu C, Heymach J, Overman M, Tran H, Kopetz S. Beyond VEGF: inhibition of the fibroblast growth factor pathway and antiangiogenesis. Clin Cancer Res. 2011 Oct 1;17(19):6130-9. doi: 10.1158/1078-0432.CCR-11-0659.
18. Allarity Therapeutics submits new drug application (NDA) to the U.S. FDA for dovitinib for third-line treatment of renal cell carcinoma (RCC). News release. Allarity Therapeutics. December 22, 2021. Consultado el 3 de marzo de 2022. https://yhoo.it/3qQwvTY.
19. Motzer RJ, Porta C, Vogelzang NJ, et al. Dovitinib versus sorafenib for third-line targeted treatment of patients with metastatic renal cell carcinoma: an open-label, randomised phase 3 trial. Lancet Oncol. 2014;15(3):286-296. doi:10.1016/S1470-2045(14)70030-0.
20. Gavine, P. R., et al. 2012. AZD4547: An orally bioavailable, potent and selective inhibitor of the Fibroblast Growth Factor Receptor tyrosine kinase family. Cancer Res, 3034.
21. Zhang, J., et al. 2012. Translating the therapeutic potential of AZD4547 in FGFR1-amplified non-small cell lung cancer through the use of patient derived tumor xenograft (PDTX) models. Clin Cancer Res, 2694
22. Xie, L., et al. 2013. FGFR2 gene amplification in gastric cancer predicts sensitivity to the selective FGFR inhibitor AZD4547. Clin Cancer Res, 3898.
23. Pàez-Ribes M, Allen E, Hudock J, Takeda T, Okuyama H, Viñals F, Inoue M, Bergers G, Hanahan D, Casanovas O. Antiangiogenic therapy elicits malignant progression of tumors to increased local invasion and distant metastasis. Cancer Cell. 2009 Mar 3;15(3):220-31. doi: 10.1016/j.ccr.2009.01.027.
24. Sun H, Zhang D, Yao Z, Lin X, Liu J, Gu Q, Dong X, Liu F, Wang Y, Yao N, Cheng S, Li L, Sun S. Anti-angiogenic treatment promotes triple-negative breast cancer invasion via vasculogenic mimicry. Cancer Biol Ther. 2017. 3;18(4):205-213. doi: 10.1080/15384047.2017.1294288.
25. Xu Y, Li Q, Li XY, Yang QY, Xu WW, Liu GL. Short-term anti-vascular endothelial growth factor treatment elicits vasculogenic mimicry formation of tumors to accelerate metastasis. J Exp Clin Cancer Res. 2012 Feb 23;31(1):16. doi: 10.1186/1756-9966-31-16.

26. Zhang D, Sun B, Zhao X, Ma Y, Ji R, Gu Q, Dong X, Li J, Liu F, Jia X, Leng X, Zhang C, Sun R, Chi J. Twist1 expression induced by sunitinib accelerates tumor cell vasculogenic mimicry by increasing the population of CD133+ cells in triple-negative breast cancer. Mol Cancer. 2014 8;13:207. doi: 10.1186/1476-4598-13-207.
27. Ribatti D, Annese T, Ruggieri S, Tamma R, Crivellato E. Limitations of Anti-Angiogenic Treatment of Tumors. Transl Oncol. 2019;12(7):981-986. doi: 10.1016/j.tranon.2019.04.022.
28. Noel B, Singh SK, Lillard JW Jr, Singh R. Role of natural compounds in preventing and treating breast cancer. Front Biosci (Schol Ed). 2020. 1;12(1):137-160. doi: 10.2741/S544.
29. Greenwell M, Rahman PK. Medicinal Plants: Their Use in Anticancer Treatment. Int J Pharm Sci Res. 2015 Oct 1;6(10):4103-4112. doi: 10.13040/IJPSR.0975-8232.6(10).4103-12.
30. Lin SR, Chang CH, Hsu CF, Tsai MJ, Cheng H, Leong MK, Sung PJ, Chen JC, Weng CF. Natural compounds as potential adjuvants to cancer therapy: Preclinical evidence. Br J Pharmacol. 2020 Mar;177(6):1409-1423. doi: 10.1111/bph.14816.
31. Lichota A, Gwozdzinski K. Anticancer Activity of Natural Compounds from Plant and Marine Environment. Int J Mol Sci. 2018 Nov 9;19(11):3533. doi: 10.3390/ijms19113533.
32. Pathak K, Pathak MP, Saikia R, Gogoi U, Sahariah JJ, Zothantluanga JH, Samanta A, Das A. Cancer Chemotherapy *via* Natural Bioactive Compounds. Curr Drug Discov Technol. 2022;19(4):e310322202888. doi: 10.2174/1570163819666220331095744.
33. Sripriya N, Ranjith Kumar M, Ashwin Karthick N, Bhuvaneswari S, Udaya Prakash N.K. *In silico* evaluation of multispecies toxicity of natural compounds. Drug Chem Toxicol. 2021 Sep;44(5):480-486. doi: 10.1080/01480545.2019.1614023
34. Lin SR, Chang CH, Hsu CF, Tsai MJ, Cheng H, Leong MK, Sung PJ, Chen JC, Weng CF. Natural compounds as potential adjuvants to cancer therapy: Preclinical evidence. Br J Pharmacol. 2020 Mar;177(6):1409-1423. doi: 10.1111/bph.14816.
35. Xu XY, Meng X, Li S, Gan RY, Li Y, Li HB. Bioactivity, Health Benefits, and Related Molecular Mechanisms of Curcumin: Current Progress, Challenges, and Perspectives. Nutrients. 2018 Oct 19;10(10):1553. doi: 10.3390/nu10101553.
36. Wang J, Jiang YF. Natural compounds as anticancer agents: Experimental evidence. World J Exp Med. 2012 Jun 20;2(3):45-57. doi: 10.5493/wjem.v2.i3.45.
37. Bachmeier B, Nerlich AG, Iancu CM, Cilli M, Schleicher E, Vené R, Dell'Eva R, Jochum M, Albini A, Pfeffer U. The chemopreventive polyphenol Curcumin prevents hematogenous breast cancer metastases in immunodeficient mice. Cell Physiol Biochem. 2007;19(1-4):137-52. doi: 10.1159/000099202.

38. Dhandapani KM, Mahesh VB, Brann DW. Curcumin suppresses growth and chemoresistance of human glioblastoma cells via AP-1 and NFkappaB transcription factors. J Neurochem. 2007 Jul;102(2):522-38. doi: 10.1111/j.1471-4159.2007.04633.x.
39. Shakeri A, Ward N, Panahi Y, Sahebkar A. Anti-Angiogenic Activity of Curcumin in Cancer Therapy: A Narrative Review. Curr Vasc Pharmacol. 2019;17(3):262-269. doi: 10.2174/1570161116666180209113014.
40. Hu A, Huang JJ, Jin XJ, Li JP, Tang YJ, Huang XF, Cui HJ, Xu WH, Sun GB. Curcumin suppresses invasiveness and vasculogenic mimicry of squamous cell carcinoma of the larynx through the inhibition of JAK-2/STAT-3 signaling pathway. Am J Cancer Res. 2014 Dec 15;5(1):278-88.
41. Chiablaem, K.; Lirdprapamongkol, K.; Keeratichamroen, S.; Surarit, R.; Svasti, J. Curcumin suppresses vasculogenic mimicry capacity of hepatocellular carcinoma cells through STAT3 and PI3K/AKT inhibition. Anticancer Res. 2014, 34, 1857-1864.
42. Chen, L.X.; He, Y.J.; Zhao, S.Z.; Wu, J.G.; Wang, J.T.; Zhu, L.M.; Lin, T.T.; Sun, B.C.; Li, X.R. Inhibition of tumor growth and vasculogenic mimicry by curcumin through down-regulation of the EphA2/PI3K/MMP pathway in a murine choroidal melanoma model. Cancer Biol Ther. 2011, 11, 229-235.
43. Bartik L, Whitfield GK, Kaczmarska M, Lowmiller CL, Moffet EW, Furmick JK, Hernandez Z, Haussler CA, Haussler MR, Jurutka PW. Curcumin: a novel nutritionally derived ligand of the vitamin D receptor with implications for colon cancer chemoprevention. J Nutr Biochem. 2010 Dec;21(12):1153-61. doi: 10.1016/j.jnutbio.2009.09.012.
44. Apprato, G.; Fiz, C.; Fusano, I.; Bergandi, L.; Silvagno, F. Natural Epigenetic Modulators of Vitamin D Receptor. *Appl. Sci.* **2020**, *10*, 4096. https://doi.org/10.3390/app10124096.
45. Garland CF, Garland FC, Gorham ED, Lipkin M, Newmark H, Mohr SB, Holick MF. The role of vitamin D in cancer prevention. Am J Public Health. 2006 Feb;96(2):252-61. doi: 10.2105/AJPH.2004.045260.
46. Garland CF, Gorham ED, Mohr SB, Garland FC. Vitamin D for cancer prevention: global perspective. Ann Epidemiol. 2009 Jul;19(7):468-83. doi: 10.1016/j.annepidem.2009.03.021. PMID: 19523595.
47. Arabnezhad L, Mohammadifard M, Rahmani L, Majidi Z, Ferns GA, Bahrami A. Effects of curcumin supplementation on vitamin D levels in women with premenstrual syndrome and dysmenorrhea: a randomized controlled study. BMC Complement Med Ther. 2022 Jan 22; 22(1):19. doi: 10.1186/s12906-022-03515-2.
48. Lips P. Vitamin D physiology. Prog Biophys Mol Biol. 2006 Sep;92(1):4-8. doi: 10.1016/j.pbiomolbio.2006.02.016.

49. Díaz L, Díaz-Muñoz M, García-Gaytán AC, Méndez I. Mechanistic Effects of Calcitriol in Cancer Biology. Nutrients. 2015 Jun 19; 7(6):5020-50. doi: 10.3390/nu7065020.
50. Wan LY, Zhang YQ, Chen MD, Liu CB, Wu JF. Relationship of structure and function of DNA-binding domain in vitamin D receptor. Molecules. 2015 Jul 7;20(7):12389-99. doi: 10.3390/molecules200712389.
51. Vanhevel, J., Verlinden, L., Doms, S., Wildiers, H., & Verstuyf, A. (2022). The role of vitamin D in breast cancer risk and progression, *Endocrine-Related Cancer*, 2022. *29*(2), R33-R55.
52. Katica, M. & Tepekoy, F. The effect of Calcitriol 1,25 (OH)2 - D3 on osteoblast-like cell proliferation during in vitro cultivation . Veterinary Journal of Mehmet Akif Ersoy University, 2020. 5 (1), 11-17. DOI: 10.24880/maeuvfd.653000.
53. Uhmann A, Niemann H, Lammering B, Henkel C, Heß I, Rosenberger A, Dullin C, Schraepler A, Schulz-Schaeffer W, Hahn H. Calcitriol inhibits hedgehog signaling and induces vitamin d receptor signaling and differentiation in the patched mouse model of embryonal rhabdomyosarcoma. Sarcoma. 2012;2012:357040. doi: 10.1155/2012/357040.
54. Humeniuk-Polaczek R, Marcinkowska E. Impaired nuclear localization of vitamin D receptor in leukemia cells resistant to calcitriol-induced differentiation. J Steroid Biochem Mol Biol. 2004 Apr;88(4-5):361-6. doi: 10.1016/j.jsbmb.2004.01.002.
55. Xu S, Zhang ZH, Fu L, Song J, Xie DD, Yu DX, Xu DX, Sun GP. Calcitriol inhibits migration and invasion of renal cell carcinoma cells by suppressing Smad2/3-, STAT3- and β-catenin-mediated epithelial-mesenchymal transition. Cancer Sci. 2020 Jan;111(1):59-71. doi: 10.1111/cas.14237.
56. Segovia-Mendoza, M.; García-Quiroz, J.; Díaz, L.; García-Becerra, R. Combinations of Calcitriol with Anticancer Treatments for Breast Cancer: An Update. *Int. J. Mol. Sci.* **2021**, *22*, 12741. https://doi.org/10.3390/ijms222312741
57. Dunlap N, Schwartz GG, Eads D, Cramer SD, Sherk AB, John V, Koumenis C. 1alpha,25-dihydroxyvitamin D(3) (calcitriol) and its analogue, 19-nor-1alpha,25(OH)(2)D(2), potentiate the effects of ionising radiation on human prostate cancer cells. Br J Cancer. 2003 Aug 18;89(4):746-53. doi: 10.1038/sj.bjc.6601161.
58. Ma Y, Yu WD, Hershberger PA, Flynn G, Kong RX, Trump DL, Johnson CS. 1alpha,25-Dihydroxyvitamin D3 potentiates cisplatin antitumor activity by p73 induction in a squamous cell carcinoma model. Mol Cancer Ther. 2008 Sep;7(9):3047-55. doi: 10.1158/1535-7163.MCT-08-0243.
59. Hershberger PA, Yu WD, Modzelewski RA, Rueger RM, Johnson CS, Trump DL. Calcitriol (1,25-dihydroxycholecalciferol) enhances paclitaxel antitumor activity in vitro and in vivo and accelerates paclitaxel-induced apoptosis. Clin Cancer Res. 2001; 7(4):1043-51.

60. Hershberger PA, McGuire TF, Yu WD, Zuhowski EG, Schellens JH, Egorin MJ, Trump DL, Johnson CS. Cisplatin potentiates 1,25-dihydroxyvitamin D3-induced apoptosis in association with increased mitogen-activated protein kinase kinase kinase 1 (MEKK-1) expression. Mol Cancer Ther. 2002;1(10):821-9.
61. Segovia-Mendoza M, González-González ME, Barrera D, Díaz L, García-Becerra R. Efficacy and mechanism of action of the tyrosine kinase inhibitors gefitinib, lapatinib and neratinib in the treatment of HER2-positive breast cancer: preclinical and clinical evidence. Am J Cancer Res. 2015 Aug 15;5(9):2531-61.
62. García-Quiroz J, García-Becerra R, Santos-Cuevas C, Ramírez-Nava GJ, Morales-Guadarrama G, Cárdenas-Ochoa N, Segovia-Mendoza M, Prado-Garcia H, Ordaz-Rosado D, Avila E, Olmos-Ortiz A, López-Cisneros S, Larrea F, Díaz L. Synergistic Antitumorigenic Activity of Calcitriol with Curcumin or Resveratrol is Mediated by Angiogenesis Inhibition in Triple Negative Breast Cancer Xenografts. Cancers (Basel). 2019 Nov 6;11(11):1739. doi: 10.3390/cancers11111739.
63. Sun, H.; Zhang, D.; Yao, Z.; Lin, X.; Liu, J.; Gu, Q.; Dong, X.; Liu, F.; Wang, Y.; Yao, N.; et al. Anti-angiogenic treatment promotes triple-negative breast cancer invasion via vasculogenic mimicry. Cancer Biol. Ther. **2017**, 18, 205–213
64. Chiablaem, K.; Lirdprapamongkol, K.; Keeratichamroen, S.; Surarit, R.; Svasti, J. Curcumin suppresses vasculogenic mimicry capacity of hepatocellular carcinoma cells through STAT3 and PI3K/AKT inhibition. Anticancer Res. **2014**, 34, 1857–1864.
65. Chen, L.X.; He, Y.J.; Zhao, S.Z.; Wu, J.G.; Wang, J.T.; Zhu, L.M.; Lin, T.T.; Sun, B.C.; Li, X.R. Inhibition of tumor growth and vasculogenic mimicry by curcumin through down-regulation of the EphA2/PI3K/MMP pathway in a murine choroidal melanoma model. Cancer Biol. Ther. **2011**, 11, 229–235.
66. Hu, A.; Huang, J.J.; Jin, X.J.; Li, J.P.; Tang, Y.J.; Huang, X.F.; Cui, H.J.; Xu, W.H.; Sun, G.B. Curcumin suppresses invasiveness and vasculogenic mimicry of squamous cell carcinoma of the larynx through the inhibition of JAK-2/STAT-3 signaling pathway. Am. J. Cancer Res. **2015**, 5, 278–288.
67. Welsh, J. Vitamin D and Breast Cancer: Mechanistic Update. JBMR Plus **2021**, 5, e10582.
68. Chang, L.C.; Sun, H.L.; Tsai, C.H.; Kuo, C.W.; Liu, K.L.; Lii, C.K.; Huang, C.S.; Li, C.C. 1,25(OH)2 D3 attenuates indoxyl sulfate-induced epithelial-to-mesenchymal cell transition via inactivation of PI3K/Akt/beta-catenin signaling in renal tubular epithelial cells. Nutrition **2020**, 69, 110554.

69. Chen, P.T.; Hsieh, C.C.; Wu, C.T.; Yen, T.C.; Lin, P.Y.; Chen, W.C.; Chen, M.F. 1alpha,25-Dihydroxyvitamin D3 Inhibits Esophageal Squamous Cell Carcinoma Progression by Reducing IL6 Signaling. Mol. Cancer Ther. **2015**, 14, 1365–1375.
70. Kulling, P.M.; Olson, K.C.; Olson, T.L.; Feith, D.J.; Loughran, T.P., Jr. Vitamin D in hematological disorders and malignancies. Eur. J. Haematol. **2017**, 98, 187–197
71. Bajbouj, K.; Al-Ali, A.; Shafarin, J.; Sahnoon, L.; Sawan, A.; Shehada, A.; Elkhalifa, W.; Saber-Ayad, M.; Muhammad, J.S.; Elmoselhi, A.B.; et al. Vitamin D Exerts Significant Antitumor Effects by Suppressing Vasculogenic Mimicry in Breast Cancer Cells. Front. Oncol. **2022**, 12, 918340.

# CAPÍTULO 3.

## DELIMITACIÓN DEL ESTUDIO

## 3.1. RELEVANCIA DEL ESTUDIO

Los agentes terapéuticos actualmente empleados en pacientes con CMTN no han logrado del todo el éxito deseado, por lo que resulta urgente desarrollar terapias más eficaces y económicamente accesibles. La falta de consistencia respecto a lo esperado se debe, en parte, a la poca comprensión que tenemos aún de los mecanismos tumorales de defensa asociados a la angiogénesis. Por ende, es requisito entender mejor la biología de la enfermedad para lograr identificar oportunidades terapéuticas que impacten positivamente en la respuesta clínica. De aquí la importancia de comprender cómo las interacciones celulares per se y después de los tratamientos, desde el modelo de estudio a emplear, generan cambios en los procesos biológicos de supervivencia del tumor.

Por otro lado, el uso de tratamientos multiblanco de baja toxicidad combinados con terapias convencionales representa una ventana de oportunidad, por lo que en este proyecto estudiaremos la combinación de calcitriol con curcumina como propuesta terapéutica adyuvante para incrementar la eficacia y reducir la toxicidad de la quimioterapia convencional.

## 3.2. PREGUNTA DE INVESTIGACIÓN

¿El tratamiento con calcitriol sólo o combinado con curcumina, previene el mimetismo vascular y sus procesos de plasticidad celular celulares asociados en CMTN?

## 3.3.HIPÓTESIS

Debido a sus potentes efectos anti-tumorales y pro-diferenciantes, el calcitriol combinado con curcumina, disminuirá significativamente el mimetismo vascular en CMTN.

## 3.4. OBJETIVOS

- Determinar el efecto del calcitriol combinado con agentes anti-angiogénicos sobre la vascularización tumoral y el mimetismo vascular.

Para alcanzar dicho objetivo, el proyecto se realizó en 3 etapas con sus respectivos objetivos particulares:

- **Establecimiento del modelo de mimetismo vascular en CMTN**
  - Caracterizar el modelo de MV en co-cultivos de las líneas celulares de CMTN, MBCDF-T y HCC-1806, con endotelio, EA.hy926.
  - Identificar la participación de la interacción cáncer-endotelio en el MV del CMTN.
  - Determinar las principales vías de señalización involucradas en el MV del CTMN.
- **Efecto del tratamiento combinado de calcitriol con curcumina sobre el MV en CMTN**
  - Determinar el efecto de la combinación de calcitriol sobre el MV en co-cultivos de MBCDF-Tum o HCC-1806 con endotelio.
  - Determinar el efecto del tratamiento con curcumina sobre el MV en co-cultivos de CMTN y endotelio.
  - Evaluar el efecto de la combinación de calcitriol y curcumina sobre el MV en el modelo de co-cultivos.
  - Identificar las vías de señalización asociadas con la respuesta a los tratamientos solos y en combinación.
- **Efecto del calcitriol combinado con inhibidores de FGFR/VEGFR sobre los procesos asociados al MV y el potencial vasculogénico de células de CMTN**
  - Evaluar el efecto de la combinación de calcitriol con dovitinib o AZD4547 sobre los procesos de plasticidad celular asociados al MV en CMTN (troncalidad y transición epitelio mesénquima).
    - *Evaluar el efecto de los tratamientos, solos o en combinación, sobre la formación de mamoesferas en las líneas celulares de CMTN, MBCDF-Tum y HCC-1806.*
    - *Evaluar el efecto de los tratamientos solos y en combinación sobre la migración celular de las células de CMTN.*
  - Determinar el efecto de la combinación de calcitriol con los inhibidores de VEGFR/FGFR, dovitinib o AZD4547, sobre el MV en CMTN.

## 3.5. DISEÑO EXPERIMENTAL

Para alcanzar los objetivos e cada etapa se establecieron diferentes estrategias experimentales, ilustradas a continuación. Los materiales y métodos de cada etapa se describen al inicio de cada capítulo.

Modelo de mimetismo vascular en CMTN

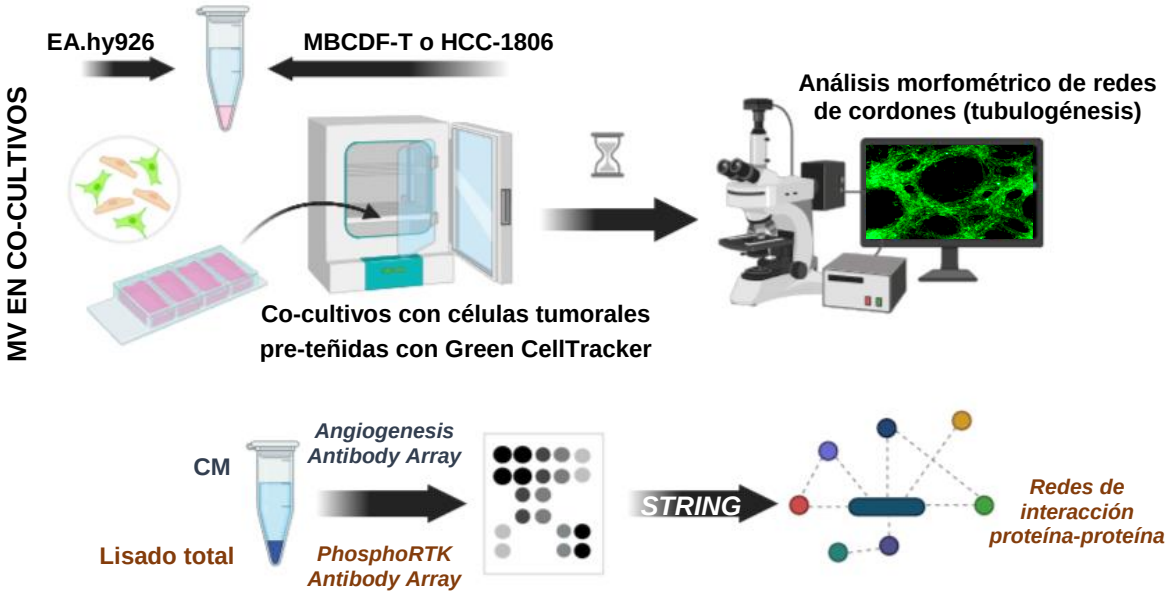


*Ilustración 3. Establecimiento de modelo de MV en co-cultivos y caracterización.*

Se realizaron co-cultivos de dos líneas celulares de cáncer de mama triple negativo, MBCDF-T/HCC-1806 con células endoteliales, EA.hy926. Las células de cáncer se pre-tiñeron con CellTracker para validar el modelo de MV y comprobar que las células de CMTN hacen las redes de cordones. Paralelamente, el secretoma inductor del MV se caracterizó mediante el arreglo en membrana *Angiogenesis Antibody Array* empleando medio condicionado (CM), mientras que las señales implicadas se evaluaron usando el *Phospho RTK Antibody Array* usando lisado total del co-cultivo. Las interacciones resultantes de los blancos obtenidos en este último sirvieron para realizar un análisis de enriquecimiento funcional en STRING y las redes de interacción proteína-proteína.

Efecto de la combinación de calcitriol y curcumina sobre el MV

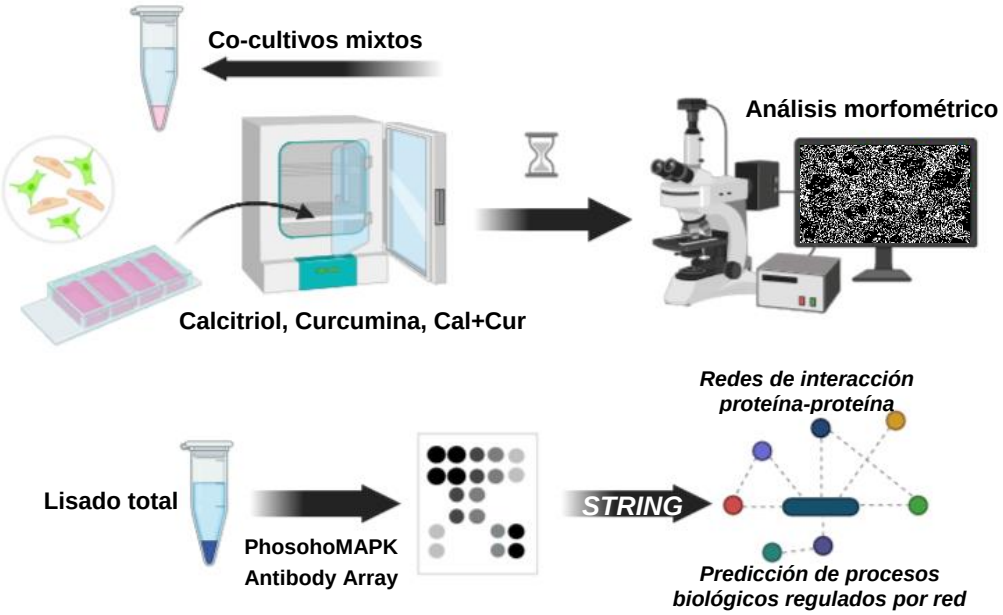


*Ilustración 4. Evaluación del tratamiento combinado de calcitriol y curcumina sobre el MV en cáncer de mama triple negativo.*

Se evaluó el efecto de los tratamientos sobre el MV de igual manera que se describe en la Ilustración 3, en esta etapa el arreglo de anticuerpos empleado fue el PhosphoMAPK antibody array a partir del cual se realizaron redes de interacción proteína-proteína y la predicción de los procesos biológicos regulados por las redes obtenidas en cada grupo de tratamiento.

# PARTE 2.

## GENERACIÓN DE UN MODELO DE MV IN VITRO EN CÁNCER DE MAMA TRIPLE NEGATIVO

# CAPÍTULO 4.

## MIMETISMO VASCULAR EN CO-CULTIVOS DE CÁNCER DE MAMA TRIPLE NEGATIVO Y ENDOTELIO

***Los resultados de este capítulo se presentaron en XXXIII Congreso Nacional de Bioquímica del 16 al 21 de octubre de 2022.***

GABRIELA MORALES-GUADARRAMA, EDGAR ARMANDO MÉNDEZ-PÉREZ, ROCÍO GARCÍA-BECERRA, JANICE GARCÍA-QUIROZ, EUCLIDES AVILA, LORENZA DÍAZ. "VASCULOGENIC MIMICRY OF TRIPLE NEGATIVE BREAST CANCER IS INHIBITED BY CALCITRIOL AND CURCUMIN THROUGH INHIBITION OF PI3K/AKT PATHWAY"

***MANUSCRITO EN PREPARACIÓN***

## 4.1. RESUMEN

La neovascularización es esencial para la diseminación y el crecimiento tumoral. Tumores altamente agresivos, como los del cáncer de mama triple negativo, son capaces de desarrollar su propia red de microcirculación mediante el mimetismo vascular. Sin embargo, el conocimiento respecto al papel de las interacciones celulares entre los componentes no tumorales (estroma/endotelio) y el tumor, siguen poco exploradas. Por ello, evaluamos los efectos del co-cultivo de células endoteliales (EC) (EA.hy926) o estromales (N30) con células de cáncer de mama triple negativo (MBCDF-T, o HCC-1806), o bien de células endoteliales con células estromales de trofoblasto (HTR-8) para conocer mejor la participación de cada linaje celular sobre el mimetismo vascular tumoral o fisiológico (MV). El MV se evaluó por medio de la formación de cordones similares a estructuras tubulares y se diferenció de la angiogénesis al pre-teñir a las células de cáncer, o a las células endoteliales (EC) con un marcador fluorescente y por medio del patrón de expresión/localización de las proteínas VE-cadherina y HK2. La participación del endotelio se estudió por medio de ensayos de expresión de proteínas o RNA, de factores reguladores de la angiogénesis, y la participación de los receptores involucrados con la vascularización se evaluó por medio de la inmunolocalización de FGFR1, su función fue validada mediante la inhibición farmacológica específica del FGFR o PI3K/Akt con las moléculas pequeñas AZD4547 o LY2904002, respectivamente.

## 4.2. MATERIALES Y MÉTODOS

### *CULTIVOS CELULARES*

En este estudio, utilizamos dos líneas celulares CMTN humanas: MBCDF-Tum (MBCDF-T), que se generó a partir de un cultivo celular primario de un carcinoma de mama ductal invasivo TNBC descrito previamente[1] y la línea celular comercial HCC1806 (ATCC). Para el modelo de co-cultivo, utilizamos la línea de células endoteliales humanas EA.hy926 (ATCC CRL-292). Como control, realizamos co-cultivos con células estromales, N30 y trofoblastos HTR-8/SVneo (ATCC).

Todas las líneas celulares se mantuvieron en condiciones de cultivo estándar en medio de mantenimiento DMEM-F12, suplementado con suero fetal bovino al 5% y penicilina 100 unidades/mL, estreptomicina 100 µg/mL. Para los experimentos con tratamientos, se usó medio suplementado con suero fetal bovino despojado de carbón.

- ***Modelo De MV En Co-Cultivos***

Para evaluar las aportaciones del estroma o el endotelio a la capacidad vasculogénica de las células de CMTN, usamos co-cultivos revueltos, donde las células de cáncer se sembraron simultáneamente en presencia de las células endoteliales (proporción 1:1), sobre cubreobjetos de vidrio colocados en placas de  pozos. Los co-cultivos se incubaron en condiciones controladas de cultivo.

  - ***Tubulogénesis en co-cultivos mixtos***

Los co-cultivos se fijaron entre las 24 y 72 horas de co-cultivo, para evaluar la formación de redes de cordones (tubulogénesis) *in vitro*. En diferentes puntos del tiempo, se llevó a cabo el seguimiento visual y registro fotográfico de los cambios en la citoarquitectura del cultivo.

Paralelamente, con el fin de determinar el origen de las células formadoras de túbulos, las células de cáncer se pre-tiñeron con CellTracker verde por 15 minutos, posteriormente se

[1] García-Quiroz J, *et. al.* Synergistic Antitumorigenic Activity of Calcitriol with Curcumin or Resveratrol is Mediated by Angiogenesis Inhibition in Triple Negative Breast Cancer Xenografts. *Cancers*, 2019. 6; 11(11):1739.

despegaron y se sembraron en combinación con las células endoteliales. La tinción inversa, pre-tiñendo las células endoteliales fue llevada a cabo como control. Posteriormente a la fijación de las laminillas, a cada laminilla se le colocó una gota de medio de montaje UltraCruz (SantaCruz) con 40,60-diamidino-2-phenylindole (DAPI) para contrateñir los núcleos de las células. Se realizó el registro fotográfico usando un microscopio de epifluorescencia convencional. Otros controles incluidos fueron co-incubación de la línea celular MBCDF-T con células estromales así como la co-incubación de las células EA.hy926 con trofoblastos, HTR-8.

- ***Co-cultivos medio condicionado***

El medio de cultivo de los co-cultivos (medio condicionado, CM) se recolectaron de diferentes experimentos, y las células en monocultivo (tanto de cáncer como de endotelio) fueron expuestas al mismo por 3 días. Cada 24 horas se llevó a cabo el seguimiento fotográfico de los cultivos para evaluar los cambios morfológicos en las células. El restante del medio de cultivo se empleó para caracterizar el perfil angiogénico del secretoma.

***PERFIL DE EXPRESIÓN DE MEDIADORES DE ANGIOGÉNESIS***

Con la finalidad de identificar la presencia de activadores o inhibidores de la angiogénesis en el secretome de los cultivos, empleamos membranas de arreglos de anticuerpo (*Human Angiogenesis Antibody Array Membranes, Abcam, ab134000)*. Este arreglo permitió la detección y cuantificación de 20 diferentes factores involucrados en la angiogénesis en los CM recuperados previamente. Todas las indicaciones se realizaron de acuerdo a lo recomendado por el fabricante. Las membranas se incubaron toda la noche a 4°C con 1 ml del CM del monocultivo de Cáncer o Endotelio, así como con el CM del co-cultivo de cáncer/endotelio. La señal obtenida por quimioluminiscencia se documentó y analizó empleando el foto-documentador ChemiDoc XRS+ System (BioRad). La comparación semicuantitativa entre las muestras se llevó a cabo empleando el software de análisis ImageLab (BioRad), usando los controles positivos incluidos en cada membrana. Los siguientes factores angiogénicos se midieron en cada una de las muestras: angiogenina (ANG), factor de crecimiento epidérmico (EGF), péptido activador de neutrófilos epiteliales (ENA-78), factor de crecimiento de fibroblastos básico (bFGF), oncogén regulado por el crecimiento (GRO), interferón gamma (IFN-γ), factor de crecimiento similar a la insulina-1 (IGF-1), interleucina- 6 (IL-6), interleucina-8 (IL-8), leptina, proteína quimioatrayente de monocitos-1 (MCP-1), factor

de crecimiento BB derivado de plaquetas (PDGF-BB), factor de crecimiento placentario (PLGF), regulado tras la activación de células T normales expresadas y secretadas (RANTES), factor de crecimiento transformante beta 1 (TGF-β1), inhibidor tisular de metaloproteinasas 1 (TIMP-1), inhibidor tisular de metaloproteinasas 2 (TIMP-2), trombopoyetina, crecimiento endotelial vascular factor A (VEGF) y factor de crecimiento endotelial vascular D (VEGF-D).

Para el análisis, únicamente se tomaron en cuenta los spots en donde hubo señal de quimioluminiscencia, los valores densitométricos obtenidos de cada blanco se categorizaron de acuerdo a sus funciones biológicas (en el caso del arreglo de angiogénesis). Finalmente la comparación visual de las diferencias relativas en los niveles de expresión de cada analito entre las diferentes muestras se representó en un mapa de calor. La medición de cada analito por membrana fue por duplicado y se evaluaron en 2 membranas distintas con diferente CM, por lo que el análisis partió de una n de 4 por cada blanco evaluado.

*RT-QPCR EN CÉLULAS ENDOTELIALES EXPUESTAS A CM*

Para estudiar el efecto de los mediadores angiogénicos en el secretoma sobre el comportamiento y la expresión de las células endoteliales, se sembraron células EA.hy926 en presencia del CM de co-cultivos mixtos durante 24 h. El ARN total se extrajo de las células utilizando Trizol (Life Technologies). Posteriormente, se transcribieron reversamente dos microgramos de ARN usando el sistema de transcripción reversa de Roche (Roche Applied Science). Los ADNc resultantes se diluyeron 1:10 para el análisis por qPCR. Las amplificaciones se realizaron en el LightCycler® 2.0 de Roche (Roche Diagnostics), según el siguiente protocolo: activación de Taq-DNA polimerasa (Roche Applied Science) y desnaturalización del ADN a 95 °C durante 10 min, seguido de 45 ciclos de amplificación que comprenden 10 s a 95 °C, 30 s a 60 °C y 1 s a 72 ◦C. Como control constitutivo de expresión, se empleó la expresión de la gliceraldehído-3-fosfato deshidrogenasa (GAPDH). Los cultivos se sembraron por triplicado y todos los experimentos se repitieron al menos tres veces.

*INMUNOFLUORESCENCIA*

Los co-cultivos mezclados de cáncer/endotelio se co-incubaron por 24 horas antes de ser fijadas y permeabilizadas con la solución Cytofix/Cytoperm (BD Biosciences, San Diego, CA) a 4°C por 15 minutos. Posteriormente, las laminillas se lavaron y se incubaron los

anticuerpos diluídos en Perm/Wash solution (BD Biosciencies). Se emplearon los anticuerpos conejo anti-HK2 (Cell Signaling Technology, dilución 1:400), anti-VEGFR-2 (Cell Signaling Technology, dilución 1:400), conejo anti-FGFR-1 (Cell Signaling Technology, dilución 1:200), ratón anti-VE-cadherina (Santa Cruz Biotechnology, dilución 1:200) o mouse anti-Vimentina (Santa Cruz Biotechnology, dilución 1:200). Tras incubarse toda la noche a 4°C, en ausencia de luz, se realizaron lavados y se incubó en presencia de los anticuerpos secundarios por 2 horas, se emplearon: anti-mouse-Cy3 (Life Technologies Inc, dilución 1:1000) y anti-conejo-FITC (Jackson Immunoresearch, dilución 1:500) a temperatura ambiente. posteriormente se hicieron lavados y se llevó a cabo el montaje con usando el medio UltraCruz (SantaCruz) con DAPI. El registro fotográfico se llevó a cabo usando un microscopio de epifluorescencia convencional.

*INHIBICIÓN FARMACOLÓGICA DE FGFR/PI3K*

El efecto funcional de la señalización dependiente de FGFR o PI3K/Akt sobre el MV se evaluó mediante la inhibición farmacológica de FGFR o PI3K. Para ello se trató a los co-cultivos con N-(5-(3,5-dimetoxifenetil)-1H-pirazol-3-il)-4-((3S,5R)-3,5-dimetilpiperazin-1-il) benzamida, AZD4547 (AstraZeneca), (Santa Cruz Biotechnology Inc), un inhibidor específico de FGFR1, FGFR2 y FGFR3, o bien con un inhibidor específico de PI3K, LY294002 (Calbiochem, SigmaAldrich), que inhibe la señalización PI3K/Akt. Su efecto sobre el MV se evaluó por medio de tubulogénesis en co-cultivo, tras 3 días de co-incubación se contabilizó la cantidad de segmentos por grupo de tratamiento; los segmentos se definieron como los cordones de células en la red formada por las células de CMTN. Las concentraciones usadas para dicho efecto fueron de 3µM (LY294002) y 5µM (AZD4547). Los experimentos se repitieron por triplicado y se tomó el registro fotográfico de cada uno, al final se analizaron de 8 a 10 imágenes por tratamiento y fueron contabilizados por 3 observadores distintos.

*PERFIL DE FOSFORILACIÓN DE RTK*

Para evaluar la respuesta de la inhibición específica de FGFR en las cascadas de señalización, se empleó un arreglo de anticuerpos de las fosforilaciones de distintas cinasas de tirosina, (*Human Phospho-RTK Antibody Array, Abcam,* ab193662). Se emplearon 500µg de lisados celulares de co-cultivos, provenientes de dos experimentos diferentes. Las incubaciones se realizaron como indica el fabricante. Este arreglo identifica 71 fosforilaciones

de las siguientes cinasas de tirosinas: ALB1, ACK1, ALK, Axl, Blk, BMX, Btk, Csk, Dtk, EGFR, EphA1, EphA2, EphA3, EphA4, EphA5, EphA6, EphA7, EphA8, EphB1, EphB2, EphB3, EphB4, EphB6, ErbB2, ErbB3, ErbB4, FAK, FER, FGFR1, FGFR2, FGFR2 (α isoform), Fgr, FRK, Fyn, Hck, HGFR, IGF-I R, Insulin R (CD220), Itk, JAK1, JAK2, JAK3, LCK, LTK, Lyn, MATK, M-CSFR, MUSK, NGFR (TNFRSF16), PDGFR-α, PDGFR-β, PYK2, RET, ROR1, ROR2, ROS, RYK, SCF R (CD117/c-kit), SRMS, SYK, Tec, Tie-1, Tie-2, TNK1, TRKB, TXK, Tyk2, TYRO10 (DDR2/TKT), VEGFR2, VEGFR3, ZAP70.

Para el análisis, todo fue igual que para el arreglo de angiogénesis. La comparación visual de los niveles de expresión/fosforilación de cada analito se representó en un mapa de calor. Ya que el lisado total analizado se obtuvo del co-cultivo mezclado, se realizó una búsqueda en la plataforma Human Protein Atlas (https://www.proteinatlas.org/), para categorizar el perfil de expresión asociado a cada estirpe celular, al para predecir qué célula (endotelial o con origen mamario) estaría expresando cada uno de estos blancos.

Finalmente, para entender más la implicación de dichos perfiles, con o sin la inhibición de FGFR, se elaboraron redes de interacción proteína-proteína, mediante un análisis de enriquecimiento funcional en STRING (https://string-db.org/), que predice las interacciones físicas y funcionales de un *input* de proteínas determinadas y arroja los procesos biológicos en los que los nodos de cada red participan en las células.

### *ANÁLISIS ESTADÍSTICO*

Las representaciones gráficas mostradas y los análisis estadísticos se realizaron en el software GraphPad Prism 7, para determinar si la expresión en endotelio, o si los efectos de los tratamientos tenían diferencias significativas respecto a los controles se realizó ANOVA de una vía y t-student en casos específicos. Se consideraron diferencias significativas cuando la $p \leq 0.001$. Las gráficas de barra muestran promedios ± error estándar.

## 4.3. RESULTADOS

De manera clásica, se sabe que las señales enviadas por el tumor al microambiente contribuyen a la formación de nuevos vasos sanguíneos. Sin embargo, de manera paralela, el endotelio puede regular el comportamiento del estroma y las propias células del tumor mediante la producción parácrina de factores pro-angiogénicos [1, 2]. Para determinar si estas comunicaciones contribuyen en el mimetismo vascular del CTMN, empleamos co-cultivos de

endotelio o estroma con cáncer (CMTN) y el MV se evaluó por medio de la formación de cordones (tubulogénesis) en los co-cultivos.

***El endotelio induce el mimetismo vascular tumoral y fisiológico in vitro.***

Inicialmente, las células MBCDF-T se co-cultivaron con células EA.hy926 en medio de mantenimiento. Tras 24 horas de co-incubación se identificó la presencia de dos planos focales caracterizados por la formación de redes de cordones formadas por células fusiformes alargadas y, al fondo del cultivo, una población de células con núcleos grandes y de alta adhesión a la superficie de cultivo parece fungir como soporte de las células formadoras de redes (Figura 1).

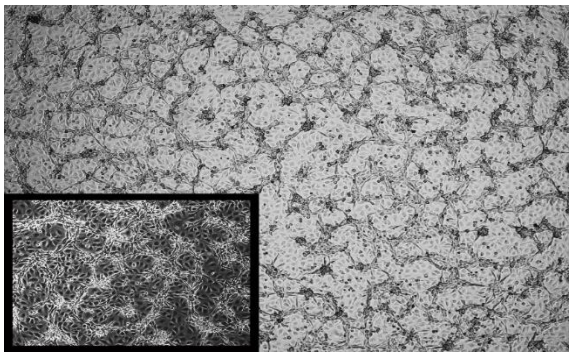

*Figura. 1. Formación de redes de cordones en co-cultivos de células de CMTN con endotelio en 4x y acercamiento en 10x.*

Este resultado nos permitió identificar la tubulogénesis en co-cultivos de cáncer/endotelio. Sin embargo, para corroborar que se trataba de mimetismo vascular, y no de tubulogénesis endotelial, realizamos co-cultivos donde las células de cáncer fueron previamente teñidas con un marcador permeable (GreenCellTracker™) para distinguir al componente celular encargado de formar las redes. Como control teñimos a las células de CMTN, MBCDF-T en monocultivo (Figura 1a).

De manera interesante, cuando pre-teñimos y co-cultivamos dos diferentes líneas células de CMTN, MBCD-F o HCC-1806, con endoteliales, identificamos que son exclusivamente las células tumorales quienes se encuentran involucradas en la formación de las redes de cordones, como se observa en la Figura 1b. Este resultado demostró que nuestro modelo efectivamente refleja la capacidad tubulogénica de las células de cáncer, la cual es el parámetro estándar *in vitro* de las células capaces de hacer MV.

No obstante para descartar que una parte del modelo incluyera tubulogénesis endotelial, el principal modelo de angiogénesis *in vitro*, realizamos co-cultivos

cáncer/endotelio, pre-tiñendo ahora a las EC, EA.hy926. En el panel de la Figura 1c, se muestra como no sólo no participan en la estructura de las redes, sino que se encuentran debajo de las células de cáncer, a manera de andamio para la formación de las redes.

Una de las características que observamos en las células formadoras de red fue su particular morfología fusiforme, nos preguntamos si algo en el secretoma de estos co-cultivos tenía un efecto sobre la morfología y el comportamiento de las células de cáncer, así que cultivamos a las células en presencia del medio condicionado (CM) del co-cultivo y

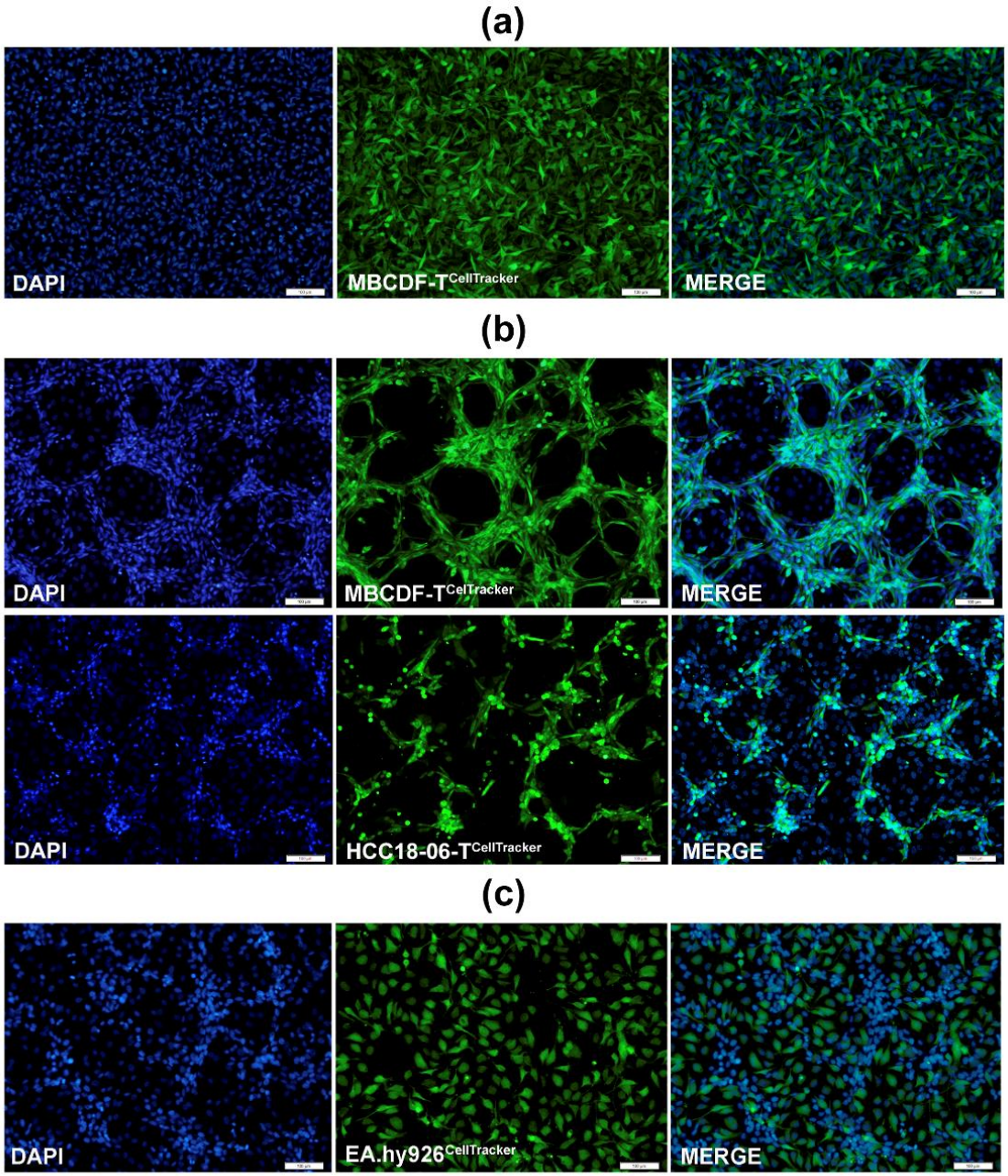

*Figura 1 El co-cultivo con células endoteliales induce mimetismo vascular in vitro en CMTN.* (a) Las células de cáncer MBCDF-T o HCC-1806, o de endotelio, fueron pre-teñidas con Green CellTracker™ antes de co-incubarse para identificar a las células formadoras de redes de cordones. Los núcleos fueron contrastados con DAPI, para observar las células restantes del co-cultivo. (b) Control de monocultivo de CMTN, se observa la ausencia de redes de cordones en MBCDF-T. Aumentos en 10x.

observamos que la presencia de estas células fusiformes aumentó radicalmente, incluso llegando a encontrarse ciertas células acomodadas a manera de "canal" en el co-cultivo con CM sin que se identifiquen estructuras tridimensionales o planos focales distintivos (Figura 33a). Son precisamente las células con estas características morfológicas las que parecieran enriquecerse y encontrarse en los co-cultivos mixtos con endotelio, formando las redes de cordones (Figura 33b). Para respaldar que el efecto es dependiente de endotelio, co-cultivamos en las mismas condiciones a las células de CMTN con células de estroma, en co-

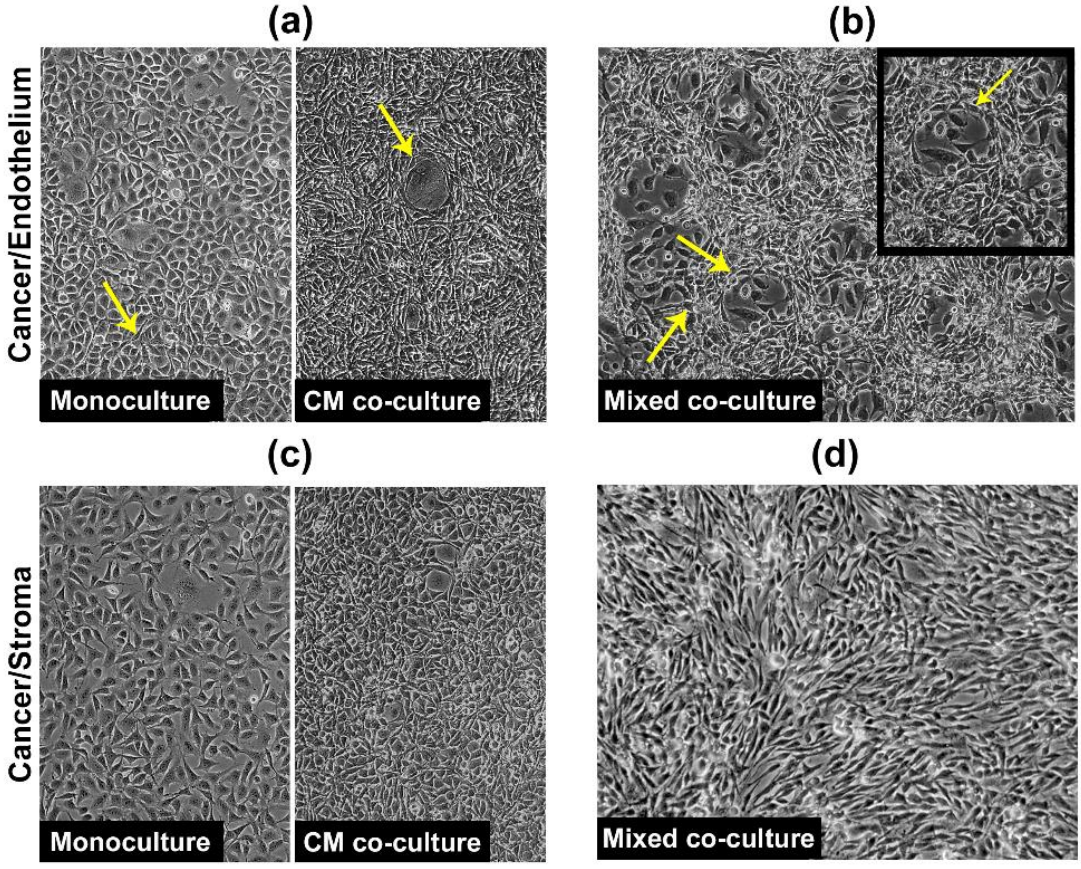


*Figura 3. Co-cultivo con células endoteliales induce mimetismo vascular in vitro en CMTN.* (a) Las células de cáncer MBCDF-T en monocultivo y en presencia del medio condicionado (CM) del co-cultivo. Se observa un claro aumento de células fusiformes, señaladas por una flecha amarilla. (b) Co-cultivos mixtos de cáncer y endotelio, las flechas señalan las células fusiformes distinguibles encargadas de formar las redes de cordones. Fotografías en campo claro, aumentos en 10x y 20x.

cultivos mixtos o de CM (Figura 33c, d). Sin embargo, ni el secretoma ni las interacciones célula-célula indujeron la formación de redes en los co-cultivos, corroborando el papel del endotelio en el MV. Lo anterior sugiere, que la participación parácina de señales que favorecen el cambio en la morfología y el comportamiento de las células de cáncer, las cuales parecieran estar haciendo algún tipo de transición fenotípica. A su vez, sugiere que son necesarias tanto las señales parácrinas como yuxtacrinas para el MV de las células de CMTN, pues sin la comunicación célula-célula entre cáncer/endotelio, la formación de las redes no se da de manera eficiente.

Con lo anterior y para finalizar la validación de la inducción de MV por el endotelio, en co-cultivos, probamos si el endotelio también era capaz de inducir el MV en células no tumorales. En condiciones fisiológicas, durante la vascularización de la placenta existe un mimetismo vascular fisiológico, en el cual las células gigantes trofoblásticas forman canales sanguíneos en la placenta y adquieren características similares al endotelio [3]. Por ello, co-incubamos células EA.hy926 con células trofoblásticas, HTR-8, y encontramos que a los 6 días de co-cultivo, se observa la formación de redes tubulares en el co-cultivo endotelio/trofoblastos, confirmando que el endotelio no sólo estimula el MV tumoral, sino también el fisiológico (Figura 4).

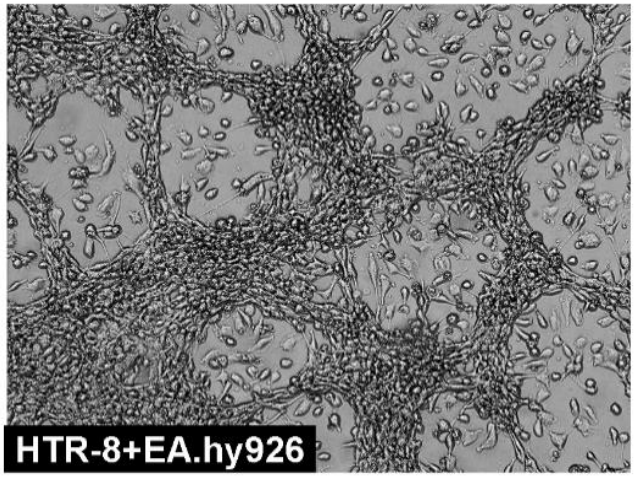


*Figura 4. El endotelio induce el MV fisiológico en co-cultivos con HTR-8.* Imagen representativa de co-cultivos de 6 días de trofoblastos (HTR-8) con células endoteliales, EA.HY926. Se observan los dos planos focales característicos del modelo de MV de co-cultivos donde una subpoblación celular se encuentra organizada en redes de cordones. Aumento 10x.

***El endotelio induce un microambiente pro-angiogénico en co-cultivos con CMTN.***

Como se mostró en la Figura 3, la exposición al CM de co-cultivo indujo cambios morfológicos en las células de CMTN, sin embargo la comunicación entre estos dos

componentes celulares puede ser bidireccional. Por ello quisimos explorar el efecto del mismo CM sobre la morfología/comportamiento del endotelio, sembramos las células EA.hy926 en presencia del CM de co-cultivo, como se muestra en la Figura 5a cuando las células se exponen al CM, cambian su morfología y comportamiento, puesto que se logran identificar dos planos focales con células morfológicamente distintas. En el acercamiento mostrado en el panel de Figura b, observamos células formadoras de cordones, que si bien no alcanzan la tridimensionalidad, si se presentan cambios en su polaridad. Además, al fondo del cultivo, se distinguen una subpoblación de células grande similares a las que se observan enriquecidas en el co-cultivo mixto cuando están con las células de cáncer. Este resultado nos indica que el secretoma producido en conjunto por las células de cáncer y endotelio tiene potentes efectos pro-angiogénicos en el endotelio, y de pro-MV en las células tumorales.

Para identificar si el co-cultivo efectivamente afecta la composición del secretoma, evaluamos la presencia de moléculas mediadoras de la angiogénesis en los monocultivos de cáncer y endotelio, así como en el co-cultivo, por medio de arreglos de anticuerpos sobre membrana. Como se muestra en el mapa de calor (Figura c) el monocultivo de cáncer no presentó, al menos en niveles detectables para esta técnica, ninguna de las moléculas evaluadas en el arreglo de anticuerpos. Sin embargo el CM de endotelio presentó un balance: tanto una gran variedad de moléculas pro-angiogénicas: IL-8, MCP-1, GRO, PlGF, como una gran abundancia de inhibidores de la angiogénesis, TIMP-1, TIMP-2. En contraste, cuando se encuentran ambas líneas en co-cultivo, las moléculas pro-angiogénicas aumentan drásticamente, principalmente IL-6 e IL-8 y PlGF, mientras que las anti-angiogénicas disminuyen, sugiriendo un desequilibrio entre ambos reguladores y promoviendo un ambiente pro-angiogénico.

Lo anterior se reforzó cuando cultivamos las células endoteliales en presencia del CM y evaluamos la expresión a nivel de RNA de diversas proteínas involucradas en la respuesta angiogénica: VEGFR2, FGFR1, HK2, VEGF-A y TSP-1 (Figura d). Interesantemente, observamos que el CM induce un aumento significativo de las moléculas pro-angiogénicas, especialmente de VEGF-A, mientras que disminuye significativamente el anti-angiogénico TSP-1. En conjunto estos resultados sugieren que el endotelio participa de manera importante en el establecimiento de un microambiente tumoral pro-angiogénico capaz de regular la

tubulogénesis en el endotelio por sí solo, y en las células de CMTN cuando se encuentran en co-cultivo.

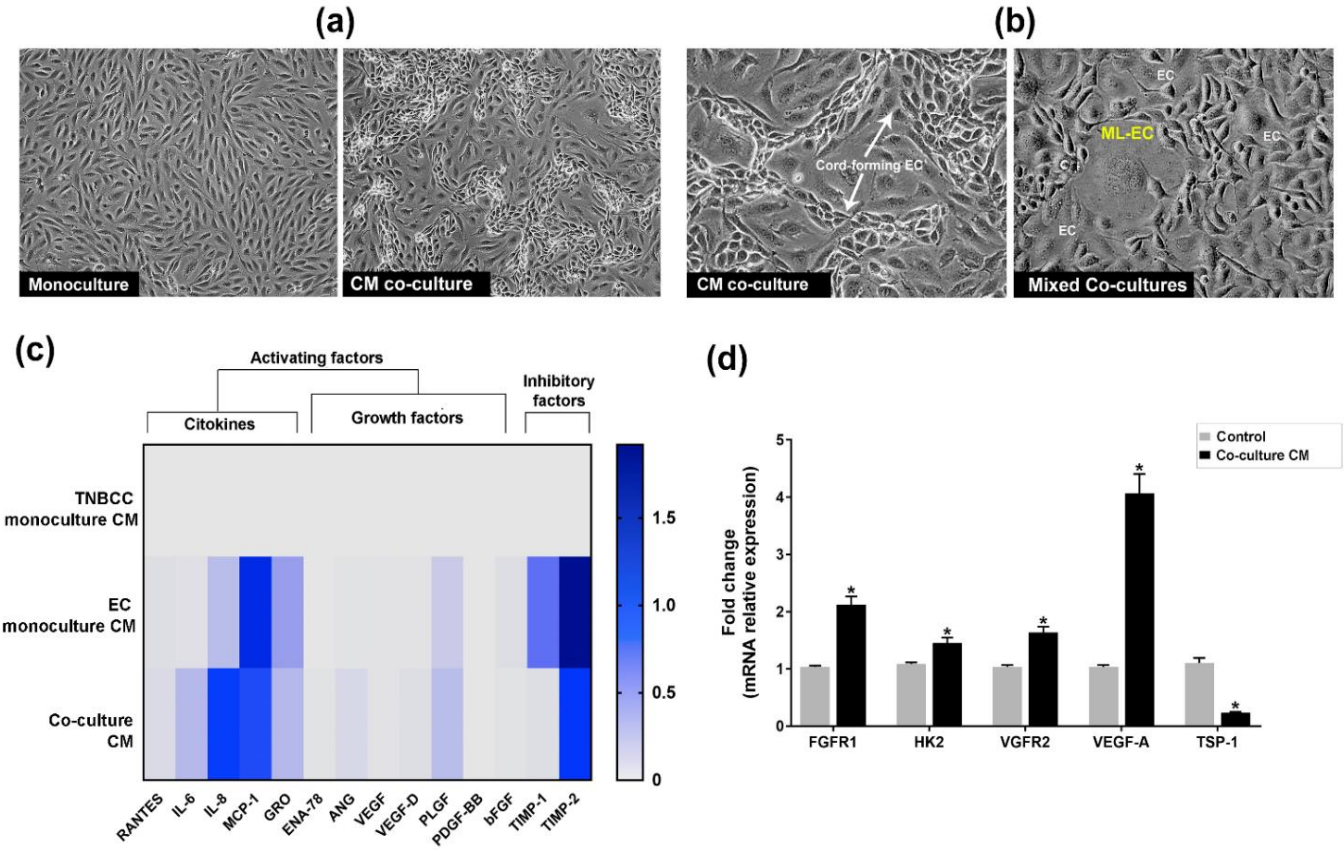


*Figura 5. Las células endoteliales inducen un secretoma pro-angiogénico capaz de regular la tubulogénesis endoteliales y tumoral.* (a) Las células de endotelio EA.hy926 en monocultivo y en presencia del medio condicionado (CM) del co-cultivo. Se observa la formación de cordones en el co-cultivo con CM. (b) Las células endoteliales formadoras de cordones desaparecen en el co-cultivo mixto con cáncer, favoreciendo la presencia de células endoteliales similares a mesénquima (ML-EC like). (c) Perfil de moléculas mediadoras de la angiogénesis en medio condicionado de monocultivos de cáncer y endotelio y de co-cultivo. (d) Expresión relativa de mediadores de la angiogénesis en células endoteliales expuestas a MC, las barras muestran el promedio ± error estándar. Con * se representan las diferencias estadísticas respecto al control de 3 experimentos diferentes con sus respectivos triplicados, $p \leq 0.01$

### *El MV de las células de CMTN es independiente de VE-cadherina*

Uno de los marcadores clásicos, propuestos, para identificar las células capaces de hacer el MV es la cadherina de endotelio vascular, VE-cadherina. Por otra parte, uno de los principales cambios metabólicos en las células durante la angiogénesis es un swich metabólico pro-glucolítico, donde la hexocinasa 2, HK-2 juega un papel esencial. La inmunolocalización de

estos dos marcadores se evaluó en los co-cultivos de cáncer y endotelio y en sus monocultivos. Por separado, las células endoteliales presentan una baja expresión de HK2, y una fuerte expresión de la VE-cadherina, principalmente localizada en la membrana celular (Figura 6a). Mientras, las células MBCDF-T, expresan abundantemente HK2 con un patrón de localización núcleo/citoplasma bien definido, mientras que también expresan, de forma aberrante, a VE-cadherina (Figura 6b). En co-cultivo, se observó un aumento de VE-cadherina aumenta en el citoplasma, de las células endoteliales, mientras HK-2 incrementó en núcleo y la región perinuclear; en contraste, las células de cáncer mantienen su expresión de HK-2 pero prácticamente pierden la expresión de VE-cadherina (Figura 6c).

***Papel funcional de FGFR/PI3K/Akt en el MV en co-cultivos de CMT***

Otro de los receptores de gran importancia en la respuesta angiogénica es el receptor de los factores de crecimiento de fibroblasto (FGFR). Evaluamos por inmunofluorescencia el estado de expresión/localización del FGFR1 y FGFR2, en los co-cultivos de MBCDF-T y EA.hy926. Como se observa en la  (Figura 7a), FGFR1 se encuentra principalmente expresado por las células de cáncer, formadoras de redes de cordones, por su parte las células endoteliales presentan una alta expresión de Vimentina. Sin embargo, en el acercamiento del lado derecho se muestra cómo, al observar de cerca, es notable que algunas células endoteliales presentan expresión del FGFR1, con un patrón de localización granulado en el interior del citoplasma, siendo mayor en aquellas células más cercanas a las células de cáncer (Figura  7 derecha). Un patrón similar fue observado en la expresión/localización de FGFR2, el cual se observa en mayor proporción en las células de la red, donde vimentina está prácticamente ausente, mientras que en las células endoteliales podemos observar que cuando están cercanas a la red, algunas presentan expresión del receptor con localización nuclear/perinuclear (Figura 7b).

El peculiar perfil de expresión de los receptores de FGFR en las células capaces de hacer MV nos llevó a preguntarnos si las señales mediadas por éste son de importancia en el MV, ya que el papel funcional de estos receptores a la fecha permanece sin explorarse en el MV del CMTN. Entre las varias vías de señalización que son reguladas por la activación del FGFR, la vía de PI3K/Akt es una de las que mayor participación ha tenido en el MV y procesos asociados al MV (como la EMT), en tumores como pulmón y glioblastoma [4].

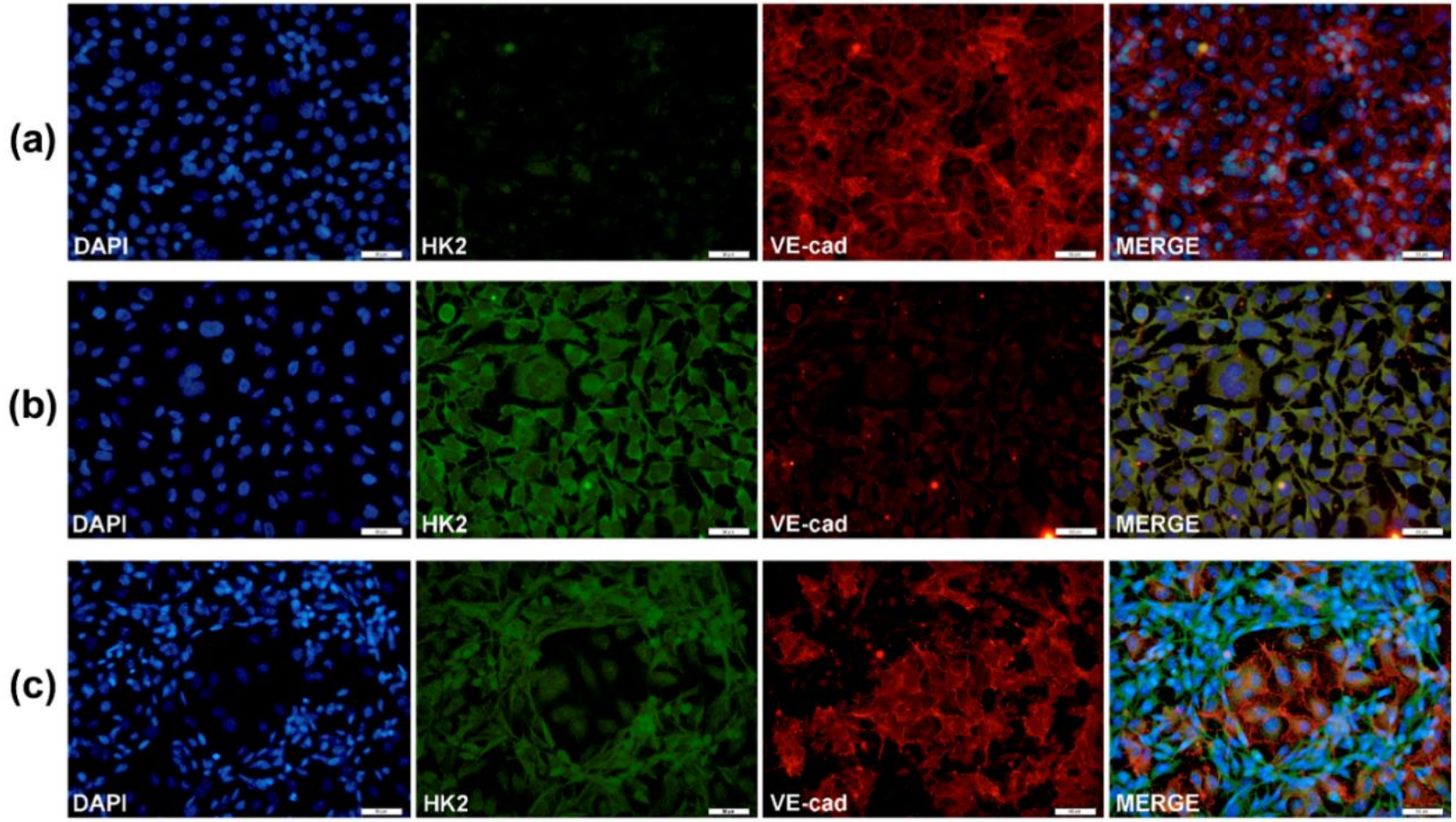


*Figura 6 Inmunolocalización de la hexocinasa 2 (HK2) y la cadherina de endotelio vascular (VE-cad) en monocultivos de endotelio (a), cáncer (b) y co-cultivos de cáncer/endotelio (c).* Inmunofluorescencias (IF) contra HK2, VE-cadherina en monocultivos y co-cultivo cáncer/endotelio, los núcleos se contratiñieron con DAPI. Imágenes representativas de cada grupo, en microscopia de epifluorescencia. Aumento 20x.

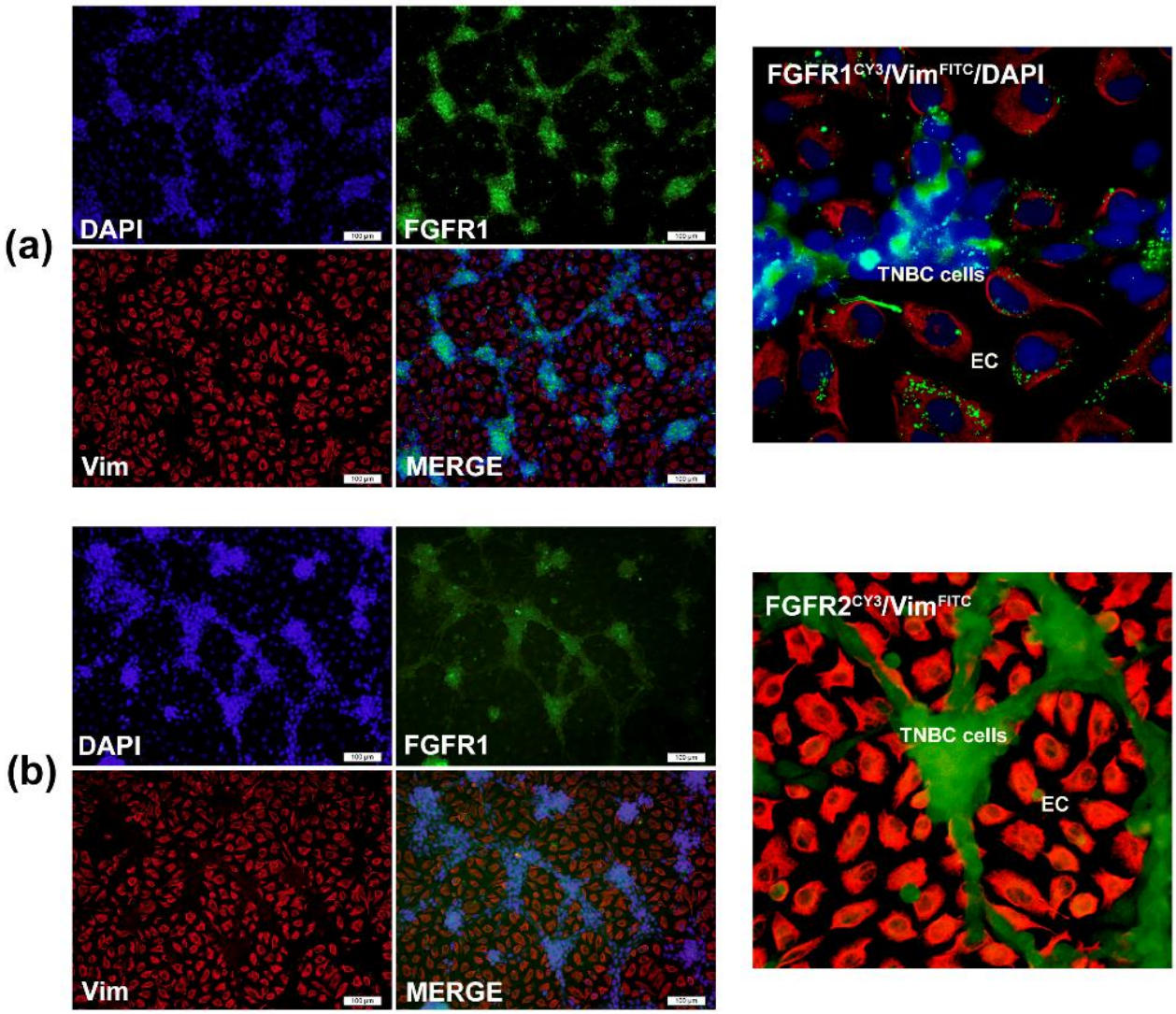


*Figura 7. Inmunolocalización de FGFR1 en co-cultivos de cáncer/endotelio.* IF contra FGFR1 y Vimentina (a) en co-cultivos cáncer/endotelio. Aumento 10x (izq.) y 40x (der), núcleos contrateñidos con con DAPI. IF contra FGFR2 y Vimentina (b) en co-cultivo de cáncer/endotelio. Aumentos 10x (izq.) y 40x (derecha, sin DAPI).

Por ello, decidimos evaluar la implicación de la activación de este eje sobre la capacidad de MV de los co-cultivos de CMTN, mediante la inhibición farmacológica de FGFR y PI3K/Akt, empleando inhibidores específicos de FGFR y PI3K, AZD4547 y LY294002 respectivamente. Como se muestra en la Figura 8a, la inhibición farmacológica tanto de FGFR como de PI3K inhibe drásticamente el MV en los co-cultivos, las redes formadas al cabo de 3 días de exposición son prácticamente nulas. Sin embargo, dicho efecto es aún más drástico con el tratamiento de con AZD4547 en ambas líneas celulares (Figura 8b), no obstante, no hay diferencia entre inhibidores, reforzando la participación del eje FGFR/PI3K/Akt en el MV.

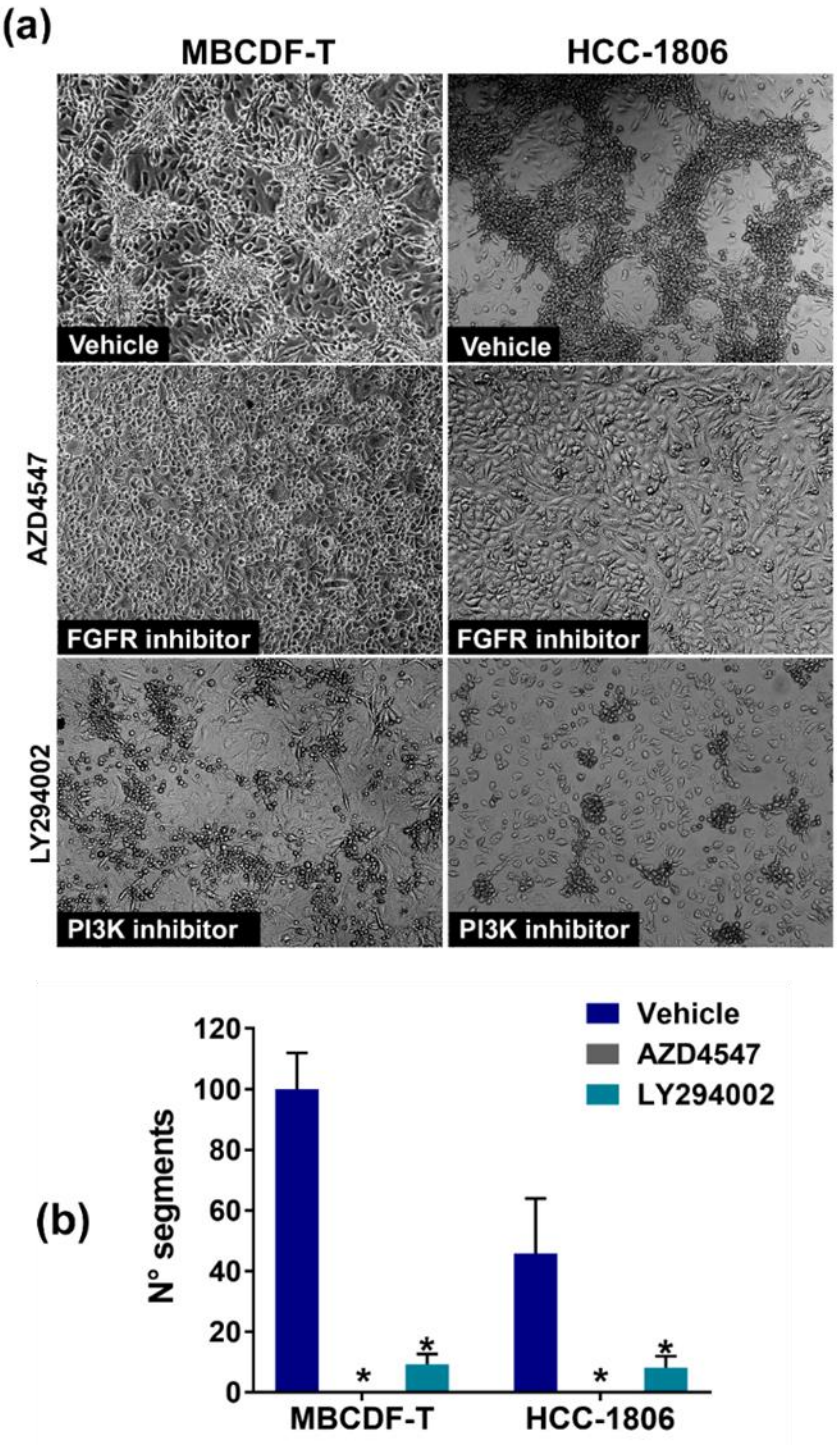


*Figura 8. La inhibición farmacológica de FGFR o PI3K inhibe el MV en co-cultivos de CMTN y endotelio.* (a) Imágenes representativas de los co-cultivos en presencia de los inhibidores de FGFR (AZD4547) o de PI3K (LY294002), tras 3 días. Imágenes obtenidas en campo claro, aumento 10x. (b) Número de segmentos por campo visual. Experimento realizado por triplicado. Las barras muestran el promedio ± error estándar. Diferencias significativas con * ($p \leq 0.001$).

.

***La señalización FGFR/PI3K/Akt involucra la participación de cinasas de tirosina no receptoras que participan en la diferenciación, comunicación celular y la producción de citosinas.***

Cabe destacar que la línea celular MBCDF-T tiene mayor potencial para hacer MV, al formar mayor cantidad de estructuras, en comparación con la línea HCC-1806, a pesar de ser del mismo fenotipo tumoral. Con lo anterior, decidimos evaluar, a partir de lisados celulares totales de MBCDF-T en co-cultivos (48h) con o sin AZD4547, el efecto de la inhibición de FGFR sobre la señalización celular mediada por fosforilaciones.

Como se muestra en la Figura 9a, de manera basal las principales cinasas fosforiladas son Ack1, Blk, Fyn, Lck, Lyn, Syk, las cuales disminuyen drásticamente en presencia del AZD4547 a excepción de Lyn la cual aumentó drásticamente. De manera interesante, hubo un aumento de la fosforilación de varias de las cinasas detectadas por el arreglo, dentro de las que tuvieron un mayor aumento, respecto al vehículo se encontró a Csk, Hck, EphB2, EphB4 y los receptores VEGFR2 y VEGFR3. El perfil obtenido proviene de la mezcla de células endoteliales y tumorales, para intentar entender mejor los fenómenos que se llevan a cabo en cada componente celular, se llevó a cabo un análisis a partir de datos proteómicos de tejido mamario en el Human Protein Atlas, para predecir qué tipo celular podríamos esperar que exprese cada una de las cinasas identificadas (Figura 9b). Encontramos que Ack1, Blk, Syk, Lyn, Lck y ZAP70, cuya fosforilación disminuyó una vez que se inhibió farmacológicamente a FGFR, es más probable que se expresen en las células de mama, así como Csk, EphB4, FAK cuya fosforilación aumentó en presencia del inhibidor AZD4547. Esto sugiere la posible participación de dichas proteínas en los en los procesos que posibilitan que las células de cáncer de mama lleven a cabo el MV. Para identificar dichos procesos, se realizó la predicción de las redes de interacción proteína-proteína en STRING, y de los procesos asociados a dichas redes. Como se muestra en las redes de Figura 9d, Figura 9e, los procesos biológicos en las células de mama incluyen diferenciación celular, regulación de las comunicaciones celulares, regulación de la actividad de cinasas y la producción de citosinas. Por otra parte, en endotelio esperaríamos encontrar reguladas a las proteínas Hck, EphB2 y KDR estarían involucradas en la diferenciación celular, la regulación positiva de la proliferación y la regulación de adhesiones celulares como se puede observar en los paneles b y c de la Figura 9.

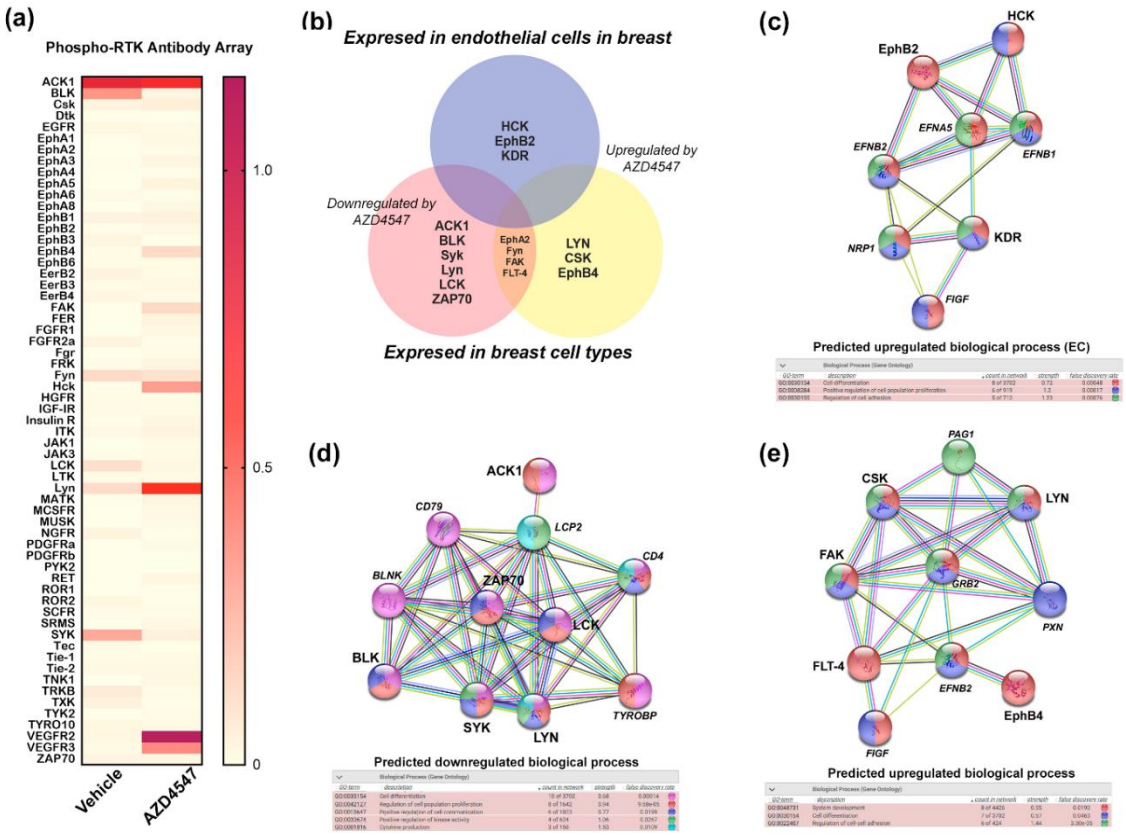


*Figura 9. Participación de FGFR/PI3K/Akt en las señalizacion involucrada con el MV en el modelo de co-cultivos en CMTN.* (a) Mapa de calor de los perfiles de fosforilación de los blancos detectados por el Human Phospho-RTK Antibody Array. (b) Las fosforilaciones con fold change mayor o menor a 0.5 se separaron para subclasificar los patrones de fosforilaciones de acuerdo al tipo celular que podría expresarlo en la mama (análisis realizado en el Human Protein). En el círculo azul, las proteínas cuya fosforilación aumentó con AZD4547 que se predice estarían expresadas principalmente en el endotelio. En amarillo, las que esperaríamos encontrar en las cpelulas de origen mamario, en rosa aquellas que se esperarían en el mismo tipo celular y cuya fosforilación disminuyó drásticamente. Al centro, las proteínas que cualquiera de los dos componentes podría expresar, que se regularon diferencialmente con el tratamiento con AZD4547. (c) Red de interacciones proteínas-proteína de los blancos regulados por AZD4547 al alta en endotelio. (d) Red de interacciones de las proteínas cuya fosforilación disminuyó en presencia del AZD454}.

## 4.4. DISCUSIÓN

La vascularización tumoral es esencial para su supervivencia y diseminación a distancia, ahora conocemos de diversos procesos por los cuales el tumor logra mantener el suministro de oxígeno y nutrientes al interior del tumor, tal como en el mimetismo vascular. En este estudio desarrollamos un modelo de co-cultivos que permite recrear el mimetismo vascular tumoral, así como la participación de cada uno de los componentes celulares. Si bien este tipo de aproximaciones experimentales han sido evaluadas ampliamente por otros en co-cultivos con trofoblastos, que son las encargadas del mimetismo endotelial fisiológico [5-7], o con cultivos primarios/tumoresferas para evaluar la angiogénesis, hasta ahora ninguno se había enfocado en el mimetismo vascular del cáncer [8]. Resulta importante tener esto en cuenta pues varias de las condiciones del microambiente, como la EMC, los componentes del secretoma, las interacciones célula-célula, son esenciales para la angiogénesis, y así mismo para el MV y sus procesos asociados.

Previamente se ha reportado que en co-cultivos en pozos tipo transwell, la angiogénesis es dependiente de la secreción de factores pro-angiogénicos, la concentración de la matriz y la duración de los co-cultivos [8]. En contraste, nosotros observamos que precisamente además de estos tres puntos esenciales, la comunicación yuxtácrina entre cáncer y endotelio, es de suma importancia para la formación de las redes de cordones por parte de las células de cáncer y no las de endotelio *in vitro*. Esto es consistente además con el fenómeno observado en la Figura , en donde vimos que cuando las células endoteliales son co-cultivadas en medio condicionado pero sin interacción espacial con el cáncer, un fenotipo angiogénico comienza a diferenciarse dentro de éstas células. Sin embargo, al entrar en contacto y comunicación directa con las células de CMTN, dicho fenotipo se inhibe dando paso a la tubulogénesis controlada por las células tumorales. Esto sugiere que de alguna manera, el endotelio en co-cultivo podría estarse autorregulando e inhibiendo sus características fenotípicas angiogénicas, pero manteniendo las características pro-angiogénicas del microambiente para estimular la plasticidad celular que observamos en los co-cultivos al incrementarse la población de células tumorales fusiformes, formadoras de redes. Es posible que las interacciones célula-célula entre el endotelio y el cáncer, mantengan la producción de matriz así como de factores pro-angiogénicos.

Observamos también que en endotelio, hay un aumento de la expresión relativa de VEGF y VEGFR2, que además también se encuentra altamente expresado en las células de cáncer formadoras de redes, más que en las endoteliales. Ambas moléculas se han asociado con la participación de las células troncales de cáncer en la inducción del secretoma pro-angiogénico, donde al encontrarse en una matriz ideal, producen moléculas pro-angiogénicas y estimulan la expresión del VEGFR2 en las células troncales. Sin embargo, cuando esta matriz cambia en su composición (p.e. aumentando la concentración de colágeno tipo I) se da un efecto inhibitorio sobre la proliferación y la formación de redes de MV [8].

Cuando caracterizamos el perfil de moléculas reguladoras de la angiogénesis, identificamos la presencia en abundancia de MCP-1, IL-8 e IL-6, estas tres moléculas han sido estudiadas previamente por su participación en el MV [8–10] y el "establecimiento del nicho vascular tumoral" [8]. Entre estas asociaciones, se ha reportado que la IL-6 del endotelio aumenta tras el tratamiento con cisplatino, no así el IL-6 de las células de cáncer de mama MDA-MB-231 y que además, al exponer a las células al CM del endotelio rico en IL-6, hay un aumento significativo en el MV de las células de CMTN en comparación con el CM de las células endoteliales no tratadas (con bajos niveles de IL-6) [9]. En este mismo modelo celular, se ha visto también la importancia de IL-8/CXCR2 sobre el MV, al identificarla como uno de las vías relevantes en el MV del CMT [10]. Esto nuevamente refuerza la importancia de las comunicaciones celulares a la hora de estudiar las respuestas a las terapias, pues constantemente nos enfocamos exclusivamente en uno de los componentes celulares, el cáncer, dejando de lado la importancia de las células con las que interactúa en el nicho tumoral.

A la fecha no existen biomarcadores estándar para el MV, pues es altamente dependiente del tiempo en el que se observe, el modelo, el tipo de cáncer, entre otros factores. Si bien encontramos que las células de cáncer de mama MBCDF-T, expresan basalmente VE-cadherina. Varios grupos han reportado que la expresión extra-vascular de la VE-cadherina en algunos tipos de cáncer, se asocia con el MV, la presencia de células troncales tumorales, y la transdiferenciación celular, por lo que dicho patrón de expresión se ha sugerido como marcador del MV [11]. Sin embargo, nos llamó la atención ver que en los co-cultivos, durante la formación de las redes de cordones, dicha expresión disminuye casi desapareciendo.

En contraste con lo anterior, observamos una gran expresión de los receptores FGFR1 y FGFR2 en las células tumorales formadoras de MV, y en menor proporción en las células endoteliales cercanas a las redes. Los FGFRs, son cinasas de tirosina transmembranales que contienen dos o tres dominios similares a inmunoglobulinas extracelulares y una secuencia de unión a heparina extracelular; su especificidad por varios ligandos se ve alterada por procesos que crean múltiples isoformas, las cuales pueden expresarse en las células epiteliales (isoformas IIIb) o bien en células mesénquimales (isoformas IIIc) donde median las interacciones tisulares en el desarrollo normal y la cicatrización de heridas [12]. Su señalización es una vía importante en la tumorigénesis y la angiogénesis tumoral, ya que puede activar río abajo a vías como la de PI3K/Akt, ERK1/2, STAT, entre otras [13-15].

Además de la formación de redes, el MV va acompañado de otros procesos, como la transición epitelio-mesénquima. En cáncer de mama, se ha visto que la activación IL-8 mediante la vía de PI3K/Akt es esencial para la proliferación tumoral y supervivencia [16]. Más áun, se ha visto que la IL-6, induce la angiogénesis mediada por el FGF-2 por medio de la vía de PI3K [17] y que MCP-1 tiene una función de regulación de Akt en las células del endotelio vascular [18]. En conjunto, esto resulta sumamente interesante pues ciñe la evidencia hacia la relevancia funcional de estas vías y sus grandes controladores: FGFR y PI3K/Akt.

Por ello realizamos la inhibición farmacológica de ambos componentes de la señalización para identificar si efectivamente son de relevancia para el MV. Como mostramos en la Figura 8, en dos líneas celulares de CMTN, la inhibición de FGFR con AZD4547 y de PI3K con LY294002, inhibió por completo o casi en su totalidad, en el caso de LY294002, la formación de redes de cordones. Estos resultados confirman la dependencia del modelo de co-cultivo en CMTN, de la señalización mediada por FGFR/PI3K/Akt. Posiblemente una porción de la señalización regulada por FGFR recae en otras cinasas, como podría ser STAT3 que también se ha visto implicada en el mimetismo vascular [19]. Sin embargo, la inhibición de PI3K tuvo un efecto casi comparable con el de la inhibición de FGFR, sugiriendo que la mayoría de la señalización recae en este punto de la cascada.

Finalmente, para dilucidar qué cascadas de señalización y procesos son relevantes para la capacidad vasculogénica del cáncer en el modelo de co-cultivo de CMTN, evaluamos el perfil de fosforilación global de diferentes proteínas, en células tratadas con AZD4547 por 48

horas. Interesantemente, la mayoría de las cinasas que basalmente se encontraron fosforiladas, pertenecen a subfamilias de cinasas de tirosina no receptoras, de la familia Src. Una de estas cinasas fue ACK1, que es está altamente ligada con el comportamiento tumoral, la progresión, proliferación, apoptosis, invasión y metástasis [20]. ACK1, fosforila directamente a Akt en respuesta a FGF y la fosforilación de ambas cinasas esta negativamente correlacionada con la supervivencia en pacientes de cáncer de mama [21]. Esto es consistente con lo observado en nuestro estudio, pues la inhibición de FGFR, disminuye drásticamente la expresión e ACK1 en el co-cultivo, lo que sugeriría a su vez una disminución en la activación de Akt, contribuyendo a un efecto mayor sobre el MV.

Por otra parte otras de las cinasas que se regularon positiva o negativamente tras la inhibición de FGFR fueron FAK, Syk y Csk, estas en particular se ha visto que son expresadas por células progenitoras eritroides, acompañadas de la expresión de FGFR, tras la diferenciación estas cinasas son reguladas a la baja [21], sugiriendo su participación en la diferenciación celular, como se muestra en las redes de interacción proteína-proteína, donde este proceso fue uno de los principales mecanismos biológicos asociados a la red. Así mismo, se ha reportado que Syk, así como BTK y HCK, también participan en la regulación de la expresión de genes importantes para la invasión y la angiogénesis, mediada por la vía de señalización PI3K/Akt y mTOR [22,23]. Esto es consistente con la hipótesis evaluada en el presente estudio, en el que proponemos que el FGFR/PÍ3K/Akt tiene un importante peso en la regulación funcional del mimetismo vascular al incidir sobre proteínas como MMP-2, VEGF y β-catenina de suma importancia en la angiogénesis tumoral y el MV [22-24].

## 4.5. CONCLUSIONES

- Únicamente el co-cultivo con células endoteliales indujeron la formación de cordones en los co-cultivos con las células de cáncer de mama triple negativo (MBCDF-T, HCC-1806) y en co-cultivo con trofoblastos, HTR-8.
- El MV en co-cultivos requiere tanto de señales parácrinas como yuxtacrinas entre cáncer y endotelio.
- El endotelio, en co-cultivo, induce el MV al generar un microambiente pro-angiogénico mediante la producción de citosinas y factores de crecimiento pro-angiogénicos.

- La inhibición específica de FGFR o PI3K/AKT resultó en el impedimento de la formación de redes en los co-cultivos, sugiriendo que esta vía es de suma importancia en la capacidad pro-angiogénica del endotelio y de MV en las células de cáncer de mama triple negativo.

## 4.6. LITERATURA CITADA


1. Rak, J., Filmus, J., & Kerbel, R. S. (1996). Reciprocal paracrine interactions between tumour cells and endothelial cells: the "angiogenesis progression" hypothesis. European Journal of Cancer, 32(14), 2438–2450. doi:10.1016/s0959-8049(96)00396-6
2. Park Y, Kim J. Regulation of IL-6 signaling by miR-125a and let-7e in endothelial cells controls vasculogenic mimicry formation of breast cancer cells. BMB Rep. 2019 Mar;52(3):214-219. doi: 10.5483/BMBRep.2019.52.3.308.
3. Rai A, Cross JC. Development of the hemochorial maternal vascular spaces in the placenta through endothelial and vasculogenic mimicry. Dev Biol. 2014 Mar 15;387(2):131-41. doi: 10.1016/j.ydbio.2014.01.015.
4. Hernández de la Cruz ON, López-González JS, García-Vázquez R, Salinas-Vera YM, Muñiz-Lino MA, Aguilar-Cazares D, López-Camarillo C, Carlos-Reyes Á. Regulation Networks Driving Vasculogenic Mimicry in Solid Tumors. Front Oncol. 2020 Jan 14;9:1419. doi: 10.3389/fonc.2019.01419.
5. McNally R, Alqudah A, Obradovic D, McClements L. Elucidating the Pathogenesis of Pre-eclampsia Using In Vitro Models of Spiral Uterine Artery Remodelling. Curr Hypertens Rep. 2017 Oct 23;19(11):93. doi: 10.1007/s11906-017-0786-2.
6. Buck VU, Gellersen B, Leube RE, Classen-Linke I. Interaction of human trophoblast cells with gland-like endometrial spheroids: a model system for trophoblast invasion. Hum Reprod. 2015 Apr;30(4):906-16. doi: 10.1093/humrep/dev011.
7. Ma C, Liu G, Liu W, Xu W, Li H, Piao S, Sui Y, Feng W. CXCL1 stimulates decidual angiogenesis via the VEGF-A pathway during the first trimester of pregnancy. Mol Cell Biochem. 2021 Aug;476(8):2989-2998. doi: 10.1007/s11010-021-04137-x.
8. Truelsen SLB, Mousavi N, Wei H, Harvey L, Stausholm R, Spillum E, Hagel G, Qvortrup K, Thastrup O, Harling H, Mellor H, Thastrup J. The cancer angiogenesis co-culture assay: In vitro quantification of the angiogenic potential of tumoroids. PLoS One. 2021 Jul 7;16(7):e0253258. doi: 10.1371/journal.pone.0253258.

9. Biondani G, Zeeberg K, Greco MR, Cannone S, Dando I, Dalla Pozza E, Mastrodonato M, Forciniti S, Casavola V, Palmieri M, Reshkin SJ, Cardone RA. Extracellular matrix composition modulates PDAC parenchymal and stem cell plasticity and behavior through the secretome. FEBS J. 2018 Jun;285(11):2104-2124. doi: 10.1111/febs.14471.
10. Aikins AR, Kim M, Raymundo B, Kim CW. Downregulation of transgelin blocks interleukin-8 utilization and suppresses vasculogenic mimicry in breast cancer cells. Exp Biol Med (Maywood). 2017 Mar;242(6):573-583. doi: 10.1177/1535370216685435.
11. Delgado-Bellido, D., Serrano-Saenz, S., Fernández-Cortés, M. *et al.* Vasculogenic mimicry signaling revisited: focus on non-vascular VE-cadherin. *Mol Cancer* **16**, 65 (2017). https://doi.org/10.1186/s12943-017-0631-x
12. McKeehan WL, Kan M. Heparan sulfate fibroblast growth factor receptor complex: structure-function relationships. Mol Reprod Dev. 1994 Sep;39(1):69-81; discusison 81-2. doi: 10.1002/mrd.1080390112.
13. Quan MY, Guo Q, Liu J, Yang R, Bai J, Wang W, Cai Y, Han R, Lv YQ, Ding L, Billadeau DD, Lou Z, Bellusci S, Li X, Zhang JS. An FGFR/AKT/SOX2 Signaling Axis Controls Pancreatic Cancer Stemness. Front Cell Dev Biol. 2020 May 7;8:287. doi: 10.3389/fcell.2020.00287. Erratum in: Front Cell Dev Biol. 2020 Oct 02;8:594589. PMID: 32457900
14. Hasse C, Holz O, Lange E, Pisowodzki L, Rebscher N, Christin Eder M, Hobmayer B, Hassel M. FGFR-ERK signaling is an essential component of tissue separation. Dev Biol. 2014 Nov 1;395(1):154-66. doi: 10.1016/j.ydbio.2014.08.010.
15. Dudka AA, Sweet SM, Heath JK. Signal transducers and activators of transcription-3 binding to the fibroblast growth factor receptor is activated by receptor amplification. Cancer Res. 2010 Apr 15;70(8):3391-401. doi: 10.1158/0008-5472.CAN-09-3033.
16. Wang L, Tang C, Cao H, Li K, Pang X, Zhong L, Dang W, Tang H, Huang Y, Wei L, Su M, Chen T. Activation of IL-8 via PI3K/Akt-dependent pathway is involved in leptin-mediated epithelial-mesenchymal transition in human breast cancer cells. Cancer Biol Ther. 2015;16(8):1220-30. doi: 10.1080/15384047.2015.1056409.
17. Lee SH, Chu CY, Chiu HC, Huang YL, Tsai WL, Liao YH, Kuo ML. Interleukin-6 induced basic fibroblast growth factor-dependent angiogenesis in basal cell carcinoma cell line

via JAK/STAT3 and PI3-kinase/Akt pathways. J Invest Dermatol. 2004 Dec;123(6):1169-75. doi: 10.1111/j.0022-202X.2004.23497.x.

18. Riverso M, Kortenkamp A, Silva E. Non-tumorigenic epithelial cells secrete MCP-1 and other cytokines that promote cell division in breast cancer cells by activating ERα via PI3K/Akt/mTOR signaling. *Int J Biochem Cell Biol*. 2014 Aug;53:281-94. doi: 10.1016/j.biocel.2014.05.023.
19. Liu X, Wang X, Li L, Han B. Research Progress of the Functional Role of ACK1 in Breast Cancer. *Biomed Res Int*. 2019 Oct 20;2019:1018034. doi: 10.1155/2019/1018034
20. Hu F, Liu H, Xie X, Mei J, Wang M. Activated cdc42-associated kinase is up-regulated in non-small-cell lung cancer and necessary for FGFR-mediated AKT activation. *Mol Carcinog*. 2016 May;55(5):853-63. doi: 10.1002/mc.22327.
21. Koritschoner, Nicolás P., et al. "The fibroblast growth factor receptor FGFR-4 acts as a ligand dependent modulator of erythroid cell proliferation." *Oncogene* 18.43 (1999): 5904-5914.
22. Fruchon S, Kheirallah S, Al Saati T, Ysebaert L, Laurent C, Leseux L, Fournié JJ, Laurent G, Bezombes C. Involvement of the Syk-mTOR pathway in follicular lymphoma cell invasion and angiogenesis. *Leukemia*. 2012 Apr;26(4):795-805. doi: 10.1038/leu.2011.248. Epub 2011 Sep 16. PMID: 21926965.
23. Zhu Y, Liu X, Zhao P, Zhao H, Gao W, Wang L. Celastrol Suppresses Glioma Vasculogenic Mimicry Formation and Angiogenesis by Blocking the PI3K/Akt/mTOR Signaling Pathway. *Front Pharmacol*. 2020 Feb 6;11:25. doi: 10.3389/fphar.2020.00025.
24. Tang J, Wang J, Fan L, Li X, Liu N, Luo W, Wang J, Wang Y, Wang Y. cRGD inhibits vasculogenic mimicry formation by down-regulating uPA expression and reducing EMT in ovarian cancer. *Oncotarget*. 2016 Apr 26; 7(17):24050-62. doi: 10.18632/oncotarget.8079. PMID: 26992227; PMCID: PMC5029683.

# PARTE 3.

## EFECTOS DEL CALCITRIOL Y CURCUMINA EN EL MIMETISMO VASCULAR DEL CMTN

# CAPÍTULO 5.

## EFECTOS DEL CALCITRIOL COMBINADO CON CURCUMINA SOBRE EL MIMETISMO VASCULAR EN CÉLULAS DE CÁNCER DE MAMA TRIPLE NEGATIVO

***Este capítulo está basado en el artículo:***

GABRIELA MORALES-GUADARRAMA, EDGAR A. MÉNDEZ-PÉREZ, JANICE GARCÍA-QUIROZ, EUCLIDES AVILA, ROCÍO GARCÍA-BECERRA, ALEJANDRO ZENTELLA-DEHESA, FERNANDO LARREA AND LORENZA DÍAZ. ENDOTHELIUM-DEPENDENT INDUCTION OF VASCULOGENIC MIMICRY IN HUMAN TRIPLE-NEGATIVE BREAST CANCER CELLS IS INHIBITED BY CALCITRIOL AND CURCUMIN.

***INTERNATIONAL JOURNAL OF BIOMEDICAL SCIENCES.* 2022, 23(14):7659**

## 5.1. RESUMEN

Algunos tumores con fenotipos agresivos tienen la capacidad de formar canales de sangre interconectados en redes de microcirculación mediante un proceso conocido como mimetismo vascular (MV). El MV suele asociarse con la metástasis, fenotipos mesénquimales y resistencia a las terapias. Además, puede ser desencadenado por tratamientos anti-angiogénicos y/o factores derivados del microambiente tumoral, incluidos los producidos por el endotelio. La curcumina es un producto derivado de la cúrcuma capaz de inhibir el MV in vitro en algunos tipos de cáncer, mientras que el calcitriol, el metabolito activo de la vitamina D, posee potentes efectos antineoplásicos. Sin embargo, los efectos de estos productos naturales sobre el MV en el cáncer de mama se desconocen. Por lo anterior, estudiamos el efecto de ambos compuestos por separado y en combinación, sobre la capacidad de MV de las células de cáncer de mama triple negativo (CMTN) en co-cultivo con endotelio. El MV inducido por endotelio en dos líneas celulares de CMTN fue inhibido de manera significativa por el calcitriol y la curcumina. El tratamiento con calcitriol indujo cambios morfológicos en las células de CMTN, que pasaron de una forma fusiforme a una forma redondeada. Por su parte, la curcumina disminuyó la tridimensionalidad de la arquitectura del co-cultivo. Interesantemente, los tratamientos disminuyeron de manera global el patrón de fosforilación de diversas proteínas, especialmente de las de la vía de PI3K/Akt. En conjunto, el calcitriol y la curcumina abatieron el MV inducido por el endotelio en las células de CMTN por la inhibición de la señalización mediada por Akt y la inhibición del fenotipo mesenquimal. Nuestros resultados refuerzan el uso potencial de estos compuestos de origen natural como adyuvantes para prevenir el MV, especialmente en pacientes con tumores altamente agresivos y con escasas estrategias terapéuticas como el CMTN, o bien para aquellos que reciben terapias anti-angiogénicas.

## 5.2. MATERIALES Y MÉTODOS

*CULTIVOS CELULARES, TRATAMIENTOS.*

Se emplearon las mismas líneas celulares, en las mismas condiciones de mantenimiento y co-cultivo que en los Materiales y Métodos del capítulo anterior. Para los tratamientos se emplearon calcitriol y/o curcumina, los cuales se compraron de la marca Sigma (Sigma (Sigma-Aldrich, St Louis, MO, USA). Como vehículo, etanol al 0.1% fue usado ambos compuestos. Los tratamientos se administraron al momento de la siembra de los co-cultivos de células de CMTN con células endoteliales, en concentraciones crecientes. Para calcitriol se emplearon 1nM y 10nM y 100nM, mientras que de curcumina se emplearon 10µM, 20µM y 30µM. En combinación, se evaluó el efecto de las dos concentraciones más bajas de calcitriol con las dos concentraciones más altas de curcumina. La evaluación cuantitativa del efecto de los tratamientos sobre el mimetismo vascular en las células de CMTN, se realizó como en el capítulo anterior, empleando imágenes de campo claro para identificar cambios morfológicos en las células. Los experimentos se repitieron por lo menos tres veces.

*PERFIL DE FOSFORILACIÓN DE PROTEÍNAS CINASAS*

Con el fin de identificar las vías involucradas en el efecto de la curcumina y el calcitriol sobre la capacidad de las células CMTN para formar MV, comparamos los cambios en la activación de las cinasas de las vías MAPK y PI3K/Akt mediante el uso de arreglos de anticuerpos sobre membrana, Human PhosphoMAPK, (ab211061 , Abcam), a partir de lisados totales de co-cultivos en presencia o ausencia de los tratamientos. Los sitios de fosforilación de las cinasas analizadas fueron: Akt (pS473), CREB (pS133), ERK1 (pT202/Y204), ERK2 (pT185/Y187), GSK3α (pS21), GSK3β (pS9), HSP27 (pS82), JNK (pT183), MEK (pS217/221), MKK3 (pS189), MKK6 (pS207), MSK2 (pS360), mTOR (pS2448), p38 (pT180/Y182), p53 (pS15), P70S6K (pT421/S424), RSK1 (pS380) y RSK2 (pS386).

Después de tratar los co-cultivos con el vehículo, calcitriol, curcumina o su combinación, se prepararon lisados celulares utilizando el buffer de lisis proporcionado complementado con un cóctel inhibidor de fosfatasas y proteasas, y se almacenaron a -80 °C hasta la realización del ensayo. La proteína total en los lisados celulares se cuantificó utilizando el kit de ensayo de proteínas BCA (Thermo Fisher Scientific, Rockford, IL, EE. UU.) y se emplearon 500 µg por cada

membrana. Las membranas se bloquearon e incubaron durante toda la noche a 4 °C. Posteriormente, se realizaron lavados e incubación de los anticuerpos HRP-Anti-Rabbit IgG y el cóctel de anticuerpos de detección. Las señales de quimioluminiscencia se adquirieron y analizaron utilizando el fotodocumentador ChemiDoc XRS+ (BioRad). Las comparaciones semi-cuantitativas entre tratamientos se realizaron después de la normalización con los controles positivos incluidos en cada membrana. Los puntos sin señal se descartaron. Para la comparación visual de las diferencias relativas entre los tratamientos, categorizamos los resultados positivos por vías canónicas en un mapa de calor y se representaron en un mapa de calor, elaborada en el software GraphPad Prism 7. Se realizaron dos experimentos diferentes en membranas separadas. Cada membrana contenía un duplicado para cada blanco.

- **Análisis de predicción de redes de interacción proteína-proteína (STRING)**

Para construir una red de asociación funcional para las proteínas involucradas en los efectos de los tratamientos, las proteínas cuya fosforilación tuvo un *fold-change* mayor a 0,5 se sometieron a un análisis de predicción de interacciones proteína-proteína mediante el uso de la Herramienta de búsqueda para la recuperación de genes/proteínas que interactúan (STRING, https://string-db.org/), considerando no más de 5 interactores predichos para cada condición y procesos biológicos asociados.

*ANÁLISIS ESTADÍSTICO*

Se usó ANOVA de una vía, seguida del método Holm-Sidak para la prueba de comparaciones múltiples usando un paquete de software especializado (SigmaStat, Jandel Scientific). Los datos se expresan como la media ± error estándar de la media (SEM). Los resultados se consideraron significativos a $p<0,05$.

## 5.3. RESULTADOS

***El calcitriol, la curcumina y su combinación inhibieron la formación de VM dependiente del endotelio en las células de cáncer de mama.***

Para conocer el efecto de la curcumina y el calcitriol *per se* y en combinación, sobre el MV en cáncer de mama triple negativo, evaluamos el efecto de estos tratamientos en concentraciones crecientes en co-cultivos de células MBCDF-T o HCC-1806 co-cultivadas con

células endoteliales EA.hy926 expuestas a los compuestos. Como se muestra en la Figura 10, el calcitriol afecta drásticamente la capacidad de las células para formar una red organizada de cordones entrelazados, sin embargo es en los co-cultivos de MBCDF-T donde la inhibición es definitiva y claramente observable. De manera interesante, observamos que este efecto se encontró asociado a la pérdida de la morfología fusiforme, característica de las células de cáncer formadoras de red (Suplementaria 1), dicho efecto se observa tanto en monocultivos como en co-cultivos, lo cual sugiere fuertemente que la diferenciación celular y la inhibición de EMT podrían ser las posibles causas del efecto anti-MV del calcitriol en los co-cultivos.

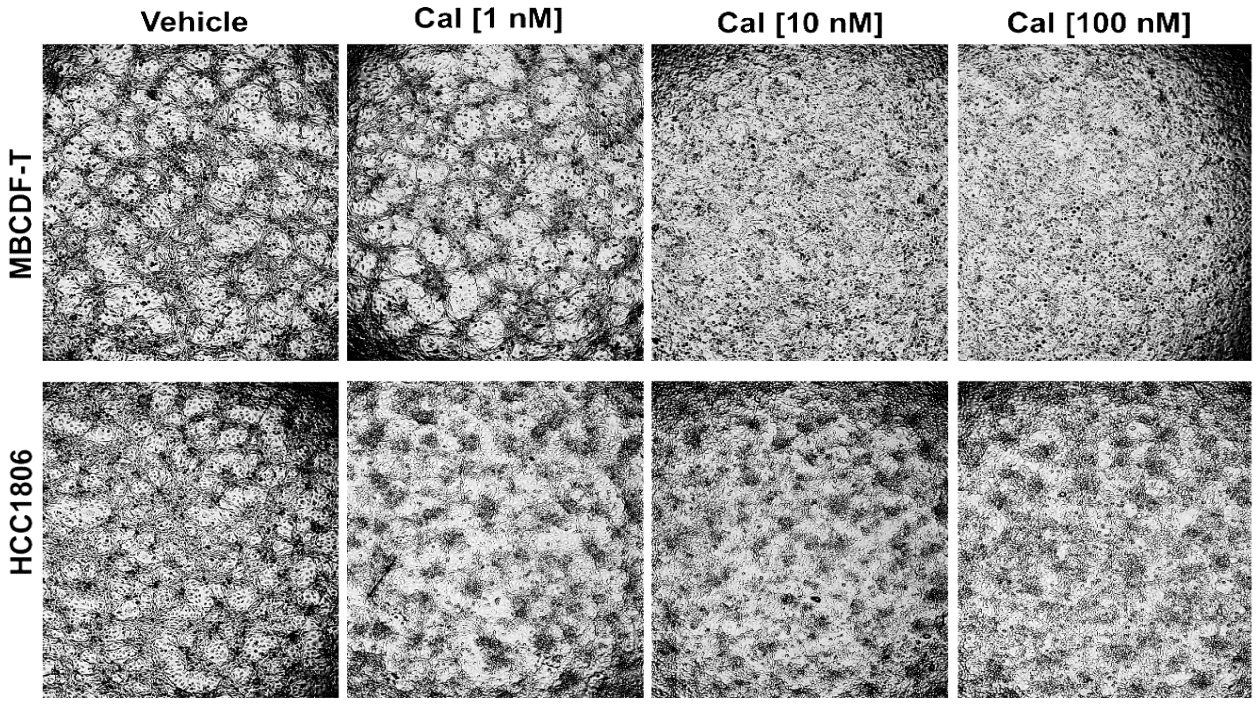


*Figura 10. Efecto del calcitriol en concentraciones nanomolares crecientes sobre el MV en co-cultivos de CMTN y endotelio a las 72 horas.* Co-cultivos de la línea MBCDF-T expuestos a calcitriol en concentraciones crecientes. Desde [10nM] la capacidad de formar redes de cordones se ve abatida. En los co-cultivos de HCC-1806, se observa un efecto similar, pero mucho menor sobre la citoarquitectura del co-cultivo.

Por otra parte, la curcumina también afectó de manera drástica la formación de las estructuras en red, en los co-cultivos. El efecto fue dependiente de la concentración en ambas líneas celulares, como se puede observar en la Figura 11. Nuevamente, es en la línea MBCDF-T donde el efecto fue más notorio. Esto sugiere que a pesar de ser células caracterizadas dentro

del mismo subtipo molecular de cáncer de mama, diferencias genotípicas podrían interferir en la respuesta a los tratamientos aquí evaluados.

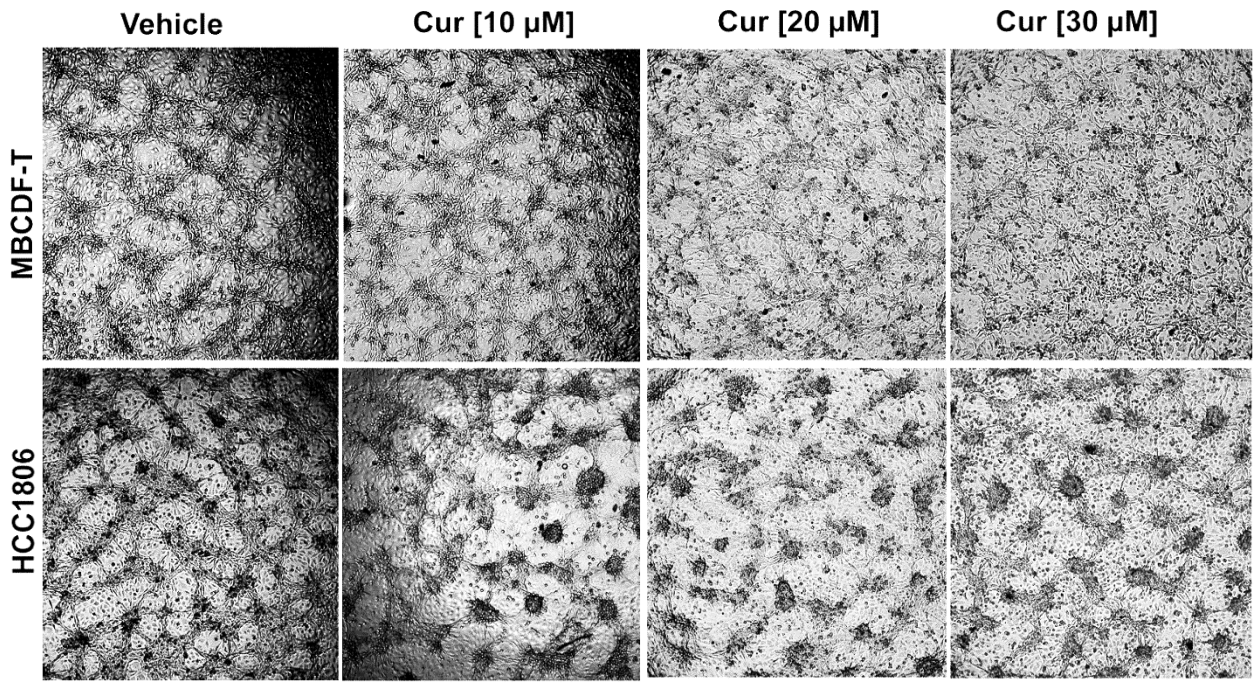


*Figura 11. Efecto de la curcumina en concentraciones nanomolares crecientes sobre el MV en co-cultivos de CMTN y endotelio a las 72 horas.* Co-cultivos de la línea MBCDF-T expuestos a curcumina en concentraciones crecientes. Se observa como desde [10µM] la capacidad de formar redes de cordones se ve completamente abatida. A la derecha, co-cultivos de la línea células HCC-1806, se observa un efecto fuerte sobre la citoarquitectura del co-cultivo, siendo menos drástico que el observado en MBCDF-T.

Las concentraciones intermedias evaluadas de cada compuesto se establecieron como las concentraciones a evaluar por separado y en combinación para determinar cuantitativamente el efecto de los tratamientos sobre el mimetismo vascular. Como se muestra en la figura Figura 12, calcitriol inhibió casi por completo la formación de redes de cordones en los co-cultivos de ambas líneas celulares. Por otra parte, curcumina también afecto la formación de dichas estructuras y modificó su tridimensionalidad; sin embargo, su efecto fue menos evidente en comparación con el del calcitriol. El tratamiento con curcumina resultó en la ruptura parcial de la estructura 3D sugiriendo que este compuesto afecta la organización/adhesión celular en las mallas formadas por las células de cáncer. El mismo efecto fue observado en ambas líneas celulares, donde los compuestos redujeron significativamente el número de segmentos (cordones observados por campo visual) respecto

al vehículo (Figura 12c). De igual manera, en ambas líneas celulares de CMTN en co-cultivo con células endoteliales, la combinación de calcitriol y curcumina disminuyó aún más la formación de MV; sin embargo, la reducción en el número de segmentos y mallas no alcanzó significación estadística en comparación con el calcitriol por sí solo.

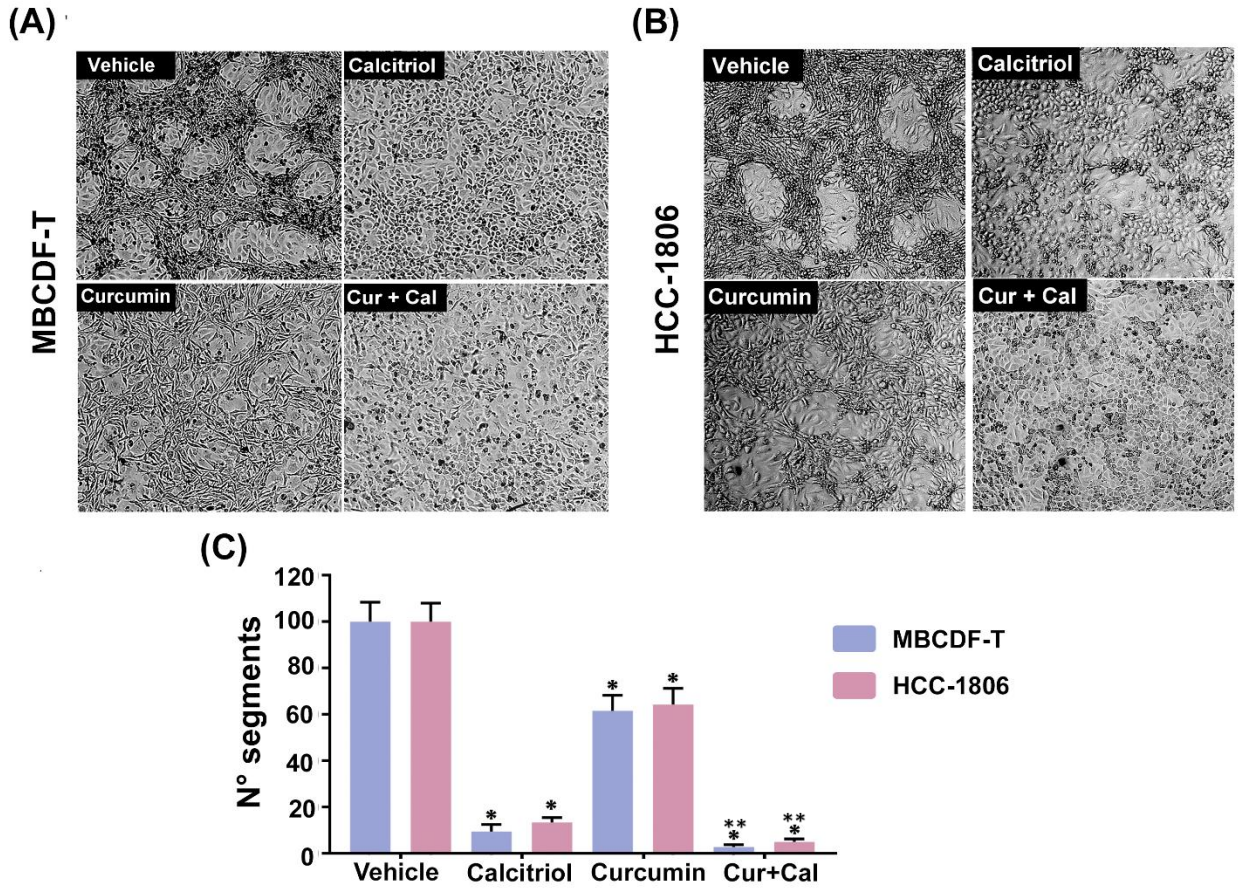


*Figura 12. El calcitriol y la curcumina inhibieron la capacidad de MV de las células de CMTN co-cultivadas con endotelio.* Se observó el MV inducido por EA.hy926 en co-cultivos de células MBCDF-T (A) o HCC1806 (B) incubadas con vehículo (etanol) o en presencia de calcitriol, curcumina o su combinación (Cur+Cal). La presencia de calcitriol (10 nM) cambió la morfología celular fusiforme a células redondeadas de cáncer de mama, evitando por casi por completo la formación de redes de cordones, mientras que la curcumina (20 µM) afectó la estructura tridimensional de las redes de cordones, puesto que se observan ambos componentes celulares en el mismo plano focal. La combinación de Cur+Cal inhibió aún más el MV en ambas células celulares de CMTN. El número de segmentos por campo visual fue contado por dos observadores diferentes en zonas enriquecidas en dichas estructuras, en al menos 5 fotografías diferentes, considerando 3 experimentos diferentes para MBCDF-T y 2 experimentos diferentes para HCC1806. Los gráficos representan el número medio de mallas/segmentos por campo visual*p < 0,05 vs VH. **p < 0,05 vs los tratamientos por separado.

***El calcitriol y la curcumina inhiben la fosforilación de cinasas de las vías de señalización MAPK, PI3K/Akt/mTOR, PI3K/Akt/CREB y PI3K/Akt/Gsk en co-cultivos de CMTN con endotelio***

Para estudiar el perfil de fosforilación de las cinasas involucradas en las vías de señalización relevantes para el mimetismo vascular, elegimos los co-cultivos MBCDF-T/EA.hy926, puesto que en estas células el efecto fue mucho más notorio. Se llevó a cabo un agrupamiento jerárquico semi-supervisado de las proteínas fosforiladas diferencialmente detectadas con un arreglo de anticuerpos en membrana (ab211061, Abcam). Luego, los resultados se representaron en un mapa de calor agrupado en tres vías de señalización principales: PI3K/Akt, mTOR y MAPK (Figura 13). Encontramos que Akt, junto con la proteína de unión al elemento de respuesta cAMP (CREB) y la glucógeno sintasa cinasa-3α (Gsk3) (Figura 13, marcada en negro), fueron las cinasas mayormente fosforiladas en los co-cultivos control. Por otro lado, las cinasas de los complejos mTOR y algunas de las MAPK, como MKK3, MKK6, MSK2, RSK1 y RSK2 (marcadas en rojo, Figura 13), fueron fuertemente inhibidas por calcitriol, mientras que el estado de fosforilación de Gsk3α, Gsk3β, p53, p38, JNK y Hsp27 (marcadas en azul, Figura 13) disminuyó mayormente en presencia de la curcumina. Estos

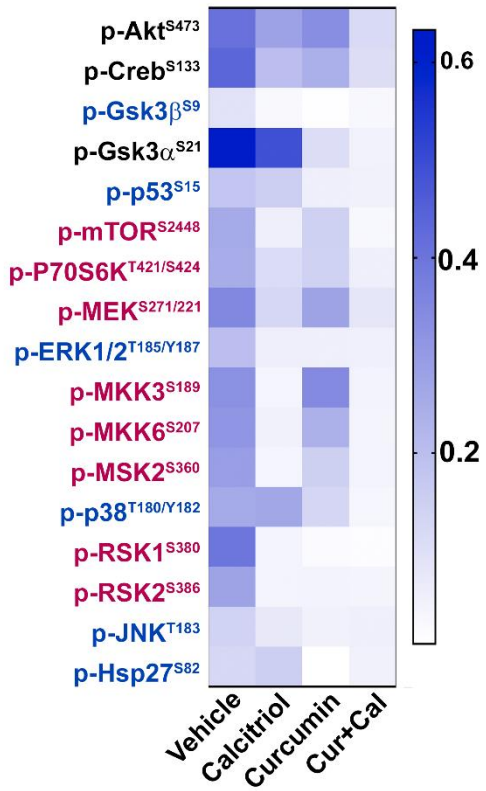


*Figura 13. En co-cultivos MBCDF-T/EA.hy926, el calcitriol y la curcumina inhibieron la fosforilación de varias proteínas de las vías de señalización MAPK, PI3K/Akt/mTOR, PI3K/Akt/CREB y PI3K/Akt/Gsk.* El perfil de fosforilación de las cinasas involucradas en las vías de señalización relevantes para el MV fue inhibido de manera diferencial por calcitriol (10 nM), curcumina (20 μM) y su combinación (Cur+Cal). Se llevó a cabo un agrupamiento jerárquico semisupervisado de las fosforilaciones diferencialmente detectados con una matriz de anticuerpos multiplex. Los resultados se muestran en el mapa de calor organizado en tres vías de señalización principales: PI3K/Akt, mTOR y MAPK. Las cinasas mayormente fosforiladas en co-cultivos control (vehículo) están marcadas en negro. Las cinasas inhibidas en su mayoría por el calcitriol están marcadas en rojo, mientras que las fosforilaciones reguladas a la baja por la curcumina, principalmente, están marcadas en azul. N=4.

resultados sugieren que cada compuesto afecta distintos niveles de las vías de señalización, confirmando uno de los porqués de su interacción sinérgica en procesos como la proliferación [1]. De manera interesante, la combinación de ambos tratamientos inhibió de manera global el estado de fosforilación (principalmente asociado a un estado de activación) de dichas proteínas/vías de señalización (Figura 13) lo que se asoció a una mayor inhibición funcional del MV.

Es notable que el efecto a nivel del patrón global de señalización obtenido con concentraciones bajas de calcitriol y curcumina es similar a lo que se esperaría de una molécula sintética multiblanco (inhibidores de RTKs). Además, por medio del análisis STRING identificamos que estas proteínas interactúan formando complejos entre ellas y que están involucradas en varias funciones biológicas, como se muestra en la Figura 14. Entre los procesos predichos regulados por calcitriol y curcumina, se identificaron las vías relacionadas con VM que involucran Wnt, VEGF, MAPK, PI3K/AKT y mTOR (Figura 15, círculo púrpura). Curiosamente, solo el calcitriol se relacionó con la vía inflamatoria que involucra la producción y respuesta de citocinas (Figura 15, círculo azul marino), mientras que la curcumina se relacionó con la señalización de TGFB, receptor del factor de crecimiento de fibroblastos (FGFR), microRNA (miRNA) y p53 (Figura 15, círculo azul claro). Además, la combinación de calcitriol y curcumina afectó las redes relacionadas con la muerte celular, como la apoptosis, la anoikis y la autofagia, mientras que la curcumina sola se asoció con la senescencia y la EMT. Finalmente, los principales impulsores involucrados en el MV son las moléculas de plasticidad y adhesión, mismas que de acuerdo con la predicción en STRING son afectadas por ambos compuestos (Figura 14).

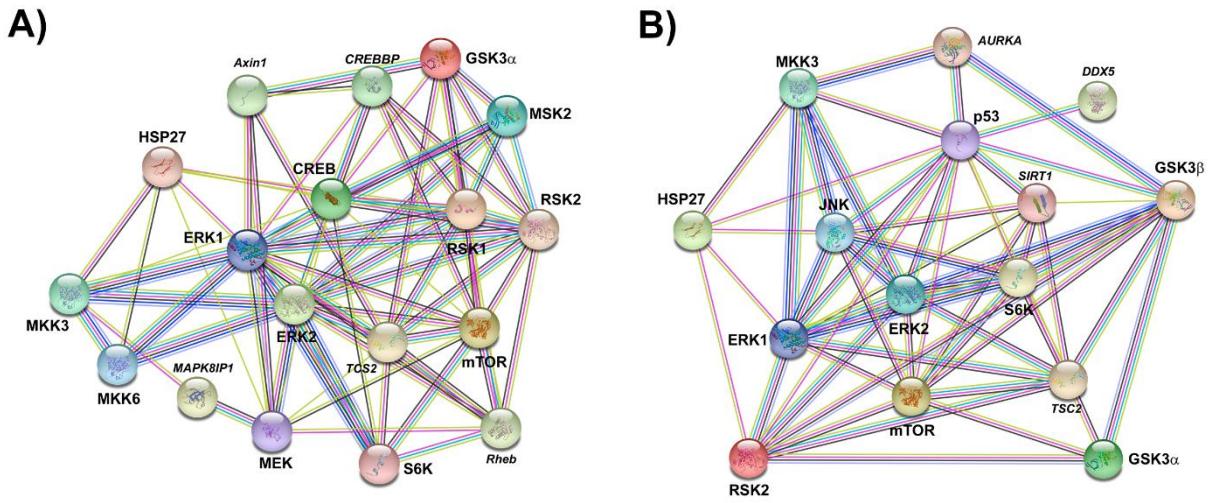


*Figura 14. Redes de interacción y procesos biológicos regulados por calcitriol, curcumina o su combinación implicados en el efecto anti-VM de los compuestos.* Análisis STRING de cinasas desreguladas en co-cultivos tratados con calcitriol (A) o curcumina (B). Las redes (A,B) muestran las interacciones proteicas físicas y funcionales. Los nombres de proteínas en cursiva representan los principales interactores predichos de la red.

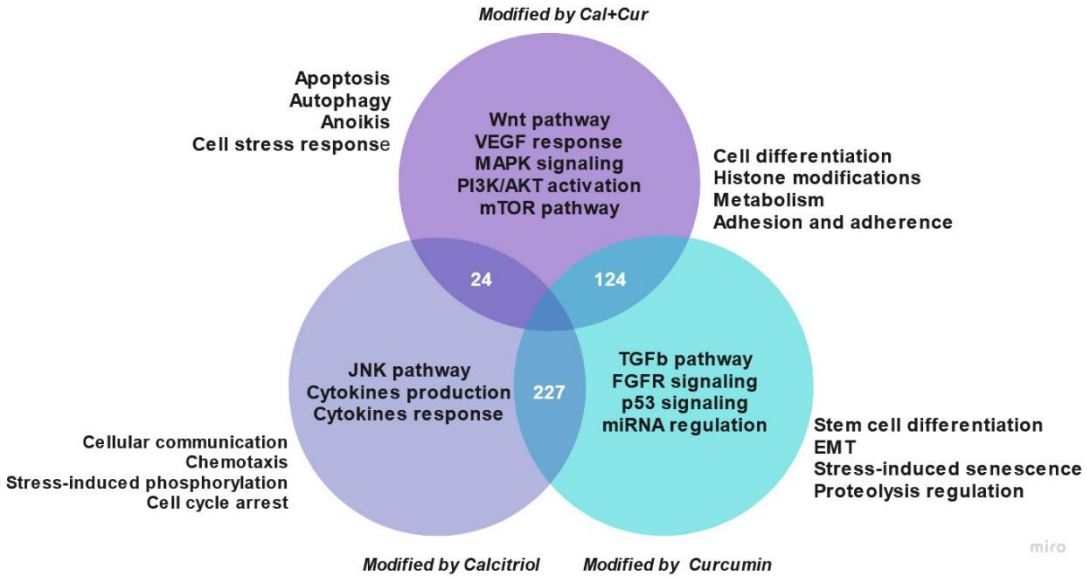


*Figura 12. Predicción de los procesos biológicos regulados diferencialmente en cada grupo de tratamiento.* Un total de 227 procesos fueron co-regulados por calcitriol (CAL) y curcumina (CUR); 24 procesos fueron compartidos por los grupos CAL y CAL+CUR (C+C), y 124 fueron compartidos en los grupos CUR y C+C. Dentro de cada círculo, se representan las principales vías involucradas. En el exterior, cerca de cada círculo, se muestran los procesos biológicos en los que se predijo podrían participar estos complejos proteicos

## 5.4. DISCUSIÓN

El crecimiento y la diseminación del tumor dependen significativamente de la formación de una red vascular funcional. En este proceso intervienen muchos mecanismos, pero entre ellos destaca el MV el cual se da zonas hipóxicas de tumores altamente agresivos. Este proceso puede generar resistencia a los fármacos destinados a bloquear la vascularización tumoral, lo que explica su fracaso en la clínica. En este estudio, encontramos que los compuestos naturales calcitriol y curcumina inhiben la formación de MV, inducida por el endotelio, en líneas celulares de CMTN. Dicho efecto fue significativamente potenciado por el uso concomitante de ambos compuestos. El modo de acción del calcitriol parece implicar la inhibición de la EMT, a juzgar por el cambio en la forma de las células cancerosas de morfología fusiforme a una forma redondead; esto explicaría la capacidad de esta hormona para bloquear drásticamente el MV. De hecho, el MV depende en gran medida del fenotipo de las células mesénquimales y de las características troncales de las células, dadas por la plasticidad celular intrínseca de las células del tumor. En este sentido, se sabe que el calcitriol bloquea la EMT a través de la inactivación de la señalización de PI3K/Akt/β-catenina y que de esta manera, induce la diferenciación celular [2]. Además, el calcitriol es una potente hormona antiinflamatoria que inhibe la expresión de citocinas inflamatorias, como la interleucina-6 (IL6) [3]. Recientemente, se ha descrito que la IL6 de origen endotelial actúa como un factor parácrino sobre las células de cáncer de mama MDA-MB-231, induciendo la formación de MV [4], lo que justifica más estudios sobre los efectos del calcitriol sobre las citocinas inflamatorias en co-cultivos de CMTN y células endoteliales. En conjunto, esto puede ayudar a explicar los fuertes efectos anti-MV del calcitriol. La curcumina, por otro lado, no inhibió la EMT en este estudio, a juzgar por la falta de modificación de la forma fusiforme de las células. Como resultado, las células cancerosas tratadas con curcumina formaron parcialmente estructuras tubulares similares a cordones. Sin embargo, en general, estas estructuras carecían de la configuración 3D característica de los co-cultivos control, sin embargo la reducción de la cantidad de segmentos, fue significativa.

En resultados previos, reportamos que la curcumina induce muerte celular en las células endoteliales, al tiempo que inhibía la proliferación y migración de células MBCDF-T y EA.hy926 [1], es posible que estos efectos estuvieran involucrados en el mecanismo anti-MV de la curcumina y que de esta manera afecte tanto a las células de cáncer como a las células

endoteliales. Además, se sabe que la curcumina ejerce actividad anti-tirosina cinasa [4], lo cual es importante para el proceso de VM, ya que algunos de sus impulsores, como VEGF, median su efecto a través de los receptores de tirosina quinasa. Otra posibilidad para explicar el efecto disruptivo de la curcumina en la estructura 3D de VM es la regulación a la baja de las moléculas de adhesión intercelular necesarias para mantener unida la estructura 3D. En este sentido, se ha descrito que la curcumina bloquea la expresión de la superficie celular de las moléculas de adhesión en las células endoteliales, reduce la unión de las células cancerosas a las proteínas de la matriz extracelular y disminuye significativamente la propensión a la adhesión de las células de cáncer de mama [5,6,7]. Estos efectos de la curcumina, junto con los efectos pro-diferenciadores, antiinflamatorios y anti-EMT del calcitriol, podrían explicar la capacidad de ambos compuestos para inhibir significativamente el MV en los co-cultivos de CMTN. Aunado a esto, entre los procesos predichos por STRING, que son regulados por la curcumina en combinación con calcitriol la adhesión, la diferenciación celular y varias vías de señalización involucradas en MV destacaron. En este sentido, la combinación de calcitriol y curcumina afectó globalmente el estado de fosforilación de diversas cinasas involucradas en la señalización asociada al MV. En particular, los componentes de señalización de la vía PI3K/Akt parecen ser los más importantes para la formación del MV en nuestro modelo de co-cultivo, incluidos Akt, CREB y Gsk3α. Esto último se relaciona estrechamente con la participación de factores derivados del microambiente tumoral capaces de activar la señalización de PI3/Akt, como FGF y VEGF [8,9,10,11,12,13]. La activación de Akt, dependiente de factores de crecimiento como estos u otros, da como resultado la inactivación de Gsk3, este mecanismo se ha visto altamente asociado al desarrollo y la progresión del cáncer. De hecho, se sabe que la actividad de Gsk3 se inhibe a través de la fosforilación de Gsk3α en la serina 21 y Gsk3β en la serina 9. Estos residuos de serina específicos en Gsk3 son blancos conocidos de Akt y otras cinasas capaces de fosforilarlos [14]. La pérdida de actividad de Gsk3 conduce al bloqueo de sus efectos antineoplásicos, ya que Gsk3 actúa como un supresor de tumor al regular negativamente moléculas pro-oncogénicas como β-catenina [14]. Sorprendentemente, en este estudio la fosforilación de Gsk3α en la serina 21 y Gsk3β en la serina 9 se encontró regulada a la baja por la curcumina y el calcitriol. Dicho esto, la disminución del estado fosforilado de Gsk3 es consistente con la disminución del estado activo de Akt en respuesta al calcitriol y la curcumina, lo que explica parcialmente la actividad anti-

MV de ambos compuestos. En particular, a través de estudios de docking, se ha descrito que la curcumina encaja en el sitio de unión a ATP de Gsk3β, modulando su actividad [15]. Además, también se ha informado que la curcumina puede de-fosforilar a Akt y Gsk3 en el modelo de leucemia linfoblástica aguda [16] y que regula negativamente la expresión de Akt en las células de CMTN, lo que resulta en la supresión de la proliferación y la migración celular [17]. De manera similar, y como se encontró en este estudio, se ha demostrado previamente que el calcitriol reduce la fosforilación de Akt en el cáncer de mama y en las células epiteliales renales [2,18].

Cabe destacar que, además de estar involucradas en el desarrollo de MV, las vías de señalización MAPK, PI3K/Akt/mTOR y PI3K/Akt/Gsk también están implicadas en diferentes funciones celulares relevantes para la progresión del cáncer, como la proliferación celular, adhesión, migración, metabolismo y supervivencia [9]. Por lo tanto, el hecho de que el calcitriol y la curcumina regulen a la baja estas vías, respalda aún más el potencial antineoplásico de estos compuestos naturales solos y combinados.

Un hallazgo interesante en este estudio fue la disminución de la fosforilación de p53 en la serina 15 por curcumina y su combinación con calcitriol. Esto podría estar relacionado con que se sabe que curcumina inhibe a las proteínas cinasas ATM y ATR, relacionadas con PI3K, y responsables de la modificación covalente en p53 [19]. La fosforilación de p53 en la serina 15 es necesaria para la activación de los promotores sensibles a p53 [20]. Por lo tanto, parece que la curcumina interfiere con la actividad transcripcional de p53 bloqueando la respuesta al daño del ADN en las células tumorales.

En general, los datos sugieren que la señalización parácrina de las células endoteliales induce a las células tumorales TNBC a formar MV mediante la activación de Akt, CREB y Gsk3α, entre otros factores importantes relacionados con la plasticidad y la angiogénesis. El calcitriol impidió significativamente la formación del MV en co-cultivos de CMTN, mientras que la curcumina inhibió la organización tridimensional de las estructuras derivadas del MV, al menos parcialmente, mediante la regulación negativa de la fosforilación de varios componentes de la vía PI3K/Akt y p53. La combinación de calcitriol y curcumina inhibió globalmente el perfil de fosforilación de las proteínas, lo cual se asoció a un mayor efecto sobre la inhibición del MV. Interesantemente, el patrón de fosforilación obtenido en el tratamiento

combinado de calcitriol y curcumina es similar a lo que podría esperarse cuando se usa un inhibidor multiblanco dirigido a cinasas. En general, el calcitriol y la curcumina son una buena opción para su uso como adyuvantes de la terapia anti-angiogénica, pues pueden ayudar a evitar la generación del MV. Además, dado que la combinación de estos compuestos naturales ha mostrado efectos anti-angiogénicos in vivo *per se* [1], el hecho de que también tenga una potente actividad anti-MV respalda aún más su plausibilidad terapéutica en un contexto clínico adyuvante. En conclusión, nuestro estudio proporciona un conocimiento novedoso, mostrando, por primera vez, que la curcumina y el calcitriol solos y combinados inhiben la formación de VM en las células de CMTN, a través de la regulación negativa de la señalización de PI3K/Akt.

## 5.5. CONCLUSIONES

El calcitriol y la curcumina suprimieron la formación de VM de células TNBC inducidas por el endotelio, al menos en parte, al bloquear la vía PI3K/Akt y, posteriormente, afectar varios procesos de supervivencia celular. Nuestros resultados sugieren el uso clínico potencial de calcitriol y curcumina para inhibir VM en tumores TNBC.

## 5.6. FIGURAS SUPLEMENTARIAS

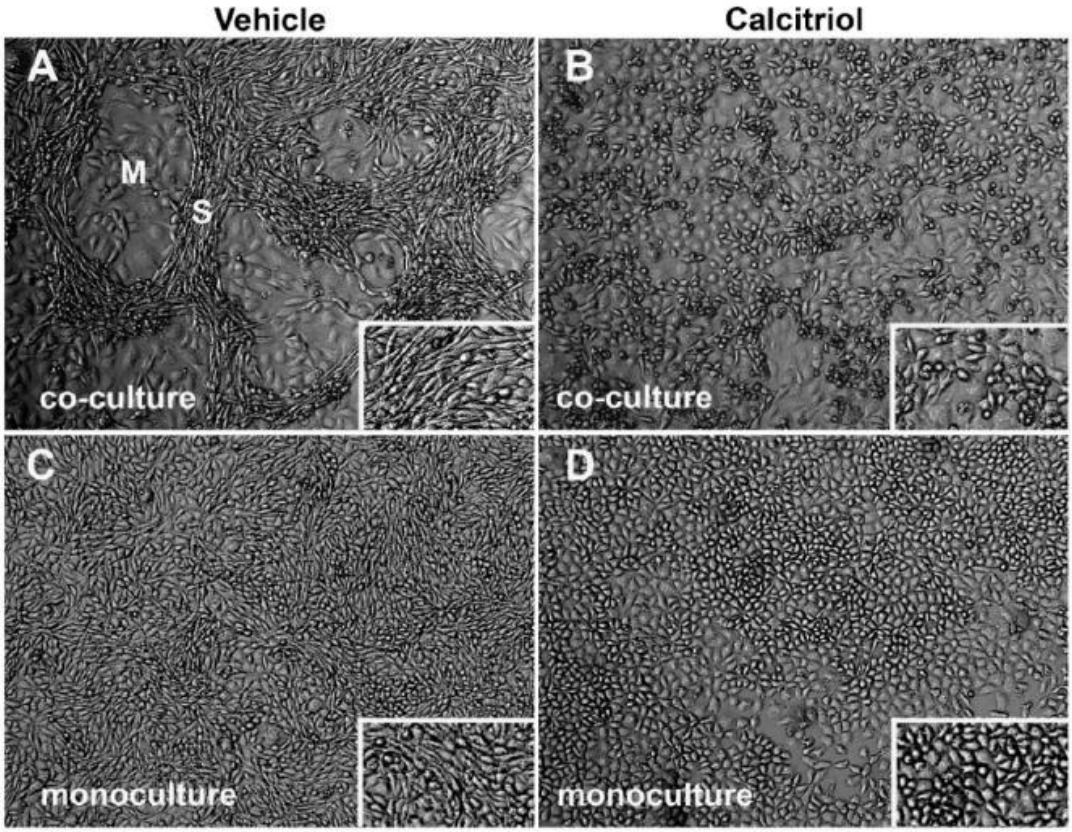


*Suplementaria 1. El calcitriol afecta el fenotipo similar a mesénquima de las células de CMTN tanto en monocultivo como en co-cultivo.*(A) Co-cultivo de células MBCDF-T y endotelio, las células formadoras de red presentan una morfología fusiforme similar a las células de cáncer que hacen EMT. (B) Las células fusiformes pierden su morfología y se vuelven más redondeadas, en presencia del calcitriol [10 nM], y la capacidad de MV se pierde. (C) Morfología típica de las células MBCDF-T. (D) Las células de cáncer en monocultivo también se redondean en presencia del calcitriol.

## 5.7. LITERATURA CITADA

1. García-Quiroz J, García-Becerra R, Santos-Cuevas C, Ramírez-Nava GJ, Morales-Guadarrama G, Cárdenas-Ochoa N, Segovia-Mendoza M, Prado-Garcia H, Ordaz-Rosado D, Avila E, Olmos-Ortiz A, López-Cisneros S, Larrea F, Díaz L. Synergistic Antitumorigenic Activity of Calcitriol with Curcumin or Resveratrol is Mediated by Angiogenesis Inhibition in Triple Negative Breast Cancer Xenografts. Cancers (Basel). 2019 Nov 6;11(11):1739. doi: 10.3390/cancers11111739.

2. Chang, L.C.; Sun, H.L.; Tsai, C.H.; Kuo, C.W.; Liu, K.L.; Lii, C.K.; Huang, C.S.; Li, C.C. 1,25(OH)2 D3 attenuates indoxyl sulfate-induced epithelial-to-mesenchymal cell transition via inactivation of PI3K/Akt/beta-catenin signaling in renal tubular epithelial cells. Nutrition 2020, 69, 110554
3. Chen, P.T.; Hsieh, C.C.; Wu, C.T.; Yen, T.C.; Lin, P.Y.; Chen, W.C.; Chen, M.F. 1alpha,25-Dihydroxyvitamin D3 Inhibits Esophageal Squamous Cell Carcinoma Progression by Reducing IL6 Signaling. Mol. Cancer Ther. 2015, 14, 1365-1375.
4. Hong, R.L.; Spohn, W.H.; Hung, M.C. Curcumin inhibits tyrosine kinase activity of p185neu and also depletes p185neu. Clin. Cancer Res. 1999, 5, 1884-1891.
5. Palange, A.L.; Di Mascolo, D.; Singh, J.; De Franceschi, M.S.; Carallo, C.; Gnasso, A.; Decuzzi, P. Modulating the vascular behavior of metastatic breast cancer cells by curcumin treatment. Front. Oncol. 2012, 2, 161.
6. Ray, S.; Chattopadhyay, N.; Mitra, A.; Siddiqi, M.; Chatterjee, A. Curcumin exhibits antimetastatic properties by modulating integrin receptors, collagenase activity, and expression of Nm23 and E-cadherin. J. Environ. Pathol. Toxicol. Oncol. 2003, 22, 49–58.
7. Gupta, B.; Ghosh, B. Curcuma longa inhibits TNF-alpha induced expression of adhesion molecules on human umbilical vein endothelial cells. Int. J. Immunopharmacol. 1999, 21, 745–757.
8. Ruan, G.X.; Kazlauskas, A. Axl is essential for VEGF-A-dependent activation of PI3K/Akt. EMBO J. 2012, 31, 1692–1703.
9. Karar, J.; Maity, A. PI3K/AKT/mTOR Pathway in Angiogenesis. Front. Mol. Neurosci. 2011, 4, 51.
10. Shao, N.; Lu, Z.; Zhang, Y.; Wang, M.; Li, W.; Hu, Z.; Wang, S.; Lin, Y. Interleukin-8 upregulates integrin beta3 expression and promotes estrogen receptor-negative breast cancer cell invasion by activating the PI3K/Akt/NF-kappaB pathway. Cancer Lett. 2015, 364, 165–172.
11. Hideshima, T.; Nakamura, N.; Chauhan, D.; Anderson, K.C. Biologic sequelae of interleukin-6 induced PI3-K/Akt signaling in multiple myeloma. Oncogene 2001, 20, 5991–6000.
12. Shi, Y.H.; Bingle, L.; Gong, L.H.; Wang, Y.X.; Corke, K.P.; Fang, W.G. Basic FGF augments hypoxia induced HIF-1-alpha expression and VEGF release in T47D breast cancer cells. Pathology 2007, 39, 396–400.
13. Jin, L.; Wessely, O.; Marcusson, E.G.; Ivan, C.; Calin, G.A.; Alahari, S.K. Prooncogenic factors miR-23b and miR-27b are regulated by Her2/Neu, EGF, and TNF-alpha in breast cancer. Cancer Res. 2013, 73, 2884–2896.
14. McCubrey, J.A.; Steelman, L.S.; Bertrand, F.E.; Davis, N.M.; Sokolosky, M.; Abrams, S.L.; Montalto, G.; D'Assoro, A.B.; Libra, M.; Nicoletti, F.; et al. GSK-3 as potential target for therapeutic intervention in cancer. Oncotarget 2014, 5, 2881–2911.

15. Bustanji, Y.; Taha, M.O.; Almasri, I.M.; Al-Ghussein, M.A.; Mohammad, M.K.; Alkhatib, H.S. Inhibition of glycogen synthase kinase by curcumin: Investigation by simulated molecular docking and subsequent in vitro/in vivo evaluation. J. Enzyme Inhib. Med. Chem. 2009, 24, 771–778.
16. Kuttikrishnan, S.; Siveen, K.S.; Prabhu, K.S.; Khan, A.Q.; Ahmed, E.I.; Akhtar, S.; Ali, T.A.; Merhi, M.; Dermime, S.; Steinhoff, M.; et al. Curcumin Induces Apoptotic Cell Death via Inhibition of PI3-Kinase/AKT Pathway in B-Precursor Acute Lymphoblastic Leukemia. Front. Oncol. 2019, 9, 484.
17. Guan, F.; Ding, Y.; Zhang, Y.; Zhou, Y.; Li, M.; Wang, C. Curcumin Suppresses Proliferation and Migration of MDA-MB-231 Breast Cancer Cells through Autophagy-Dependent Akt Degradation. PLoS ONE 2016, 11, e0146553.
18. Proietti, S.; Cucina, A.; D'Anselmi, F.; Dinicola, S.; Pasqualato, A.; Lisi, E.; Bizzarri, M. Melatonin and vitamin D3 synergistically down-regulate Akt and MDM2 leading to TGFbeta-1-dependent growth inhibition of breast cancer cells. J. Pineal Res. 2011, 50, 150–158.
19. Ogiwara, H.; Ui, A.; Shiotani, B.; Zou, L.; Yasui, A.; Kohno, T. Curcumin suppresses multiple DNA damage response pathways and has potency as a sensitizer to PARP inhibitor. Carcinogenesis **2013**, 34, 2486–2497.
20. Loughery, J.; Cox, M.; Smith, L.M.; Meek, D.W. Critical role for p53-serine 15 phosphorylation in stimulating transactivation at p53-responsive promoters. Nucleic Acids Res. **2014**, 42, 7666–7680.

# PARTE 4.

## PERSPECTIVAS DEL PROYECTO: USO COMBINADO DEL CALCITRIOL CON ANTI-ANGIOGÉNICOS SINTÉTICOS EN CMTN

# CAPÍTULO 6.

## EFECTOS DEL CALCITRIOL COMBINADO CON INHIBIDORES DE VEGFR/FGFR SOBRE EL MIMETISMO VASCULAR EN CÉLULAS DE CÁNCER DE MAMA TRIPLE NEGATIVO

***Los resultados de este capítulo se presentaron en EACR Conference: Cellular Bases for patient response to conventional therapies, que tuvo lugar del 1 al 3 de noviembre del presente año en Berlín, Alemania.***

GABRIELA MORALES-GUADARRAMA, EDGAR A. MÉNDEZ-PÉREZ, JANICE GARCÍA-QUIROZ, EUCLIDES AVILA, AND LORENZA DÍAZ. "CALCITRIOL COMBINED WITH VEGFR/FGFR INHIBITORS ABROGATE VASCULOGENIC MIMICRY BY DOWN REGULATING STEMNESS AND MESENCHYMAL TRANSITION OF TRIPLE-NEGATIVE BREAST CANCER CELLS."

***MANUSCRITO EN PREPARACIÓN***

## 6.1. RESUMEN

En los capítulos anteriores identificamos que el eje FGFR/PI3K/Akt es potencialmente una de las principales vías de señalización que regulan la capacidad de las células de CMTN de hacer el MV, y que esta vía y sus blancos río abajo son regulados a la baja por el calcitriol. Además, al evaluar el efecto de calcitriol sobre las redes de interacción proteína-proteína y los procesos biológicos asociados que se predijeron en el análisis de STRING, identificamos que la plasticidad celular (troncalidad y transición epitelio-mesénquima) son parte importante del porqué calcitriol tiene un efecto tan fuerte sobre el MV. Por ello, en estos avances prospectivos evaluamos el efecto de los inhibidores de FGFR/VEGFR, AZD4547, dovitinib y calcitriol, sobre la troncalidad, la EMT y el MV, por separado o en combinación. A la fecha el posible efecto de las moléculas pequeñas empleadas aquí, sobre el MV se desconocen, siendo este es el primer informe sobre la participación de FGFR en el MV, y los efectos del AZD4547 en dicho proceso.

## 6.2. DISEÑO EXPERIMENTAL

La troncalidad se evaluó por medio de ensayos de formación de mamosferas, en superficies de baja adherencia, empleando las mismas dos líneas celulares de CMTN. El efecto de los tratamientos sobre la troncalidad se cuantifico mediante el conteo de aquellas mamosferas con las 3 capas de un esferoide maduro y viable distinguibles. Por otra parte, el efecto de los tratamientos sobre la EMT se evaluó por medio de ensayos de migración por cierre de herida. Finalmente, el efecto de los tratamientos sobre el MV se evaluó como anteriormente se ha descrito.

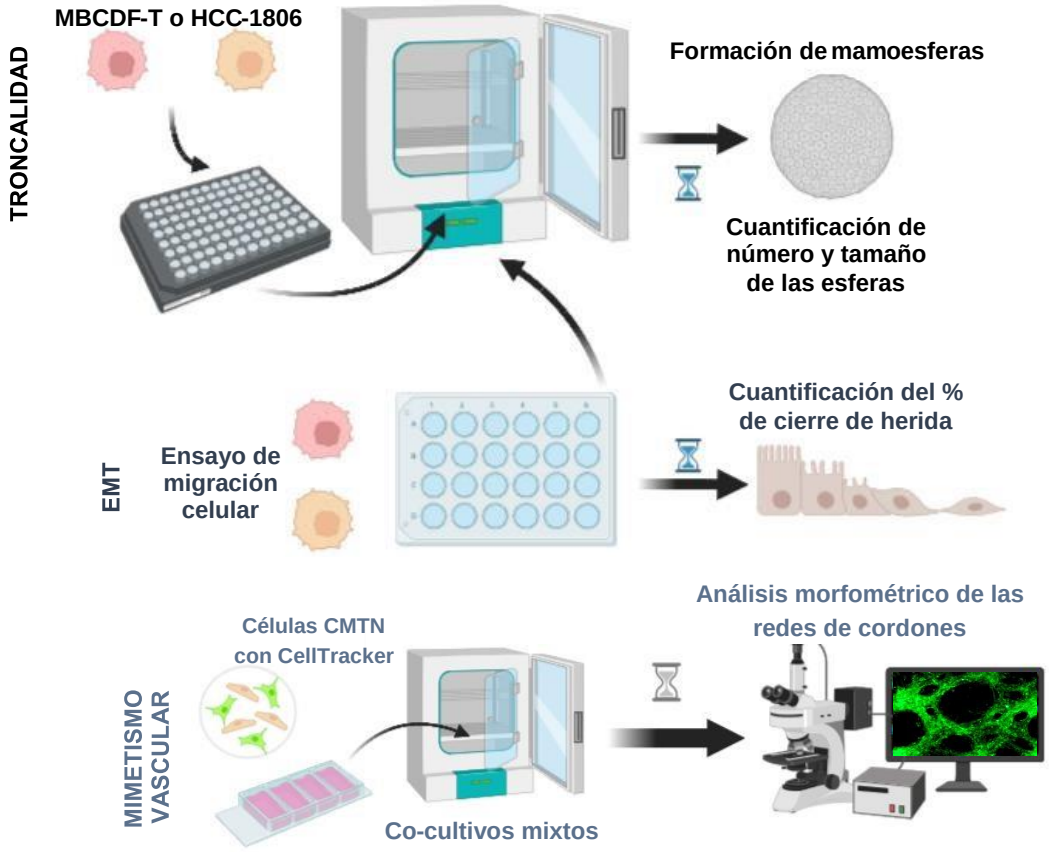


*Evaluación del efecto del calcitriol solo y combinado con inhibidores de VEGFR, dovitinib, y FGFR, AZD4547, sobre la plasticidad celular y el MV.* El efecto sobre la troncalidad se evaluó mientras que la EMT se evaluó por ensayos de migración celular por cierre de herida mediante ensayos de formación de mamoesferas. Los efectos sobre el mimetismo vascular se evaluaron por ensayos de tubulogénesis en co-cultivo y la cuantificación de las estructuras formadas. Cada experimento se repitió por triplicado biológico y duplicado técnico.

## 6.3. RESULTADOS

***El tratamiento con calcitriol mejora la inhibición de la EMT al incrementar el efecto inhibitorio de dovitinib y AZD4547 por separado.***

Las células MBCDF-T fueron tratadas con concentraciones bajas de Calcitriol [10nM], dovitinib [30nM] y AZD4547 [3μM]. Como se observa en la Figura 16a, las células MBCDF-T fueron muy sensibles al efecto de los compuestos sobre la migración celular, parámetro asociado con la EMT. Como se observa en la Figura 16b, los tratamientos por separado disminuyeron significativamente el cierre de herida, respecto al vehículo. Sin embargo, la combinación con calcitriol mejoró efecto de los compuestos por separado.

Por otra parte, en las células HCC-1806 se emplearon las mismas concentraciones que en MBCDF-T de los tratamientos (Figura 16c). En esta línea celular los tratamientos por separado inhibieron significativamente la migración celular; sin embargo, el efecto logrado entre tratamientos fue muy similar. No obstante, la combinación de calcitriol con dovitinib o AZD4547 mejoró la inhibición de cierre de la herida en HCC-1806 (Figura 16d).

De manera general, las células MBCDF-T a lo largo del estudio mostraron mayor sensibilidad, en respuesta a este proceso en particular es importante notar que después de las combinaciones, fue el dovitinib (inhibidor multiblanco de VEGFR/FGFR/PDGFR, c-kit, etc) el que más afecto la migración celular, seguido del AZD4547 (inhibidor de FGFR1-3) y de calcitriol. Esto sugiere la participación de otras vías de señalización además de las mediadas por FGFR, puesto que cuando estos receptores son específicamente bloqueados con el AZD4547, la migración no se ve abatida tan drásticamente. Precisamente es la combinación de dovitinib con calcitriol la que mejor efecto tiene, sugiriendo que los efectos pro-diferenciantes del calcitriol y la inhibición de distintas cascadas de señalización mediadas por RTKs podrían ser los mecanismos involucrados en inhibir la migración celular en este modelo celular.

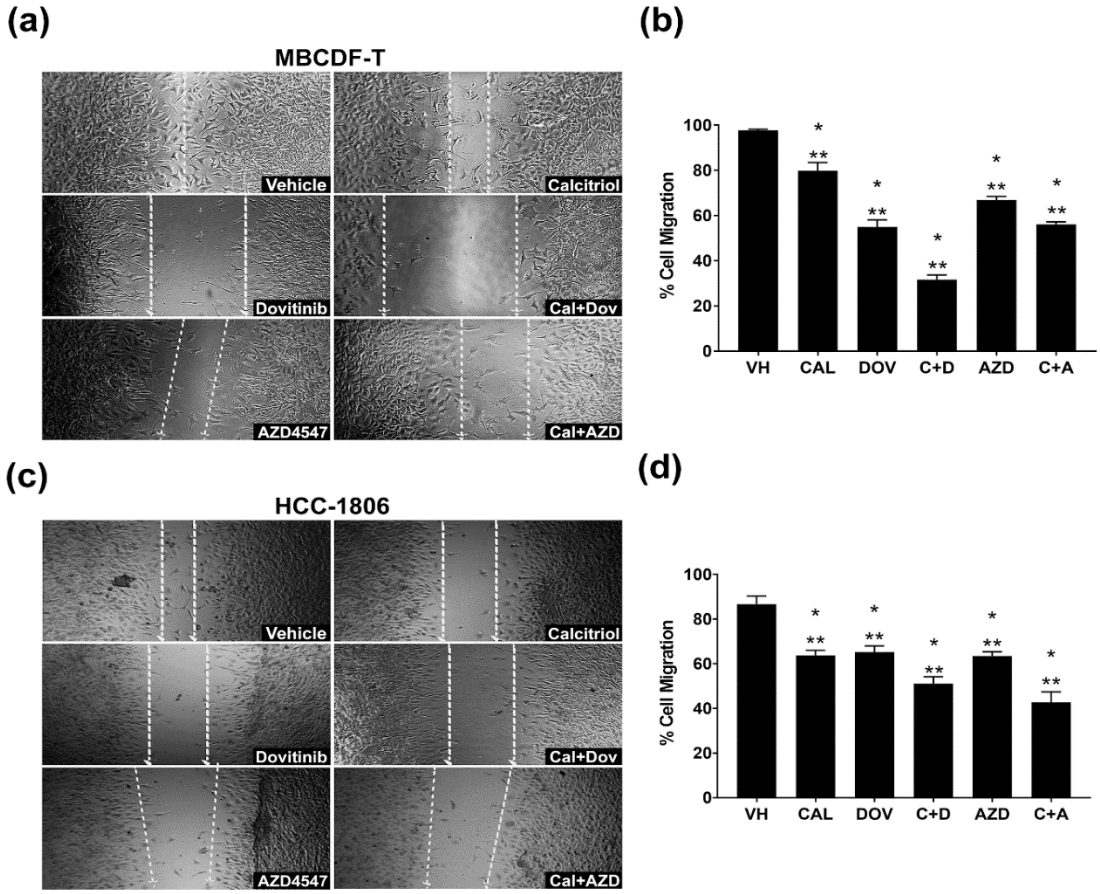


*Figura 16. Efecto del calcitriol y los inhibidores de VEGFR/FGFR, dovitinib y AZD4547, solos o en combinación, sobre la migración celular de las células de CMTN, MBCDF-T y HCC-1806.* (a) Imágenes representativas del cierre de herida a las 48 horas en la línea MBCDF-T expuesta a calcitriol [10nM], dovitinib [30nM] y AZD4547 [3μM]. Aumento 4x. (b) Media del porcentaje de migración ± SEM por tratamiento. Las diferencias significativas respecto al vehículo, (*p≤0.001 vs VH) o a cada tratamiento en combinación/separado (**p≤0.001 Cal vs C+D, vs C+A, Dov vs C+D, AZD vs C+A) se calcularon por ANOVA de una vía en GraphPad. (c) Imágenes representativas de la migración celular de las células HCC-1806 en presencia de los tratamientos (48 horas). (d) Representación gráfica del efecto de los tratamientos sobre la migración celular, si bien los tratamientos por separado inhibieron significativamente la migración celular, el efecto logrado entre tratamientos fue muy similar. La combinación de calcitriol con dovitinib o AZD4547 mejoró la inhibición de cierre de la herida en HCC-1806, n=8.

*La inhibición de FGFR afecta drásticamente el mimetismo vascular*

En presencia del calcitriol, observamos cómo las esferas formadas son prácticamente inviables puesto que la mayoría de las células están muertas. Por su parte el dovitinib tuvo un efecto drástico en la formación de mamosferas, sin embargo dicho efecto fue potenciado en presencia del calcitriol, donde observamos cómo inclusive muchas de las células ya no fueron capaces de auto-agregarse y se encuentran flotando en el pozo. Finalmente, el AZD4547 tuvo un efecto importante en la formación de mamosferas, prácticamente inhibiendo por completo esta capacidad, interesantemente se observa como en superficies de baja adherencia y en presencia del inhibidor de FGFR las células intentan agruparse en cordones pero mueren a los 5 días. En contraste, en combinación con calcitriol, las esferas formadas están prácticamente muertas o disgregadas a los 5 días. Todos los tratamientos inhibieron significativamente el número de esferas por pozo, respecto al vehículo (Figura 17c, *p≤0.001 vs VH) y entre tratamientos (**p≤0.001 Cal vs C+D, vs C+A, Dov vs C+D, AZD vs C+A).

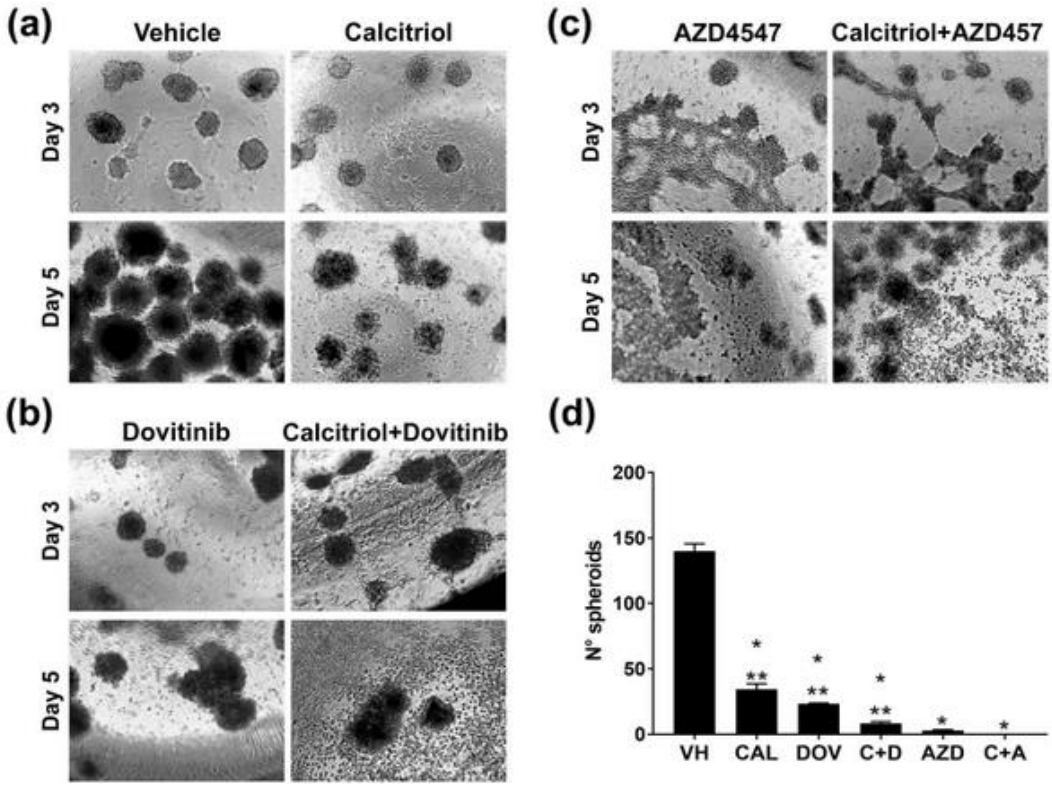


*Figura 17. Efecto de los tratamientos solos o en combinación sobre la troncalidad, evaluada por la formación de esferas en superficies de baja adherencia, en las células MBCDF-T.* ***(a) Imágenes representativas, en contraste de fases (10x), de esferas a los 3 y 5 días de incubación. (b) Todos los tratamientos inhibieron significativamente el número de esferas por pozo, respecto al vehículo, (*p≤0.001 vs VH) y entre tratamientos (**p≤0.001 Cal vs C+D, vs C+A, Dov vs C+D, AZD vs C+A).***

***El calcitriol mejora supera la resistencia al MV del dovitinib y mantiene el efecto anti-MV del AZD4547.***

Hasta el momento el efecto de los inhibidores dovitinib y AZD4547 sobre el mimetismo vascular se desconoce. Sin embargo, se sabe que algunos inhibidores de la angiogénesis similares, son capaces de inducir el MV en CMTN, por ello es interesante ver que en las células MBCDF-T tratadas con dovitinib la formación de redes no se ve afectada a nivel de la citoarquitectura (Figura 18.a) sino tampoco a nivel de la cantidad de segmentos cuantificados por campo visual (Figura 18.b). Sin embargo, esta "resistencia" es abatida cuando las células son expuestas al calcitriol combinado con dovitinib, donde sí se observa una disminución significativa de la presencia de cordones en red (Figura 18.b). Por el contrario, AZD4547 tuvo en efecto incluso mayor que el de calcitriol solo, abatiendo casi por completo la formación de redes de cordones en los co-cultivos (Figura 18.), mientras que en su combinación con calcitriol, las estructuras están prácticamente ausentes. Este resultado sugiere aunado a lo que observamos previamente sobre la formación de mamosferas, podría sugerir la gran dependencia de la troncalidad y la plasticidad celular en general, en estas células, para poder mantener la capacidad de hacer MV en los co-cultivos. Son necesarios más experimentos y la validación del efecto sobre la vía que suponemos es la principal involucrada en la capacidad de hacer MV de las células MBCDF-T, FGFR/PI3K/AKT. Hasta el momento, los resultados sugieren que la combinación de calcitriol con estos agentes podría ser beneficiosa para las pacientes de CMTN que son candidatas a recibir terapias anti-angiogénicas, para prevenir la generación de resistencia y mejorar la respuesta terapéutica a estos tratamientos. Además, el uso combinado de estas moléculas podría ser de ayuda también para aquellos pacientes que de manera clásica reciben anti-angiogénicos, para disminuir las dosis efectivas y mejorar el pronóstico de dichos pacientes. Lo ideal para escalar dichos resultados sería realizar los estudios *in vivo* de la combinación de estas terapias y evaluar el efecto que tienen sobre la vascularización tumoral en CMTN.

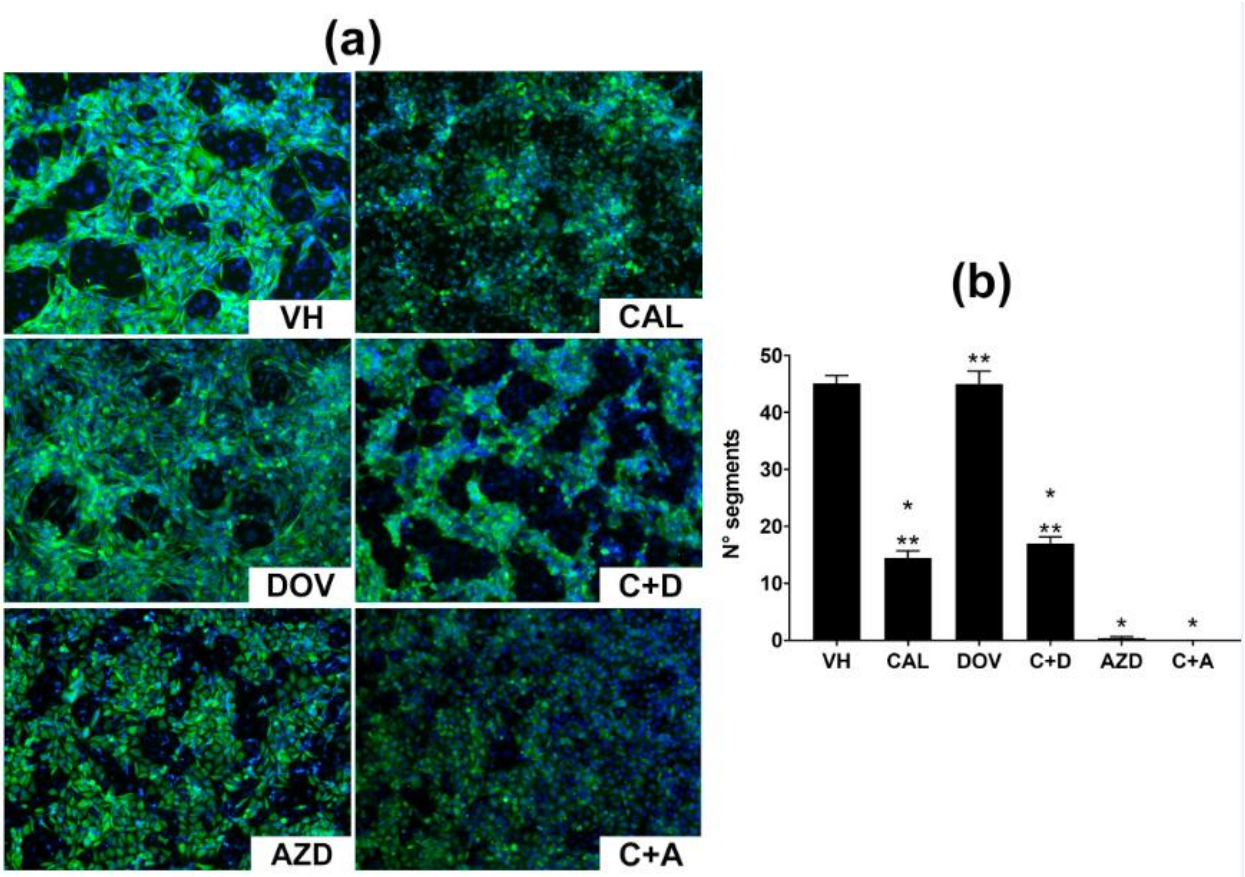


*Figura 18. Efecto de los tratamientos con calcitriol, dovitinib y AZD4547, solos o en combinación, sobre el mimetismo vascular en co-cultivos de las células de cáncer de mama triple negativo, MBCDF-T con células endoteliales.* (a) Imágenes representativas de las redes de cordones formadas por las células de cáncer MBCDF-T co-cultivadas con endotelio en presencia de los tratamientos solos o en combinación. (b) En la gráfica de barras se muestra el promedio de segmentos por campo visual (± SEM), observamos como AZD solo y combinado (C+A), seguido de calcitriol y calcitriol combinado con dovitinib (C+D) fueron los grupos con mayor efecto. Dovitinib fue el único de los compuestos que no inhibió ni afectó el mimetismo vascular en co-cultivos. (*p≤0.001 vs VH; ** p≤0.001 Cal vs C+D, vs C+A). n=6

## 6.4. CONCLUSIONES PRELIMINARES

El calcitriol mejora la respuesta a los efectos anti-migratorios, anti-tumorales, la inhibición de la troncalidad celular y la inhibición del propio MV en las células de cáncer de mama triple negativo, en combinación con inhibidores sintéticos de la angiogénesis, dirigidos contra VEGFR/FGFR.

# PARTE 5.

## PRODUCCIÓN CIENTÍFICA

# PARTICIPACIÓN EN CONGRESOS

*RESÚMENES Y POSTERS CON RESULTADOS DE LA INVESTIGACIÓN DOCTORAL, PRESENTADOS EN CONGRESOS NACIONALES E INTERNACIONALES DURANTE MI ESTANCIA EN EL LABORATORIO DE LA DRA. LORENZA DÍAZ NIETO.*

## VITAMIN D WORKSHOP 2022

Realizado en Austin, Texas del 6 al 9 de septiembre de 2022.

*Presentación en póster (co-autora).*

**# 34 CREB EXPRESSION AND IMMUNOLOCALIZATION WERE DIFFERENTIALLY REGULATED BY CALCITRIOL AND CURCUMIN WHILE INHIBITING VASCULOGENIC MIMICRY IN BREAST CANCER CELLS COCULTURED WITH ENDOTHELIAL CELLS.** Lorenza Diaz[1], Gabriela Morales-Guadarrama[1], Edgar Armando Méndez-Pérez[1], Janice García-Quiroz[1], Rocío García-Becerra[2], Euclides Avila[1], [1]Instituto Nacional de Ciencias Médicas y Nutrición Salvador Zubirán, [2]Instituto de Investigaciones Biomédicas, Universidad Nacional Autónoma de México

Vasculogenic mimicry (VM) is the process undertaken by cancer cells to form channel-like structures under hypoxic conditions and is generally associated with metastasis, treatment resistance, and bad prognosis. Recently, we showed that endothelial-dependent VM formation in triple-negative breast cancer cells (TNBC) was strongly inhibited by calcitriol, curcumin, and to a greater extent by their mixture. Calcitriol changed cell morphology from spindle to cobblestone shape, while curcumin diminished the VM 3D structure. These two parameters suggest the loss of epithelial-to-mesenchymal phenotype, a VM hallmark. Importantly, the treatments dephosphorylated several active kinases/proteins, especially those involved in the PI3K/Akt pathway. Among them, the cyclic AMP-response element-binding protein (CREB) was found to be highly activated in untreated co-cultures, while it was significantly deactivated by the compound's combination. Since the overexpression of CREB has been linked to the generation of tumor stem cells, which are thought to be responsible for VM-formation, in this study we aimed at investigating the regulation of CREB protein expression by calcitriol, curcumin and their combination in a model of endothelial-induced VM in TNBC cells. VM was evaluated by morphometric parameters including the formation of cord-like tubular structures by cancer cells. CREB expression and cell localization were studied by immunocytochemistry. As a control, we used the PI3K inhibitor LY294002. Curcumin, calcitriol, and LY294002 significantly reduced the number of segments and meshes compared to controls. Bright-field images merged with fluorescently labeled CREB showed that calcitriol, at clinically achievable concentrations, significantly reduced CREB protein expression, while curcumin changed its localization from the cell nuclei to the cytoplasm. The compounds' combination produced a similar inhibitory effect as LY294002 upon VM structures, while downregulated CREB expression to a greater extent. Our results suggest that the anti-VM activity of calcitriol and curcumin co-treatment involves the downregulation of CREB protein expression and its migration from the cell nuclei to the cytoplasm. Thus, the compounds' combination could represent a new therapeutic strategy to inhibit VM in TNBC tumors. This work was supported by CONACYT México, grant A1-S-10749 to L. Díaz.

## XXXIII NATIONAL SMB MEETING

Realizado en Mérida, Yucatán del 16 al 21 de octubre de 2022.

*Presentación en póster (autora principal, expositora)*


### Vasculogenic mimicry of triple negative breast cancer is inhibited by calcitriol and curcumin through inhibition of PI3K/AKT pathway

Gabriela Morales-Guadarrama[1], Edgar A. Méndez-Pérez[1], Janice García-Quiroz[1], Euclides Avila[1], Rocío García-Becerra[2], Fernando Larrea[1], Lorenza Díaz[1]

[1]Departamento de Biología de la Reproducción Dr. Carlos Gual Castro, Instituto Nacional de Ciencias Médicas y Nutrición Salvador Zubirán, Vasco de Quiroga No. 15, Belisario Domínguez Sección XVI, Tlálpan 14080, Ciudad de México, México
Tel. (525) 554 87 09 00 ext. 2417, e-mail: gabriela.mguadarrama@gmail.com
[2]Departamento de Biología Molecular y Biotecnología, Instituto de Investigaciones Biomédicas, Universidad Nacional Autónoma de México, Ciudad de México 04510, México; Av. Universidad 3000, Coyoacán, 04510, Ciudad de México, México,

**Abstract:**

Neo-vascularization is essential for tumor growth and dissemination. The formation of channel-like structures by cancer cells, namely vasculogenic mimicry (VM), is generally associated with epithelial-to-mesenchymal transition, metastasis and resistance to therapy in highly aggressive tumors, such as the triple-negative breast cancer (TNBC). The role of tumor-endothelial interactions on the microcirculatory network formation and the effect of natural products for VM therapeutic purposes remain poorly investigated. To address these issues, we developed an *in vitro* VM model by co-culturing endothelial cells (EAhy.926) with TNBC cells (MBCDF-T or HCC-1806), and studied the effects of curcumin, a natural phytochemical, and calcitriol, the active vitamin D metabolite, on VM formation. We considered these compounds given previous studies showing that their combination abrogated TNBC tumor growth and angiogenesis *in vivo*. Results: Co-culture of EAhy.926, but not of stromal cells, with MBCDF-T, HCC-1806 and trophoblastic cells, triggered tubular-like structures formation, suggesting participation of endothelium in both physiological and pathological VM. Tube-like formation was accompanied by increased VEGFR2 and FGFR1 expression, as well as up regulation of pro-angiogenic molecules in the co-cultures. Interestingly, the VM capacity of TNBC cells was readily inhibited by calcitriol, and to a lesser extent by curcumin; however, their combination further inhibited VM. Mechanistically, treatments inhibited the phosphorylation of several proteins, including those involved in the FGFR/PI3K/Akt pathway. Specific pharmacological inhibition of FGFR or PI3K suggested that this is the main cascade involved in VM of TNBC cells. Our results support the possibility to use these natural compounds as adjuvants for VM inactivation in patients with highly malignant tumors inherently capable of forming VM, or in patients with ongoing anti-angiogenic therapy, warranting further *in vivo* studies.

October 16-21, 2022
Mérida, Yucatán
Hotel Fiesta Americana

## CELLULAR BASES FOR PATIENT RESPONSE TO CONVENTIONAL CANCER THERAPIES, EACR CONFERENCE

Realizado en Berlín, Alemania del 1 al 3 de noviembre de 2022.

*Presentación en póster (autora principal, expositora)*

# Calcitriol combined with VEGFR/FGFR inhibitors abrogate vasculogenic mimicry by downregulating stemness and mesenchymal transition of triple-negative breast cancer cells

Euclides Ávila[1], Lorenza Díaz[1], Janice García-Quiroz[1], Edgar Armando Méndez-Pérez[1], Silvia Gabriela Morales-Guadarrama[1,2]

[1] Instituto Nacional de Ciencias Médicas y Nutrición Salvador Zubirán, Mexico City, MEXICO. [2] Universidad Nacional Autónoma de México, Mexico City, MEXICO

In highly aggressive tumors, such as the triple-negative breast cancer (TNBC), neoplastic cells may develop an alternative microcirculatory system by forming channel-like structures through a process known as vasculogenic mimicry (VM). VM can be driven by antiangiogenic treatments and tumor microenvironment-derived factors. Recently we reported that calcitriol, the most active metabolite of Vitamin D, inhibited VM of TNBC cells by dephosphorylating several kinases involved in the PI3K/Akt signaling pathway. Further, calcitriol has potent antitumor effects on TNBC and can enhance anti-neoplastic activity of antiangiogenic compounds such as the VEGFR and FGFR inhibitors dovitinib and AZD4547, on tumor growth and angiogenesis. However, the role of these receptor tyrosine kinase inhibitors (RTKIs) upon VM on TNBC, alone or in combination with calcitriol remains unknown. Therefore, in this study we aimed to investigate the effect of dovitinib and AZD4547, alone or combined with calcitriol, on the VM capacity of TNBC cells. Since stemness and mesenchymal transition are the main plasticity-associated VM hallmarks, we evaluated the treatments' effect on spheroid formation and migration of MBCDF-T and HCC-1806 TNBC cell lines. Furthermore, VM capacity was assessed by tubulogenesis assays on co-cultured TNBC cells with endothelial cells. Among all compounds tested, AZD4547 was the most efficient one to inhibit VM, as well as spheroid formation and cell migration in both TNBC cell lines, suggesting a main role of FGFR on the VM capacity of TNBC. This is the first report on the participation of FGFR on VM as well as the effects of AZD4547 regarding this. Remarkably, calcitriol enhanced the anti-VM effects of the RTKIs. Altogether, our results suggest that calcitriol as adjuvant, could be a promising option for TNBC patients undergoing anti-angiogenic therapy by preventing VM as a resistance mechanism. This work was supported by CONACYT México, grant A1-S-10749 to LD.

# MANUSCRITOS PUBLICADOS

A CONTINUACIÓN SE PRESENTAN ARTÍCULOS EN LOS QUE PARTICIPÉ DURANTE MI ESTANCIA EN EL LABORATORIO DE LA DRA. LORENZA DÍAZ NIETO

# MANUSCRITOS PUBLICADOS CON DATOS DERIVADOS DE LA INVESTIGACIÓN DE TESIS DOCTORAL

cells

MDPI

*Review*

# Vasculogenic Mimicry in Breast Cancer: Clinical Relevance and Drivers

**Gabriela Morales-Guadarrama [1], Rocío García-Becerra [2], Edgar Armando Méndez-Pérez [1], Janice García-Quiroz [1], Euclides Avila [1] and Lorenza Díaz [1,*]**

[1] Departamento de Biología de la Reproducción, Instituto Nacional de Ciencias Médicas y Nutrición Salvador Zubirán, Ciudad de México 14080, Mexico; gabriela.mguadarrama@gmail.com (G.M.-G.); edgar.mendez.p3@gmail.com (E.A.M.-P.); janice.garciaq@incmnsz.mx (J.G.-Q.); euclides.avilac@incmnsz.mx (E.A.)

[2] Departamento de Biología Molecular y Biotecnología, Instituto de Investigaciones Biomédicas, Universidad Nacional Autónoma de México, Ciudad de México 04510, Mexico; rocio.garciab@iibiomedicas.unam.mx

* Correspondence: lorenza.diazn@incmnsz.mx; Tel.: +52-(55)-5487-0900

**Abstract:** In solid tumors, vasculogenic mimicry (VM) is the formation of vascular structures by cancer cells, allowing to generate a channel-network able to transport blood and tumor cells. While angiogenesis is undertaken by endothelial cells, VM is assumed by cancer cells. Besides the participation of VM in tumor neovascularization, the clinical relevance of this process resides in its ability to favor metastasis and to drive resistance to antiangiogenic therapy. VM occurs in many tumor types, including breast cancer, where it has been associated with a more malignant phenotype, such as triple-negative and HER2-positive tumors. The latter may be explained by known drivers of VM, like hypoxia, TGFB, TWIST1, EPHA2, VEGF, matrix metalloproteinases, and other tumor microenvironment-derived factors, which altogether induce the transformation of tumor cells to a mesenchymal phenotype with a high expression rate of stemness markers. This review analyzes the current literature in the field, including the participation of some microRNAs and long noncoding RNAs in VM-regulation and tumorigenesis of breast cancer. Considering the clinical relevance of VM and its association with the tumor phenotype and clinicopathological parameters, further studies are granted to target VM in the clinic.

**Keywords:** vasculogenic mimicry; breast cancer; tumor neovascularization; HER2; triple-negative



**Citation:** Morales-Guadarrama, G.; García-Becerra, R.; Méndez-Pérez, E.A.; García-Quiroz, J.; Avila, E.; Díaz, L. Vasculogenic Mimicry in Breast Cancer: Clinical Relevance and Drivers. *Cells* **2021**, *10*, 1758. https://doi.org/10.3390/cells10071758

Academic Editor: Francesco Pezzella

Received: 17 June 2021
Accepted: 8 July 2021
Published: 12 July 2021



## 1. Introduction

*What Is Vascular Mimicry?*

Tumor growth and dissemination depend on vascularization, a process that is achieved through vasculogenesis and/or angiogenesis. Vasculogenesis is de novo blood vessel formation by newly differentiated endothelial cells (ECs), while angiogenesis is the formation of blood vessels from pre-existing ones, either by sprouting or intussusception [1]. Intussusception refers to the formation of pillars inside the blood vessel, resulting in its division into segments [2]. In the context of cancer, both vasculogenesis and angiogenesis are regulated by microenvironment-derived factors, tumor heterogeneity, cell–cell interactions (including malignant and non-transformed cells), as well as modifications on extracellular matrix (ECM) components [3]. In addition, there are alternative non-angiogenic mechanisms used by tumor cells to obtain nutrients and oxygen and to disseminate to distant sites, for instance vessel co-option, which consists in the hijacking of pre-existing blood vessels from non-tumoral surrounding tissue [4]. While all these processes and their related pathways play an essential role in the growth, proliferation, migration, invasion, and metastasis of highly aggressive tumors, they are not the only mechanisms by which tumors generate vasculature and escape routes [5,6]. In 1999, Maniotis and collaborators described for the

first time an endothelial-independent vascularization mechanism in highly aggressive and metastatic uveal and cutaneous melanoma tumors. They observed the presence of patterned networks of interconnected loops and cord formation, composed of cancer cells and ECM that stained with the periodic acid-Schiff (PAS) reagent, but that in relation to EC markers such as CD31 or factor VIII-related antigen, showed weak, focal, and discontinuous staining. Erythrocytes could be found inside these structures, suggesting that they actually conducted blood and represented an intratumor microcirculatory system. Moreover, it was shown that highly invasive M619 human melanoma cells were able to form three-dimensional channel-like structures resembling vascular networks. This process was termed "vasculogenic mimicry" (VM) [7–10].

Vascular channels in VM share several characteristics with endothelial-dependent vasculature; however, distinctive features differentiate them (Table 1). For instance, ECs express vascular endothelial (VE)-Cadherin, also known as CD144, the major molecule related to cell–cell adhesion in endothelial adherent junctions. However, in cancer cells capable of forming VM, VE-Cadherin is aberrantly expressed and seems to be involved in a different function, namely, the acquisition of tubule-like structures [11]. Even if at present time there is no infallible biomarker for VM channels identification, some specific characteristics and the expression of particular markers associated with these cellular arrangements have been described (Table 1).

**Table 1.** Distinctive features/markers between vasculogenic mimicry and angiogenesis.

| Vasculogenic Mimicry | Angiogenesis | References |
|---|---|---|
| Formation of vascular channels from cancer stem cells (tumor cells). | Development of new blood vessels and capillaries from pre-existing ones. | [1,12] |
| Patterned networks of interconnected loops and cords formation | Formation by sprouting or intussusception | [1,7] |
| Formed by tumor cells and cancer stem cells | Formed by endothelial cells | [7] |
| Aberrant expression of VE-Cadherin | VE-Cadherin localization in cell membranes | [13] |
| PAS+, $CD31^{-/low}$ staining | $PAS^{-/low}$, CD31+ staining | [7] |
| Factor VIII-related antigen negative or low | Factor VIII-related antigen highly positive | [7] |
| Unaffected by endostatin and other antiangiogenic factors | Inhibited by antiangiogenic factors | [14,15] |
| EPHA2, TIE1, LAMC2, overexpression | EPHA2, TIE1, LAMC2 generally negative. | [16] |
| Express stemness markers, e.g., CD133, ALDH1 | CD133 positivity mostly in endothelial precursor cells | [17–20] |
| More abundant in poorly differentiated tumors, such as HER2+ and TNBC | Present in embryogenesis, wound healing and tumor growth | [16,21] |

There are two types of VM described up to now. The tubular type and the patterned matrix type [22] (Figure 1). In vitro, the first type refers to networks of cellular cords above a thin matrix, encircling cell-free spaces (Figure 1a). In vivo, this type would appear as matrix "rivers" that may arrange as parallel PAS+ ECM deposits (Figure 1b). This matrix is produced by cancer cells. In some cases, PAS+ tumor endothelial-like cells can be found forming cords or lining blood channels. In the second type, PAS+ ECM patterns enclose packs of tumor cells wedged into the matrix arrays (Figure 1c,d). This last one is characteristic of highly invasive tumors [22]. It may be possible that the patterned type gives rise to the tubular type, after the enclosed cells die. In Figure 2, we provide photographs depicting VM-structures formed in vitro and in vivo by the triple-negative breast cancer (TNBC) cell line MBCDF-Tum, reported as highly tumorigenic [23] (Figure 2).

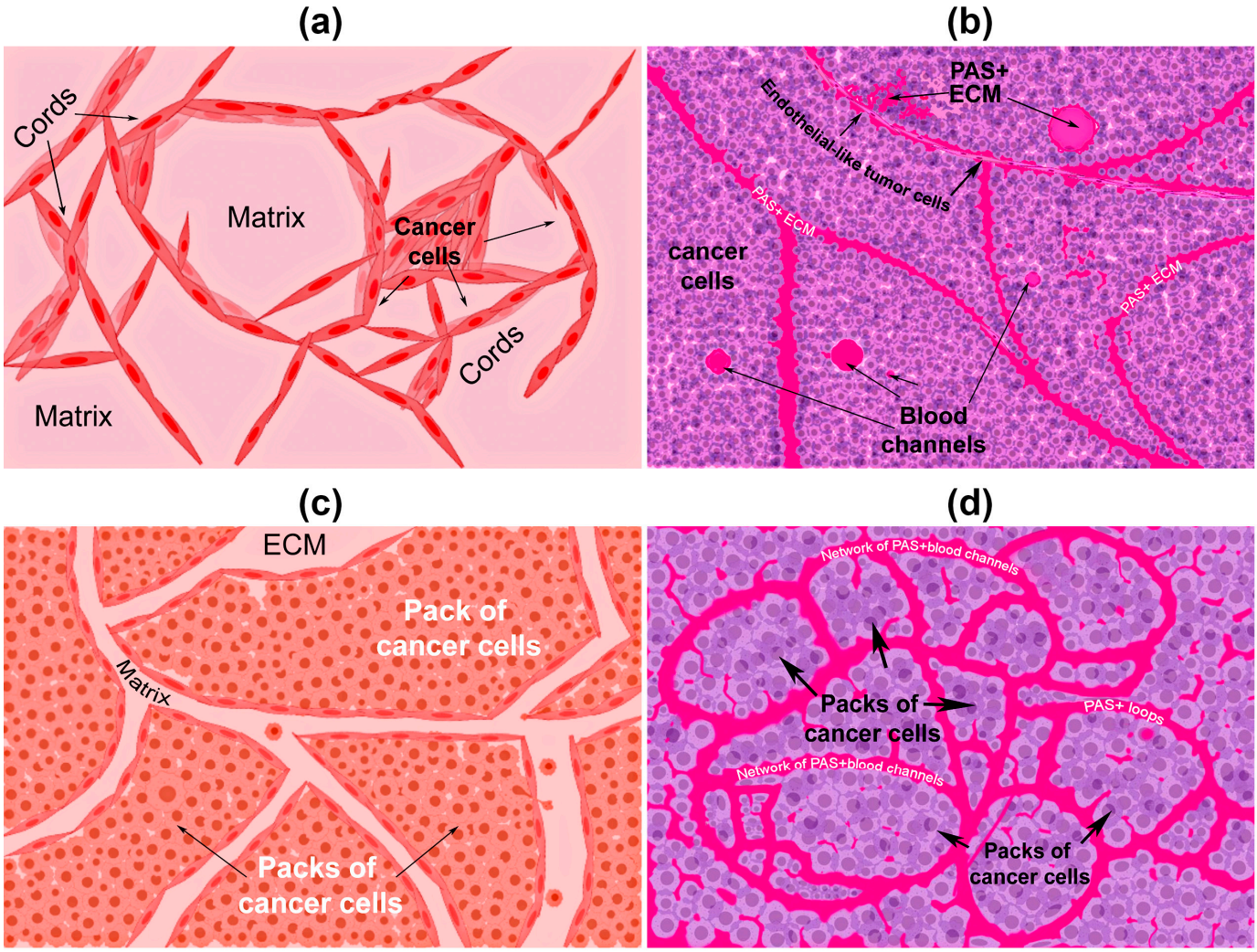


**Figure 1.** Graphical representation of the types of vasculogenic mimicry structures formed in vitro and in vivo by cancer cells. (**a**) In vitro tubular type. Is formed by networks of cellular cords encircling cell-free spaces above a matrix rich in collagen such as Matrigel. Tumor cells aligned in cords or tubular-like interconnected structures are depicted. (**b**) In vivo tubular type (parallel PAS+ patterned). Deposits of PAS+ proteoglycan/laminin-enriched matrix derived from cancer cells resembling "matrix rivers" may contain PAS+ tumor cells able to form channels and may be flanked by endothelial-like tumor cells. (**c**) In vitro patterned matrix type. Flattened tumor cells lodged into the matrix form packages of cells that deposit matrix enriched in collagen, laminin, and proteoglycans. Tumor endothelial-like cells may be found surrounding the packs. (**d**) In vivo patterned matrix type (network or back-to-back loops PAS+ patterned). Several layers of extracellular matrix rich in laminin, fibronectin, and collagens IV and VI form loops surrounding packs of tumor cells.

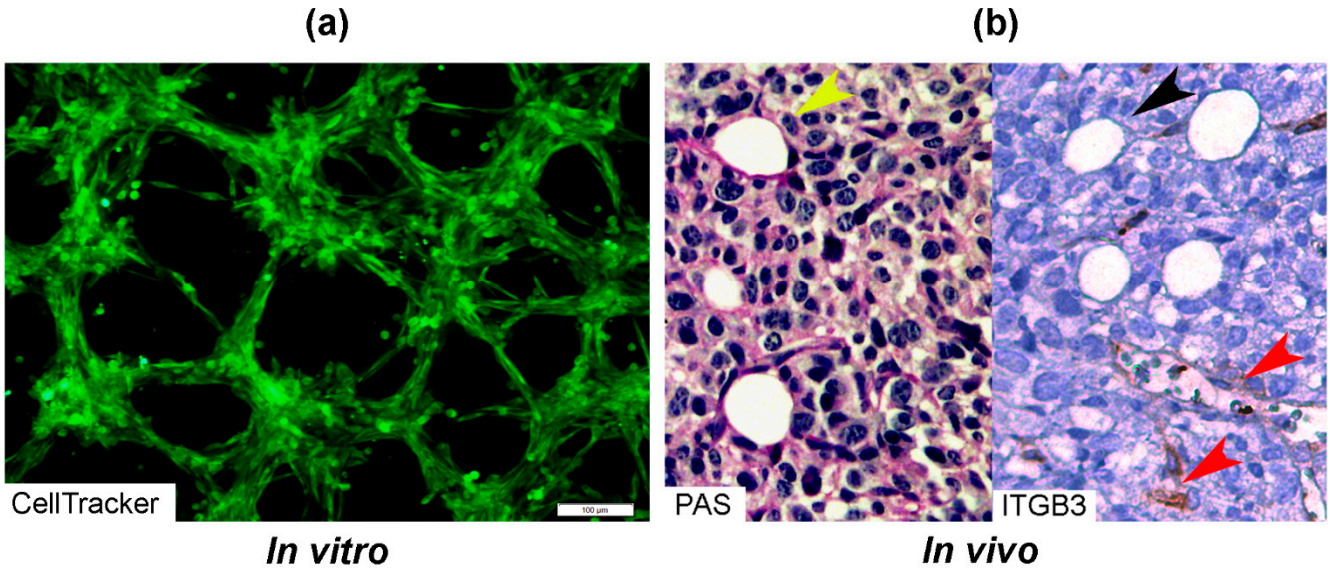


**Figure 2.** Photographs of vascular mimicry structures formed by the TNBC cell line MBCDF-Tum in vitro and in vivo. (**a**) MBCDF-Tum cells were labeled using Cell tracker-green (Abcam) and photographed by epifluorescence microscopy at 24 h of seeding (10 magnification, Olympus BX51). (**b**) MBCDF-Tum cells xenografted in nude mice generated VM-forming tumors. VM structures (yellow arrow heads) were identified by PAS-staining (magenta color, left side of the picture) in a tumor section. In the right part of the picture, a similar section of the same tumor was stained for Integrin-β3 (ITGB3) as an endothelial marker, identifying tumor endothelial-vasculature (brown staining, red arrow heads) in a hot spot of ITGB3-negative VM channels (black arrow heads) (40 magnification).

## 2. First Highlights of VM in Breast Cancer

VM has been identified in numerous types of highly aggressive tumors including breast cancer. Only two years later from the first report of VM in melanoma, a group in Japan identified the presence of blood pooling without a lining of ECs on hyper vascularized xenografts of inflammatory breast cancer. Remarkably, these cells were able to form tube-like structures and loops in vitro, and were associated with lung metastasis in vivo, representing the first evidence of VM in breast cancer [24]. These results helped to establish the relationship between angiogenesis and VM. Shirakawa et al. observed that the hyper vascularized zone in the tumor periphery contained vessels lined by ECs positive to murine CD31, consistent with angiogenesis, while the central highly hypoxic area of the tumor exhibited channels that were PAS positive, presented weak expression of human integrin $\alpha_v\beta_3$ and lacked ECs, consistent with VM. Altogether, this suggested that in some instances, tumors can develop hybrid vascular networks combining angiogenesis and VM to efficiently obtain oxygen and nutrients [25,26]. In addition, structural heterogeneity (mosaic vessels) has also been described in solid tumors, including breast cancer, where a vessel may be lined by ECs in some parts and by tumor cells in others, forming hybrid vascular structures associated with intravasation and systemic dissemination of cancer cells [27]. Since it has been demonstrated that VM can enhance metastasis after an anti-angiogenic treatment [28], research in the VM field will surely improve cancer therapeutics.

## 3. Clinical Relevance of VM in Breast Cancer and Association with Clinicopathological Parameters

There is no doubt that a major drawback of anti-angiogenic treatment is the formation of VM. Indeed, by inducing hypoxia, VM may be favored, which in turn enhances distant metastasis [28,29]. Notably, the angiogenesis inhibitor endostatin readily inhibits proangiogenic factors such as vascular endothelial growth factor (VEGF), fibroblast growth factor 2 (FGF2), matrix metalloproteinases (MMPs), and hypoxia-inducible factor 1-α (HIF1A), blocking endothelial tube formation. However, endostatin does not affect VM-forming

cells, which after being exposed to this collagen-derived factor remain fully active and capable to configure vascular channels [14]. Other antiangiogenic factors have shown similar results [15], suggesting a differential response of EC-dependent angiogenesis and cancer-dependent VM channels formation. In addition, as with the well-established relationship between microvascular density and metastasis in invasive breast cancer [30], VM also has been associated with malignant cells dissemination and bad prognosis, including higher recurrence, lower survival, larger tumor size, and poorer differentiation grade [16,25,31,32], linking this feature to a more malignant breast cancer phenotype [25,31,32]. The VM-positivity rate and its impact on clinicopathological parameters and prognosis in breast cancer patients have been largely studied in the last two decades. For instance, the study from Shirakawa K et al. [25] showed that from 331 surgically resected breast cancer specimens, only 26 (7.9%) evidenced the presence of VM. A high proportion of these VM-positive tumors exhibited pseudo-comedo formations, which are channels containing blood cells instead of necrotic tumor cells. Notably, in these 26 cases, patients were more likely to have hematogenous recurrence and lower percentage of 5-year survival [25]. However, in another study involving eight clinical reports with 1238 breast cancer patients, the VM-cases rate was higher, specifically 24%, and this was associated with larger tumor size (>2 cm), lymph node metastasis, poorer differentiation grade (grades 2 and 3), and shorter overall survival than those without VM, corroborating that this feature is associated with more aggressive breast cancer tumors and poorer prognosis [32].

Interestingly, in invasive ductal carcinoma samples, VM was detected in 13.3% of the analyzed tumors. Still, in this VM-positive group, 75% were significantly associated with bad clinicopathological characteristics, including axillary lymph node metastasis (95.6%), tumor size larger than 3 cm (56.25%), higher histological grade (stage 3, 75%), and overall poor prognosis [33]. Similarly, another study showed that breast cancer patients with VM-positive tumors were related to positive nodal status and advanced clinical stage, being the majority of VM-cases in progressive stage 2 and 3, thus, again, associating VM to a poorer outcome [34]. Of note, a meta-analysis on the role of VM in cancer progression and its prognostic value was undertaken considering different types of tumors, corroborating that the presence of VM predicts poorer survival outcomes in cancer patients [35].

## 4. Relationship between VM and Tumor Phenotype

Human breast cancer tumors are classified mainly considering clinic and histopathologic features, as well as molecular markers. Regarding this, the vast majority of these tumors belong to a group that expresses estrogen receptor alpha (ERα) and progesterone receptor (PR). Tumors overexpressing epidermal growth factor receptor 2 (HER2) generally lack ER and PR, while those that do not express neither of these three proteins are collectively called TNBC tumors. HER2 and TNBC are commonly considered as the most aggressive phenotypes of breast cancer.

The association between VM and breast tumor phenotype has been investigated. In vitro studies have shown that TNBC aggressive cells are particularly prone to form tubular structures, in contrast to more differentiated breast cancer cells. For example, the TNBC MDA-MB-231 and HCC1937 cells readily formed tubular-like structures in Matrigel [36,37]. In comparison, the ERα-positive cell line MCF-7 has been reported to be incapable of forming VM in this matrix [36]; however, in the presence of some VM drivers such as interleukin 1β, MCF-7 cells formed microvessel-like intersections and cords [38]. Further studies are needed to corroborate the effects of VM-drivers upon tubular-like structure formation in ER-positive breast cancer cells.

The link between VM and a more malignant breast cancer phenotype is coherent with the previously discussed association between VM and poor prognosis, as well as with the stemness features and increased plasticity characterizing cells with high VM-forming potential [18,39]. Indeed, some stemness markers have been negatively related to the hormone receptor status, while their expression has been found significantly increased in TNBC [18,39]. There are important features of the genotypic and phenotypic differences

in breast cancer that confer a greater capacity to develop VM, like in TNBC compared to hormone receptor-positive or HER2-positive tumors. For instance, BRCA1 mutations have been shown to predispose for the basal-like/TNBC tumor subtype [40].

On the other hand, there is also solid evidence showing a positive association between VM and the overexpression of HER2. In a study using the MCF-7 cells, forced exogenous HER2 overexpression allowed these cells to form vessel-like structures in Matrigel, a characteristic previously absent in the parental cell line. Interestingly, this process was associated with increased VE-Cadherin protein expression, which abundance and interaction with the epithelial cell kinase 2 (EPHA2) are known to be linked to VM induction [34,41]. Strongly supporting these observations, studies undertaken in aggressive melanoma cells have shown that knockdown or downregulation of VE-cadherin, EPHA2, or laminin subunit gamma 2 (LAMC2) results in abolishing of their ability to form VM [42–44]. Notably, in invasive breast carcinoma specimens, HER2 overexpression highly correlated with VM, further corroborating the in vitro results in MCF-7 cells [33,34]. However, other studies have not found a statistically significant association between HER2 overexpression and VM [32]. The reason for this discrepancy is not known, but may be related to an incomplete transformation to a full vasculogenic phenotype in HER2-positive cells, probably due to a lesser level of aggressiveness or the development of alternative survival pathways not related to HER2. Supporting this hypothesis, it is known that HER2-positive tumor cells previously treated with trastuzumab express antigens normally associated with endothelial and stemness phenotypes, together with VM markers, indicating that the treatment may induce VM. However, and interestingly, these cells were not able to form VM structures unless they had fully developed resistance to trastuzumab. Indeed, trastuzumab-resistant cells readily formed tubular structures on Matrigel, which suggested that while HER2-positive cells remain sensitive to treatment, an incomplete vasculogenic phenotype prevails, while fully resistant cells have already experienced a complete transformation and therefore can form VM channels [45].

## 5. Drivers of Vascular Mimicry in Breast Cancer

Many drivers of VM have been described, but in general, these are factors associated with the epithelial-to-mesenchymal transition (EMT) and stemness acquisition processes. In breast cancer, EMT has shown to be important for stem cell-like characteristics acquisition and maintenance, resulting in VM development [46]. Particularly in patients with TNBC tumors, cancer stem cells are considered the source of VM [19]. Among the stemness markers, CD133 and aldehyde dehydrogenase 1 (ALDH1) are closely related to VM formation [18,39]. In this regard, Liu and collaborators found that CD133-positivity displayed in holoclones of the TNBC cell line MDA-MB-231 correlated with VM-forming capacity and self-renew potential. Notably, these holoclones also expressed ECs markers such as VE-Cadherin, MMP2 and MMP9, demonstrating that CD133-positive cancer stem cells contribute to VM in TNBC by inducing transdifferentiation [19].

On the other hand, some tumor microenvironment-derived factors associated with EMT promotion are known to induce VM as well, like the cytokine transforming growth factor beta (TGFB) and the transcription factor TWIST1 [17,47]. In hepatocellular carcinoma, it is known that TGFB promotes VM in vitro and in vivo by inducing VE-Cadherin, MMP2, and LAMC2 [47]. Even though this cytokine has not yet been described as a VM-driver in breast cancer, in mice carrying TNBC xenografts the hypoxia-dependent induction of TWIST1 (a known target of TGFB) increased CD133 positivity, causing resistance to sunitinib treatment due to VM development [17]. In addition, and as previously discussed, aberrant extra-vascular expression of VE-Cadherin has been tightly associated with VM formation in cancer cells, a process thought to be related to the acquisition of an undifferentiated embryonic-like phenotype and possibly to a mesenchymal-to-endothelial transition that renders cancer cells able to form vessel-like structures. Speculatively, this would imply the loss of some mesenchymal markers and the gain of endothelial ones, such as vimentin and VE-Cadherin, respectively.

As mentioned earlier in this review, hypoxia, either as a result of an antiangiogenic treatment or induced naturally in tumor core niches, is involved in VM-formation, and therefore should be considered as an important driver by itself. Indeed, a hypoxic environment causes that tumor cells and those from the microenvironment increase their production of factors involved in VM, such as VE-Cadherin, VEGF, MMPs, TWIST1, and HIF1A [17,48–50]. Indeed, HIF1A starts multiple signaling cascades resulting in VM induction, as shown in the MDA-MB-231 and MCF-7 breast cancer cell lines [51].

Five years after the first report of VM in breast tumors by Shirakawa [24], Basu G.D. and colleagues reported the involvement of Cyclo-oxygenase (COX)-2 as a driver of VM in breast cancer [9]. They found that the invasive MDA-MB-231 and MDA-MB-435 cells overexpressing COX-2 were able to form VM-channels on Matrigel, while non-invasive MCF-7 and ZR-75-1 expressing null or low COX-2 were unable to do so. Moreover, by using the COX-2 inhibitor celecoxib, the authors concluded that the COX-2-dependent induction of VM implicated pathways related to angiogenesis, proliferation, apoptosis, and cell cycle. In a similar manner as the in vitro results, vascular channels were frequently observed in high grade invasive breast ductal carcinoma overexpressing COX-2, but not in low-grade breast tumors, whereas tumor-bearing mice treated with celecoxib corroborated in vitro results [9]. A decade later, Majumder M. and collaborators linked COX-2 expression in breast cancer cells to the induction of stemness, which is a hallmark of VM. Prostaglandin and the EP4 agonist PGE1OH, acting through the prostaglandin E-2 receptor EP4, upregulated NOTCH/WNT expression via PI3K/AKT signaling pathway, which increased migration, invasion, proliferation, EMT, and spheroid formation. Regarding this, increased ALDH activity was found in COX-2 overexpressing tumorospheres, while COX-2 colocalized with the stemness markers ALDH1, CD44, Catenin, NANOG, OCT3/4, and SOX-2 [52,53]. Altogether, the implication of COX-2/prostaglandin signalization in VM formation by highly aggressive breast cancer cells opens new avenues for the use of COX-2/EP4 as a therapeutic target in breast cancer.

Another known player in VM development is sphingosine-1 phosphate receptor 1 (S1PR1), a bioactive signaling lipid regulating vascular development, function, and maturation. However, its participation in this process is more as an "anti-driver", since its suppression impairs angiogenesis but contributes to VM generation as well as the promotion of invasion and metastasis [54]. Indeed, a recent study demonstrated that S1PR1 deficiency or knockdown contributed to the generation or increase of VM. This was attributed to the S1PR1-dependent promotion of VE-Cadherin phosphorylation, leading to its separation from β-catenin. Interestingly, the survival analysis suggested that in non-TNBC, S1PR1 significantly correlated with poor patient survival, warranting further studies [54].

A very interesting study published in 2015 by Wagenblast E. and colleagues, clearly identified the contribution of two anticoagulant secreted proteins in driving VM in breast cancer cells in vitro and in vivo. These proteins were Serpine2 and Slpi, which were overexpressed in clones from a heterogeneous population of breast cancer cells that could efficiently enter the vasculature and form lung metastasis [55]. The authors were able to prove that the enforced expression of Serpine2 and Slpi in non-intravasating clones efficiently induced in vitro formation of tubular structures in cells previously incapable of forming VM. They concluded that the expression of Serpine2 and Slpi was "sufficient and necessary" to program breast cancer cells for VM, as if this combination worked as a vasculogenic inductive cocktail. Moreover, due to their anticoagulant properties, Serpine2 and Slpi seemed to promote both the passage of erythrocytes into the tumor as well as that of cancer cells into the bloodstream [55]. In accordance with the tumor phenotypes mostly associated with VM, Serpine2 and Slpi were significantly more expressed in HER2+, TNBC (basal) and claudin-low tumors of relapsing patients [55].

TNBC has been described as the breast cancer subtype with the highest rate of tumor infiltrating lymphocytes [56]. Although in the clinic the presence of these cells has been associated with a more favorable prognosis due to their ability to synergize chemother-

apy [56], they also secrete a variety of chemokines and cytokines to the tumor microenvironment that may contribute to the oncogenic process. Regarding this, interleukin (IL)-6, signaling through the signal transducer and activator of transcription 3 (STAT3), has shown to promote tube formation by tumor cells in vivo and in vitro by upregulating VE-Cadherin expression and MMP2 activity [57]. Particularly in breast cancer, other inflammatory cytokines have also proven to be drivers of VM, for instance IL-1β and IL-8. On this subject, it is known that TNBC MDA-MB-231 cells express IL-8 as well as its receptors CXCR1/CXCR2, and notably, it has been shown that IL-8 uptake increases during VM formation and that IL-8/CXCR2 signaling is necessary for tube formation, a process that correlates with increased IL-8 levels [58]. In a similar manner but using a different signalization pathway, IL-1β has shown to stimulate VM formation by MCF-7 and MDA-MB-231 cells [38]. Indeed, when these cells were incubated in the presence of IL-1β, they readily formed tube-like structures in Matrigel and expressed VM biomarkers, including VE-Cadherin, VEGF receptor-1, MMP-9, and MMP-2. Of note, this effect was preserved under both normoxic and hypoxic conditions and involved the p38/MAPK and PI3K/Akt signaling pathways [38].

Additionally contributing to VM induction is the BRCA-human chorionic gonadotropin (hCG) axis. The BRCA1 protein is involved in DNA repair mechanisms, and it has been demonstrated that BRCA1-deficient mouse mammary tumors are enriched in CD44+/CD24$^{-/(low)}$ and CD133+ cells. These highly tumorigenic cells show expression of stem cell-associated genes such as *OCT4, NOTCH1, ALDH1, FFGR1, SOX1* [59]. On the other hand, an inverse correlation between BRCA1 and hCG has been found. Indeed, BRCA1 directly represses the expression of β-hCG by binding to its promoter [60]. This hormone is known to exert a potent proangiogenic effect on hCG/luteinizing hormone receptor (hCG/LH-R)-expressing uterine ECs. Moreover, it has been reported that hCG-secreting tumors promote neovascularization and capillary sprouting on in vitro models [61]. Interestingly, mutated BRCA1 in breast cancer cells is associated with β-hCG overexpression, which results in pluripotency and EMT. Besides, this correlated with enhanced migration, invasion, and greater tumorigenic capacity along with expression of EMT and stem cell markers [60]. Notably, all the cellular processes aberrantly activated in BRCA1-mutated cancers are closely related to the VM capacity of tumors, and it has been documented that hCG is crucial for the transdifferentiation of cancer cells into endothelial-like cells by inducing expression of ECs markers such as CD31 and VEGF among others [62]. Remarkably, in breast cancer with mutated BRCA1, β-hCG can signal through transforming growth factor beta receptor II (TGFβRII) regardless of the hCG/LH-R status, resulting in increased cell proliferation [60]. The activation of the TGFB signaling pathway also induces the expression of Snail, Slug, TWIST, and ZEB-1, which in turn increase the expression of mesenchymal markers leading to EMT, a well-known driver of VM. Nevertheless, the role of hCG in VM induction may vary depending on the tumor phenotype. For instance, in hCG/LH-R-positive luminal-A breast cancer cell lines, hCG inhibited cell proliferation and tumor growth [63], whereas, in HER2 positive breast cancer cells, hCG enhanced growth and metastasis in vivo [64]. Therefore, the subtype of breast cancer should be taken into consideration for a clinical approach targeting hCG.

Another important axis involved in VM is the leucine rich repeats and immunoglobulin like domains 1 (LRIG1)-HER2 axis. LRIG1 is a tumor suppressor that negatively regulates tyrosine kinase receptors (TKRs) signaling by inducing their degradation via ubiquitination and/or hindering the TKRs heterodimeric conformation. This results in the inhibition of PI3K/AKT and ERK1/2 signaling pathways [65]. Among the TKRs regulated by LR1G1 is HER2, which, as previously discussed in this review, has important relevance on the processes associated with the VM capacity of HER2-enriched breast cancer cells. In addition, in other breast tumor subtypes, including the TNBC, LRIG1 expression is known to be decreased, a clinical feature associated with decreased relapse-free survival, higher-grade tumors, and EMT activation [66,67]. Conversely, restoration of LRIG1 expression provokes a mesenchymal-to-epithelial transition, as well as loss of tumorigenic and

invasiveness potentials of highly invasive basal breast cancer cells [68]. Interestingly, a proposed molecular mechanism involved in the down-regulation of LRIG1 in breast cancer is mediated by HER2 itself. Indeed, a study from 2008 showed that HER2-induced mammary tumors in transgenic mice had significantly suppressed LRIG1 protein levels, and the activation of HER2 induced a further dramatic loss of endogenous LRIG1 expression and enhancement of proliferation via Akt/Erk, showing that HER2 oncogenic signaling actively contributes to suppression of LRIG [66]. In contrast, LRIG1 gene expression was found enriched in ERα-positive breast cancer, and consistently, LRIG1 has proven to be a transcriptional target of ERα. Moreover, LRIG1 restricts estrogen-driven tumor cell growth, suggesting that it can suppress ERα-positive tumors [67]. This might explain why ERα-positive breast cancer has a lower incidence of VM compared to HER2 and TNBC.

## 6. VM Regulation by Noncoding RNAs in Breast Cancer

Noncoding RNAs (ncRNAs), such as microRNAs (miRNAs) and long noncoding RNAs (lncRNAs), are involved in VM regulation and tumorigenesis of breast cancer. Herein, we review some ncRNAs known to be involved in this process.

The miRNA-299-5p is downregulated in cell lines and tumor and serum samples from breast cancer patients [69,70], and the restoration of its expression inhibited cell migration, invasion, and metastasis [70]. Interestingly, this miRNA is also critical for the development of vascular-like structures by regulating *de novo* expression of osteopontin, which plays a critical role in the VM process of spheroid-forming cells in breast cancer [71]. Another ncRNA involved in breast cancer progression is the tumor-suppressive miRNA-193b [72]. It has been demonstrated that this molecule regulates VM by targeting the dimethylarginine dimethylaminohydrolase 1 (DDAH1) enzyme involved in the metabolism of asymmetric dimethylarginine and monomethyl arginine that are inhibitors of nitric oxide synthesis. Ectopic expression of miR-193b reduced DDAH1 expression and completely inhibited tube formation in MDA-MB-231 cells [73].

P73 antisense RNA 1T (TP73-AS1) is a lncRNA that promotes breast cancer cell invasion and migration [74,75]. In TNBC, TP73-AS1 also participates in VM formation since it decreases miR-490-3p levels implicated in the negative regulation of the TWIST1 gene, which participates in EMT promotion and VM formation [76].

The miR-204 is a tumor suppressor down-regulated in breast cancer and associated with poor prognostic [77]. An overall survival analysis of 3951 breast cancer patients indicated that low miRNA-204 and high FAK/SRC levels were associated with low overall survival of patients. Interestingly, ectopic restoration of miR-204 in MDA-MB-231 cells produced a potent inhibition of VM by reducing the number of branch points and patterned 3D channels. This was associated with the downregulation of several transducers involved in the activation of PI3K/AKT, RAF1, MAPK, VEGF, and FAK/SRC signaling [78].

HOX transcript antisense RNA (HOTAIR) is a lncRNA that sponges tumor-suppressive miRNAs. Interestingly, knockdown of HOTAIR resulted in an increment of miR-204 levels, as well as the reduction of migration and hypoxia-induced VM formation by targeting the FAK signaling in TNBC cells [79].

The miR-126-3p expression was significantly downregulated in TNBC cells, where its overexpression inhibited cell proliferation, migration, invasion, colony formation capacity and VM by targeting the regulator of G protein signaling 3 (RGS3), which promotes these processes [80].

As discussed earlier in this review, IL-6 signaling is implicated in chemoresistance and metastasis of various tumors, including breast cancer [81–83]. Interestingly, cisplatin treatment upregulated IL-6 levels in ECs, and the resulting conditioned medium induced VM formation in MDA-MB-231 breast cancer cells that might eventually promote drug resistance and metastasis. The mechanism that contributes to VM implicates miR-125a and let-7e downregulation in response to cisplatin treatment, affecting the IL-6 pathway due to IL-6 targeting by these miRNAs, as well as the IL-6 receptor and the STAT3 genes in ECs [84]. Another known miRNA involved in hampering IL-6-stimulated VM in vitro

and in vivo is miR-29b, which represses the expression of STAT3 and MMP2 by directly binding to the UTRs of their mRNAs [57].

The signaling of AXL receptor tyrosine kinase promotes cancer stem cell-like phenotypes, drug resistance, metastasis, and EMT. Overexpression of this receptor promotes the regulation of VM formation in breast cancer cells [73] through miRNA-34a that targets the 3′-untranslated region (UTR) [85,86]. In this sense, it was demonstrated that miRNA-34a overexpression downregulated AXL receptor expression resulting in the inhibition of VM formation, migration, and invasion in MDA-MB 231 cells [28].

The miR-93 levels are enriched in TNBC tissue, which has been associated with the occurrence of EMT and VM formation. Accordingly, knockdown of this miRNA resulted in an increase of E-Cadherin and Occludin gene expression and reduction of Vimentin and N-Cadherin levels, as well as the decrease in microtubule forming ability by MDA-MB-231 cells [87,88]. Likewise, forced expression of miR-93 in MT-1 human breast carcinoma cells resulted in tumors containing more blood vessels than those formed by non-miR-93 expressing cells. Accordingly, the expression of miR-93 promoted tumor cell metastasis to lung tissue. It was concluded that the potential target mediating miR-93′s effects was the large tumor suppressor, homolog 2 (LATS2). Indeed, increased expression of LATS2 was associated with tumor cells death and decreased cell survival and invasion [89].

The ncRNAs represent an attractive approach in cancer since they may be considered biomarkers associated with tumors' biological and clinical characteristics with an important diagnostic and prognostic value. Their implication in VM formation may provide the theoretical basis for anti-vascular therapy in human TNBC as therapeutic targets to inhibit tumor neovascularization.

## 7. Targeting Microenvironment to Overcome VM in Breast Cancer

As discussed earlier in this review, many factors deriving from the tumor microenvironment are involved in VM induction. Likewise, resident cells such as lymphocytes, macrophages, fibroblasts, and tumor cells themselves may produce VM-promoting factors including the inflammatory cytokines IL-6, IL-8, TGFB, and IL-1β. Therefore, the signaling pathways associated with these cytokines offer potential oncological targets to design therapeutic strategies aimed to control the aggressiveness of breast cancer tumor cells. In this regard, since aberrant TGFB signaling is of primordial importance for VM induction, this pathway offers a good opportunity for a VM-targeted therapy. Indeed, TGFB from the tumor microenvironment significantly stimulates tumor growth, migration, invasion, and angiogenesis, which results in an overall poor prognosis. Conversely, blockade of this signalization pathway has been associated with significant inhibition of human basal-like breast cancer metastasis [90], while TGFB-targeted clinical/preclinical studies in breast cancer have shown delayed tumor growth [91]. Furthermore, TGFB inhibition has been shown to enhance chemotherapy action against TNBC [92]. All considered TGFB-targeting warrants further studies for VM inhibition.

The participation of platelets in tumorigenesis and metastasis is a well described process; however, only recently the inhibitory effect of platelets on VM formation by breast cancer has been revealed [93]. Indeed, the ability of HS-578T and MDA-MB-231 TNBC cells to form VM structures on Matrigel was significantly inhibited by their coculture with platelets, while already existing VM structures were readily disassembled by these clotting agents as well. This anti-VM capacity was attributed to the release of soluble factors from the platelets, opening new avenues for further studies aimed to identify these factors in order to target VM-formation.

On the other hand, and as described before, phenotype-related signaling pathways could be useful for targeting microenvironmental changes involved in VM development. This is related especially with modifications on the ECM and plasticity involved in EMT, transdifferentiation, and stemness. A clear example is the use of inhibitors against heat shock protein of 90 kDa (Hsp90). This is a subfamily of molecular chaperones that regulate folding, unfolding, activation, degradation, and intra- or extracellular localization of

more than 200 proteins named "client proteins" such as hormone receptors and several kinases [94]. As a chaperone, Hsp90 can rescue functionality on mutated client proteins that would be degraded or inactivated in its absence. In evolution, this increases genetic diversity [95]; however, in cancer, this can lead to the up-regulation of signaling client proteins involved in carcinogenesis, invasion, or metastasis. Therefore, Hsp90 functional inhibition has shown promising effects by degradation of client proteins and shutdown of the processes involved in tumor progression [96]. Particularly in BRCA1-deficient mice, spheroid-forming cells resistant to DNA-damaging drugs could be efficiently re-sensitized by the Hsp90 inhibitor 17-DMAG [59]. Furthermore, this same strategy but with Geldanamycin, an antitumor antibiotic that inhibits Hsp90 function by binding to its ADP/ATP-binding pocket, successfully suppressed breast cancer stem cell population in mammospheres, along with proliferation and migration [97]. One of the possible mechanisms involved in such effects is the regulation of MMP-2 and MMP-9 by cytosolic isoforms Hsp90α and Hsp90β since it has been demonstrated that the interaction between Hsp90 and MMP-2/9 is necessary for its secretion and activation [98]. Taken together, Hsp90 inhibition might represent a highlight in the regulation of the microenvironment factors that trigger VM in breast cancer.

Another strategy to take into account is the targeting of β-hCG, due to its immune suppressor functions and its vasculogenic effects on BRCA1 defective tumors; however, as mentioned above, this is highly dependent on the molecular characteristics of patients [60], warranting further studies.

## 8. Conclusions

In cancer, VM is an alternative survival strategy adopted by cancer cells under hypoxic stress that allows them to adapt, grow, and disseminate and that is significantly related to poor prognosis and adverse clinicopathological parameters. Besides hypoxic stress, other drivers may also initiate this process, including antiangiogenic therapies and molecules derived from the microenvironment. In breast cancer, VM has been generally associated with HER2-positive and triple-negative breast tumors, as well as with stemness and EMT markers. A scheme summarizing the molecular regulators of VM as well as its relationship with stemness and prognosis is provided in Figure 3.

It is of paramount importance to understand VM biology in order to efficiently target its drivers and to avoid its consequences.

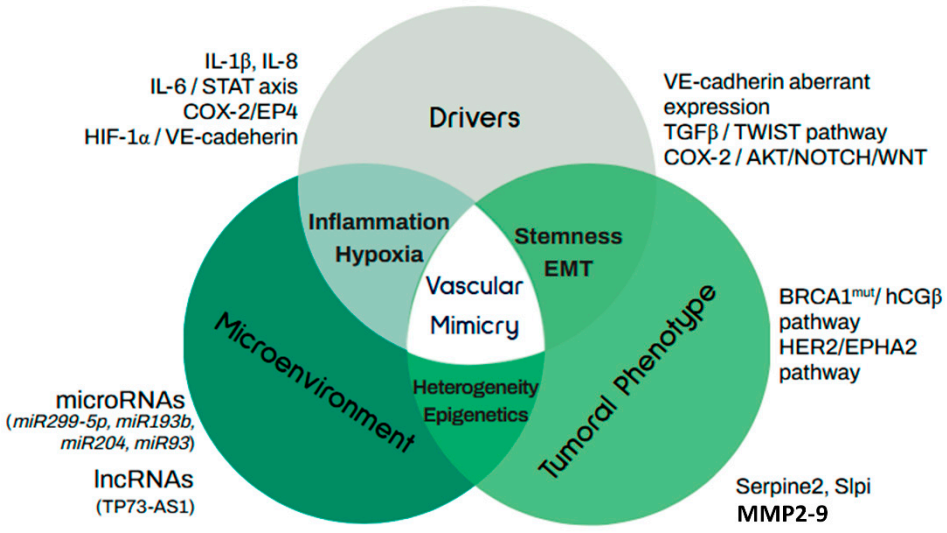


**Figure 3.** Molecular regulators of vascular mimicry. Vascular mimicry in cancer is activated by several drivers associated with phenotypic features of tumors and microenvironmental factors and

signals. Tumor phenotype relates to stemness and EMT capacity of cancer cells. Molecular drivers include TGFB/TWIST regulation of the stem cellular subpopulation and the aberrant expression of VE-cadherin, while the COX-2 axis regulates stemness and VM capacity by PI3K/AKT activation and induction of NOTCH/WNT expression. In the context of breast cancer, the main mechanisms associated with stemness are mediated by hCGβ in BRCA1 mutated patients and by EPHA2 in HER2+ tumors. Heterogeneity in breast cancer tumors is associated with the activation of VM and metastasis through the expression of anti-coagulant factors Serpine2 and Slpi. Along with this, highly invasive breast tumors overexpress metalloproteinases as MMP2 and MMP9, which participate in VM by remodeling the extracellular matrix. Regarding epigenetic regulation of VM, ncRNAs, including several microRNAs as well as lncRNA participate in this process. Well-known microenvironment factors and drivers inducing VM include IL-1β, IL-8, and IL-6. Finally, HIF1A activation in response to hypoxic conditions is highly involved with VE-cadherin expression through TWIST1.

**Author Contributions:** Conceptualization, writing—original draft preparation and visualization, G.M.-G., E.A.M.-P. and L.D.; writing—review and editing, R.G.-B., J.G.-Q., and E.A. All authors have read and agreed to the published version of the manuscript.

**Funding:** This research was funded by Consejo Nacional de Ciencia y Tecnología (CONACyT), México, grant number A1-S-10749 to L.D.

**Institutional Review Board Statement:** Not applicable.

**Informed Consent Statement:** Not applicable.

**Data Availability Statement:** Not applicable.

**Acknowledgments:** This review is part of the Ph.D. work of G.M.-G. who is a student from El Programa de Doctorado en Ciencias Biomédicas, Universidad Nacional Autónoma de México (UNAM). G.M.-G. is receiving a fellowship from Consejo Nacional de Ciencia y Tecnología de México (CONACyT).

**Conflicts of Interest:** The authors declare no conflict of interest.

## Abbreviations

| | |
|---|---|
| DDAH1 | Dimethylarginine dimethylaminohydrolase 1 |
| ECM | Extracellular matrix |
| ECs | Endothelial cells |
| EMT | Epithelial-to-mesenchymal transition |
| hCG | Human chorionic gonadotropin |
| HOTAIR | HOX transcript antisense RNA |
| IL | Interleukin |
| LATS2 | Large tumor suppressor, homology 2 |
| LH | Luteinizing hormone |
| LHCGR | Luteinizing hormone/chorionic gonadotropin receptor |
| lncRNAs | Long noncoding RNAs |
| LRIG1 | Leucine rich repeats and immunoglobulin like domains 1 |
| miRNAs | MicroRNAs |
| ncRNAs | Noncoding RNAs |
| PAS | Periodic acid-Schiff |
| RGS3 | G protein signaling 3 |
| RR | Relative risk |
| S1PR1 | Sphingosine-1 phosphate receptor 1 |
| STAT3 | Signal transducer and activator of transcription 3 |
| TNBC | Triple-negative breast cancer |
| TKR | Tyrosine kinase receptor |
| TP73-AS1 | P73 antisense RNA 1T |
| UTR | Untranslated region |
| VM | Vasculogenic mimicry |

## References


1. Kolte, D.; McClung, J.A.; Aronow, W.S. Chapter 6—Vasculogenesis and Angiogenesis. In *Translational Research in Coronary Artery Disease*; Aronow, W.S., McClung, J.A., Eds.; Academic Press: Boston, MA, USA, 2016; pp. 49–65.
2. Patan, S.; Munn, L.L.; Jain, R.K. Intussusceptive Microvascular Growth in a Human Colon Adenocarcinoma Xenograft: A Novel Mechanism of Tumor Angiogenesis. *Microvasc. Res.* **1996**, *51*, 260–272. [CrossRef]
3. Rodríguez-Núñez, I.; Romero, F.; González, M.; Campos, R.R. Biología del Desarrollo Vascular: Mecanismos en Condiciones Fisiológicas y Estrés Flujo. *Int. J. Morphol.* **2015**, *33*, 1348–1354. [CrossRef]
4. Kuczynski, E.A.; Vermeulen, P.B.; Pezzella, F.; Kerbel, R.S.; Reynolds, A.R. Vessel co-option in cancer. *Nat. Rev. Clin. Oncol.* **2019**, *16*, 469–493. [CrossRef]
5. Bergers, G.; Benjamin, L.E. Tumorigenesis and the angiogenic switch. *Nat. Reviews Cancer* **2003**, *3*, 401–410. [CrossRef] [PubMed]
6. Folberg, R.; Hendrix, M.J.; Maniotis, A.J. Vasculogenic mimicry and tumor angiogenesis. *Am. J. Pathol.* **2000**, *156*, 361–381. [CrossRef]
7. Maniotis, A.J.; Folberg, R.; Hess, A.; Seftor, E.A.; Gardner, L.M.; Pe'er, J.; Trent, J.M.; Meltzer, P.S.; Hendrix, M.J. Vascular channel formation by human melanoma cells in vivo and in vitro: Vasculogenic mimicry. *Am. J. Pathol.* **1999**, *155*, 739–752. [CrossRef]
8. Folberg, R.; Arbieva, Z.; Moses, J.; Hayee, A.; Sandal, T.; Kadkol, S.; Lin, A.Y.; Valyi-Nagy, K.; Setty, S.; Leach, L.; et al. Tumor cell plasticity in uveal melanoma: Microenvironment directed dampening of the invasive and metastatic genotype and phenotype accompanies the generation of vasculogenic mimicry patterns. *Am. J. Pathol.* **2006**, *169*, 1376–1389. [CrossRef] [PubMed]
9. Basu, G.D.; Liang, W.S.; Stephan, D.A.; Wegener, L.T.; Conley, C.R.; Pockaj, B.A.; Mukherjee, P. A novel role for cyclooxygenase-2 in regulating vascular channel formation by human breast cancer cells. *Breast Cancer Res.* **2006**, *8*, 69. [CrossRef]
10. Chiao, M.T.; Yang, Y.C.; Cheng, W.Y.; Shen, C.C.; Ko, J.L. CD133+ glioblastoma stem-like cells induce vascular mimicry in vivo. *Curr. Neurovascular Res.* **2011**, *8*, 210–219. [CrossRef] [PubMed]
11. Delgado-Bellido, D.; Serrano-Saenz, S.; Fernández-Cortés, M.; Oliver, F.J. Vasculogenic mimicry signaling revisited: Focus on non-vascular VE-cadherin. *Mol. Cancer* **2017**, *16*, 65. [CrossRef]
12. Andonegui-Elguera, M.A.; Alfaro-Mora, Y.; Caceres-Gutierrez, R.; Caro-Sanchez, C.H.S.; Herrera, L.A.; Diaz-Chavez, J. An Overview of Vasculogenic Mimicry in Breast Cancer. *Front. Oncol.* **2020**, *10*, 220. [CrossRef]
13. Breier, G.; Grosser, M.; Rezaei, M. Endothelial cadherins in cancer. *Cell Tissue Res.* **2014**, *355*, 523–527. [CrossRef]
14. Hendrix, M.J.; Seftor, E.A.; Hess, A.R.; Seftor, R.E. Vasculogenic mimicry and tumour-cell plasticity: Lessons from melanoma. *Nat. Rev. Cancer* **2003**, *3*, 411–421. [CrossRef]
15. van der Schaft, D.W.; Seftor, R.E.; Seftor, E.A.; Hess, A.R.; Gruman, L.M.; Kirschmann, D.A.; Yokoyama, Y.; Griffioen, A.W.; Hendrix, M.J. Effects of angiogenesis inhibitors on vascular network formation by human endothelial and melanoma cells. *J. Natl. Cancer Inst.* **2004**, *96*, 1473–1477. [CrossRef]
16. Mitra, D.; Bhattacharyya, S.; Alam, N.; Sen, S.; Mitra, S.; Mandal, S.; Vignesh, S.; Majumder, B.; Murmu, N. Phosphorylation of EphA2 receptor and vasculogenic mimicry is an indicator of poor prognosis in invasive carcinoma of the breast. *Breas Cancer Res Treat.* **2020**, *179*, 359–370. [CrossRef]
17. Zhang, D.; Sun, B.; Zhao, X.; Ma, Y.; Ji, R.; Gu, Q.; Dong, X.; Li, J.; Liu, F.; Jia, X.; et al. Twist1 expression induced by sunitinib accelerates tumor cell vasculogenic mimicry by increasing the population of CD133+ cells in triple-negative breast cancer. *Mol. Cancer* **2014**, *13*, 207. [CrossRef]
18. Brugnoli, F.; Grassilli, S.; Al-Qassab, Y.; Capitani, S.; Bertagnolo, V. CD133 in Breast Cancer Cells: More than a Stem Cell Marker. *J. Oncol.* **2019**, *2019*, 7512632. [CrossRef]
19. Liu, T.J.; Sun, B.C.; Zhao, X.L.; Zhao, X.M.; Sun, T.; Gu, Q.; Yao, Z.; Dong, X.Y.; Zhao, N.; Liu, N. CD133+ cells with cancer stem cell characteristics associates with vasculogenic mimicry in triple-negative breast cancer. *Oncogene* **2013**, *32*, 544–553. [CrossRef]
20. Rossi, E.; Poirault-Chassac, S.; Bieche, I.; Chocron, R.; Schnitzler, A.; Lokajczyk, A.; Bourdoncle, P.; Dizier, B.; Bacha, N.C.; Gendron, N.; et al. Human Endothelial Colony Forming Cells Express Intracellular CD133 that Modulates their Vasculogenic Properties. *Stem Cell Rev Rep.* **2019**, *15*, 590–600. [CrossRef]
21. Ribatti, D.; Pezzella, F. Overview on the Different Patterns of Tumor Vascularization. *Cells* **2021**, *10*, 639. [CrossRef]
22. Folberg, R.; Maniotis, A.J. Vasculogenic mimicry. *Acta Pathol. Microbiol. Et Immunol. Scand.* **2004**, *112*, 508–525. [CrossRef]
23. Garcia-Quiroz, J.; Garcia-Becerra, R.; Santos-Cuevas, C.; Ramirez-Nava, G.J.; Morales-Guadarrama, G.; Cardenas-Ochoa, N.; Segovia-Mendoza, M.; Prado-Garcia, H.; Ordaz-Rosado, D.; Avila, E.; et al. Synergistic Antitumorigenic Activity of Calcitriol with Curcumin or Resveratrol is Mediated by Angiogenesis Inhibition in Triple Negative Breast Cancer Xenografts. *Cancers* **2019**, *11*, 1739. [CrossRef]
24. Shirakawa, K.; Tsuda, H.; Heike, Y.; Kato, K.; Asada, R.; Inomata, M.; Sasaki, H.; Kasumi, F.; Yoshimoto, M.; Iwanaga, T.; et al. Absence of endothelial cells, central necrosis, and fibrosis are associated with aggressive inflammatory breast cancer. *Cancer Res.* **2001**, *61*, 445–451.
25. Shirakawa, K.; Wakasugi, H.; Heike, Y.; Watanabe, I.; Yamada, S.; Saito, K.; Konishi, F. Vasculogenic mimicry and pseudo-comedo formation in breast cancer. *Int. J. Cancer* **2002**, *99*, 821–828. [CrossRef]
26. Shirakawa, K.; Kobayashi, H.; Heike, Y.; Kawamoto, S.; Brechbiel, M.W.; Kasumi, F.; Iwanaga, T.; Konishi, F.; Terada, M.; Wakasugi, H. Hemodynamics in vasculogenic mimicry and angiogenesis of inflammatory breast cancer xenograft. *Cancer Res.* **2002**, *62*, 560–566.

27. Silvestri, V.L.; Henriet, E.; Linville, R.M.; Wong, A.D.; Searson, P.C.; Ewald, A.J. A Tissue-Engineered 3D Microvessel Model Reveals the Dynamics of Mosaic Vessel Formation in Breast Cancer. *Cancer Res.* **2020**, *80*, 4288–4301. [CrossRef]
28. Xu, Y.; Li, Q.; Li, X.Y.; Yang, Q.Y.; Xu, W.W.; Liu, G.L. Short-term anti-vascular endothelial growth factor treatment elicits vasculogenic mimicry formation of tumors to accelerate metastasis. *J. Exp. Clin. Cancer Res.* **2012**, *31*, 1–7. [CrossRef]
29. Valencia-Cervantes, J.; Huerta-Yepez, S.; Aquino-Jarquín, G.; Rodríguez-Enríquez, S.; Martínez-Fong, D.; Arias-Montaño, J.A.; Dávila-Borja, V.M. Hypoxia increases chemoresistance in human medulloblastoma DAOY cells via hypoxia-inducible factor 1α-mediated downregulation of the CYP2B6, CYP3A4 and CYP3A5 enzymes and inhibition of cell proliferation. *Oncol. Rep.* **2019**, *41*, 178–190. [CrossRef]
30. Weidner, N.; Semple, J.P.; Welch, W.R.; Folkman, J. Tumor angiogenesis and metastasis–correlation in invasive breast carcinoma. *N. Engl. J. Med.* **1991**, *324*, 1–8. [CrossRef] [PubMed]
31. Sun, B.; Zhang, S.; Zhang, D.; Du, J.; Guo, H.; Zhao, X.; Zhang, W.; Hao, X. Vasculogenic mimicry is associated with high tumor grade, invasion and metastasis, and short survival in patients with hepatocellular carcinoma. *Oncol. Rep.* **2006**, *16*, 693–698. [CrossRef]
32. Shen, Y.; Quan, J.; Wang, M.; Li, S.; Yang, J.; Lv, M.; Chen, Z.; Zhang, L.; Zhao, X.; Yang, J. Tumor vasculogenic mimicry formation as an unfavorable prognostic indicator in patients with breast cancer. *Oncotarget* **2017**, *8*, 56408–56416. [CrossRef]
33. Jafarian, A.H.; Kooshkiforooshani, M.; Rasoliostadi, A.; Mohamadian Roshan, N. Vascular Mimicry Expression in Invasive Ductal Carcinoma; A New Technique for Prospect of Aggressiveness. *Iran. J. Pathol.* **2019**, *14*, 232–235. [CrossRef]
34. Liu, T.; Sun, B.; Zhao, X.; Gu, Q.; Dong, X.; Yao, Z.; Zhao, N.; Chi, J.; Liu, N.; Sun, R.; et al. HER2/neu expression correlates with vasculogenic mimicry in invasive breast carcinoma. *J. Cell. Mol. Med.* **2013**, *17*, 116–122. [CrossRef] [PubMed]
35. Yang, J.P.; Liao, Y.D.; Mai, D.M.; Xie, P.; Qiang, Y.Y.; Zheng, L.S.; Wang, M.Y.; Mei, Y.; Meng, D.F.; Xu, L.; et al. Tumor vasculogenic mimicry predicts poor prognosis in cancer patients: A meta-analysis. *Angiogenesis* **2016**, *19*, 191–200. [CrossRef]
36. Quiros-Gonzalez, I.; Tomaszewski, M.R.; Aitken, S.J.; Ansel-Bollepalli, L.; McDuffus, L.A.; Gill, M.; Hacker, L.; Brunker, J.; Bohndiek, S.E. Optoacoustics delineates murine breast cancer models displaying angiogenesis and vascular mimicry. *Br. J. Cancer* **2018**, *118*, 1098–1106. [CrossRef]
37. Luan, Y.Y.; Liu, Z.M.; Zhong, J.Y.; Yao, R.Y.; Yu, H.S. Effect of grape seed proanthocyanidins on tumor vasculogenic mimicry in human triple-negative breast cancer cells. *Asian Pac. J. Cancer Prev.* **2015**, *16*, 531–535. [CrossRef] [PubMed]
38. Nisar, M.A.; Zheng, Q.; Saleem, M.Z.; Ahmmed, B.; Ramzan, M.N.; Ud Din, S.R.; Tahir, N.; Liu, S.; Yan, Q. IL-1β Promotes Vasculogenic Mimicry of Breast Cancer Cells Through p38/MAPK and PI3K/Akt Signaling Pathways. *Front. Oncol.* **2021**, *11*, 1–13. [CrossRef] [PubMed]
39. Xing, P.; Dong, H.; Liu, Q.; Zhao, T.; Yao, F.; Xu, Y.; Chen, B.; Zheng, X.; Wu, Y.; Jin, F.; et al. ALDH1 Expression and Vasculogenic Mimicry Are Positively Associated with Poor Prognosis in Patients with Breast Cancer. *Cell. Physiol. Biochem. Int. J. Exp. Cell. Physiol. Biochem. Pharmacol.* **2018**, *49*, 961–970. [CrossRef]
40. Sorlie, T.; Tibshirani, R.; Parker, J.; Hastie, T.; Marron, J.S.; Nobel, A.; Deng, S.; Johnsen, H.; Pesich, R.; Geisler, S.; et al. Repeated observation of breast tumor subtypes in independent gene expression data sets. *Proc. Natl. Acad. Sci. USA* **2003**, *100*, 8418–8423. [CrossRef] [PubMed]
41. Hess, A.R.; Seftor, E.A.; Gruman, L.M.; Kinch, M.S.; Seftor, R.E.; Hendrix, M.J. VE-cadherin regulates EphA2 in aggressive melanoma cells through a novel signaling pathway: Implications for vasculogenic mimicry. *Cancer Biol. Ther.* **2006**, *5*, 228–233. [CrossRef]
42. Hess, A.R.; Seftor, E.A.; Gardner, L.M.; Carles-Kinch, K.; Schneider, G.B.; Seftor, R.E.; Kinch, M.S.; Hendrix, M.J. Molecular regulation of tumor cell vasculogenic mimicry by tyrosine phosphorylation: Role of epithelial cell kinase (Eck/EphA2). *Cancer Res.* **2001**, *61*, 3250–3255. [PubMed]
43. Hendrix, M.J.; Seftor, E.A.; Meltzer, P.S.; Gardner, L.M.; Hess, A.R.; Kirschmann, D.A.; Schatteman, G.C.; Seftor, R.E. Expression and functional significance of VE-cadherin in aggressive human melanoma cells: Role in vasculogenic mimicry. *Proc. Natl. Acad. Sci. USA* **2001**, *98*, 8018–8023. [CrossRef] [PubMed]
44. Seftor, R.E.; Seftor, E.A.; Koshikawa, N.; Meltzer, P.S.; Gardner, L.M.; Bilban, M.; Stetler-Stevenson, W.G.; Quaranta, V.; Hendrix, M.J. Cooperative interactions of laminin 5 gamma2 chain, matrix metalloproteinase-2, and membrane type-1-matrix/metalloproteinase are required for mimicry of embryonic vasculogenesis by aggressive melanoma. *Cancer Res.* **2001**, *61*, 6322–6327. [PubMed]
45. Hori, A.; Shimoda, M.; Naoi, Y.; Kagara, N.; Tanei, T.; Miyake, T.; Shimazu, K.; Kim, S.J.; Noguchi, S. Vasculogenic mimicry is associated with trastuzumab resistance of HER2-positive breast cancer. *Breast Cancer Res.* **2019**, *21*, 88. [CrossRef]
46. Kotiyal, S.; Bhattacharya, S. Epithelial Mesenchymal Transition and Vascular Mimicry in Breast Cancer Stem Cells. *Crit. Rev. Eukaryot. Gene Expr.* **2015**, *25*, 269–280. [CrossRef]
47. Yang, J.; Lu, Y.; Lin, Y.Y.; Zheng, Z.Y.; Fang, J.H.; He, S.; Zhuang, S.M. Vascular mimicry formation is promoted by paracrine TGF-β and SDF1 of cancer-associated fibroblasts and inhibited by miR-101 in hepatocellular carcinoma. *Cancer Lett.* **2016**, *383*, 18–27. [CrossRef]
48. Tang, N.N.; Zhu, H.; Zhang, H.J.; Zhang, W.F.; Jin, H.L.; Wang, L.; Wang, P.; He, G.J.; Hao, B.; Shi, R.H. HIF-1α induces VE-cadherin expression and modulates vasculogenic mimicry in esophageal carcinoma cells. *World J. Gastroenterol.* **2014**, *20*, 17894–17904. [CrossRef]

49. Li, S.; Meng, W.; Guan, Z.; Guo, Y.; Han, X. The hypoxia-related signaling pathways of vasculogenic mimicry in tumor treatment. *Biomed. Pharmacother.* **2016**, *80*, 127–135. [CrossRef]
50. Wei, X.; Chen, Y.; Jiang, X.; Peng, M.; Liu, Y.; Mo, Y.; Ren, D.; Hua, Y.; Yu, B.; Zhou, Y.; et al. Mechanisms of vasculogenic mimicry in hypoxic tumor microenvironments. *Mol. Cancer* **2021**, *20*, 7. [CrossRef]
51. Li, S.; Zhang, Q.; Zhou, L.; Guan, Y.; Chen, S.; Zhang, Y.; Han, X. Inhibitory effects of compound DMBT on hypoxia-induced vasculogenic mimicry in human breast cancer. *Biomed. Pharmacother.* **2017**, *96*, 982–992. [CrossRef]
52. Majumder, M.; Xin, X.; Liu, L.; Tutunea-Fatan, E.; Rodriguez-Torres, M.; Vincent, K.; Postovit, L.M.; Hess, D.; Lala, P.K. COX-2 Induces Breast Cancer Stem Cells via EP4/PI3K/AKT/NOTCH/WNT Axis. *Stem Cells* **2016**, *34*, 2290–2305. [CrossRef]
53. Majumder, M.; Xin, X.; Liu, L.; Girish, G.V.; Lala, P.K. Prostaglandin E2 receptor EP4 as the common target on cancer cells and macrophages to abolish angiogenesis, lymphangiogenesis, metastasis, and stem-like cell functions. *Cancer Sci.* **2014**, *105*, 1142–1151. [CrossRef]
54. Liu, S.; Ni, C.; Zhang, D.; Sun, H.; Dong, X.; Che, N.; Liang, X.; Chen, C.; Liu, F.; Bai, J.; et al. S1PR1 regulates the switch of two angiogenic modes by VE-cadherin phosphorylation in breast cancer. *Cell Death Dis.* **2019**, *10*, 200. [CrossRef] [PubMed]
55. Wagenblast, E.; Soto, M.; Gutiérrez-Ángel, S.; Hartl, C.A.; Gable, A.L.; Maceli, A.R.; Erard, N.; Williams, A.M.; Kim, S.Y.; Dickopf, S.; et al. A model of breast cancer heterogeneity reveals vascular mimicry as a driver of metastasis. *Nature* **2015**, *520*, 358–362. [CrossRef] [PubMed]
56. Stanton, S.E.; Adams, S.; Disis, M.L. Variation in the Incidence and Magnitude of Tumor-Infiltrating Lymphocytes in Breast Cancer Subtypes: A Systematic Review. *JAMA Oncol.* **2016**, *2*, 1354–1360. [CrossRef] [PubMed]
57. Fang, J.H.; Zheng, Z.Y.; Liu, J.Y.; Xie, C.; Zhang, Z.J.; Zhuang, S.M. Regulatory Role of the MicroRNA-29b-IL-6 Signaling in the Formation of Vascular Mimicry. *Mol. Therapy. Nucleic Acids* **2017**, *8*, 90–100. [CrossRef]
58. Aikins, A.R.; Kim, M.; Raymundo, B.; Kim, C.-W. Downregulation of transgelin blocks interleukin-8 utilization and suppresses vasculogenic mimicry in breast cancer cells. *Exp. Biol Med.* **2017**, *242*, 573–583. [CrossRef]
59. Wright, M.H.; Calcagno, A.M.; Salcido, C.D.; Carlson, M.D.; Ambudkar, S.V.; Varticovski, L. Brca1 breast tumors contain distinct CD44+/CD24- and CD133+ cells with cancer stem cell characteristics. *Breast Cancer Res.* **2008**, *10*, 10. [CrossRef]
60. Sengodan, S.K.; Nadhan, R.; Nair, R.S.; Hemalatha, S.K.; Somasundaram, V.; Sushama, R.R.; Rajan, A.; Latha, N.R.; Varghese, G.R.; Thankappan, R.K.; et al. BRCA1 regulation on β-hCG: A mechanism for tumorigenicity in BRCA1 defective breast cancer. *Oncogenesis* **2017**, *6*, 376. [CrossRef]
61. Zygmunt, M.; Herr, F.; Keller-Schoenwetter, S.; Kunzi-Rapp, K.; Münstedt, K.; Rao, C.V.; Lang, U.; Preissner, K.T. Characterization of human chorionic gonadotropin as a novel angiogenic factor. *J. Clin. Endocrinol. Metab.* **2002**, *87*, 5290–5296. [CrossRef]
62. Su, M.; Xu, X.; Wei, W.; Gao, S.; Wang, X.; Chen, C.; Zhang, Y. Involvement of human chorionic gonadotropin in regulating vasculogenic mimicry and hypoxia-inducible factor-1α expression in ovarian cancer cells. *Cancer Cell Int.* **2016**, *16*, 50. [CrossRef] [PubMed]
63. Yuri, T.; Kinoshita, Y.; Emoto, Y.; Yoshizawa, K.; Tsubura, A. Human chorionic gonadotropin suppresses human breast cancer cell growth directly via p53-mediated mitochondrial apoptotic pathway and indirectly via ovarian steroid secretion. *Anticancer Res.* **2014**, *34*, 1347–1354. [PubMed]
64. Iezzi, M.; Quaglino, E.; Cappello, P.; Toto, V.; Sabatini, F.; Curcio, C.; Garotta, G.; Musiani, P.; Cavallo, F. HCG hastens both the development of mammary carcinoma and the metastatization of HCG/LH and ERBB-2 receptor-positive cells in mice. *Int. J. Immunopathol. Pharmacol.* **2011**, *24*, 621–630. [CrossRef]
65. Laederich, M.B.; Funes-Duran, M.; Yen, L.; Ingalla, E.; Wu, X.; Carraway, K.L., 3rd; Sweeney, C. The leucine-rich repeat protein LRIG1 is a negative regulator of ErbB family receptor tyrosine kinases. *J. Biol. Chem.* **2004**, *279*, 47050–47056. [CrossRef] [PubMed]
66. Miller, J.K.; Shattuck, D.L.; Ingalla, E.Q.; Yen, L.; Borowsky, A.D.; Young, L.J.; Cardiff, R.D.; Carraway, K.L., 3rd; Sweeney, C. Suppression of the negative regulator LRIG1 contributes to ErbB2 overexpression in breast cancer. *Cancer Res.* **2008**, *68*, 8286–8294. [CrossRef]
67. Krig, S.R.; Frietze, S.; Simion, C.; Miller, J.K.; Fry, W.H.; Rafidi, H.; Kotelawala, L.; Qi, L.; Griffith, O.L.; Gray, J.W.; et al. Lrig1 is an estrogen-regulated growth suppressor and correlates with longer relapse-free survival in ERα-positive breast cancer. *Mol. Cancer Res.* **2011**, *9*, 1406–1417. [CrossRef] [PubMed]
68. Yokdang, N.; Hatakeyama, J.; Wald, J.H.; Simion, C.; Tellez, J.D.; Chang, D.Z.; Swamynathan, M.M.; Chen, M.; Murphy, W.J.; Carraway Iii, K.L.; et al. LRIG1 opposes epithelial-to-mesenchymal transition and inhibits invasion of basal-like breast cancer cells. *Oncogene* **2016**, *35*, 2932–2947. [CrossRef] [PubMed]
69. van Schooneveld, E.; Wouters, M.C.; Van der Auwera, I.; Peeters, D.J.; Wildiers, H.; Van Dam, P.A.; Vergote, I.; Vermeulen, P.B.; Dirix, L.Y.; Van Laere, S.J. Expression profiling of cancerous and normal breast tissues identifies microRNAs that are differentially expressed in serum from patients with (metastatic) breast cancer and healthy volunteers. *Breast Cancer Res.* **2012**, *14*, R34. [CrossRef]
70. Li, C.; Wang, A.; Chen, Y.; Liu, Y.; Zhang, H.; Zhou, J. MicroRNA-299-5p inhibits cell metastasis in breast cancer by directly targeting serine/threonine kinase 39. *Oncol. Rep.* **2020**, *43*, 1221–1233. [CrossRef]
71. Shevde, L.A.; Metge, B.J.; Mitra, A.; Xi, Y.; Ju, J.; King, J.A.; Samant, R.S. Spheroid-forming subpopulation of breast cancer cells demonstrates vasculogenic mimicry via hsa-miR-299-5p regulated de novo expression of osteopontin. *J. Cell. Mol. Med.* **2010**, *14*, 1693–1706. [CrossRef]

72. Yang, Z.; He, M.; Wang, K.; Sun, G.; Tang, L.; Xu, Z. Tumor suppressive microRNA-193b promotes breast cancer progression via targeting DNAJC13 and RAB22A. *Int. J. Clin. Exp. Pathol.* **2014**, *7*, 7563–7570.
73. Hulin, J.A.; Tommasi, S.; Elliot, D.; Hu, D.G.; Lewis, B.C.; Mangoni, A.A. MiR-193b regulates breast cancer cell migration and vasculogenic mimicry by targeting dimethylarginine dimethylaminohydrolase 1. *Sci. Rep.* **2017**, *7*, 13996. [CrossRef]
74. Zou, Q.; Zhou, E.; Xu, F.; Zhang, D.; Yi, W.; Yao, J. A TP73-AS1/miR-200a/ZEB1 regulating loop promotes breast cancer cell invasion and migration. *J. Cell. Biochem.* **2018**, *119*, 2189–2199. [CrossRef] [PubMed]
75. Yao, J.; Xu, F.; Zhang, D.; Yi, W.; Chen, X.; Chen, G.; Zhou, E. TP73-AS1 promotes breast cancer cell proliferation through miR-200a-mediated TFAM inhibition. *J. Cell. Biochem.* **2018**, *119*, 680–690. [CrossRef]
76. Tao, W.; Sun, W.; Zhu, H.; Zhang, J. Knockdown of long non-coding RNA TP73-AS1 suppresses triple negative breast cancer cell vasculogenic mimicry by targeting miR-490-3p/TWIST1 axis. *Biochem. Biophys. Res. Commun.* **2018**, *504*, 629–634. [CrossRef]
77. Li, W.; Jin, X.; Zhang, Q.; Zhang, G.; Deng, X.; Ma, L. Decreased expression of miR-204 is associated with poor prognosis in patients with breast cancer. *Int. J. Clin. Exp. Pathol.* **2014**, *7*, 3287–3292.
78. Salinas-Vera, Y.M.; Marchat, L.A.; García-Vázquez, R.; González de la Rosa, C.H.; Castañeda-Saucedo, E.; Tito, N.N.; Flores, C.P.; Pérez-Plasencia, C.; Cruz-Colin, J.L.; Carlos-Reyes, Á.; et al. Cooperative multi-targeting of signaling networks by angiomiR-204 inhibits vasculogenic mimicry in breast cancer cells. *Cancer Lett.* **2018**, *432*, 17–27. [CrossRef] [PubMed]
79. Lozano-Romero, A.; Astudillo-de la Vega, H.; Terrones-Gurrola, M.; Marchat, L.A.; Hernandez-Sotelo, D.; Salinas-Vera, Y.M.; Ramos-Payan, R.; Silva-Cazares, M.B.; Nunez-Olvera, S.I.; Hernandez-de la Cruz, O.N.; et al. HOX Transcript Antisense RNA HOTAIR Abrogates Vasculogenic Mimicry by Targeting the AngiomiR-204/FAK Axis in Triple Negative Breast Cancer Cells. *Non-Coding RNA* **2020**, *6*, 19. [CrossRef] [PubMed]
80. Hong, Z.; Hong, C.; Ma, B.; Wang, Q.; Zhang, X.; Li, L.; Wang, C.; Chen, D. MicroRNA-126-3p inhibits the proliferation, migration, invasion, and angiogenesis of triple-negative breast cancer cells by targeting RGS3. *Oncol. Rep.* **2019**, *42*, 1569–1579. [CrossRef] [PubMed]
81. Rossi, J.F.; Lu, Z.Y.; Jourdan, M.; Klein, B. Interleukin-6 as a therapeutic target. *Clin. Cancer Res. Off. J. Am. Assoc. Cancer Res.* **2015**, *21*, 1248–1257. [CrossRef] [PubMed]
82. Wang, Y.; Niu, X.L.; Qu, Y.; Wu, J.; Zhu, Y.Q.; Sun, W.J.; Li, L.Z. Autocrine production of interleukin-6 confers cisplatin and paclitaxel resistance in ovarian cancer cells. *Cancer Lett.* **2010**, *295*, 110–123. [CrossRef]
83. Zhang, G.J.; Adachi, I. Serum interleukin-6 levels correlate to tumor progression and prognosis in metastatic breast carcinoma. *Anticancer Res.* **1999**, *19*, 1427–1432.
84. Park, Y.; Kim, J. Regulation of IL-6 signaling by miR-125a and let-7e in endothelial cells controls vasculogenic mimicry formation of breast cancer cells. *BMB Rep.* **2019**, *52*, 214–219. [CrossRef]
85. Lim, D.; Cho, J.G.; Yun, E.; Lee, A.; Ryu, H.Y.; Lee, Y.J.; Yoon, S.; Chang, W.; Lee, M.S.; Kwon, B.S.; et al. MicroRNA 34a-AXL Axis Regulates Vasculogenic Mimicry Formation in Breast Cancer Cells. *Genes* **2020**, *12*, 9. [CrossRef]
86. Mudduluru, G.; Ceppi, P.; Kumarswamy, R.; Scagliotti, G.V.; Papotti, M.; Allgayer, H. Regulation of Axl receptor tyrosine kinase expression by miR-34a and miR-199a/b in solid cancer. *Oncogene* **2011**, *30*, 2888–2899. [CrossRef] [PubMed]
87. Hu, J.; Xu, J.; Wu, Y.; Chen, Q.; Zheng, W.; Lu, X.; Zhou, C.; Jiao, D. Identification of microRNA-93 as a functional dysregulated miRNA in triple-negative breast cancer. *Tumour Biol. J. Int. Soc. Oncodevelopmental Biol. Med.* **2015**, *36*, 251–258. [CrossRef]
88. An, G.; Lu, F.; Huang, S.; Bai, J.; He, L.; Liu, Y.; Hou, L. Effects of miR-93 on epithelial-to-mesenchymal transition and vasculogenic mimicry in triple-negative breast cancer cells. *Mol. Med. Rep.* **2021**, *23*, 1–8. [CrossRef] [PubMed]
89. Fang, L.; Du, W.W.; Yang, W.; Rutnam, Z.J.; Peng, C.; Li, H.; O'Malley, Y.Q.; Askeland, R.W.; Sugg, S.; Liu, M.; et al. MiR-93 enhances angiogenesis and metastasis by targeting LATS2. *Cell Cycle* **2012**, *11*, 4352–4365. [CrossRef] [PubMed]
90. Ganapathy, V.; Ge, R.; Grazioli, A.; Xie, W.; Banach-Petrosky, W.; Kang, Y.; Lonning, S.; McPherson, J.; Yingling, J.M.; Biswas, S.; et al. Targeting the Transforming Growth Factor-beta pathway inhibits human basal-like breast cancer metastasis. *Mol. Cancer* **2010**, *9*, 122. [CrossRef]
91. Herbertz, S.; Sawyer, J.S.; Stauber, A.J.; Gueorguieva, I.; Driscoll, K.E.; Estrem, S.T.; Cleverly, A.L.; Desaiah, D.; Guba, S.C.; Benhadji, K.A.; et al. Clinical development of galunisertib (LY2157299 monohydrate), a small molecule inhibitor of transforming growth factor-beta signaling pathway. *Drug Des. Dev. Ther.* **2015**, *9*, 4479–4499. [CrossRef]
92. Bhola, N.E.; Balko, J.M.; Dugger, T.C.; Kuba, M.G.; Sánchez, V.; Sanders, M.; Stanford, J.; Cook, R.S.; Arteaga, C.L. TGF-β inhibition enhances chemotherapy action against triple-negative breast cancer. *J. Clin. Investig.* **2013**, *123*, 1348–1358. [CrossRef] [PubMed]
93. Martini, C.; Thompson, E.J.; Hyslop, S.R.; Cockshell, M.P.; Dale, B.J.; Ebert, L.M.; Woods, A.E.; Josefsson, E.C.; Bonder, C.S. Platelets disrupt vasculogenic mimicry by cancer cells. *Sci. Rep.* **2020**, *10*, 5869. [CrossRef]
94. Taipale, M.; Krykbaeva, I.; Koeva, M.; Kayatekin, C.; Westover, K.D.; Karras, G.I.; Lindquist, S. Quantitative analysis of HSP90-client interactions reveals principles of substrate recognition. *Cell* **2012**, *150*, 987–1001. [CrossRef]
95. Rohner, N.; Jarosz, D.F.; Kowalko, J.E.; Yoshizawa, M.; Jeffery, W.R.; Borowsky, R.L.; Lindquist, S.; Tabin, C.J. Cryptic variation in morphological evolution: HSP90 as a capacitor for loss of eyes in cavefish. *Science* **2013**, *342*, 1372–1375. [CrossRef]
96. Neckers, L.; Trepel, J.B. Stressing the development of small molecules targeting HSP90. *Clin. Cancer Res. Off. J. Am. Assoc. Cancer Res.* **2014**, *20*, 275–277. [CrossRef] [PubMed]

97. Lee, C.H.; Hong, H.M.; Chang, Y.Y.; Chang, W.W. Inhibition of heat shock protein (Hsp) 27 potentiates the suppressive effect of Hsp90 inhibitors in targeting breast cancer stem-like cells. *Biochimie* **2012**, *94*, 1382–1389. [CrossRef] [PubMed]
98. Sims, J.D.; McCready, J.; Jay, D.G. Extracellular heat shock protein (Hsp)70 and Hsp90α assist in matrix metalloproteinase-2 activation and breast cancer cell migration and invasion. *PLoS ONE* **2011**, *6*, 18848. [CrossRef]

International Journal of
*Molecular Sciences*

MDPI

*Article*

# Endothelium-Dependent Induction of Vasculogenic Mimicry in Human Triple-Negative Breast Cancer Cells Is Inhibited by Calcitriol and Curcumin

**Gabriela Morales-Guadarrama [1], Edgar A. Méndez-Pérez [1], Janice García-Quiroz [1], Euclides Avila [1], Rocío García-Becerra [2,3], Alejandro Zentella-Dehesa [2,4,5], Fernando Larrea [1] and Lorenza Díaz [1,*]**

[1] Departamento de Biología de la Reproducción Dr. Carlos Gual Castro, Instituto Nacional de Ciencias Médicas y Nutrición Salvador Zubirán, Vasco de Quiroga No. 15, Belisario Domínguez Sección XVI, Tlalpan, Ciudad de México 14080, Mexico; gabriela.mguadarrama@gmail.com (G.M.-G.); edgar.mendez.p3@gmail.com (E.A.M.-P.); janice.garciaq@incmnsz.mx (J.G.-Q.); euclides.avilac@incmnsz.mx (E.A.); fernando.larreag@incmnsz.mx (F.L.)
[2] Programa de Investigación de Cáncer de Mama, Instituto de Investigaciones Biomédicas, Universidad Nacional Autónoma de México, Ciudad de México 04510, Mexico; rocio.garciab@iibiomedicas.unam.mx (R.G.-B.); azentell@iibiomedicas.unam.mx (A.Z.-D.)
[3] Departamento de Biología Molecular y Biotecnología, Instituto de Investigaciones Biomédicas, Universidad Nacional Autónoma de México, Ciudad de México 04510, Mexico
[4] Departamento de Medicina Genómica y Toxicología Ambiental, Instituto de Investigaciones Biomédicas, Universidad Nacional Autónoma de México, Ciudad de México 04510, Mexico
[5] Unidad de Bioquímica, Instituto Nacional de Ciencias Médicas y Nutrición Salvador Zubirán (INCMNSZ), Ciudad de México 14080, Mexico
* Correspondence: lorenza.diazn@incmnsz.mx; Tel.: +52-(55)-5487-0900 (ext. 2417)

**Citation:** Morales-Guadarrama, G.; Méndez-Pérez, E.A.; García-Quiroz, J.; Avila, E.; García-Becerra, R.; Zentella-Dehesa, A.; Larrea, F.; Díaz, L. Endothelium-Dependent Induction of Vasculogenic Mimicry in Human Triple-Negative Breast Cancer Cells Is Inhibited by Calcitriol and Curcumin. *Int. J. Mol. Sci.* **2022**, *23*, 7659. https://doi.org/10.3390/ijms23147659

Academic Editor: Hwan-Suck Chung

Received: 28 May 2022
Accepted: 9 July 2022
Published: 11 July 2022



**Abstract:** In highly aggressive tumors, cancer cells may form channel-like structures through a process known as vasculogenic mimicry (VM). VM is generally associated with metastasis, mesenchymal phenotype, and treatment resistance. VM can be driven by antiangiogenic treatments and/or tumor microenvironment-derived factors, including those from the endothelium. Curcumin, a turmeric product, inhibits VM in some tumors, while calcitriol, the most active vitamin D metabolite, exerts potent antineoplastic effects. However, the effect of these natural products on VM in breast cancer remains unknown. Herein, we studied the effect of both compounds on triple-negative breast cancer (TNBC) VM-capacity in a co-culture model. The process of endothelial cell-induced VM in two human TNBC cell lines was robustly inhibited by calcitriol and partially by curcumin. Calcitriol promoted TNBC cells' morphological change from spindle-like to cobblestone-shape, while curcumin diminished VM 3D-structure. Notably, the treatments dephosphorylated several active kinases, especially those involved in the PI3K/Akt pathway. In summary, calcitriol and curcumin disrupted endothelium-induced VM in TNBC cells partially by PI3K/Akt inactivation and mesenchymal phenotype inhibition. Our results support the possible use of these natural compounds as adjuvants for VM inactivation in patients with malignant tumors inherently capable of forming VM, or those with antiangiogenic therapy, warranting further in vivo studies.

**Keywords:** co-culture; tubulogenesis; vascular mimicry; breast cancer; epithelial-to-mesenchymal transition

## 1. Introduction

Triple-negative breast cancer (TNBC), the most aggressive tumor phenotype of the mammary gland, is commonly resistant to conventional therapy, has very limited approved targeted treatments, and is commonly associated with poor prognosis and a high recurrence risk. Among the signaling pathways known to be involved in the

malignant features of TNBC tumors, the phosphatidylinositol-3-kinase/Protein kinase B (PI3K/Akt) signaling pathway plays a fundamental oncogenic role in promoting proliferation and survival of cancer cells [1,2]. Notably, the activation of this and other canonical pathways, such as p38/Mitogen-activated protein kinase (MAPK), is critical for vasculogenic mimicry (VM) formation in breast cancer [3–5]. VM is the process cancer cells undertake to form tube-like or micro-vessel-like structures in solid tumors, and is clinically relevant given its association with metastasis and resistance to antiangiogenic treatments. The VM vessel network compensates for the lack of endothelial-derived vessels in avascular tumors, allowing access to blood and providing an escape route to invade distant sites. Besides hypoxia, tumor microenvironment-derived factors may act as drivers of VM, including vascular endothelial growth factor (VEGF) and cytokines, such as transforming growth factor beta (TGFB) [5–7]. Notably, some of these factors are related to the promotion of epithelial-to-mesenchymal transition (EMT), a process that in breast cancer has been linked with the generation of cancer cells with a stem cell-like phenotype, which are believed to be the source of VM [8]. Due to the intrinsic plasticity of VM-forming cells, they may transdifferentiate into endothelial-like cells, displaying stemness features, high renewal ability, metastatic capacity, and chemoresistance [8,9]. All these properties may contribute to the poor prognosis and compromised therapeutic response of patients with breast tumors undergoing VM [5]. Therefore, implementing VM targeting strategies is of utmost importance, especially for TNBC tumors, in which a significantly higher VM rate has been reported, compared to non-TNBC [10]. Importantly, antiangiogenic treatments can induce VM by generating hypoxia, which is why their combination with anti-VM compounds can help reduce treatment-resistance.

Regarding VM targeting, the natural compound curcumin, derived from *Curcuma longa*, is known to suppress VM-drivers and VM-formation in different types of cancer cells; however, to date, its effects on VM in breast cancer has remained unexplored [11,12]. The anti-VM potential of curcumin in hepatocellular carcinoma, a tumor characterized by hyper-vascularization and enriched vascular networks, was shown to involve the inhibition of the PI3K/Akt signaling pathway. Likewise, in choroidal melanoma, the curcumin anti-VM effect involved the down-regulation of the EphA2/PI3K/matrix metalloproteinase (MMP) pathway [11,12]. In addition, curcumin has also been shown to inhibit VM in squamous cell carcinoma of the larynx through the inhibition of the Janus kinase-2 (JAK-2)/signal transducer activator of transcription protein (STAT) signaling pathway, and the downregulation of MMP-2 and VEGF expression [13].

On the other hand, calcitriol, the most active vitamin D metabolite, exerts pro-differentiating and antiproliferative effects in breast cancer [14], and has shown an anti-EMT effect in epithelial cells through inhibiting the PI3K/Akt/β-catenin pathway [15]. Also, calcitriol exerts potent anti-inflammatory activity, partially through downregulating JAK-STAT pathway activation and inflammatory cytokine production, processes known to be involved in carcinogenesis and VM [16,17]; however, calcitriol's effects upon VM has not been explored. Regarding this, while this article was under peer review, Khuloud Bajbouj et al. reported that calcitriol differentially downregulated VM-related pathways and the expression of key VM markers in calcitriol-treated breast cancer cells by an in silico analysis of transcriptomic databases [18]. The same research group also showed that a very high concentration of calcitriol (10 μM) stimulated the expression of tissue inhibitors of MMPs (TIMPs) and decreased that of MMPs, lowering the formation of VM in MDA-MB-231 cells [18]. The effects of curcumin, those of nanomolar calcitriol concentrations, and those exerted by the combination of these compounds on VM development in breast cancer, as well as the mechanisms potentially involved, do, however, remain unknown, which were the originating concepts of our research question. To address this matter, we implemented a model that included the participation of tumor microenvironment-derived factors involved in VM-induction. Knowing that endothelial cells can induce tumor cells to undergo VM [19], we used an in vitro co-culture model of endothelial-induced VM in TNBC cells co-cultured with endothelial cells. Once we

characterized the VM-process in our experimental model, we tested the effects of calcitriol, curcumin, and their combination on the ability of tumor cells to form tube-like structures. Furthermore, for mechanistic insights, we explored the ability of the natural compounds to dephosphorylate several kinases known to be involved in VM formation. Part of the novelty of this research resides in the experimental model that we used, the calcitriol concentrations tested that can be safely achieved in patients, and the compounds combinatorial effect upon VM.

## 2. Results

### *2.1. Calcitriol, Curcumin and Their Combination Inhibited Endothelial-Dependent VM Formation by Breast Cancer Cells*

Paracrine pro-vasculogenic factors from endothelial origin are known to act on tumor cells, altering their behavior [19,20]. As a result of this communication, endothelial cells can enable tumor cells to undergo trans-differentiation, forming cords with a tube-like structure, namely, VM [19,21]. In this study, we used an in vitro co-culture model of endothelial-induced VM in TNBC cells to study the anti-VM effect of calcitriol and curcumin (Figure 1A). As a control, we first validated VM by staining TNBC cells with a green fluorescent Cell Tracker to distinguish which cell type was located in the cord-like tubular formations of the co-cultures. Co-culturing TNBC MBCDF-T cells with EA.hy926 endothelial cells resulted in the development of defined tridimensional interconnecting cord-like tubular networks. These structures were formed by green-stained cancer cells, localized in an elevated focal plane above the endothelial monolayer that seemed to provide the extracellular matrix to support them (Figure 1B, upper panels). Depending on the confluence, the cord-like tubular structures started forming within 24 h of co-culturing, developing meshes containing unstained-endothelial cells underneath, evident only by their blue colored nuclei (Figure 1B). Note that nuclei from endothelial cells in co-cultures appear less bright than those from cancer cells, probably due to the different focal planes and the fact that endothelial cells have the tendency of spreading out. The cells that formed VM in the higher focal plane had a spindle-shaped fibroblast-like phenotype, suggestive of trans-differentiation into a mesenchymal-like lineage (Figure 1B, upper panels). Of note, monocultures of both TNBC cell lines tested in this study could not form VM by themselves, as seen in Figure 1B for MBCDF-T (Figure 1B, lower panels), supporting the pro-VM activity of the endothelial secretome and extracellular matrix.

Interestingly, both TNBC cell lines co-cultured with endothelial EA.hy926 cells and incubated in the presence of calcitriol failed to form VM, and changed their shape from spindle-like to cobblestone form (Figures 2 and S1). This morphological change of TNBC cells was also observed in monocultures (Figure S1), strongly suggesting cell differentiation and EMT inhibition as possible causes of calcitriol-dependent VM deterrence in co-cultures. Curcumin treatment also affected TNBC-VM formation in the co-cultures; however, its effect was less evident compared with that of calcitriol. Actually, curcumin treatment resulted in the partial breakdown of the VM-3D structure, suggesting that this compound affects cell organization/adhesion in the meshes formed by cancer cells (Figure 2). Regarding morphometric parameters, both curcumin and calcitriol significantly reduced the number of segments and meshes compared to controls, as seen in the graphics of Figure 2. In fact, the compounds were able to inhibit VM in a concentration-dependent manner (Figures S2 and S3). Remarkably, in both TNBC cell lines co-cultured with endothelial cells, the combination of calcitriol and curcumin further abrogated VM formation (Figures 2 and S4).

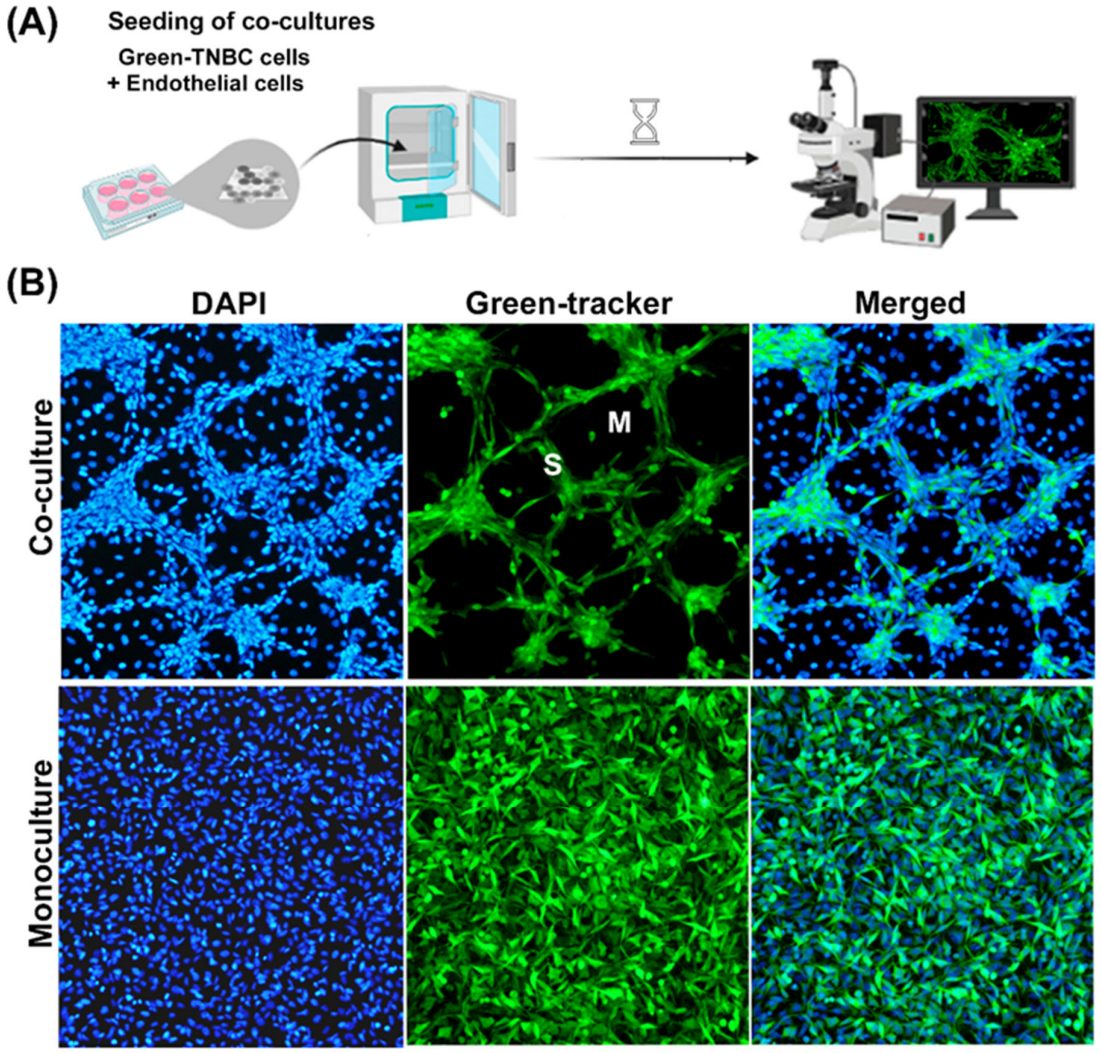


**Figure 1.** Characterization of the co-culture model of TNBC cells with endothelial cells. (**A**) Illustration of the vasculogenic mimicry process in vitro. TNBC cells stained with a green tracker were seeded with endothelial cells (1:1) and allowed to interact for 2 days. The formation of cord-like networks was evaluated with epifluorescence microscopy. (**B**) MBCDF-T cells stained with a green cell fluorescent tracker were incubated in the presence (upper panels, co-cultures) or the absence (lower panels, monocultures) of unstained endothelial cells (EA.hy926). Afterwards, cells were fixed with ethanol. A mounting medium containing DAPI was used to label cell nuclei in blue (left panels). TNBC cells- vasculogenic mimicry was identified only in co-cultures by the formation of meshes (M) and segments (S) stained in green (upper panels). Merged pictures are shown in right panels. Magnification is 10×.

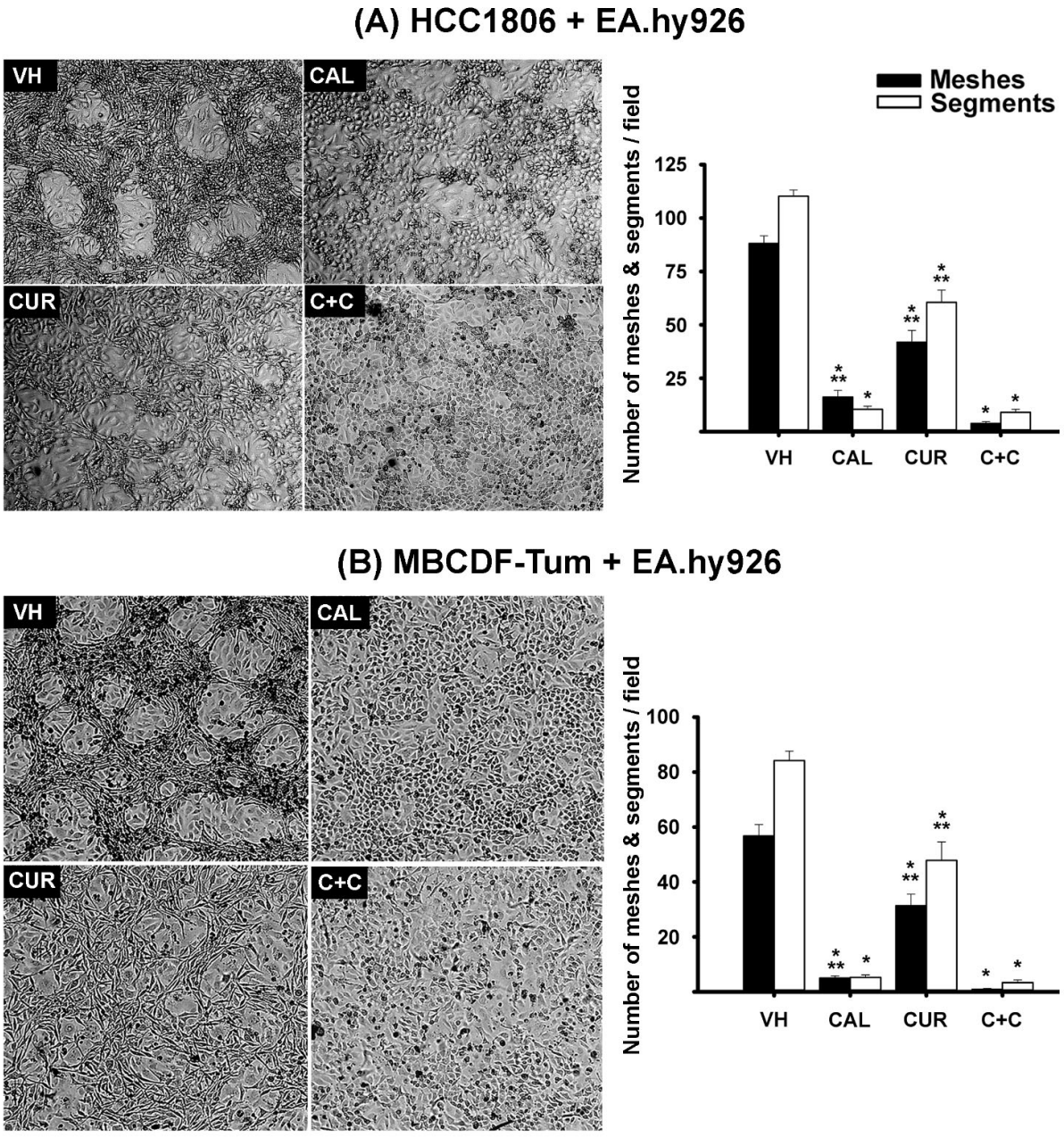


**Figure 2.** Calcitriol and curcumin inhibited endothelium-induced TNBC-VM capacity in co-cultures. EA.hy926-induced VM was observed in co-cultures of HCC1806 (**A**) and MBCDF-T (**B**) cells incubated with vehicle (VH, ethanol). The presence of calcitriol (CAL, 10 nM) changed cell morphology from spindle-shape to cobblestone-like and abrogated VM formation, while curcumin (CUR, 20 μM) affected the 3D VM structure. The combination of calcitriol with curcumin (C+C) further inhibited VM in both TNBC cells. The number of meshes and segments *per* visual field were counted by three different observers in hot spots in at least 10 different photographs, considering 3 different experiments for each cell line. The graphics depict the average number of meshes and segments *per* visual field. * $p < 0.001$ vs. VH. ** $p < 0.01$ vs. C+C. Magnification is 10×.

### *2.2. In TNBC Cells Co-Cultured with Endothelial Cells, Calcitriol and Curcumin Inhibited the Phosphorylation of Several Kinases of the MAPK, PI3K/Akt/mTOR, PI3K/Akt/CREB and PI3K/Akt/Gsk Signaling Pathways*

To study the phosphorylation profile of kinases involved in signaling pathways relevant to VM, we chose MBCDF-T/EA.hy926 co-cultures. A semi-supervised hierarchical clustering of the targets differentially phosphorylated detected with an antibody array (human MAPK Phosphorylation Antibody Array, ab211061, Abcam) was carried out. Results were then represented on a heat map clustered in groups encompassing three main signaling pathways: PI3K/Akt, mammalian target of rapamycin (mTOR), and MAPK (Figure 3). We found that Akt, together with the cAMP response element-binding protein (CREB) and glycogen synthase kinase-3 (Gsk3)$\alpha$ (labeled in black, Figure 3), were the kinases more strongly phosphorylated in control co-cultures. Remarkably, calcitriol or curcumin downregulated the phosphorylation of these proteins as well as p53, P70S6K, and p38, while their combination further inhibited the overall kinases activation status (Figures 3 and S2). On the other hand, the kinases of mTOR complexes and some of the MAPK, such as MKK3, MKK6, MSK2, RSK1 and RSK2 (labeled in red, Figure 3), were strongly inhibited by calcitriol, while the phosphorylation status of Gsk3$\alpha$, Gsk3$\beta$, p53, p38, JNK and Hsp27 (labeled blue, Figure 3) was more intensely downregulated by curcumin. The graphical representation of symbolic kinases inactivated by the compounds with statistical significance is provided in Figure S5. These results suggested that each treatment differentially targeted distinctive parts of the signaling pathways. When combined, a global effect upon dephosphorylation was enhanced, leading to a more potent VM functional inhibition. Furthermore, the STRING analysis indicated that these proteins interacted forming complexes between them, and were involved in several biological functions, as shown in Figure 4A,B. Among predicted processes regulated by calcitriol and curcumin, the VM-related pathways involving Wnt, VEGF, MAPK, PI3K/AKT and mTOR were identified (purple circle, Figure 4C). Interestingly, only calcitriol was related to the inflammatory pathway involving cytokine production and response (navy blue circle, Figure 4C), while curcumin was related to signaling of TGFB, fibroblast growth factor receptor (FGFR), microRNA (miRNA) and p53 (light blue circle, Figure 4C). Moreover, the combination of calcitriol and curcumin affected networks related to cell death, such as apoptosis, anoikis and autophagy, while curcumin alone was associated with senescence and EMT. Finally, major drivers involved in VM are plasticity and adhesion molecules, which were predicted to be affected by both compounds (Figure 4C).

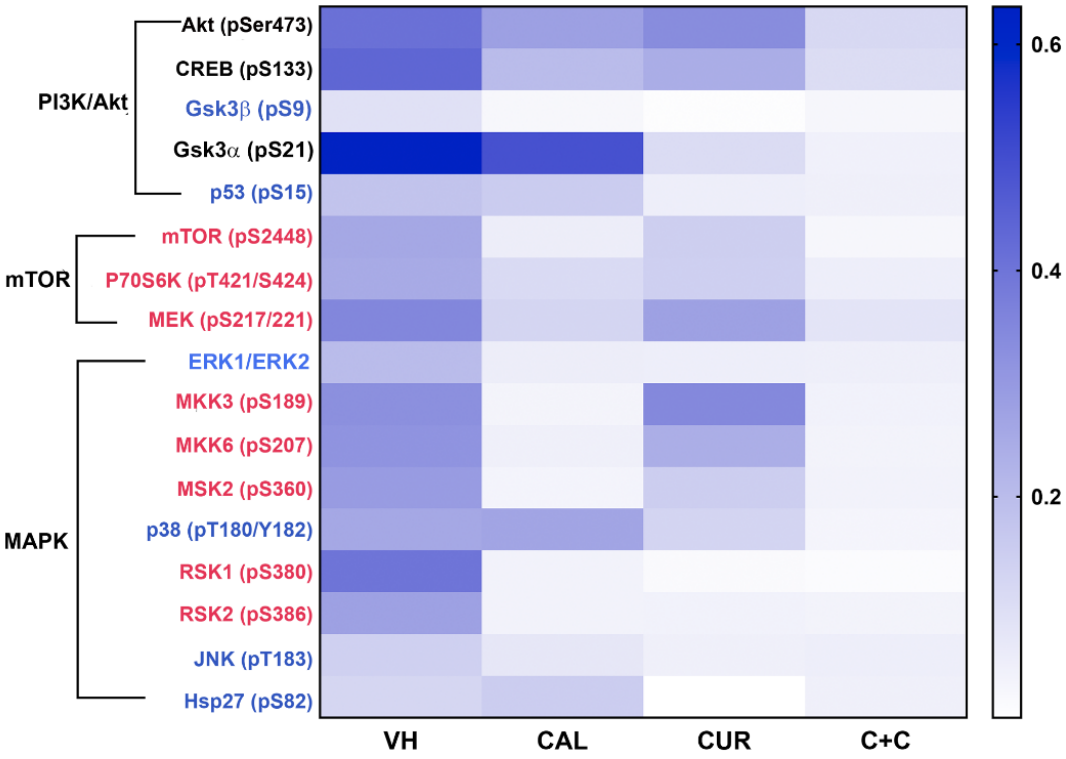


**Figure 3.** In MBCDF-T/EA.hy926 co-cultures, calcitriol and curcumin inhibited the phosphorylation of several protein targets of the MAPK, PI3K/Akt/mTOR, PI3K/Akt/CREB and PI3K/Akt/Gsk signaling pathways. The phosphorylation profile of kinases involved in signaling pathways relevant to VM was differentially inhibited by calcitriol (CAL, 10 nM), curcumin (CUR, 20 μM) and their combination (C+C). A semi-supervised hierarchical clustering of the targets differentially phosphorylated detected with a multiplex antibody array was carried out and results are shown in the heat map clustered in three main signaling pathways: PI3K/Akt, mTOR and MAPK. The more strongly phosphorylated kinases in vehicle-treated co-cultures (VH) are labeled in black. Kinases mostly inhibited by calcitriol are labeled in red, while phosphorylated protein targets more strongly downregulated by curcumin are labeled in blue. N = 4.

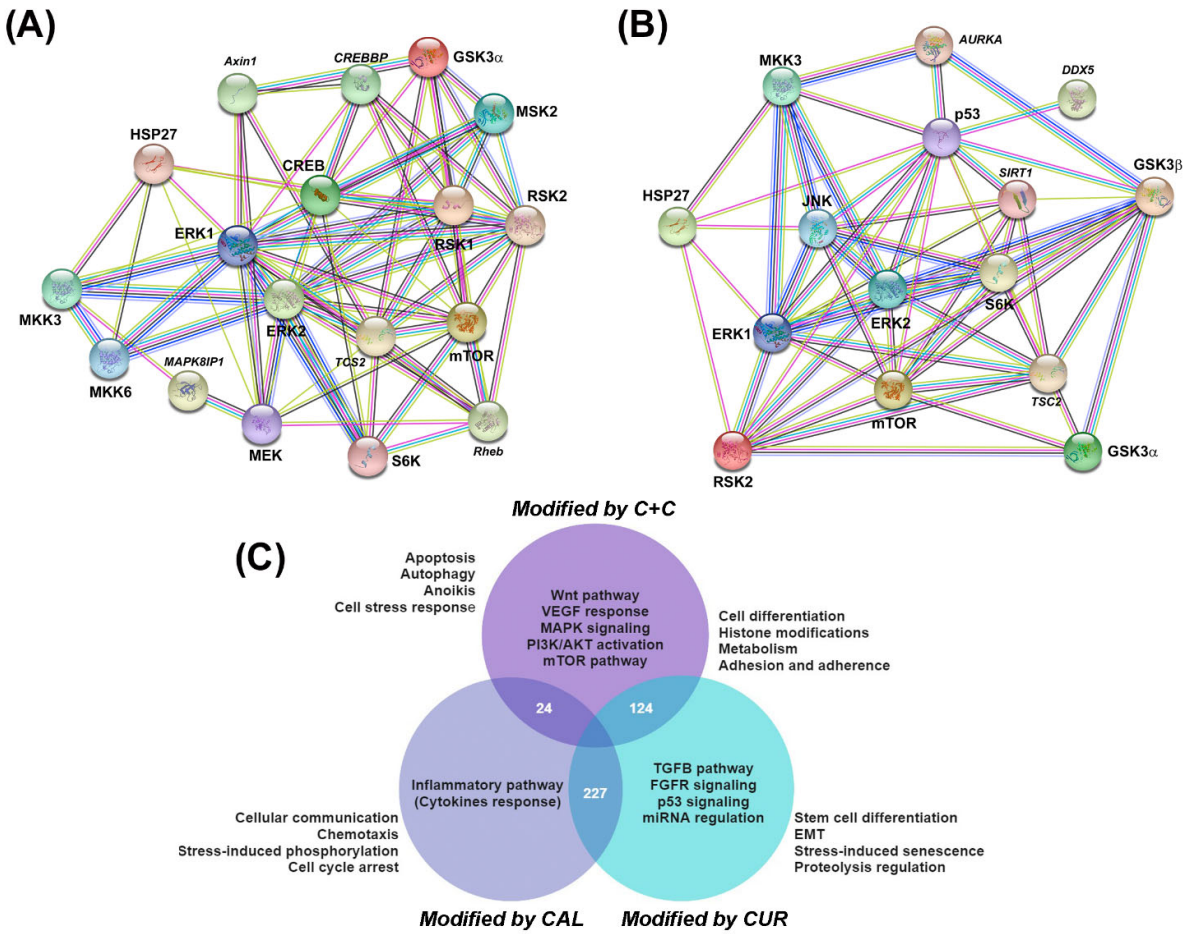


**Figure 4**. Interaction networks and biological processes regulated by calcitriol, curcumin or their combination involved in the anti-VM effect of the compounds. STRING analysis of deregulated kinases in calcitriol (**A**) or curcumin (**B**) treated co-cultures. Images in (**A**,**B**) show the physical and functional protein interactions. Protein names in italics represent the top predicted interactors of the network. (**C**) Prediction of the biological processes differentially regulated in each treatment group. A total of 227 processes were co-regulated by calcitriol (CAL) and curcumin (CUR); 24 processes were shared by the CAL and CAL+CUR (C+C), and 124 were shared in the CUR and C+C groups. Inside each circle, the main pathways involved are depicted. Outside, near each circle, the biological processes in which protein complexes were predicted to participate are shown.

## 3. Discussion

Tumor growth and dissemination significantly depend on forming a functional vascular network. Many mechanisms are involved in this process, but VM stands out among them in the case of highly malignant hypoxic tumors. VM comprises de novo generation of vessels lined with tumor cells, bypassing the lack of functional endothelial vessels. This process can lead to resistance to drugs intended to block tumor vascularization, explaining their failure in the clinic. In this study, we found that the natural compounds calcitriol and curcumin inhibited endothelial-induced VM-formation in TNBC cell lines in vitro, which was significantly potentiated by the concomitant use of both compounds. Calcitriol's mode of action seemed to involve EMT inhibition, as judged by the change in the cancer cells' shape from spindle-like to cobblestone, which would explain the ability of this hormone to robustly block VM from the start. Indeed, VM is highly dependent on the mesenchymal cell phenotype and the stemness characteristics of the cells, which confer cell plasticity. In this regard, calcitriol is known to block EMT via

the inactivation of PI3K/Akt/β-catenin signaling, and to induce cell differentiation [15]. In addition, calcitriol is a potent anti-inflammatory hormone that inhibits inflammatory cytokine expression, such as interleukin-6 (IL6) [16]. Recently, it has been described that IL6 from endothelial origin acts as a paracrine factor upon MDA-MB-231 breast cancer cells, inducing VM formation [19], warranting further studies on calcitriol effects upon inflammatory cytokines in co-cultures of TNBC and endothelial cells. Altogether, this may help to explain the strong anti-VM effects of calcitriol. Curcumin, on the other hand, did not inhibit EMT in this study, as judged by the lack of modification of the cells' fusiform shape. As a result, cord like tubular structures were partially formed by curcumin-treated cancer cells. However, in general, these structures lacked the 3D configuration observed in control cultures, and significantly fewer segments and meshes were formed in comparison to vehicle-treated co-cultures of HCC1806. Considering a previous study showing that curcumin induced cell death in endothelial cells, while inhibiting both MBCDF-T and EA.hy926 cell proliferation and migration [22], it is possible that these effects were involved in the anti-VM mechanism of curcumin observed herein, affecting both cell components of the co-culture. In addition, curcumin is known to exert anti-tyrosine kinase activity [23], which is important to the VM process, since some of its drivers, such as VEGF, mediate their effect through tyrosine kinase receptors. Another possibility to explain curcumin's disruptive effect on the VM 3D structure is the downregulation of intercellular-adhesion molecules required for holding the 3D structure together. In this regard, it has been described that curcumin blocks the cell surface expression of adhesion molecules in endothelial cells, reduces cancer cell binding to extracellular matrix proteins, and significantly decreases the adhesion propensity of breast cancer cells [24–26]. These curcumin effects, together with calcitriol pro-differentiating, anti-inflammatory and anti-EMT effects, might explain the ability of both compounds to significantly inhibit VM in our co-cultured TNBC cells. Supporting this, among the predicted processes regulated by curcumin in combination with calcitriol in our STRING analysis were adhesion, cell differentiation and several signaling pathways involved in VM. In this regard, calcitriol and curcumin in combination globally affected the phosphorylation status of a panel of kinases relevant to the VM process. In particular, signaling components of the PI3K/Akt pathway seemed to be the most important for VM formation in our co-culture system, including Akt, CREB and Gsk3$\alpha$. The latter was in line with known drivers of the VM process that activate PI3K/Akt signaling, including some tumor microenvironment-derived factors such as cytokines, FGF and VEGF [27–32]. These and other growth factor-dependent activation of the PI3K/Akt pathway results in Gsk3 inactivation, a process associated with cancer progression. Indeed, Gsk3 activity is known to be inhibited through phosphorylation of Gsk3$\alpha$ at serine 21 and Gsk3β at serine 9. These specific serine residues in Gsk3 are known targets of Akt and other kinases able to phosphorylate them [33]. Loss of Gsk3 activity leads to the blockade of its antineoplastic effects, since Gsk3 acts as a tumor suppressor by negatively regulating molecules involved in cancer development [33]. Remarkably, the phosphorylation of Gsk3$\alpha$ at serine 21 and Gsk3β at serine 9 was found downregulated by curcumin and calcitriol in this study. Since Gsk3 is phosphorylated by Akt, the calcitriol and curcumin-dependent downregulation of Akt phosphorylation found herein was likely the cause of Gsk3 dephosphorylation, partially explaining the anti-VM activity of both compounds. Notably, through docking, it has been described that curcumin fits into the binding pocket of Gsk3β, modulating its activity [34]. Furthermore, curcumin has also been reported to dephosphorylate Akt and Gsk3 in acute lymphoblastic leukemia [35] and to dramatically downregulate the expression of Akt in TNBC cells, resulting in the suppression of cellular proliferation and migration [36]. Similarly, and as found in this study, calcitriol has previously been shown to reduce Akt phosphorylation in breast cancer and renal epithelial cells [15,37].

Noteworthy is the fact that, besides being involved in VM development, the MAPK, PI3K/Akt/mTOR and PI3K/Akt/Gsk signaling pathways are also implicated in different cellular functions relevant to cancer progression, such as cell proliferation, adhesion,

migration, metabolism, and survival [4,28]. Therefore, the fact that calcitriol and curcumin significantly downregulated these pathways further supports the antineoplastic potential of these natural compounds alone and combined.

An interesting finding in this study was the dephosphorylation of p53 at serine 15 by curcumin and its combination with calcitriol. Such dephosphorylation is expected because PI3K-related protein kinases ATM and ATR, responsible for the covalent modification on p53, are inhibited by curcumin [38]. Phosphorylation of p53 at serine 15 is required for the activation of p53-responsive promoters [39]. Thus, it seems that curcumin interferes with the p53 transcriptional activity blocking the DNA damage response in cancer cells.

Overall, the data suggest that endothelial cells' paracrine signaling induced TNBC tumor cells to form VM by activating Akt, CREB and Gsk3$\alpha$ among other important factors related to plasticity and angiogenesis. Calcitriol significantly prevented VM formation in TNBC co-cultures, while curcumin deterred VM 3D structures, at least partially, through downregulating the phosphorylation of several PI3K/Akt pathway components and p53. The combination of calcitriol and curcumin further inhibited the global protein phosphorylation status, explaining the improved effect on VM inhibition. Interestingly, the phosphorylation pattern evoked by the combination of calcitriol and curcumin, is similar to what could be expected when using a multi-kinase inhibitor drug. All considered, calcitriol and curcumin are a good option to use as antiangiogenic therapy adjuvants to help avoid VM generation. Moreover, since these natural compounds' combination has shown in vivo antiangiogenic effects *per se* [22], the fact that it also exerts anti-VM activity further supports its therapeutic plausibility in a clinical adjuvant context, warranting more studies. In conclusion, our study provides novel knowledge, showing, for the first time, that curcumin and calcitriol alone and combined inhibit VM formation in TNBC cells, through the downregulation of PI3K/Akt signaling.

## 4. Materials and Methods

### *4.1. Cell Cultures and Treatments*

In this study we used two human TNBC cell lines: the MBCDF-Tum (MBCDF-T), which was generated from a primary cell culture of a TNBC invasive ductal breast carcinoma [22], and the commercial cell line HCC1806 (ATCC, Manassas, VA, USA). For the co-culture model, we used the human endothelial cell line EA.hy926 (ATCC CRL-292). Both cell lines were maintained under standard culture conditions in control medium (DMEM-F12 medium, 100 units/mL penicillin, 100 μg/mL streptomycin, 5% fetal bovine serum), while experimental procedures were carried out in the same medium, but supplemented with charcoal-stripped fetal bovine serum. Co-cultures were implemented by simultaneously seeding endothelial cells with breast cancer cells (1:1 ratio, 150,000 cells *per* cell line) on square glass coverslips placed into 6-well plates.

### *4.2. Reagents*

The curcumin and calcitriol used for our in vitro studies were from Sigma (Sigma–Aldrich, St Louis, MO, USA). Ethanol (0.1%) was used as a vehicle for both compounds. For characterization of cell co-cultures, TNBC cells were labeled by incubation of live cells with 5-chloromethylfluorescein diacetate, CellTracker Green CMFDA Dye (Invitrogen, Eugene, OR, USA). Cell culture media, antibiotics, and fetal bovine serum were from Gibco/Invitrogen (Invitrogen, CA, USA).

### *4.3. Evaluation of Calcitriol and Curcumin Effects on VM Networks in TNBC Cells*

To validate our VM model, TNBC cells were stained with a fluorescent green Cell Tracker™ (ab138891, Abcam, Cambridge, MA, USA) and seeded in monoculture or co-cultured with endothelial cells (1:1). After 2 days, cells were washed and fixed in 80% ethanol for 10 min. After air drying, a drop of UltraCruz™ mounting medium containing

4′,6-diamidino-2-phenylindole (DAPI, Santa Cruz Biotechnology, Santa Cruz, CA, USA) was added to coverslips, which were then placed onto slides and further photographed with a conventional fluorescence microscope equipped with an Olympus DP72 camera (Olympus Optical Co., Ltd., Tokyo, Japan), a 100 W high-pressure mercury burner and suitable filters.

To quantitatively evaluate the effect of curcumin and calcitriol on the vasculogenic capacity of TNBC cells, the treatments were introduced at the time of co-cultures seeding. Ethanol (0.1%) was used as the vehicle, and different calcitriol and curcumin concentrations were tested, either alone or combined. Co-cultures were visually inspected daily, and after VM formation in vehicle-treated co-cultures, bright field images were acquired in VM-hot spots by conventional microscopy. We chose bright-field images to assess cell morphology, since it yields the possibility to evaluate more descriptive features, such as cell shape and texture in live cells, considering the two cell types of the co-cultures. Experiments were repeated at least three times. Three different observers counted segments and meshes *per* visual field in hot spots of several 4X images. Segments were cords/branches formed by cells, delimited by two junctions, while meshes referred to closed areas surrounded by segments (Figure 1).

### *4.4. MAPK Activation/Phosphorylation Array and Analysis of Protein–Protein Interaction Networks*

In order to unveil pathways involved in the inhibitory effect of curcumin and calcitriol on the ability of TNBC cells to form VM, we compared the changes in kinase activation of the MAPK and PI3K/Akt pathways by using the human MAPK Phosphorylation Antibody Array (ab211061, Abcam), which allowed us to simultaneously evaluate several phosphorylated proteins in our co-cultures cell lysates. All steps were carried out as recommended by the manufacturer. The phosphorylation sites on each protein tested were: Akt (pS473), CREB (pS133), ERK1 (pT202/Y204), ERK2 (pT185/Y187), GSK3α (pS21), GSK3β (pS9), HSP27 (pS82), JNK (pT183), MEK (pS217/221), MKK3 (pS189), MKK6 (pS207), MSK2 (pS360), mTOR (pS2448), p38 (pT180/Y182), p53 (pS15), P70S6K (pT421/S424), RSK1 (pS380) and RSK2 (pS386). After treating the co-cultures with the vehicle, calcitriol, curcumin, or their combination, cell lysates were prepared using the provided lysis buffer supplemented with a phosphatase and protease inhibitor cocktail, and stored at −80°C until assay performance. Total protein in cell lysates was quantified using the BCA Protein Assay kit (Thermo Fisher Scientific, Rockford, IL, USA) and 500 µg were applied to previously blocked membranes and incubated overnight at 4 °C. The membranes were washed and subsequently incubated with HRP-Anti-Rabbit IgG and detection antibody cocktail. Chemiluminescent signals were acquired and analyzed using the ChemiDoc XRS+ System (BioRad). Semi-quantitative comparisons between treatments were performed after normalization against positive controls, which are included in each membrane. Spots with no signal were disregarded. For visual comparison of relative differences among treatments, we categorized the positive results by canonical pathways in a heat map and also used graphic representation for specific phosphorylated kinases using the GraphPad Prisma 7 software. Two different experiments were run in separate membranes. We tested every target in each membrane twice. To construct a functional association network for the proteins involved in the effects of the treatments, targets with fold changes greater than 0.5 were subjected to a prediction analysis for protein-protein interactions by using the Search Tool for the Retrieval of Interacting Genes/Proteins (STRING, https://string-db.org/, last accessed on 25 April 2022), considering no more than 5 predicted interactors for each condition and associated biological processes.

### *4.5. Statistical Analysis*

One-way ANOVA followed by the Holm-Sidak method was used for multiple comparisons using a specialized software package (SigmaStat, Jandel Scientific). Data were expressed as the mean ± standard error of the mean (SEM). The differences between

calcitriol and calcitriol + curcumin in Figure 2 were analyzed by Student's *t*-test. The results were considered significant at $p < 0.05$.

## 5. Conclusions

Calcitriol and curcumin suppressed endothelial-induced TNBC cell VM formation, at least in part, by blocking the PI3K/Akt pathway, and subsequently affecting several cellular survival processes. Our results suggest the potential clinical use of calcitriol and curcumin to inhibit VM in TNBC tumors.

**Supplementary Materials:** The following supporting information can be downloaded at: www.mdpi.com/article/10.3390/ijms23147659/s1.

**Author Contributions:** Validation, methodology, investigation, formal analysis, visualization and Writing-review and editing, G.M.-G.; validation, methodology, investigation, formal analysis and visualization, E.A.M.-P.; methodology, investigation, formal analysis and visualization, J.G.-Q.; formal analysis, writing review, editing and visualization, R.G.-B.; writing-review and editing, A.Z.-D.; writing-review and editing, E.A.; writing-review and editing, F.L.; conceptualization, validation, methodology, investigation, formal analysis, visualization, writing-original draft preparation, supervision, project administration and funding acquisition, L.D. All authors have read and agreed to the published version of the manuscript.

**Funding:** This study was funded by Consejo Nacional de Ciencia y Tecnología de México (CONACyT), grant number A1-S-10749 to L.D. The funders had no role in the study design, analysis and interpretation of the data, writing of the manuscript or the decision to submit the article for publica-tion.

**Institutional Review Board Statement:** Not applicable.

**Informed Consent Statement:** Not applicable.

**Data Availability Statement:** The authors confirm that the data supporting the findings of this study are available within the article [and/or] its Supplementary Materials.

**Acknowledgments:** Gabriela Morales-Guadarrama is a student from Programa de Doctorado en Ciencias Biomédicas, Universidad Nacional Autónoma de México (UNAM) and received fellowship 662170 from CONACyT, México, for which we are very grateful. This study was part of GM-G thesis work to obtain her PH.D. degree in Biomedical Sciences. We are also grateful for the support from Fundación amigos del INCMNSZ, A.C. (Grant number 348 to GM-G). The authors would like to thank Salvador Ramirez Jiménez, who is responsible of the repository of cell lines from "Programa de Investigación en Cáncer de Mama" Universidad Nacional Autónoma de México, for providing TNBC HCC1806 cell line.

**Conflicts of Interest:** The authors declare no conflict of interest.

## References

1. Khan, M.A.; Jain, V.K.; Rizwanullah, M.; Ahmad, J.; Jain, K. PI3K/AKT/mTOR pathway inhibitors in triple-negative breast cancer: A review on drug discovery and future challenges. *Drug Discov. Today* **2019**, *24*, 2181–2191.
2. Pascual, J.; Turner, N.C. Targeting the PI3-kinase pathway in triple-negative breast cancer. *Ann. Oncol.* **2019**, *30*, 1051–1060.
3. Salinas-Vera, Y.M.; Marchat, L.A.; Garcia-Vazquez, R.; Gonzalez de la Rosa, C.H.; Castaneda-Saucedo, E.; Tito, N.N.; Flores, C.P.; Perez-Plasencia, C.; Cruz-Colin, J.L.; Carlos-Reyes, A.; et al. Cooperative multi-targeting of signaling networks by angiomiR-204 inhibits vasculogenic mimicry in breast cancer cells. *Cancer Lett.* **2018**, *432*, 17–27.
4. Nisar, M.A.; Zheng, Q.; Saleem, M.Z.; Ahmmed, B.; Ramzan, M.N.; Ud Din, S.R.; Tahir, N.; Liu, S.; Yan, Q. IL-1beta Promotes Vasculogenic Mimicry of Breast Cancer Cells Through p38/MAPK and PI3K/Akt Signaling Pathways. *Front. Oncol.* **2021**, *11*, 618839.
5. Morales-Guadarrama, G.; Garcia-Becerra, R.; Mendez-Perez, E.A.; Garcia-Quiroz, J.; Avila, E.; Diaz, L. Vasculogenic Mimicry in Breast Cancer: Clinical Relevance and Drivers. *Cells.* **2021**, *10*, 1758.
6. Angara, K.; Borin, T.F.; Arbab, A.S. Vascular Mimicry: A Novel Neovascularization Mechanism Driving Anti-Angiogenic Therapy (AAT) Resistance in Glioblastoma. *Transl. Oncol.* **2017**, *10*, 650–660.
7. Yao, X.; Ping, Y.; Liu, Y.; Chen, K.; Yoshimura, T.; Liu, M.; Gong, W.; Chen, C.; Niu, Q.; Guo, D.; et al. Vascular endothelial growth factor receptor 2 (VEGFR-2) plays a key role in vasculogenic mimicry formation, neovascularization and tumor initiation by Glioma stem-like cells. *PLoS ONE.* **2013**, *8*, e57188.

8. Kotiyal, S.; Bhattacharya, S. Epithelial Mesenchymal Transition and Vascular Mimicry in Breast Cancer Stem Cells. *Crit. Rev. Eukaryot. Gene Expr.* **2015**, *25*, 269–280.
9. Maniotis, A.J.; Folberg, R.; Hess, A.; Seftor, E.A.; Gardner, L.M.; Pe'er, J.; Trent, J.M.; Meltzer, P.S.; Hendrix, M.J. Vascular channel formation by human melanoma cells in vivo and in vitro: Vasculogenic mimicry. *Am. J. Pathol.* **1999**, *155*, 739–752.
10. Sun, H.; Zhang, D.; Yao, Z.; Lin, X.; Liu, J.; Gu, Q.; Dong, X.; Liu, F.; Wang, Y.; Yao, N.; et al. Anti-angiogenic treatment promotes triple-negative breast cancer invasion via vasculogenic mimicry. *Cancer Biol. Ther.* **2017**, *18*, 205–213.
11. Chiablaem, K.; Lirdprapamongkol, K.; Keeratichamroen, S.; Surarit, R.; Svasti, J. Curcumin suppresses vasculogenic mimicry capacity of hepatocellular carcinoma cells through STAT3 and PI3K/AKT inhibition. *Anticancer Res.* **2014**, *34*, 1857–1864.
12. Chen, L.X.; He, Y.J.; Zhao, S.Z.; Wu, J.G.; Wang, J.T.; Zhu, L.M.; Lin, T.T.; Sun, B.C.; Li, X.R. Inhibition of tumor growth and vasculogenic mimicry by curcumin through down-regulation of the EphA2/PI3K/MMP pathway in a murine choroidal melanoma model. *Cancer Biol. Ther.* **2011**, *11*, 229–235.
13. Hu, A.; Huang, J.J.; Jin, X.J.; Li, J.P.; Tang, Y.J.; Huang, X.F.; Cui, H.J.; Xu, W.H.; Sun, G.B. Curcumin suppresses invasiveness and vasculogenic mimicry of squamous cell carcinoma of the larynx through the inhibition of JAK-2/STAT-3 signaling pathway. *Am. J. Cancer Res.* **2015**, *5*, 278–288.
14. Welsh, J. Vitamin D and Breast Cancer: Mechanistic Update. *JBMR Plus* **2021**, *5*, e10582.
15. Chang, L.C.; Sun, H.L.; Tsai, C.H.; Kuo, C.W.; Liu, K.L.; Lii, C.K.; Huang, C.S.; Li, C.C. 1,25(OH)2 D3 attenuates indoxyl sulfate-induced epithelial-to-mesenchymal cell transition via inactivation of PI3K/Akt/beta-catenin signaling in renal tubular epithelial cells. *Nutrition* **2020**, *69*, 110554.
16. Chen, P.T.; Hsieh, C.C.; Wu, C.T.; Yen, T.C.; Lin, P.Y.; Chen, W.C.; Chen, M.F. 1alpha,25-Dihydroxyvitamin D3 Inhibits Esophageal Squamous Cell Carcinoma Progression by Reducing IL6 Signaling. *Mol. Cancer Ther.* **2015**, *14*, 1365–1375.
17. Kulling, P.M.; Olson, K.C.; Olson, T.L.; Feith, D.J.; Loughran, T.P., Jr. Vitamin D in hematological disorders and malignancies. *Eur. J. Haematol.* **2017**, *98*, 187–197.
18. Bajbouj, K.; Al-Ali, A.; Shafarin, J.; Sahnoon, L.; Sawan, A.; Shehada, A.; Elkhalifa, W.; Saber-Ayad, M.; Muhammad, J.S.; Elmoselhi, A.B.; et al. Vitamin D Exerts Significant Antitumor Effects by Suppressing Vasculogenic Mimicry in Breast Cancer Cells. *Front. Oncol.* **2022**, *12*, 918340. doi: 10.3389/fonc.2022.918340.
19. Park, Y.; Kim, J. Regulation of IL-6 signaling by miR-125a and let-7e in endothelial cells controls vasculogenic mimicry formation of breast cancer cells. *BMB Rep.* **2019**, *52*, 214–219.
20. Rak, J.; Filmus, J.; Kerbel, R.S. Reciprocal paracrine interactions between tumour cells and endothelial cells: The 'angiogenesis progression' hypothesis. *Eur. J. Cancer* **1996**, *32A*, 2438–2450.
21. Furlan, A.; Vercamer, C.; Heliot, L.; Wernert, N.; Desbiens, X.; Pourtier, A. Ets-1 drives breast cancer cell angiogenic potential and interactions between breast cancer and endothelial cells. *Int. J. Oncol.* **2019**, *54*, 29–40.
22. Garcia-Quiroz, J.; Garcia-Becerra, R.; Santos-Cuevas, C.; Ramirez-Nava, G.J.; Morales-Guadarrama, G.; Cardenas-Ochoa, N.; Segovia-Mendoza, M.; Prado-Garcia, H.; Ordaz-Rosado, D.; Avila, E.; et al. Synergistic Antitumorigenic Activity of Calcitriol with Curcumin or Resveratrol is Mediated by Angiogenesis Inhibition in Triple Negative Breast Cancer Xenografts. *Cancers* **2019**, *11*, 1739.
23. Hong, R.L.; Spohn, W.H.; Hung, M.C. Curcumin inhibits tyrosine kinase activity of p185neu and also depletes p185neu. *Clin. Cancer Res.* **1999**, *5*, 1884–1891.
24. Palange, A.L.; Di Mascolo, D.; Singh, J.; De Franceschi, M.S.; Carallo, C.; Gnasso, A.; Decuzzi, P. Modulating the vascular behavior of metastatic breast cancer cells by curcumin treatment. *Front. Oncol.* **2012**, *2*, 161.
25. Ray, S.; Chattopadhyay, N.; Mitra, A.; Siddiqi, M.; Chatterjee, A. Curcumin exhibits antimetastatic properties by modulating integrin receptors, collagenase activity, and expression of Nm23 and E-cadherin. *J. Environ. Pathol. Toxicol. Oncol.* **2003**, *22*, 49–58.
26. Gupta, B.; Ghosh, B. Curcuma longa inhibits TNF-alpha induced expression of adhesion molecules on human umbilical vein endothelial cells. *Int. J. Immunopharmacol.* **1999**, *21*, 745–757.
27. Ruan, G.X.; Kazlauskas, A. Axl is essential for VEGF-A-dependent activation of PI3K/Akt. *EMBO J.* **2012**, *31*, 1692–1703.
28. Karar, J.; Maity, A. PI3K/AKT/mTOR Pathway in Angiogenesis. *Front. Mol. Neurosci.* **2011**, *4*, 51.
29. Shao, N.; Lu, Z.; Zhang, Y.; Wang, M.; Li, W.; Hu, Z.; Wang, S.; Lin, Y. Interleukin-8 upregulates integrin beta3 expression and promotes estrogen receptor-negative breast cancer cell invasion by activating the PI3K/Akt/NF-kappaB pathway. *Cancer Lett.* **2015**, *364*, 165–172.
30. Hideshima, T.; Nakamura, N.; Chauhan, D.; Anderson, K.C. Biologic sequelae of interleukin-6 induced PI3-K/Akt signaling in multiple myeloma. *Oncogene* **2001**, *20*, 5991–6000.
31. Shi, Y.H.; Bingle, L.; Gong, L.H.; Wang, Y.X.; Corke, K.P.; Fang, W.G. Basic FGF augments hypoxia induced HIF-1-alpha expression and VEGF release in T47D breast cancer cells. *Pathology* **2007**, *39*, 396–400.
32. Jin, L.; Wessely, O.; Marcusson, E.G.; Ivan, C.; Calin, G.A.; Alahari, S.K. Prooncogenic factors miR-23b and miR-27b are regulated by Her2/Neu, EGF, and TNF-alpha in breast cancer. *Cancer Res.* **2013**, *73*, 2884–2896.
33. McCubrey, J.A.; Steelman, L.S.; Bertrand, F.E.; Davis, N.M.; Sokolosky, M.; Abrams, S.L.; Montalto, G.; D'Assoro, A.B.; Libra, M.; Nicoletti, F.; et al. GSK-3 as potential target for therapeutic intervention in cancer. *Oncotarget* **2014**, *5*, 2881–2911.
34. Bustanji, Y.; Taha, M.O.; Almasri, I.M.; Al-Ghussein, M.A.; Mohammad, M.K.; Alkhatib, H.S. Inhibition of glycogen synthase kinase by curcumin: Investigation by simulated molecular docking and subsequent in vitro/in vivo evaluation. *J. Enzyme Inhib. Med. Chem.* **2009**, *24*, 771–778.

35. Kuttikrishnan, S.; Siveen, K.S.; Prabhu, K.S.; Khan, A.Q.; Ahmed, E.I.; Akhtar, S.; Ali, T.A.; Merhi, M.; Dermime, S.; Steinhoff, M.; et al. Curcumin Induces Apoptotic Cell Death via Inhibition of PI3-Kinase/AKT Pathway in B-Precursor Acute Lymphoblastic Leukemia. *Front. Oncol.* **2019**, *9*, 484.
36. Guan, F.; Ding, Y.; Zhang, Y.; Zhou, Y.; Li, M.; Wang, C. Curcumin Suppresses Proliferation and Migration of MDA-MB-231 Breast Cancer Cells through Autophagy-Dependent Akt Degradation. *PLoS ONE* **2016**, *11*, e0146553.
37. Proietti, S.; Cucina, A.; D'Anselmi, F.; Dinicola, S.; Pasqualato, A.; Lisi, E.; Bizzarri, M. Melatonin and vitamin D3 synergistically down-regulate Akt and MDM2 leading to TGFbeta-1-dependent growth inhibition of breast cancer cells. *J. Pineal Res.* **2011**, *50*, 150–158.
38. Ogiwara, H.; Ui, A.; Shiotani, B.; Zou, L.; Yasui, A.; Kohno, T. Curcumin suppresses multiple DNA damage response pathways and has potency as a sensitizer to PARP inhibitor. *Carcinogenesis* **2013**, *34*, 2486–2497.
39. Loughery, J.; Cox, M.; Smith, L.M.; Meek, D.W. Critical role for p53-serine 15 phosphorylation in stimulating transactivation at p53-responsive promoters. *Nucleic Acids Res.* **2014**, *42*, 7666–7680.

# OTROS MANUSCRITOS PUBLICADOS

*A continuación se presentan artículos en los que participé durante mi estancia en el laboratorio de la Dra. Lorenza Díaz Nieto*

Journal of Steroid Biochemistry and Molecular Biology 223 (2022) 106132

Contents lists available at ScienceDirect

Journal of Steroid Biochemistry and Molecular Biology

journal homepage: www.elsevier.com/locate/jsbmb

# AZD4547 and calcitriol synergistically inhibited BT-474 cell proliferation while modified stemness and tumorsphere formation

Gabriela Morales-Guadarrama [a,b,1], Edgar A. Méndez-Pérez [a,1], Janice García-Quiroz [a], Euclides Avila [a], Fernando Larrea [a], Lorenza Díaz [a,*]

[a] Departamento de Biología de la Reproducción, Dr. Carlos Gual Castro, Instituto Nacional de Ciencias Médicas y Nutrición Salvador Zubirán, Av. Vasco de Quiroga No. 15, Belisario Domínguez Sección XVI, Tlalpan 14080, Ciudad de México, Mexico

[b] Programa de Doctorado en Ciencias Biomédicas, Universidad Nacional Autónoma de México, Ciudad de México, Mexico

ARTICLE INFO

*Keywords:*
Breast cancer
AZD4547
Calcitriol
Combination index
Dose-reduction index
Synergism

ABSTRACT

Fibroblast growth factor receptor (FGFR) overamplification/activation in cancer leads to increased cell proliferation. AZD4547, a FGFR selective inhibitor, hinders breast cancer cells growth. Although luminal B breast tumors may respond to chemotherapy and endocrine therapy, this subtype is associated with poor prognosis, inadequate response and/or acquired drug resistance. Calcitriol, the vitamin D most active metabolite, exerts anti-neoplastic effects and enhances chemotherapeutic drugs activity. In this study, we sought to decrease the concentration of AZD4547 needed to inhibit the luminal-B breast cancer cell line BT-474 proliferation by its combination with calcitriol. Anti-proliferative inhibitory concentrations, combination index and dose-reduction index were analyzed from Sulforhodamine B assays. Western blot and qPCR were used to study FGFR molecular targets. The compound's ability to inhibit BT-474 cells tumorigenic capacity was assessed by tumorspheres formation. Results: BT-474 cells were dose-dependently growth-inhibited by calcitriol and AZD4547 ($IC_{50}$ = 2.9 nM and 3.08 μM, respectively). Calcitriol at 1 nM synergistically improved AZD4547 antiproliferative effects, allowing a 2-fold AZD4547 dose-reduction. Mechanistically, AZD4547 downregulated p-FGFR1, p-Akt and tumorsphere formation. Calcitriol also decreased tumorspheres, while induced cell differentiation. Both compounds inhibited *MYC* and *CCND1* expression, as well as ALDH, a stemness marker that positively correlated with *FGFR1* and negatively with *VDR* expression in breast cancer transcriptomic data. In conclusion, the drugs impaired self-aggregation capacity, reduced stemness features, induced cell-differentiation and when combined, synergistically inhibited cell proliferation. Overall, our results suggest that calcitriol, at low pharmacological doses, may be a suitable candidate to synergize AZD4547 effects in luminal B breast tumors, allowing to reduce dose and adverse effects.

## 1. Introduction

Breast cancer is a heterogeneous molecular entity representing the most frequent malignancy among women worldwide [1]. Breast cancer tumors are commonly divided into distinct subtypes based on immunohistochemical status of the molecular markers estrogen receptor α (ERα), progesterone receptor (PR), human epidermal growth factor receptor 2 (HER2) and Ki-67 proliferation index [2]. Histopathological subgroups can also be presented as surrogate intrinsic molecular subtypes, including luminal A, luminal B, HER2-enriched or triple negative breast cancer [3]. Luminal B breast cancer represents 10–20 % of all cases, is identified by the ER+ /$PR^{low}$/HER2 + /Ki-$67^{high}$ phenotype [2] and is commonly associated with poor response and *de novo* resistance to chemo-endocrine therapy [4–7]. Due to ERα expression, luminal B

*Abbreviations:* CI, Combination index; DRI, Dose-reduction index; EGFR, Epidermal growth factor receptor; ER, Estrogen receptor; FBS, Fetal bovine serum; FGF, Fibroblast growth factor; FGFR, Fibroblast growth factor receptor; HER2, Human epidermal growth factor receptor 2; IC, Inhibitory concentrations; MBCDF-T, MBCDF-Tum; PR, Progesterone receptor; RTK, Receptor tyrosine kinase; RXR, Retinoid X receptor; VDR, Vitamin D receptor.

* Corresponding author.
*E-mail addresses:* gabriela.mguadarrama@gmail.com (G. Morales-Guadarrama), edgar.mendez.p3@gmail.com (E.A. Méndez-Pérez), janice.garciaq@incmnsz.mx (J. García-Quiroz), euclides.avilac@incmnsz.mx (E. Avila), fernando.larreag@incmnsz.mx (F. Larrea), lorenza.diazn@incmnsz.mx (L. Díaz).
[1] These authors equally contributed to this work

https://doi.org/10.1016/j.jsbmb.2022.106132
Received 1 December 2021; Received in revised form 2 April 2022; Accepted 22 May 2022
Available online 31 May 2022

cancer cells growth is expected to be estradiol-dependent; however, the activity of several ER-independent cell cycle proteins and the overexpression of receptors tyrosine kinase (RTKs) and/or their downstream targets, make these cells partially independent of estrogens [8]. In this regard, the amplification of *FGFR1*, the gene encoding for the fibroblast growth factor receptor 1 (FGFR1), has been described in 16–27 % of luminal B breast tumors, and has been identified as an underlying mechanism of endocrine resistance, ligand independent signaling and poor prognosis [9]. In fact, breast cancer cells overexpressing FGFR1 have shown resistance to 4-hydroxytamoxifen and anchorage independent proliferation, linking FGFR1 to the failure of antiestrogenic treatments and distant metastasis formation [9]. Liganded-FGFR downstream signaling includes activation of PI3K/AkT, MAPK/ERK, and crosstalk with the Wnt signaling pathway [10,11], favoring metastasis and treatment-resistance through epithelial to mesenchymal transition (EMT) and stemness induction [11]. Therefore, strategies directed to block FGFRs represent a promising therapeutic approach [12]. In particular, a previous report showed that the RTK inhibitor (RTKI) AZD4547 impaired stem cell-like characteristics in primary mammary epithelial cells in premalignant tissue, and downregulated FGFR's signaling pathways [13]. AZD4547, a potent and selective inhibitor of FGFRs, has shown to inhibit cancer cells proliferation and tumor growth in preclinical models, and is currently in clinical trials for breast cancer [13–15]. Despite the good tolerability of AZD4547 shown in these trials, patients tend to present adverse events, including dysgeusia, stomatitis, diarrhea, hyperphosphatemia, dry mouth, nausea, neutropenia, and thrombocytopenia [16,17]. To prevent treatment-associated toxicity and the development of resistance mechanisms, AZD4547 may be combined with other antineoplastic agents to block alternative tumor survival pathways, with the aim of reducing the therapeutic dose. In several experimental models, calcitriol, the most active vitamin D metabolite, has shown anti-proliferative and pro-differentiating effects on cancer cells [18–25], as well as the ability to sensitize tumor cells to various chemotherapeutic agents [26–29]. In this regard, we have previously reported the synergistic effect of calcitriol in combination with the RTKIs dovitinib and gefitinib in breast cancer models [27,28]. Hence, in this study, we explored whether an improved antiproliferative effect could be achieved in a luminal B cell line by combining AZD4547 with calcitriol *in vitro*. In addition, given the potential of AZD4547 and calcitriol to prevent stemness [21,30–33], we explored the possibility that their combination would greatly affect BT-474 tumorigenic potential by impairing BT-474 stem population.

## 2. Materials and methods

### 2.1. Reagents and cell cultures

N-(5-(3,5-dimethoxyphenethyl)− 1H-pyrazol-3-yl)− 4-((3S,5R)− 3,5-dimethylpiperazin-1-yl) benzamide, AZD4547 (AstraZeneca) was acquired from Santa Cruz (Santa Cruz Biotechnology Inc., Dallas, TX, USA). Calcitriol, sulforhodamine B (SRB) and trichloroacetic acid (TCA) were from Sigma (Sigma–Aldrich, USA). The vehicle for AZD4547 was water, while calcitriol was diluted in ethanol as we previously reported [28].

The human luminal B breast cancer cell line used in this study (BT-474, ATCC, Manassas, VA) was maintained in DMEM-F12 medium supplemented with 100 units/mL penicillin plus 100 μg/mL streptomycin and 5% heat-inactivated fetal bovine serum (FBS). All experimental procedures were carried out with supplemented medium using charcoal-stripped-FBS.

### 2.2. Cells phenotype characterization by immunofluorescence analysis

The expression of the vitamin D receptor (VDR), its heteropartner retinoid X receptor (RXR), ERα, PR, HER2 and FGFR 1–2 was analyzed in BT-474 cells as described before [25]. Briefly, cells ($1 \times 10^3$ cells *per* well) were seeded onto sterile 12-well slides and incubated for 24 h. Cells were fixed in ethanol at 4 °C and permeabilized in Fixation/Permeabilization solution at 4 °C (Cytofix/Cytoperm BD Biosciences, San Diego, CA). Washing steps and antibodies dilutions were performed with Perm/Wash solution (BD Biosciences). Slides were co-incubated overnight at 4 °C with antibodies against VDR (mouse monoclonal antibody against human VDR, 1:1000, Santa Cruz sc-13133X), RXR (rabbit polyclonal antibody against human RXRα/β/γ, 1:1000, Santa Cruz sc-774X), ERα (mouse monoclonal antibody against human ERα, 1:100, Santa Cruz sc-8002), PR (rabbit monoclonal antibody against human PR, 1:500, Bio SB 5886), HER-2 (rabbit monoclonal antibody against human HER-2 neu, 1:500, Bio SB 2040) and FGFR1 (mouse monoclonal antibody against FGFR1, 1:200, Santa Cruz sc-393911). Negative controls were incubated in the absence of primary antibodies. After washing, a coincubation for 1 h at room temperature with secondary antibodies was performed using goat anti-mouse-Cy3 (1:1000, Life Technologies Inc.) and goat anti-rabbit-FITC (1:500, Jackson ImmunoResearch Laboratories, West Grove, PA). UltraCruz mounting medium (Santa Cruz) containing 4',6-diamidino-2-phenylindole (DAPI) was used as final step. Cells were photographed with a conventional epifluorescence microscope.

### 2.3. Effect of AZD4547 and calcitriol upon ALDH positivity in BT-474 cells

To study the basal expression and regulation of aldehyde dehydrogenase (ALDH), a marker of stemness, BT-474 cells were seeded onto sterile 12-well slides and incubated for 24 h in the presence of AZD4547 [5 μM], calcitriol [10 nM] or their combination. Afterward, cells were fixed and set with rabbit anti-ALDH (Abcam, Cambridge, MA, USA). After washing, goat anti-rabbit IgG Alexa Fluor 488 (green fluorophore, 1:10,000, Invitrogen, Thermo Fisher Scientific, Rockford, IL) was incubated for 1 h at room temperature. Mounting was carried out as described in Section 2.2. The intensity of ALDH-Alexa 488 signal was measured by using ImageJ (Fiji) software in at least six hot spots *per* group. In the acquired digital fluorescent images, the densitometric analysis considered green channel intensity *per* hot spot area. Results depict mean values. ANOVA was used for comparison.

### 2.4. Proliferation studies

Cells were seeded in 96-well plates (500–1000 cells/well). After incubation overnight, cells were treated with AZD4547 (0.05–8.0 μM), calcitriol (0.01–100 nM) and their respective vehicles (water and ethanol 0.1 %, respectively). Cell proliferation was assessed by SRB colorimetric assay as previously described [34]. Briefly, after 6 days of exposure to the compounds, cells were fixed with TCA and dyed with SRB (0.057%). Absorbance was read at 492 nm in a microplate reader (Synergy HT Multi-Mode Microplate Reader, BioTek, VT, USA). Concentration values that inhibited cell proliferation at 20% ($IC_{20}$) and 50% ($IC_{50}$) were calculated considering the minimum and maximum effect, using the dose-response fitting function, with the scientific plotting software Origin 9.0 (OriginLab Corporation, Northampton, MA, USA).

### 2.5. Combination index and dose reduction index determination

To identify the type of combinatory pharmacological effect of the compounds, we calculated the combination index value, which is based on the median effect principle of the mass-action law described by Chou and Talalay, and the dose-reduction index (DRI), a measure of how many folds the dose of each drug in a combination may be reduced [35]. To interpret the results, we took into consideration that combination index values $< 1$, $= 1$ or $> 1$ depict synergistic, additive, or antagonistic effects, respectively, while synergism is subdivided into nearly additive (0.90–1.10), slight synergism (0.85–0.90), moderate synergism (0.7–0.85), synergism (0.3–0.7), strong synergism (0.1–0.3), and very

strong synergism (<0.1) [36]. On the other hand, DRI values ≤ 1 or > 1 indicate not favorable dose-reduction or favorable dose-reduction, respectively [35,36].

### 2.6. Immunoblotting

To get mechanistic insights into the compound's activity, $1 \times 10^6$ cells were seeded in the presence of AZD4547 [5 μM] and calcitriol [10 nM], alone or combined. Cells were lysed in Lysis buffer in the presence of phosphatase and protease inhibitor cocktails (Abcam) after 24 h of incubation. Total protein content in cell lysates was assessed by the bicinchoninic acid method [37]. For SDS-PAGE, 30 μg of the cell lysate were charged onto polyacrylamide gels prepared with TGX Stain-Free™ FastCast™ Acrylamide Kit, (10 %, BioRad, 1610183) and ran for 40 min at high voltage. Electroblotting to PVDF membranes was carried out at 4 °C for 60 min (100 V). For stain-free protocol, after electrophoresis gels were activated 1 min by UV light on the ChemiDoc XRS System (BioRad), and protein transfer assessed the same by rapid exposure of membranes to UV light. Later, membranes were incubated for 1 h at room temperature in blocking buffer (Abcam, AB126587), and after that incubated in the presence of one of the following antibodies: mouse anti-phosphorylated-FGFR Y653/654 (p-FGFR, 1:1000, Cell Signaling Technology, 55H2), rabbit anti-phospho-Akt (p-Akt) S473 (1:1000, Cell Signaling, 9271) and mouse anti- glyceraldehyde-3-phosphate dehydrogenase (GAPDH, 1:1000, Santa Cruz, CA, 0411, sc-47724) at 4 °C overnight. Washing steps and antibody dilutions were performed with 1× Tris Buffered Saline-Tween (20 mM Tris, 150 mM NaCl, 0.1 % Tween 20). After washing, goat anti- mouse secondary antibody (1:5000, Santa Cruz) or goat anti-rabbit (1:5000, Santa Cruz) were incubated for 1 h at room temperature. Then, membranes were processed with the ECL + Plus Western blotting detection system (GE Healthcare, UK). Total protein normalization or GAPDH optical density were used as controls.

### 2.7. RT-qPCR

Total RNA was extracted from cells using Trizol® (Life Technologies, Carlbad, USA). After estimating the concentration of RNA at 260/280 nm, 2 μg of RNA were reverse-transcribed using a commercial kit (Roche Diagnostics, Basel, Switzerland) and resulting cDNAs were used for qPCR amplifications using the Roche master mix in combination with hydrolysis probes (Roche, Universal Probe Library) in the LightCycler® 480 II system (Roche), according to standard protocols. Gene expression was normalized using the housekeeping gene *GAPDH* or *RPL32* (*L32*) as internal controls. Forward and reverse primers sequences were as follows: *GAPDH* (NM_002046.3): agccacatcgctcagacac - gcccaatacgaccaaatcc; epidermal growth factor receptor (*EGFR*, NM_005228.3): gccttgactgaggacagca - tttgggaacggactggttta, *FGFR1* (NM_001174063.1): agactccggcctctatgctt - aggaggggagagcatctga, *FGFR2* (NM_000141.4): tgcatggttgacagttctgc - aggcgattaagaagacccta, *HER2* (NM_004448.2): gggaaacctggaactcaccta – ccctgcacctcctggata; Cyclin D1 (*CCND1* NM_053056.2): gaagatcgtcgccacctg - gacctcctcctcgcacttct); Myc (*MYC*, NM_002467.3): caccagcagcgactctga – gatccagactctgacctttgc; *CYP24A1* (NM_000782.3): catcatggccatcaaaacaa – gcagctcgactggagtgac); *L32* (NM_000994.3) gaagttcctggtccacaacg – gagcgatctcggcacagta.

### 2.8. Self-aggregation capacity and formation of cellular spherical aggregates

To evaluate the effect of treatments on tumorigenic ability of breast cancer cells, BT-474, tumorsphere formation was assessed, as a measure of self-renewal and aggregation capacity. Briefly, $1 \times 10^5$ cells were seeded in low-attachment culture flasks and incubated with AZD4547 [5 μM] or calcitriol [10 nM] alone or in combination for 7–10 days. We chose higher compounds concentrations than their calculated inhibitory concentrations considering that tridimensional models may reduce the ability of treatments to reach all cells. Flask were incubated at 37 °C in absence of $CO_2$, in a sterile environment. After 6 days, cellular aggregates and spheres were counted in each treatment. The results were expressed as tumorsphere efficiency (number of tumorspheres formed/ $1 \times 10^5$ cells plated).

### 2.9. Statistical analysis

Statistical differences were established by one-way ANOVA using a specialized software package (SigmaStat 3.5, Jandel Scientific, CA, USA). Differences were considered statistically significant at $P'<0.05$.

## 3. Results

### 3.1. Characterization of receptors status on BT-474 cell line

To address whether BT-474 cells could respond to calcitriol, we first assessed VDR/RXR expression by immunofluorescence. As depicted in Fig. 1A, both receptors are expressed in this cell line, suggesting sensibility to calcitriol. RXR was localized into the nucleus, while VDR was preferentially found in the cell membrane and alongside fibers in the cytoplasm. We also evaluated ERα and PR protein expression in BT-474 cells. As shown in Fig. 1A, both receptors are mainly localized at the nuclear compartment, particularly in the nucleolus, suggesting responsiveness to steroid hormone signaling (Fig. 1A). On the other hand, the RTKs FGFR1, FGFR2, HER2, and EGFR, were evaluated either by immunocytochemistry and/or by qPCR. As depicted in Fig. 1B, HER2 receptor is highly enriched in BT-474 cells at the cytoplasmic compartment and in cell membranes, while FGFR1 was immunolocalized both in the cytoplasm and in the nuclear compartment (Fig. 1B), a localization associated with oncogenic functions of this protein in breast cancer cells, and with poor prognosis [38,39]. FGFR2 was not detected by immunocytochemistry (data not shown), while very low mRNA expression was detected by qPCR (Fig. 1C). By using this molecular technique, we also found that BT-474 cells highly express EGFR and HER2 (Fig. 1D).

### 3.2. AZD4547 and calcitriol inhibited cellular proliferation in a concentration-dependent manner

To study the sensitivity of BT-474 cells to the antiproliferative effects of AZD4547 and calcitriol, we used SRB assays. Our results showed a concentration-dependent inhibition of BT-474 cells proliferation by both compounds (Fig. 2). Based on the concentration-response curves, $IC_{20}$ and $IC_{50}$ were calculated. As depicted in Table 1, inhibitory concentrations of AZD4547 were found in the micromolar range. On the other hand, calcitriol displayed a potent anti-proliferative effect on BT-474 cells (Fig. 2B), showing inhibitory concentrations in the nanomolar range (Table 1).

### 3.3. Anti-proliferative effects of AZD4547 on BT-474 cells are increased by calcitriol

Combination schemes of AZD4547 $IC_{20}$ and $IC_{50}$ with calcitriol at 1 nM and 10 nM were performed to analyze the pharmacological interaction of both compounds. As depicted in Fig. 3, calcitriol, at nanomolar concentrations, significantly increased the antiproliferative effects of AZD4547. Next, we evaluated the nature of this pharmacological interaction by calculating the combination index and DRI values. Interestingly, calcitriol synergized AZD4547 antiproliferative effects only at its lowest concentration (1 nM), while the highest concentration tested (10 nM) resulted antagonistic (Table 2). Of note, similar results were obtained by cell counting (data not shown).

As depicted in Table 2, AZD4547, at both concentrations tested in combination with 1 nM calcitriol, not only produced a synergic antiproliferative effect, but also resulted in a favorable DRI, which is relevant considering that 1 nM calcitriol is a safe achievable concentration

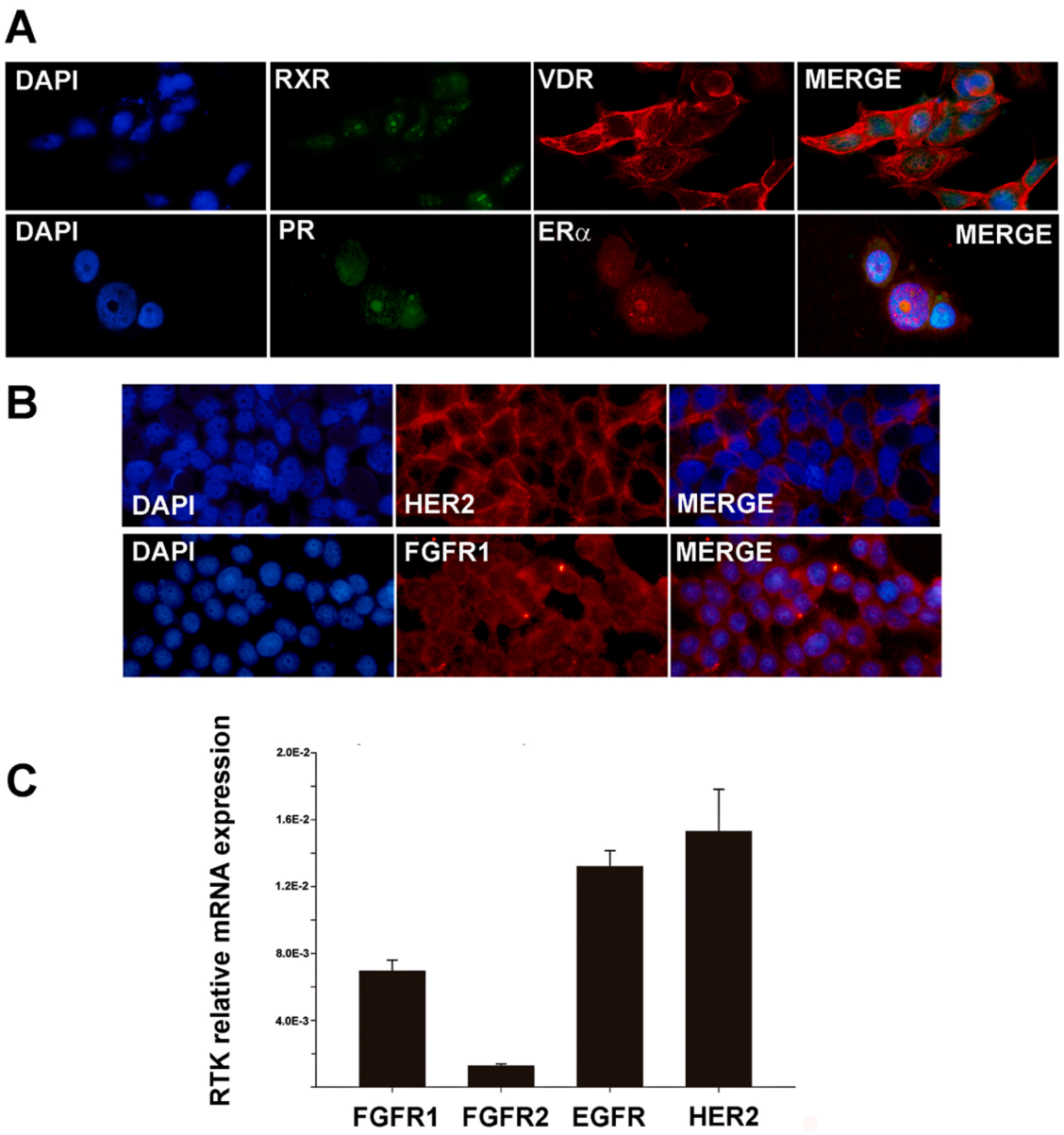


**Fig. 1.** Characterization of BT-474 cells. (A) Immunolocalization of vitamin D receptor (VDR, red, upper panel), retinoid X receptor α,β/γ (RXR, green, upper panel), progesterone receptor (PR, green, lower panel) and estrogen receptor alpha (ERα, red, lower panel) was studied by immunocytochemistry in BT-474 cells using specific antibodies. Secondary antibodies were goat anti-rabbit-FITC and goat anti-mouse-Cy3. DAPI shows nuclei in blue. Merged channels green, red and blue are included. Magnification 40X. PR and ERα photographs are amplified from 40x pictures. (B) Immunolocalization for human epidermal growth factor receptor 2 (HER2, red, upper panel) and Fibroblast growth factor receptor 1 (FGFR1, red, lower panel) in BT-474 cells. Magnification 40X. (C) Relative mRNA expression of different RTKs in BT-474 cells. RT-qPCR was performed using specific primers for FGFR1, FGFR2, and epidermal growth factor receptor 1 and 2 (EGFR, HER2).

in cancer treated patients [40,41]. However, and consistently with the type of pharmacological effect, the use of a higher calcitriol concentration in combination with AZD4547 resulted in antagonism and lower DRI values, as compared with calcitriol 1 nM. This may be due to convergence of effects at some point of the signaling path involved in each compound's activity, probably acting upon the same molecular targets. Therefore, next we analyzed possible mechanisms involved in the compound's anticancer effects to further understand their interaction.

### *3.4. AZD4547 and calcitriol impair Akt/ Myc/Cyclin D1 signaling in BT-474 cells*

As has been previously described, the inhibition of FGFR and/or the treatment with calcitriol impair mammary tumor growth by blocking PI3K/Akt signaling and/or by inducing a G1 growth arrest of breast cancer cells partly through cyclin D1 (*CCND1*) and myc downregulation, as well as p21 induction [42–47]. Therefore, we analyzed p-Akt S473 protein abundance as well as *MYC* and *CCND1* gene expression in BT-474 cells treated for 24 h with the compounds by Western blot or qPCR. We found that AZD4547 alone and combined significantly reduced p-Akt compared with vehicle-treated cells (Fig. 4A and B). On the other hand, both compounds downregulated *MYC* and *CCND1* gene expression (Fig. 4C and D), although *MYC* inhibition by calcitriol *per se* did not reach statistical significance. As a control, we evaluated AZD4547 and calcitriol bioactivity by analyzing FGFR phosphorylation and *CYP24A1* gene expression, which is a main transcriptional target of calcitriol. AZD4547 significantly reduced p-FGFR abundance, while calcitriol induced more than 400-folds *CYP24A1* gene expression (Supplementary Figure 1).

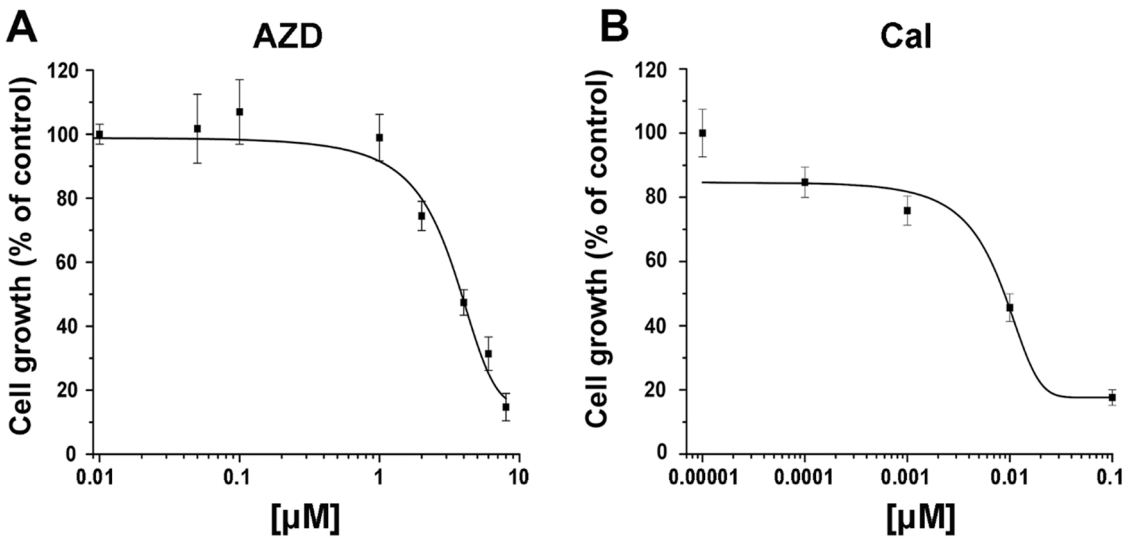


**Fig. 2.** Antiproliferative effects of AZD4547 and calcitriol in BT-474 cells. Cells were incubated for 6 days with AZD4547 (AZD, A) or calcitriol (Cal, B) at different concentrations. The results are depicted as the mean ± S.D. of at least three independent experiments by sextuplicate, and were normalized *vs.* control values, which were set to 100 %.

**Table 1**
$IC_{20}$ and $IC_{50}$ values of AZD4547 and calcitriol in the luminal B BT474 cells. Inhibitory concentrations at 20 % ($IC_{20}$) and 50 % ($IC_{50}$) were calculated based on the dose-response curves of AZD4547 and calcitriol. Results are depicted as the mean of N ≥ 3 experiments.

| AZD4547 (μM) | | Calcitriol (nM) | |
|---|---|---|---|
| **$IC_{20}$** | **$IC_{50}$** | **$IC_{20}$** | **$IC_{50}$** |
| 1.73 | 3.08 | 0.511 | 2.9 |

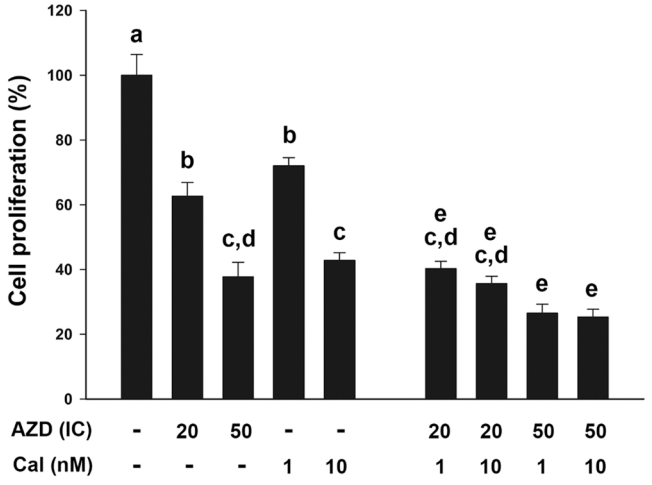


**Fig. 3.** Calcitriol increased AZD4547 antiproliferative activity in the luminal B breast cancer cell line BT-474. BT-474 cells were incubated in the presence of AZD4547 (AZD), calcitriol (Cal) or the combination of AZD4547 inhibitory concentration (IC) values at 20% or 50% with Cal 1 nM or 10 nM. Each bar represents the mean ± SEM of at least three independent experiments by triplicate, after normalization *vs.* control values, which were set to 100 %. Different letters indicate statistical significance ($P < 0.05$).

### *3.5. AZD4547 and calcitriol reduced self-aggregation capacity of BT-474 cells and decreased ALDH+ subpopulation*

To further study possible mechanisms involved in the effects of AZD4547 and calcitriol on BT-474 cells, and considering that in mammary cells the pharmacological inhibition of FGFR impairs stemness [13], while calcitriol reduces cancer stem cell population and induces pro-differentiation in breast cancer [48,49], we studied tumorsphere formation and cell-differentiation capacity by these compounds. In the tumorsphere formation assay, we found that BT-474 cells have the intrinsic capacity to form spherical cell aggregates from free-floating cells (Fig. 5A). Vehicle-treated cells appeared mostly aggregated, with no cells attached (monolayer panel shows the cells at the level of the flask surface). Remarkably, in calcitriol treatments, we found a considerable enrichment of adherent cells alongside with the reduction in their capacity to form cellular aggregates. Indeed, a subpopulation of adherent cells formed patches of well-differentiated cells (Fig. 5A), in a similar manner as cells grown on flasks normally used for maintaining the cell line, suggesting the possible participation of adhesion molecules in this process and the acquisition of a more differentiated phenotype. Whilst in AZD4547 treated cells, self-aggregation capacity in tridimensional structures was almost fully repressed, leading to cell death after 6 days of incubation (Fig. 5A, B). In contrast, combination of both compounds (C+A) resulted in the reduction of cell aggregates together with lack of compaction, enhanced formation of adhered cellular patches and induction of a differentiated phenotype (Fig. 5A, B).

To explore if self-aggregation inhibition was due to the reduction of cells with stemness properties, we evaluated ALDH-positive populations on the cell culture. ALDH was used as marker of stem population, as it is expressed in tumor initiating cells [13]. As assessed by

**Table 2**
Combination index values and dose-reduction index for AZD4547/calcitriol treatment in BT-474 cells.

| Combination schemes AZD (IC) / Cal (nM) | Combination index | Effect | DRI (folds) | |
|---|---|---|---|---|
| | | | AZD | Cal |
| $IC_{20}$ / 1 | 0.686 | Synergism | 2.10 | 4.78 |
| $IC_{20}$ / 10 | 2.072 | Antagonism | 2.28 | 0.61 |
| $IC_{50}$ / 1 | 0.748 | Moderate synergism | 1.53 | 10.56 |
| $IC_{50}$ / 10 | 1.514 | Antagonism | 1.56 | 1.14 |

The combination index values and dose-reduction index (DRI) were calculated after incubating BT-474 cells in the presence of the inhibitory concentrations (IC) 20 or 50 of AZD4547 (AZD), and calcitriol (Cal) 1 nM and 10 nM.

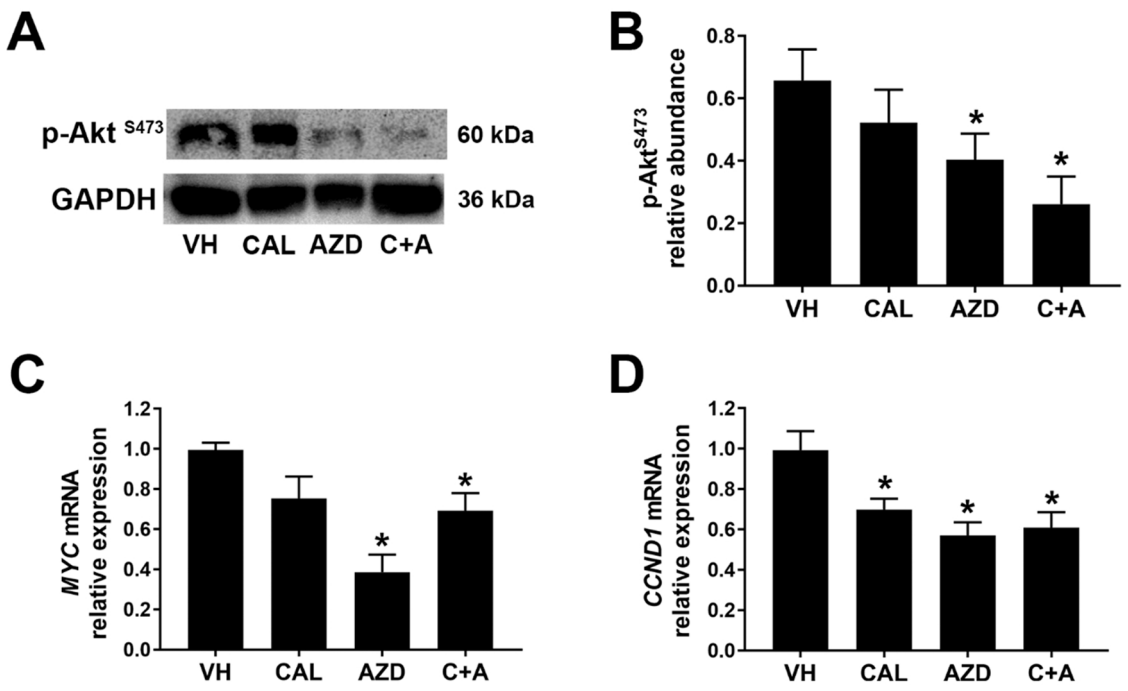


**Fig. 4.** Disruption of FGFR signaling pathway by calcitriol and AZD4547 involves Akt/Myc and *CCND1*. (A) Cell lysates of BT-474 cells treated for 24 h in the presence of vehicle (VH), calcitriol (Cal, 10 nM), AZD4547 (AZD, 5 μM) or their combination (C+A) were used to study p-Akt by Western blot. GAPDH expression was used as a loading control. A representative cropped image of three different experiments is shown. (B) Graphical representation of the relative abundance of Akt phosphorylated at serine 473. Bars depict mean ± SEM, * $P < 0.05$) *vs.* VH. (C, D) The gene expression of downstream transcriptional targets of FGFR activation, *MYC* (C) and *CCND1* (D), was studied by RT-qPCR in three different experiments by triplicate and is shown as the mean ± SEM of normalized values using *L32* as housekeeping gene. * $P < 0.05$ *vs.* VH.

immunofluorescence, ALDH protein expression was reduced by calcitriol and AZD4547 compared to control cells; however, the RTKI more potently inhibited this marker (Fig. 5C, D). These results suggest that both compounds impair tumorsphere formation at least in part through the reduction of stemness in BT-474 cells.

To explore the relationship and possible clinical relevance between the stemness marker ALDH and AZD4547 or calcitriol molecular targets (FGFR1 and VDR, respectively) in breast cancer tumorigenesis, we used the Breast Cancer Gene-Expression Miner database (http://bcgenex.ico.unicancer.fr/BC-GEM/GEM-requete.php). By means of this mining module, we performed gene expression correlation analyses for ALDH and FGFR1 and for ALDH and VDR, using RNA-sequencing databases of patients with breast cancer. As depicted in Fig. 5E, the Pearson correlation graphic representation shows that increased ALDH expression positively correlated with FGFR1 expression in all patients ($r = 0.24$, $P < 0.0001$, n = 4421). On the contrary, we found a significant negative correlation between ALDH and VDR expression in normal-like tumors ($r = -0.32$, $P < 0.0001$, n = 602, Fig. 5 F).

### 3.6. *FGFR1 and its downstream targets association in HER-2 enriched breast cancer tumors*

Finally, to further understand the relationship between FGFR1 signaling and its downstream targets *AKT, CCND1*, and β-catenin *(CTNNB1)* gene expression, we explored their correlation using the Breast Cancer Gene-Expression Miner database. Of note, *CTNNB1* is involved in anti-tumoral effects of both AZD4547 and calcitriol [13,50]. Since BT-474 cells overexpress FGFR1 and HER2 receptors, we used the HER-2 enriched breast cancer database from 693 patients. We found significative positive correlations between FGFR1 gene expression and *AKT*, *CCND1* and *CTNNB1* (Supplementary Figure 2A, 2B, 2C). Similarly, we found positive correlations between *AKT* expression and *CTNNB1* and *ALDH* (Supplementary Figure 2D, 2E).

All considered, we propose that AZD4547 and calcitriol disrupt signaling of FGFR/Akt/c-myc axis at different levels in BT-474 cell line, resulting in cell proliferation inhibition, promotion of cell differentiation and impairment of self-aggregation capacity (Fig. 6).

## 4. Discussion

Luminal B breast cancer tumors usually display poor response and *de novo* resistance to chemo-endocrine therapy, representing a clinical challenge [8]. Nonetheless, in this tumor subtype, the overexpression of RTKs, such as FGFR, and the overactivation of their downstream molecular targets, makes them potential anti-neoplastic targets [12]. Small molecules with inhibitory activity on FGFR are a good option to treat luminal B breast cancer patients, considering the promising results reported [13–15, 51]. However, some adverse effects might develop; therefore, dose reduction by using combinatorial regimens is a good option to achieve a beneficial therapeutic outcome while preventing treatment-associated toxicity and resistance development. Regarding this, in this study we evaluated the pharmacological interaction between AZD4547 and calcitriol in BT-474 cells, with the aim to increase their antitumoral effects while allowing for dose-reduction. Our results showing a strong AZD4547 antiproliferative effect on BT-474 cells suggested the sensitivity of this cell line to FGFR blockade. The latter was further confirmed by FGFR phosphorylation and downstream targets regulation. The basal FGFR1 expression and activity in BT-474 cells found herein are consistent with previous reports, including one showing that in comparison with other breast cancer cells, FGFR1 gene is significantly highly expressed in BT-474 cells [13,52]. On the other hand, BT-474 cells were also highly sensitive to calcitriol antineoplastic effects, displaying an $IC_{50}$ value of 2.9 nM. As a reference, clinical studies have reported calcitriol peak blood levels of 3–16 nM in cancer patients treated with the secosteroid, resulting in little toxicity [40,41]. The high sensitivity of BT-474 cells to calcitriol may result from the strong VDR expression and its cytoplasmic localization, as calcitriol genomic effects have been associated with the interaction between VDR

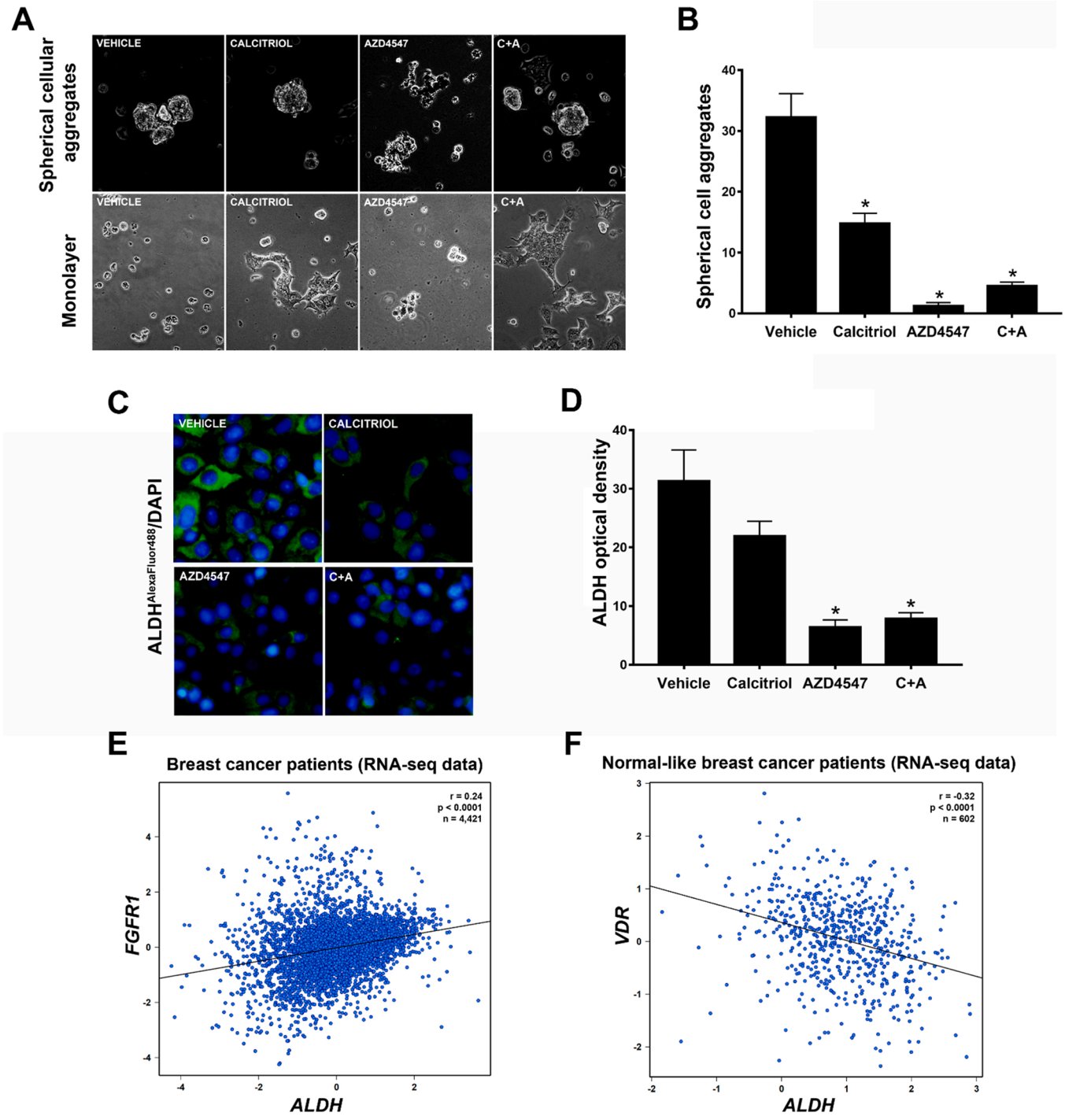


**Fig. 5.** Calcitriol and AZD4547 decreased BT-474 cell tumorsphere formation capacity, impaired cell-aggregation, induced cell differentiation and decreased ALDH+ cell subpopulation. (A) Cells were seeded in low-attachment culture flasks, and incubated with AZD4547 [AZD, 5 μM] or calcitriol [Cal, 10 nM] alone or combined (C+A). After 6 days with shaking, spheres were counted in each treatment. The graphical result of spheres count is shown in **(B)**, depicting mean values ± SEM of at least 8 visual fields. * $P < 0.05$ *vs* vehicle-treated cells. (C) Immunocytochemistry was used to evaluate the presence of ALDH+ subpopulations. Cells were treated for 24 h with AZD4547 [5 μM], calcitriol [10 nM] or their combination; fixed and incubated with rabbit anti-ALDH. For detection, goat anti-rabbit IgG Alexa Fluor 488 (green fluorophore) was used. DAPI was used to stain nuclei. Magnification 40 X. (D) Intensity of ALDH-Alexa 488 signal in each group is shown as mean optical density values ± SEM * $P < 0.05$ *vs* vehicle-treated cells. (E) Pearson pairwise correlation plot depicting the positive correlation between ALDH and FGFR1, and the negative correlation between ALDH and VDR expression (F), in breast cancer patient's transcriptomic data.

and microtubules in the cytoplasm [53,54]. Interestingly, when both compounds were combined, calcitriol at 1 and 10 nM equipotently and significantly enhanced AZD4547 antiproliferative activity, showing a pharmacologically synergic effect when using the secosteroid at its lowest concentration, as deduced by the combination index values. This low concentration of calcitriol also resulted in favorable DRI values for both compounds, with the possibility to reduce AZD4547 dose in 2-folds, and up to 10-folds for calcitriol. The latter is consistent with other reports describing the ability of calcitriol to synergize the anti-tumor effects of chemotherapeutic agents and RTKIs [27,29]. Overall, these results strongly suggest the possibility of combining both drugs in the clinic, reducing the RTKI dose while maintaining robust anticancer

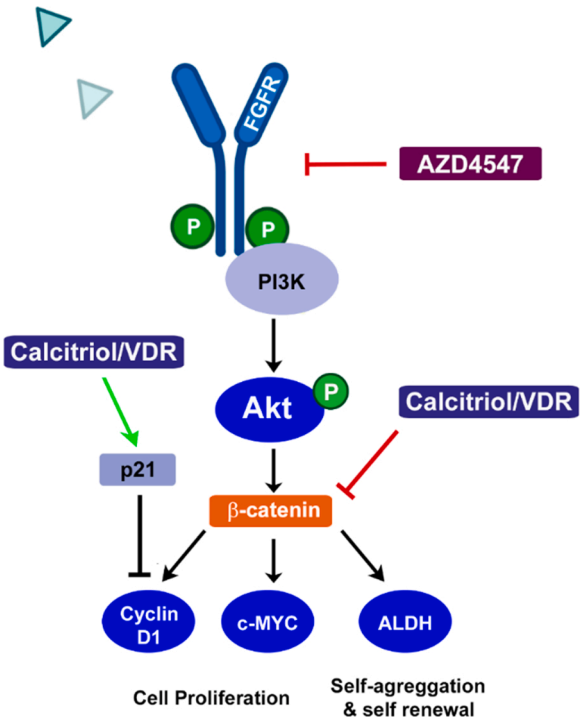


**Fig. 6.** AZD4547 and calcitriol disrupt signaling of FGFR/Akt/Myc axis at different levels in BT-474 cell line. Activation of FGFR through phosphorylation involves the modulation of expression and activation of downstream targets as Akt, ALDH, Myc and cyclin D1. Protein or mRNA expression of targets assessed in this study are shown in blue. Treatment with AZD4547 significantly reduced p-Akt, resulting in *MYC*, *CCND1* and ALDH downregulation, cell proliferation inhibition, as well as self-aggregation capacity impairment. β-catenin could be an important mediator of these effects, since *CTNNB1* expression positively correlated with *FGFR1* and *AKT* gene expression. On the other hand, it is known that calcitriol inhibits downstream targets of β-catenin including *MYC* and *CCND1*, while induces p21 expression repressing cyclin D1 and arresting cells in G1 phase.

activity, avoiding adverse effects or resistance development. Of note, the use of a higher calcitriol concentration with AZD4547, although significantly different from each compound alone, did not result in an increased benefit compared to that obtained with 1 nM calcitriol, and resulted in an antagonistic interaction, which we believe was probably due to an increment in the population of differentiated cells, due to the well-known pro-differentiating effect of calcitriol in cancer cells [26,48,49]. Indeed, differentiation-induction by calcitriol has been associated with the expression of adhesion molecules [55–57], which might explain the enrichment in the adherent cell population observed in low-attachment flasks of BT-474 cells treated with calcitriol. Supporting this, Palmer et al. previously described that calcitriol transformed cell shape to become more adhesive, by inducing E-cadherin and inhibiting β-catenin signaling in colon cancer cells [55]. Moreover, the increase of αVβ3 integrin expression has been associated with calcitriol-mediated cellular differentiation of stem cells [58,59]. Even though adhesion molecules were not assessed in this work, further experiments would help to clarify the role of calcitriol in the regulation of differentiation/adhesion markers. On the other hand, it has been described that calcitriol inhibits cancer stem-like cells, decrease their capacity to form spheres and reduce the frequency of tumor-initiating cells [21,60]. Similarly, it is known that AZD4547 has the potential to prevent stemness of certain subpopulations of cancer cells [30–33]. All these characteristics are essential for carcinogenesis and tumor progression. Therefore, we hypothesized that the combination of both compounds would greatly affect BT-474 tumorigenic potential by impairing their self-aggregation capacity and reducing their stem population. In this regard, we found that calcitriol and AZD4547 significantly compromised the ability of the cells to form tumorspheres. However, their combination did not further improve this capacity. This could be due to the robust effect of AZD4547 on this feature, impeding an enhanced response. It is also possible that the compounds interacted on the same pathway involved in the regulation of self-aggregation. This possibility seems to be supported by our results showing calcitriol and AZD4547-dependent disruption of FGFR/Akt/Myc axis signaling at different levels, including the downregulation of downstream targets such as Akt, cyclin D1, Myc and ALDH.

ALDH has been proposed as a marker of tumor-initiating cells population, associated with spheroid formation capacity *in vitro*, and metastasis *in vivo* [13,31]. Hence, we evaluated the effect of treatments on ALDH expression. Interestingly, we observed that both calcitriol and AZD4547 reduced ALDH positivity in BT-474 cells, being the RTKI more potent than the secosteroid. Interestingly, we found a positive correlation between *ALDH* and *FGFR1*, and a negative correlation between *ALDH* and *VDR* expression in breast cancer patient's transcriptomic data. The latter suggests that FGFR1 overexpression relates to increased stemness features and worst prognostic, while VDR to a better one, supporting the benefit of a FGFR-VDR targeted therapy in breast cancer. As a selective inhibitor of FGFR1–3, AZD4547 effects are given by the regulation of FGFR signaling. In our model, we showed that FGFR1 was overexpressed, suggesting that BT-474 stem population is mainly dependent on FGFR1 activity. In this regard, FGFR1 overexpression is known to enhance Akt/Erk/ER signaling, which has been associated with stemness induction in ER+ breast cancer cells [33]. For this reason, we propose that FGFR1 signaling is highly involved in the stemness features of BT-474 cells and their tumorigenic potential. Moreover, the correlation results generated with the Breast Cancer Gene-Expression Miner database support an intrinsic relationship between *FGFR1* gene expression and that of *AKT, CCND1* and *CTNNB1* in HER2-enriched breast tumors that share similar molecular characteristics with BT-474 cells. As judged by the BT-474 phenotypic characterization performed in this study, this cell line may be considered as luminal B-like HER2 + surrogate intrinsic subtype [13]. Considering the correlations between *CTNNB1* expression with *FGFR1* and *AKT,* we hypothesize that β-catenin could be participating in AZD4547-calcitriol antiproliferative effects, which deserves further studies. On the other hand, calcitriol inhibits downstream targets of β-catenin such as *MYC* and *CCND1*, while induces p21 expression to repress cyclin D1 and arrest cells in G1 phase. Therefore, the use of AZD4547 and calcitriol in combination in patients bearing tumors that co-express FGFR and VDR could result beneficial to inhibit tumor growth and dissemination.

Taken together, our results suggest that AZD4547 combined with calcitriol inhibit BT-474 stemness capacity through the inhibition of FGFR1 activation and pro-differentiating activity. As far as we know, this is the first study addressing the antineoplastic effects of AZD4547 in combination with calcitriol. Our results can contribute to the proposal of a better therapeutic strategy for luminal B-like HER2 + breast cancer, to achieve a synergic antineoplastic response while avoiding adverse effects and treatment resistance.

## 5. Conclusions

Calcitriol, at a clinically achievable low concentration (1 nM), synergized AZD4547 antiproliferative effects in BT-474 cells, allowing for a favorable dose reduction. Mechanistically, calcitriol induced cell differentiation, AZD4547 inhibited FGFR1 phosphorylation, and both compounds promoted the inhibition of stemness and tumorsphere formation capacity of the luminal B breast cancer cells BT-474. Furthermore, the results suggest that these effects were partially mediated by disruption of the FGFR/Akt/Myc axis.

## Funding

This study was funded by Consejo Nacional de Ciencia y Tecnología de México (CONACyT), grant number A1-S-10749 to LD. The funders had no role in study design, analysis and interpretation of the data, writing of the manuscript or the decision to submit the article for publication.

## CRediT authorship contribution statement

**Gabriela Morales-Guadarrama**: Validation, Methodology, Investigation, Formal analysis, Writing-original draft preparation and Visualization; **Edgar A. Méndez-P é rez**: Validation, Methodology, Investigation, Formal analysis and Visualization; **Janice García-Quiroz** Methodology, Investigation, Formal analysis and Visualization; **Euclides Avila**: Writing-review and editing; **Fernando Larrea**: Writing-review and editing; **Lorenza Díaz**: Conceptualization, Validation, Methodology, Investigation, Formal analysis, Writing-original draft preparation, Supervision, Project administration and Funding acquisition.

## Acknowledgments

Gabriela Morales-Guadarrama is a doctoral student from Programa de Doctorado en Ciencias Biomédicas, Universidad Nacional Autónoma de México (UNAM), and received fellowship 662170 from CONACyT, México. We are also grateful for the support from Fundación amigos del INCMNSZ, A.C. (Grant number 348 to GM-G). Part of this study was included on the thesis work to obtain the bachelor's degree in Chemical Pharmaceutical Biologist of EAM from Universidad Simón Bolívar, México.

*Declarations of interest*

None.

## Appendix A. Supporting information

Supplementary data associated with this article can be found in the online version at doi:10.1016/j.jsbmb.2022.106132.

## References

[1] H. Sung, J. Ferlay, R.L. Siegel, M. Laversanne, I. Soerjomataram, A. Jemal, F. Bray, Global cancer statistics 2020: GLOBOCAN estimates of incidence and mortality worldwide for 36 cancers in 185 countries, CA Cancer J. Clin. 71 (2021) 209–249.
[2] C.M. Perou, T. Sorlie, M.B. Eisen, M. van de Rijn, S.S. Jeffrey, C.A. Rees, J. R. Pollack, D.T. Ross, H. Johnsen, L.A. Akslen, O. Fluge, A. Pergamenschikov, C. Williams, S.X. Zhu, P.E. Lonning, A.L. Borresen-Dale, P.O. Brown, D. Botstein, Molecular portraits of human breast tumours, Nature 406 (2000) 747–752.
[3] N. Harbeck, F. Penault-Llorca, J. Cortes, M. Gnant, N. Houssami, P. Poortmans, K. Ruddy, J. Tsang, F. Cardoso, Breast cancer, Nat. Rev. Dis. Prim. 5 (2019) 66.
[4] R. Clarke, M.C. Liu, K.B. Bouker, Z. Gu, R.Y. Lee, Y. Zhu, T.C. Skaar, B. Gomez, K. O'Brien, Y. Wang, L.A. Hilakivi-Clarke, Antiestrogen resistance in breast cancer and the role of estrogen receptor signaling, Oncogene 22 (2003) 7316–7339.
[5] M.C. Cheang, S.K. Chia, D. Voduc, D. Gao, S. Leung, J. Snider, M. Watson, S. Davies, P.S. Bernard, J.S. Parker, C.M. Perou, M.J. Ellis, T.O. Nielsen, Ki67 index, HER2 status, and prognosis of patients with luminal B breast cancer, J. Natl. Cancer Inst. 101 (2009) 736–750.
[6] B. Linderholm, J. Bergqvist, H. Hellborg, U. Johansson, M. Linderholm, E. von Schoultz, G. Elmberger, L. Skoog, J. Bergh, Shorter survival-times following adjuvant endocrine therapy in oestrogen- and progesterone-receptor positive breast cancer overexpressing HER2 and/or with an increased expression of vascular endothelial growth factor, Med. Oncol. 26 (2009) 480–490.
[7] L. Braun, F. Mietzsch, P. Seibold, A. Schneeweiss, P. Schirmacher, J. Chang-Claude, H. Peter Sinn, S. Aulmann, Intrinsic breast cancer subtypes defined by estrogen receptor signalling-prognostic relevance of progesterone receptor loss, Mod. Pathol. 26 (2013) 1161–1171.
[8] C.J. Creighton, The molecular profile of luminal B breast cancer, Biologics 6 (2012) 289–297.
[9] N. Turner, A. Pearson, R. Sharpe, M. Lambros, F. Geyer, M.A. Lopez-Garcia, R. Natrajan, C. Marchio, E. Iorns, A. Mackay, C. Gillett, A. Grigoriadis, A. Tutt, J. S. Reis-Filho, A. Ashworth, FGFR1 amplification drives endocrine therapy resistance and is a therapeutic target in breast cancer, Cancer Res. 70 (2010) 2085–2094.
[10] M. Katoh, H. Nakagama, FGF receptors: cancer biology and therapeutics, Med. Res. Rev. 34 (2014) 280–300.
[11] X. Qian, A. Anzovino, S. Kim, K. Suyama, J. Yao, J. Hulit, G. Agiostratidou, N. Chandiramani, H.M. McDaid, C. Nagi, H.W. Cohen, G.R. Phillips, L. Norton, R. B. Hazan, N-cadherin/FGFR promotes metastasis through epithelial-to-mesenchymal transition and stem/progenitor cell-like properties, Oncogene 33 (2014) 3411–3421.
[12] M.F. Santolla, M. Maggiolini, The FGF/FGFR system in breast cancer: oncogenic features and therapeutic perspectives, Cancers 12 (2020).
[13] Q. Zhao, A.B. Parris, E.W. Howard, M. Zhao, Z. Ma, Z. Guo, Y. Xing, X. Yang, FGFR inhibitor, AZD4547, impedes the stemness of mammary epithelial cells in the premalignant tissues of MMTV-ErbB2 transgenic mice, Sci. Rep. 7 (2017) 11306.
[14] C. Aggarwal, M.W. Redman, P.N. Lara Jr., H. Borghaei, P. Hoffman, J.D. Bradley, A.J. Newman 3rd, M.J. Feldman, K. Minichiello, J. Miao, P.C. Mack, V. A. Papadimitrakopoulou, R.S. Herbst, K. Kelly, D.R. Gandara, SWOG S1400D (NCT02965378), a phase II study of the fibroblast growth factor receptor inhibitor AZD4547 in previously treated patients with fibroblast growth factor pathway-activated stage IV squamous cell lung cancer (Lung-MAP Substudy), J. Thorac. Oncol. 14 (2019) 1847–1852.
[15] P.R. Gavine, L. Mooney, E. Kilgour, A.P. Thomas, K. Al-Kadhimi, S. Beck, C. Rooney, T. Coleman, D. Baker, M.J. Mellor, A.N. Brooks, T. Klinowska, AZD4547: an orally bioavailable, potent, and selective inhibitor of the fibroblast growth factor receptor tyrosine kinase family, Cancer Res. 72 (2012) 2045–2056.
[16] H. Saka, C. Kitagawa, Y. Kogure, Y. Takahashi, K. Fujikawa, T. Sagawa, S. Iwasa, N. Takahashi, T. Fukao, C. Tchinou, D. Landers, Y. Yamada, Safety, tolerability and pharmacokinetics of the fibroblast growth factor receptor inhibitor AZD4547 in Japanese patients with advanced solid tumours: a Phase I study, Investig. N. Drugs 35 (2017) 451–462.
[17] Y.K. Chae, F. Hong, C. Vaklavas, H.H. Cheng, P. Hammerman, E.P. Mitchell, J. A. Zwiebel, S.P. Ivy, R.J. Gray, S. Li, L.M. McShane, L.V. Rubinstein, D. Patton, P. M. Williams, S.R. Hamilton, A. Mansfield, B.A. Conley, C.L. Arteaga, L.N. Harris, P. J. O'Dwyer, A.P. Chen, K.T. Flaherty, Phase II study of AZD4547 in patients with tumors harboring aberrations in the FGFR pathway: results From the NCI-MATCH trial (EAY131) subprotocol W, J. Clin. Oncol.: Off. J. Am. Soc. Clin. Oncol. 38 (2020) 2407–2417.
[18] I. Martinez-Reza, L. Diaz, D. Barrera, M. Segovia-Mendoza, S. Pedraza-Sanchez, G. Soca-Chafre, F. Larrea, R. Garcia-Becerra, Calcitriol inhibits the proliferation of triple-negative breast cancer cells through a mechanism involving the proinflammatory cytokines IL-1beta and TNF-alpha, J. Immunol. Res. 2019 (2019), 6384278.
[19] G. Wang, L. Lei, X. Zhao, J. Zhang, M. Zhou, K. Nan, Calcitriol inhibits cervical cancer cell proliferation through downregulation of HCCR1 expression, Oncol. Res. 22 (2014) 301–309.
[20] R. Garcia-Becerra, L. Diaz, J. Camacho, D. Barrera, D. Ordaz-Rosado, A. Morales, C. S. Ortiz, E. Avila, E. Bargallo, M. Arrecillas, A. Halhali, F. Larrea, Calcitriol inhibits Ether-a go-go potassium channel expression and cell proliferation in human breast cancer cells, Exp. Cell Res. 316 (2010) 433–442.
[21] N.L. Shan, J. Wahler, H.J. Lee, M.J. Bak, S.D. Gupta, H. Maehr, N. Suh, Vitamin D compounds inhibit cancer stem-like cells and induce differentiation in triple negative breast cancer, J. Steroid Biochem. Mol. Biol. 173 (2017) 122–129.
[22] Y. Lee, B.E. Dunlap, W.S. Mellon, Induction of monocytic differentiation by calcitriol (1,25-dihydroxyvitamin D3) in the human promyelocytic leukemic cell line (HL-60) in serum-free medium, Biochem. Pharmacol. 36 (1987) 3893–3901.
[23] T. Takahashi, K. Nakamura, S. Iho, Differentiation of myeloid cells and 1,25-dihydroxyvitamin D3, Leuk. Lymphoma 27 (1997) 25–33.
[24] P.J. Hughes, E. Marcinkowska, E. Gocek, G.P. Studzinski, G. Brown, Vitamin D3-driven signals for myeloid cell differentiation – implications for differentiation therapy, Leuk. Res. 34 (2010) 553–565.
[25] J. Garcia-Quiroz, R. Garcia-Becerra, C. Santos-Cuevas, G.J. Ramirez-Nava, G. Morales-Guadarrama, N. Cardenas-Ochoa, M. Segovia-Mendoza, H. Prado-Garcia, D. Ordaz-Rosado, E. Avila, A. Olmos-Ortiz, S. Lopez-Cisneros, F. Larrea, L. Diaz, Synergistic antitumorigenic activity of calcitriol with curcumin or resveratrol is mediated by angiogenesis inhibition in triple negative breast cancer xenografts, Cancers 11 (2019).
[26] N. Santos-Martinez, L. Diaz, D. Ordaz-Rosado, J. Garcia-Quiroz, D. Barrera, E. Avila, A. Halhali, H. Medina-Franco, M.J. Ibarra-Sanchez, J. Esparza-Lopez, J. Camacho, F. Larrea, R. Garcia-Becerra, Calcitriol restores antiestrogen responsiveness in estrogen receptor negative breast cancer cells: a potential new therapeutic approach, BMC Cancer 14 (2014) 230.
[27] M. Segovia-Mendoza, L. Diaz, M.E. Gonzalez-Gonzalez, I. Martinez-Reza, J. Garcia-Quiroz, H. Prado-Garcia, M.J. Ibarra-Sanchez, J. Esparza-Lopez, F. Larrea, R. Garcia-Becerra, Calcitriol and its analogues enhance the antiproliferative activity of gefitinib in breast cancer cells, J. Steroid Biochem. Mol. Biol. 148 (2015) 122–131.
[28] J. Garcia-Quiroz, N. Cardenas-Ochoa, R. Garcia-Becerra, G. Morales-Guadarrama, E.A. Mendez-Perez, C. Santos-Cuevas, G.J. Ramirez-Nava, M. Segovia-Mendoza, H. Prado-Garcia, E. Avila, F. Larrea, L. Diaz, Antitumoral effects of dovitinib in triple-negative breast cancer are synergized by calcitriol in vivo and in vitro, J. Steroid Biochem. Mol. Biol. 214 (2021), 105979.
[29] M. Segovia-Mendoza, J. García-Quiroz, L. Díaz, R. García-Becerra, Combinations of calcitriol with anticancer treatments for breast cancer: an update, Int. J. Mol. Sci. 22 (2021).
[30] M.Y. Quan, Q. Guo, J. Liu, R. Yang, J. Bai, W. Wang, Y. Cai, R. Han, Y.Q. Lv, L. Ding, D.D. Billadeau, Z. Lou, S. Bellusci, X. Li, J.S. Zhang, An FGFR/AKT/SOX2

signaling axis controls pancreatic cancer stemness, Front. Cell Dev. Biol. 8 (2020) 287.
[31] T. Yamamoto, H. Miyoshi, F. Kakizaki, H. Maekawa, T. Yamaura, T. Morimoto, T. Katayama, K. Kawada, Y. Sakai, M.M. Taketo, Chemosensitivity of patient-derived cancer stem cells identifies colorectal cancer patients with potential benefit from FGFR inhibitor therapy, Cancers 12 (2020).
[32] Y.R. Na, J.Y. Kim, C.H. Song, M. Kim, Y.T. Do, T.T.L. Vo, E. Choi, E. Ha, J.H. Seo, S. J. Shin, The FGFR family inhibitor AZD4547 exerts an antitumor effect in ovarian cancer cells, Int. J. Mol. Sci. 22 (2021).
[33] Q. Cheng, Z. Ma, Y. Shi, A.B. Parris, L. Kong, X. Yang, FGFR1 overexpression induces cancer cell stemness and enhanced Akt/Erk-ER signaling to promote palbociclib resistance in luminal A breast cancer cells, Cells 10 (2021).
[34] V. Vichai, K. Kirtikara, Sulforhodamine B colorimetric assay for cytotoxicity screening, Nat. Protoc. 1 (2006) 1112–1116.
[35] T.C. Chou, P. Talalay, Quantitative analysis of dose-effect relationships: the combined effects of multiple drugs or enzyme inhibitors, Adv. Enzym. Regul. 22 (1984) 27–55.
[36] T.C. Chou, The mass-action law based algorithm for cost-effective approach for cancer drug discovery and development, Am. J. Cancer Res. 1 (2011) 925–954.
[37] P.K. Smith, R.I. Krohn, G.T. Hermanson, A.K. Mallia, F.H. Gartner, M. D. Provenzano, E.K. Fujimoto, N.M. Goeke, B.J. Olson, D.C. Klenk, Measurement of protein using bicinchoninic acid, Anal. Biochem. 150 (1985) 76–85.
[38] P.T. Nguyen, T. Tsunematsu, S. Yanagisawa, Y. Kudo, M. Miyauchi, N. Kamata, T. Takata, The FGFR1 inhibitor PD173074 induces mesenchymal-epithelial transition through the transcription factor AP-1, Br. J. Cancer 109 (2013) 2248–2258.
[39] A.M. Chioni, R. Grose, FGFR1 cleavage and nuclear translocation regulates breast cancer cell behavior, J. Cell Biol. 197 (2012) 801–817.
[40] M.G. Fakih, D.L. Trump, J.R. Muindi, J.D. Black, R.J. Bernardi, P.J. Creaven, J. Schwartz, M.G. Brattain, A. Hutson, R. French, C.S. Johnson, A phase I pharmacokinetic and pharmacodynamic study of intravenous calcitriol in combination with oral gefitinib in patients with advanced solid tumors, Clin. Cancer Res.: Off. J. Am. Assoc. Cancer Res. 13 (2007) 1216–1223.
[41] T.M. Beer, Development of weekly high-dose calcitriol based therapy for prostate cancer, Urol. Oncol. 21 (2003) 399–405.
[42] J.H. Dey, F. Bianchi, J. Voshol, D. Bonenfant, E.J. Oakeley, N.E. Hynes, Targeting fibroblast growth factor receptors blocks PI3K/AKT signaling, induces apoptosis, and impairs mammary tumor outgrowth and metastasis, Cancer Res. 70 (2010) 4151–4162.
[43] C. Dombrowski, T. Helledie, L. Ling, M. Grunert, C.A. Canning, C.M. Jones, J. H. Hui, V. Nurcombe, A.J. van Wijnen, S.M. Cool, FGFR1 signaling stimulates proliferation of human mesenchymal stem cells by inhibiting the cyclin-dependent kinase inhibitors p21(Waf1) and p27(Kip1), Stem Cells 31 (2013) 2724–2736.
[44] S.S. Jensen, M.W. Madsen, J. Lukas, L. Binderup, J. Bartek, Inhibitory effects of 1alpha,25-dihydroxyvitamin D(3) on the G(1)-S phase-controlling machinery, Mol. Endocrinol. 15 (2001) 1370–1380.
[45] K.C. Chiang, C.N. Yeh, S.C. Chen, S.C. Shen, J.T. Hsu, T.S. Yeh, J.H. Pang, L.J. Su, M. Takano, A. Kittaka, H.H. Juang, T.C. Chen, MART-10, a new generation of vitamin D analog, is more potent than 1alpha,25-dihydroxyvitamin D(3) in inhibiting cell proliferation and inducing apoptosis in ER+ MCF-7 breast cancer cells, Evid. -Based Complement. Altern. Med. 2012 (2012), 310872.
[46] H. Liu, J. Ai, A. Shen, Y. Chen, X. Wang, X. Peng, H. Chen, Y. Shen, M. Huang, J. Ding, M. Geng, c-Myc alteration determines the therapeutic response to FGFR inhibitors, Clin. Cancer Res.: Off. J. Am. Assoc. Cancer Res. 23 (2017) 974–984.
[47] M. Koziczak, T. Holbro, N.E. Hynes, Blocking of FGFR signaling inhibits breast cancer cell proliferation through downregulation of D-type cyclins, Oncogene 23 (2004) 3501–3508.
[48] J. Welsh, Targets of vitamin D receptor signaling in the mammary gland, J. Bone Min. Res. 22 (Suppl 2) (2007) V86–V90.
[49] N. Kocak, S. Nergiz, I.H. Yildirim, Y. Duran, Vitamin D can be used as a supplement against cancer stem cells, Cell. Mol. Biol. 64 (2018) 47–51.
[50] M.J. Larriba, J.M. Gonzalez-Sancho, A. Barbachano, N. Niell, G. Ferrer-Mayorga, A. Munoz, Vitamin D is a multilevel repressor of Wnt/b-catenin signaling in cancer cells, Cancers 5 (2013) 1242–1260.
[51] S. Navid, C. Fan, O.F.-V. P, D. Generali, Y. Li, The fibroblast growth factor receptors in breast cancer: from oncogenesis to better treatments, Int. J. Mol. Sci. 21 (2020).
[52] T. Kroll, L. Odyvanova, J.H. Clement, C. Platzer, A. Naumann, N. Marr, K. Hoffken, S. Wolfl, Molecular characterization of breast cancer cell lines by expression profiling, J. Cancer Res. Clin. Oncol. 128 (2002) 125–134.
[53] S. Kamimura, M. Gallieni, M. Zhong, W. Beron, E. Slatopolsky, A. Dusso, Microtubules mediate cellular 25-hydroxyvitamin D3 trafficking and the genomic response to 1,25-dihydroxyvitamin D3 in normal human monocytes, J. Biol. Chem. 270 (1995) 22160–22166.
[54] J. Barsony, W. McKoy, Molybdate increases intracellular 3',5'-guanosine cyclic monophosphate and stabilizes vitamin D receptor association with tubulin-containing filaments, J. Biol. Chem. 267 (1992) 24457–24465.
[55] H.G. Palmer, J.M. Gonzalez-Sancho, J. Espada, M.T. Berciano, I. Puig, J. Baulida, M. Quintanilla, A. Cano, A.G. de Herreros, M. Lafarga, A. Munoz, Vitamin D(3) promotes the differentiation of colon carcinoma cells by the induction of E-cadherin and the inhibition of beta-catenin signaling, J. Cell Biol. 154 (2001) 369–387.
[56] E. Gocek, G.P. Studzinski, Vitamin D and differentiation in cancer, Crit. Rev. Clin. Lab Sci. 46 (2009) 190–209.
[57] R. Gniadecki, B. Gajkowska, M. Hansen, 1,25-dihydroxyvitamin D3 stimulates the assembly of adherens junctions in keratinocytes: involvement of protein kinase C, Endocrinology 138 (1997) 2241–2248.
[58] F. Posa, A. Di Benedetto, E.A. Cavalcanti-Adam, G. Colaianni, C. Porro, T. Trotta, G. Brunetti, L. Lo Muzio, M. Grano, G. Mori, Erratum to vitamin D promotes MSC osteogenic differentiation stimulating cell adhesion and alphaVbeta3 expression, Stem Cells Int. 2018 (2018), 1865084.
[59] F. Posa, A. Di Benedetto, E.A. Cavalcanti-Adam, G. Colaianni, C. Porro, T. Trotta, G. Brunetti, L. Lo Muzio, M. Grano, G. Mori, Vitamin D promotes MSC osteogenic differentiation stimulating cell adhesion and alphaVbeta3 expression, Stem Cells Int. 2018 (2018), 6958713.
[60] A.K. Srivastava, A. Rizvi, T. Cui, C. Han, A. Banerjee, I. Naseem, Y. Zheng, A. A. Wani, Q.E. Wang, Depleting ovarian cancer stem cells with calcitriol, Oncotarget 9 (2018) 14481–14491.

Journal of Steroid Biochemistry and Molecular Biology 214 (2021) 105979

Contents lists available at ScienceDirect

Journal of Steroid Biochemistry and Molecular Biology

journal homepage: www.elsevier.com/locate/jsbmb

# Antitumoral effects of dovitinib in triple-negative breast cancer are synergized by calcitriol *in vivo* and *in vitro*

Janice García-Quiroz [a,1], Nohemí Cárdenas-Ochoa [a,1], Rocío García-Becerra [b], Gabriela Morales-Guadarrama [a], Edgar A. Méndez-Pérez [a], Clara Santos-Cuevas [c], Gerardo J. Ramírez-Nava [c], Mariana Segovia-Mendoza [d], Heriberto Prado-García [e], Euclides Avila [a], Fernando Larrea [a], Lorenza Díaz [a,*]

[a] *Departamento de Biología de la Reproducción Dr. Carlos Gual Castro, Instituto Nacional de Ciencias Médicas y Nutrición Salvador Zubirán, Av. Vasco de Quiroga No. 15, Belisario Domínguez Sección XVI, Tlalpan, 14080, Ciudad de México, Mexico*

[b] *Departamento de Biología Molecular y Biotecnología, Instituto de Investigaciones Biomédicas, Universidad Nacional Autónoma de México, Av. Universidad 3000, Coyoacán, 04510, Ciudad de México, Mexico*

[c] *Departamento de Materiales Radioactivos, Instituto Nacional de Investigaciones Nucleares, Ocoyoacac, 52750, Estado de México, Mexico*

[d] *Departamento de Farmacología, Facultad de Medicina, Universidad Nacional Autónoma de México, Av. Universidad 3000, Coyoacán, 04510, Ciudad de México, Mexico*

[e] *Departamento de Enfermedades Crónico-Degenerativas, Instituto Nacional de Enfermedades Respiratorias Ismael Cosío Villegas, Calzada de Tlalpan 4502, Belisario Domínguez Sección XVI, C.P. 14080, Tlalpan, Ciudad de México, Mexico*

ARTICLE INFO

*Keywords:*
Breast cancer
Dovitinib
Calcitriol
Combination index
Dose-reduction index
Synergism

ABSTRACT

Chemotherapy is a standard therapeutic option for triple-negative breast cancer (TNBC); however, its effectiveness is often compromised by drug-related toxicity and resistance development. Herein, we aimed to evaluate whether an improved antineoplastic effect could be achieved *in vitro* and *in vivo* in TNBC by combining dovitinib, a multi-kinase inhibitor, with calcitriol, a natural anticancer hormone. *In vitro*, cell proliferation and cell-cycle distribution were studied by sulforhodamine B-assays and flow cytometry. *In vivo*, dovitinib/calcitriol effects on tumor growth, angiogenesis, and endothelium activation were evaluated in xenografted mice by caliper measures, Itgb3/VEGFR2-immunohistochemistry and $^{99m}$Tc-Ethylenediamine-N,N-diacetic acid/hydrazinonicotinamyl-Glu[cyclo(Arg-Gly-Asp-D-Phe-Lys)]$_2$ ($^{99m}$Tc-RGD$_2$)-tumor uptake. The drug combination elicited a synergistically improved antiproliferative effect in TNBC-derived cells, which allowed a 7-fold and a 3.3-fold dovitinib dose-reduction in MBCDF-Tum and HCC-1806 cells, respectively. Mechanistically, the co-treatment induced a cell cycle profile suggestive of cell death and DNA damage (accumulation of cells in SubG1, S, and G2/M phases), increased the number of multinucleated cells and inhibited tumor growth to a greater extent than each compound alone. Tumor uptake of $^{99m}$Tc-RGD$_2$ was reduced by dovitinib, suggesting angiogenesis inhibition, which was corroborated by decreased endothelial cell growth, tumor-vessel density and VEGFR2 expression. In summary, calcitriol synergized dovitinib anticancer effects *in vitro* and *in vivo*, allowing for a significant dose-reduction of dovitinib while maintaining its antiproliferative potency. Our results suggest the beneficial convergence of independent antitumor mechanisms of dovitinib and calcitriol to inhibit TNBC-tumor growth.

*Abbreviations:* TNBC, Triple-negative breast cancer; HER-2, human epidermal growth factor receptor 2; RTK, receptor tyrosine kinase; RTKI, receptor tyrosine kinase inhibitor; FGF, fibroblast growth factor; FGFR, fibroblast growth factor receptor; VEGF, vascular endothelial growth factor; VEGFR, vascular endothelial growth factor receptor; PDGFR, platelet derived growth factor receptor; VDR, vitamin D receptor; MBCDF-T, MBCDF-Tum; DRI, dose-reduction index; SPECT/CT, single–photon emission computed tomography and radiographic computed tomography; IC, Inhibitory concentrations; $^{99m}$Tc-RGD$_2$, $^{99m}$Tc-Ethylenediamine-N,N-diacetic acid/hydrazinonicotinamyl-Glu[cyclo(Arg-Gly-Asp-D-Phe-Lys)]$_2$.

* Corresponding author.

*E-mail addresses:* janice.garciaq@incmnsz.mx (J. García-Quiroz), cardenas9501@gmail.com (N. Cárdenas-Ochoa), rocio.garciab@iibiomedicas.unam.mx (R. García-Becerra), gabriela.mguadarrama@gmail.com (G. Morales-Guadarrama), edgar.mendez.p3@gmail.com (E.A. Méndez-Pérez), clara.cuevas@inin.gob.mx (C. Santos-Cuevas), gerardo.r.servicios@inin.gob.mx (G.J. Ramírez-Nava), mariana.segovia@facmed.com (M. Segovia-Mendoza), hpradog@yahoo.com (H. Prado-García), euclides.avilac@incmnsz.mx (E. Avila), fernando.larreag@incmnsz.mx (F. Larrea), lorenzadiaz@gmail.com, lorenza.diazn@incmnsz.mx (L. Díaz).

[1] These authors contributed equally to this work.

https://doi.org/10.1016/j.jsbmb.2021.105979
Received 18 March 2021; Received in revised form 25 July 2021; Accepted 18 August 2021
Available online 24 August 2021

## 1. Introduction

Breast cancer is the most commonly diagnosed neoplasm and the leading cause of cancer death among women worldwide [1]. According to the tumor molecular expression profile, this neoplasm has been classified mainly into four different subtypes: Luminal A, luminal B, human epidermal growth factor receptor 2 (HER-2)-enriched and triple-negative breast cancer (TNBC) [2]. Identifying breast cancer subtypes led to personalized treatment, including endocrine and anti-HER-2 therapy; however, the therapeutic possibilities for the TNBC-subtype are limited due to the lack of specific targets. In this regard, options targeting different receptor tyrosine kinases (RTKs) are currently underway, like those directed to members of the fibroblast growth factor receptors (FGFRs) [3]. Indeed, abnormal FGFR signaling has been reported in TNBC-tumors [4], including overamplifications that may result in FGF addiction [4–7]. Blocking the FGFR pathway *in vivo* has the additional benefit of reducing tumor angiogenesis due to its involvement in endothelial activation [8]. Regarding this, dovitinib, a potent orally bioavailable RTK inhibitor (RTKI), blocks not only FGFR 1–3 but also the vascular endothelial growth factor receptor (VEGFR) subtypes 1–3 and the platelet-derived growth factor receptor (PDGFR), whose signaling pathways are involved in carcinogenesis, neovascularization, invasion, and metastasis [7]. Of note, dovitinib has been shown to inhibit FGFR, VEGFR, and PDGFR in preclinical breast cancer models [9,10].

Although dovitinib has been generally associated with low-grade side effects such as diarrhea, nausea, vomiting, and/or headache [11], its long-term use may result in more severe adverse events and/or acquired resistance [12–14]. Concerning this, a good strategy to avoid treatment-associated toxicity and resistance is to combine dovitinib with other antineoplastic agents to block additional tumor survival pathways, allowing to reduce the dose and/or frequency of administration. In this regard, a recent RNA-sequencing data analysis undertaken to identify potential targeting therapeutic candidates for TNBC revealed that one of the highly expressed genes in these tumors was the vitamin D receptor (VDR), encoding the target of calcitriol [15]. Calcitriol, the vitamin D most active metabolite, exerts potent antineoplastic activity by modulating diverse signaling networks involved in inhibition of cell proliferation, anti-inflammatory effects, acquisition of a more differentiated phenotype and induction of apoptosis [16]. Moreover, calcitriol has been shown to increase the sensitivity of tumor cells to various chemotherapeutic agents [17–21], with the added benefit of being a natural compound derived from dietary sources or by sun exposure. Notably, low vitamin D serum levels have been shown to correlate with an increased risk of certain neoplasms, including breast cancer [22]. Therefore, herein we explored whether an improved *in vitro* and *in vivo* antineoplastic effect could be achieved in TNBC by combining dovitinib with calcitriol. We also used a vascular endothelial cell line as a control for endothelial activation.

## 2. Materials and methods

### 2.1. Cell culture

In this study, we used the human TNBC cell lines MBCDF-Tum (MBCDF-T) [23] and HCC-1806 (ATCC CRL-2335, Manassas VA). The human endothelial cell line EA.hy926 (ATCC CRL-292, Manassas VA) was also used. Regarding MBCDF-Tum, these cells were derived from the parental cell line MBCDF (kindly donated by María de Jesus Ibarra-Sánchez and José Esparza López, Instituto Nacional de Ciencias Médicas y Nutrición Salvador Zubirán), which was generated by growing explants obtained from a radical mastectomy of a patient diagnosed with ductal infiltrating carcinoma stage IV with bone metastasis [24]. MBCDF was implanted in a mouse, and the cell line derived from the resulting tumor was named MBCDF-Tum [23]. After characterization, this cell line showed lack of expression of estrogen receptor, progesterone receptor, cytokeratin 7 and epidermal growth factor receptor 2. However, they were positive for vimentin, which expression by cancer cells has been largely recognized as a marker of epithelial-to-mesenchymal transition. Therefore, MBCDF-Tum may be considered as a TNBC subtype with a mesenchymal-like phenotype [23]. In addition, this and the other cell lines used herein have been shown to express VDR, making them calcitriol targets [23,25]. The cells were maintained under standard cell culture conditions. All experimental procedures were performed in DMEM-F12 medium supplemented with 100 units/mL penicillin plus 100 μg/mL streptomycin and 5% charcoal-stripped-heat-inactivated fetal bovine serum.

### 2.2. Proliferation studies

Cells were seeded in 96-well plates (500–1000 cells/well) and the day after treated with dovitinib (0.005–5.0 μM, Santa Cruz Biotechnology, Santa Cruz, CA), calcitriol (0.01–100 nM, Sigma-Aldrich, St Louis, MO) or their respective vehicles (water or ethanol 0.1 %, respectively). Cell proliferation was evaluated by the sulforhodamine B colorimetric assay, as previously described [26]. After 3 and 6 days from initial exposure to treatment, incubations of HCC-1806 and MBCDF-T, respectively, were stopped, and absorbance was read at 492 nm in a microplate reader (Synergy HT Multi-Mode Microplate Reader, BioTek, VT, USA). The concentration values that inhibited cell proliferation at 20 % ($IC_{20}$) and 50 % ($IC_{50}$) were calculated considering the minimum and maximum effect, using the dose-response fitting function, with the scientific plotting software Origin 9.0 (OriginLab Corporation, Northampton, MA, USA).

Photographs of MBCDF-T were taken after 4 days of treatments to assess the formation of multinucleated cells.

### 2.3. Combination index and dose reduction index determination

To identify the nature of the compounds combination effect, the combination index and dose-reduction index (DRI) were calculated as previously reported [27–29]. Results were evaluated considering that combination index values $< 1$, $= 1$ or $>1$ depict synergistic, additive, or antagonistic effects, respectively, while synergism is subdivided into nearly additive (0.90–1.10), slight synergism (0.85–0.90), moderate synergism (0.7–0.85), synergism (0.3–0.7), strong synergism (0.1–0.3), and very strong synergism ($<0.1$) [29]. On the other hand, DRI values $\leq 1$ or $>1$ indicate not favorable dose-reduction or favorable dose-reduction, respectively [29].

### 2.4. Cell cycle analysis

Flow cytometry analyses were performed using a FACS Aria II flow cytometer (Becton Dickinson, San Jose, CA, USA). Briefly, MBCDF-T cells were treated with dovitinib ($IC_{50}$) and/or calcitriol (10 nM) for 72 h. After that, the cells were harvested, washed in PBS pH 7.2, fixed in 70 % ethanol, and kept at -20 ° C until analysis. DNA staining with 7-amino-actinomycin D (BioLegend, San Diego, CA) was done as reported previously [23]. The results were analyzed using FlowJo Software (LLC, Ashland, OR, USA).

### 2.5. Induction of tumors in athymic nude mice and therapeutic protocol

This study was approved by the Internal Committee for the Care and Use of Laboratory Animals (CICUAL: BRE-1820−16/19−1) of the Instituto Nacional de Ciencias Médicas y Nutrición Salvador Zubirán, and the handling of mice was performed according to the national and international rules, including the Official Mexican Rule (NOM-062-ZOO-1999). Six-week-old female athymic nude mice (BALB/c homozygous, Crl:NU(NCr)-Foxn1nu, Charles River Laboratories, Wilmington, MA) were maintained under controlled temperature, humidity and 12 h light/dark cycles with sterile food (standard PMI 5053) and water *ad*

*libitum*. Mice were randomly divided into four experimental groups (N = 4 each): 1) Control (C, 100 μL sterile saline 0.9 % NaCl *i.p.* once a week), 2) Calcitriol (Cal, 0.25 μg/ 100 μL *i.p.* once a week, Geldex, GELpharma, México), 3) Dovitinib (Dov, 20 mg/kg twice a week *i.p*, CAS 852433−84-2, Santa Cruz), and 4) Dovitinib plus calcitriol (Dov + Cal). The treatments were initiated the next day after the subcutaneous injection of MBCDF-T cells ($1.0 \times 10^6$ / 0.1 mL sterile 0.9 % NaCl) into the back of mice and were maintained for 3 weeks. To determine any toxic effect of the drug, mice were weighed three times *per* week. Tumor volume was calculated by caliper measures and the standard formula (length x width$^2$)/2, where length and width are the largest and smallest dimension, respectively. At the end of the experiments, mice were sacrificed by cervical dislocation under anesthesia (sodium pentobarbital 80 mg/kg *i.p.*), and tumors were fixed in paraformaldehyde for immunohistochemical staining.

### 2.6. SPECT/CT imaging

To acquire tumor images of activated endothelium, one mouse from each group was placed in a prone position in an induction chamber and anesthetized (2% isoflurane in 100 % oxygen). Under anesthesia, an intravenous injection of $^{99m}$Tc-RGD$_2$ (7.4 MBq/ 0.05 mL, ININ, México), a marker of endothelial activation, was administered. After 3−4 h, the radiopharmaceutical tumor uptake was evaluated using a micro single-photon emission computed tomography and radiographic computed tomography (SPECT/CT) scanner (Albira, ONCOVISION; Gem Imaging S.A., Valencia, Spain). Acquisition parameters were the same as reported previously [23].

### 2.7. Itgb3 immunohistochemistry and tumor vessel density evaluation

To visualize blood vessels, formaldehyde-fixed and paraffin-embedded tumor sections placed on glass coverslips were dewaxed and rehydrated using standard protocols. Antigen retrieval was accomplished by autoclaving in retriever citrate solution (BioSB, Santa Barbara, CA, USA). Tumor slides were blocked with immunodetector peroxidase blocker (BioSB) and incubated for 1 h with the primary antibody rabbit anti-Integrin 3 (Itgb3 1:100, Cell Signaling Technology, Beverly, MA 13166, USA), a marker of activated endothelium. After washing, slides were sequentially incubated with Immuno-Detector Biotin-Link and Immuno-Detector horseradish peroxidase (HRP) label (BioSB) 10 min each. Staining was completed with diaminobenzidine (DAB) and slides were counterstained with hematoxylin. Images were taken with a conventional microscope. Microvessel count was undertaken by three different observers using 20X photographs considering Itgb3-positive vessels in at least three hot spots areas (high-density fields) of each tumor, as described previously [30].

### 2.8. Semi-quantitative determination of tumor VEGFR2 expression by immunohistochemistry

The immunohistochemistry protocol for VEGFR2 was the same as described in 2.7, but using a rabbit anti-VEGFR2 antibody (1:500, Cell signaling Technology). A semi-quantitative analysis of VEGFR2-DAB staining was carried out in acquired images according to the protocol described by Crow and Yue [31]. This method is based on the deconvolution of immunohistochemistry images considering hematoxylin and DAB staining by using the ImageJ Fiji software. The intensity of DAB staining was normalized against the total number of nucleus present in each picture; therefore, considering both cancer and endothelial cells.

### 2.9. Statistical analysis

Statistical differences were established by one-way ANOVA followed by appropriate post-hoc tests for multiple comparisons using a specialized software package (SigmaStat 3.5, Jandel Scientific, CA, USA). In the case of multinucleated cells, the analysis of the statistical difference between groups was performed by Kruskal-Wallis ANOVA on Ranks followed by Dunn's method. Differences were considered statistically significant at $P < 0.05$.

## 3. Results

### 3.1. Dovitinib and calcitriol differentially regulated TNBC and endothelial cell proliferation

The effects of dovitinib and calcitriol on MBCDF-T, HCC-1806, and EA.hy926 cell proliferation are shown in Fig. 1. As depicted, dovitinib significantly inhibited breast cancer and endothelial cell proliferation in a concentration-dependent manner (Fig. 1A, C and E). On the other hand, as expected and as previously reported [23], calcitriol only inhibited tumor cells proliferation (Fig. 1B and D), and did not affect endothelial cells growth (Fig. 1F).

Based on the dose-response curves, $IC_{20}$ and $IC_{50}$ values were calculated (Table 1). Considering dovitinib $IC_{50}$ values, this drug inhibited more potently TNBC cells growth compared to EA.hy926 (Table 1).

Inhibitory concentrations at 20 % ($IC_{20}$) and 50 % ($IC_{50}$) were calculated based on the dose-response curves of dovitinib and calcitriol. Results are depicted as the mean of N ≥ 3 experiments. The ICs of calcitriol in EA.hy926 cells were not determined due to the lack of antiproliferative effect of this compound in these cells (ND = Not determined).

### 3.2. The combination of dovitinib and calcitriol synergistically inhibited the growth of TNBC-cells

Next, we sought to determine the nature of the pharmacological interaction between dovitinib and calcitriol in TNBC cells. For this, the following combination schemes were evaluated in MBCDF-T: dovitinib/calcitriol $IC_{20}/IC_{20}$, $IC_{20}/IC_{50}$, $IC_{50}/IC_{20}$ and $IC_{50}/IC_{50}$. For HCC-1806, we decided to evaluate concentrations equal or below the $IC_{20}$ of both compounds in combination: $IC_5/IC_5$, $IC_5/IC_{10}$, $IC_{20}/IC_5$ and $IC_{20}/IC_{10}$.

With all the combinations evaluated in MBCDF-T, a significantly stronger cell growth inhibitory effect was achieved as compared to each drug alone (Fig. 2A). Notably, the calculated combination index values (< 1) implicated a synergic effect (Table 2). Regarding HCC-1806, only the $IC_{20}/IC_5$ and $IC_{20}/IC_{10}$ combination schemes resulted in a significant cell growth inhibitory effect, compared to each drug alone (Fig. 2B), which resulted in being synergic (Table 2). Then, we studied the combined effect of both drugs in EA.hy926 cells. Since calcitriol did not change endothelial growth, we tested dovitinib $IC_{20}$ and $IC_{50}$ values with calcitriol 0.1 and 10 nM. As seen in Fig. 2C, calcitriol did not change dovitinib potency to inhibit endothelial cells proliferation.

The combination (Comb.) index values and dose-reduction index (DRI) were calculated after co-incubating TNBC cells in the presence of the indicated inhibitory concentrations (IC) of dovitinib (Dov) and calcitriol (Cal). Combination index <1, = 1, and >1 indicate synergistic, additive, or antagonistic effects, respectively. In the synergy scale, values <0.1, 0.1−0.3, 0.3−0.7, 0.7−0.85, 0.85−0.90, and 0.90–1.10 indicate very strong synergism, strong synergism, synergism, moderate synergism, slight synergism, and nearly additive, respectively. DRI values <1 and >1 indicate not favorable dose-reduction and favorable dose-reduction, respectively, for each drug in combination. DRI values higher than 1 represent the folds of dose-reduction allowed in combination for a given degree of effect compared with the dose of each drug alone. DRI values in bold font indicate the highest DRI value for Dov and Cal.

### 3.3. The combination of dovitinib with calcitriol allows for a significant dovitinib dose-reduction

Considering the synergism elicited by the combination of dovitinib with calcitriol in tumor cells, we calculated the DRI values to determine

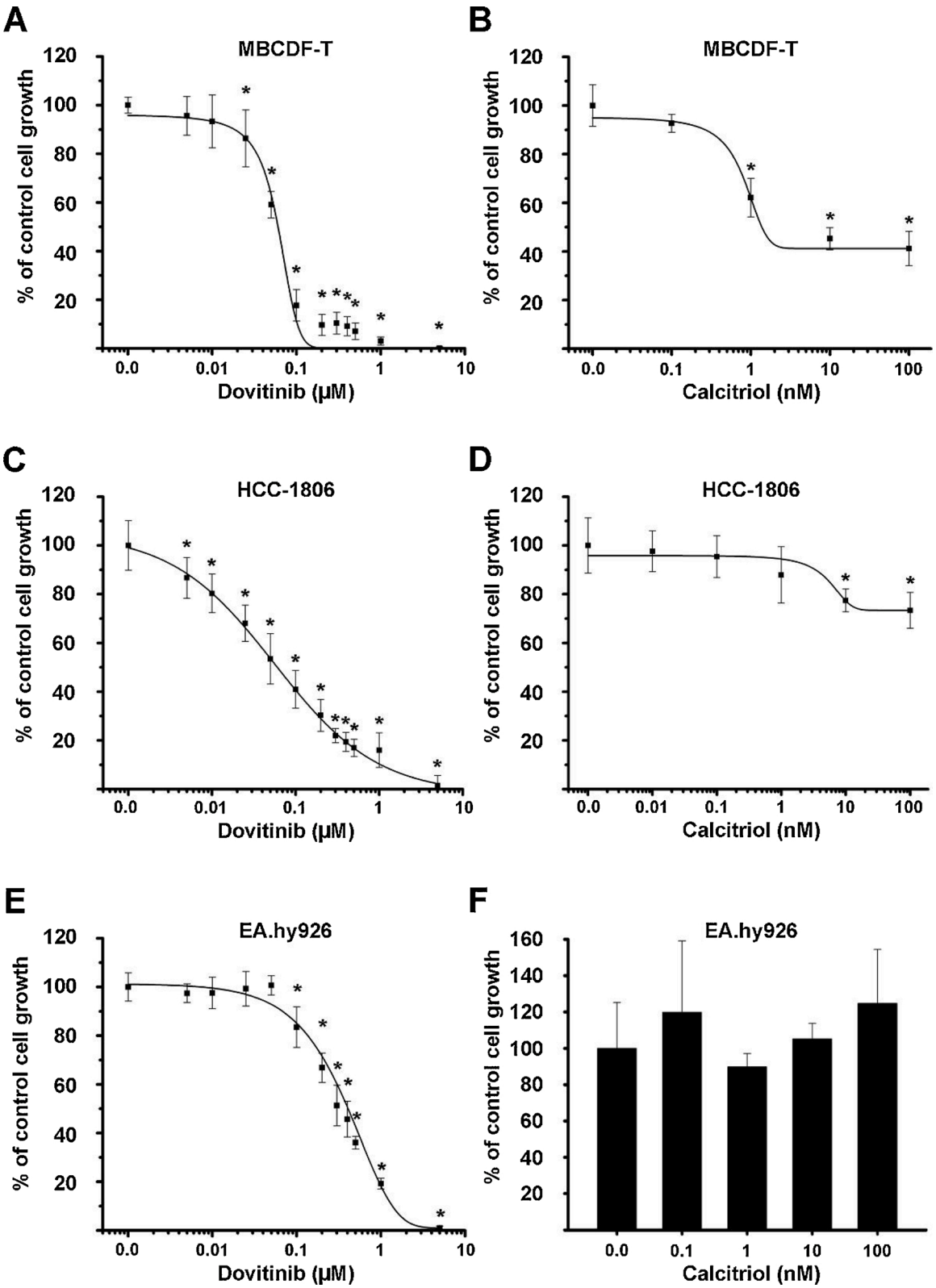


**Fig. 1.** Dose-response curves of dovitinib and calcitriol in MBCDF-T, HCC-1806 and EA.hy926 cells. MBCDF-T (A, B), HCC-1806 (C, D) and endothelial (E, F) cells were incubated with dovitinib (A, C and E) or calcitriol (B, D and F). The results are depicted as the mean ± S.D. of at least three independent experiments by sextuplicate and were normalized *vs.* control values, which were set to 100 %. * $P < 0.05$ *vs.* control.

how many folds the concentration of each compound could be reduced while maintaining the same efficacy as the drug alone (Table 2). Remarkably, in all combination schemes tested, both dovitinib and calcitriol concentrations showed favorable DRI values (DRI > 1), in accordance with the intensity of synergism (Table 2). As depicted in this table, the most favorable combination schemes in MBCDF-T were $IC_{50}$/$IC_{50}$ and $IC_{50}$/$IC_{20}$ for dovitinib/calcitriol, since dovitinib may be reduced up to 7 folds while calcitriol up to 28 folds, respectively. In the

**Table 1**
$IC_{20}$ and $IC_{50}$ values of dovitinib and calcitriol in endothelial and TNBC-cells.

| Cell line | Dovitinib (nM) | | Calcitriol (nM) | |
|---|---|---|---|---|
| | $IC_{20}$ | $IC_{50}$ | $IC_{20}$ | $IC_{50}$ |
| MBCDF-T | 18 | 56 | 0.296 | 0.619 |
| HCC-1806 | 11 | 60 | 0.141 | 0.974 |
| EA.hy926 | 153 | 378 | ND | ND |

case of HCC-1806, dovitinib/calcitriol $IC_{20}/IC_5$ and $IC_{20}/IC_{10}$ showed favorable results. Taken together, these data show that the combination of dovitinib and calcitriol is synergic, with favorable dose-reduction values.

### 3.4. The combination of dovitinib and calcitriol promoted breast cancer cell death

To gain insight into the mechanisms associated with the synergic antiproliferative effect of calcitriol and dovitinib, we studied the cell cycle distribution of MBCDF-T cells when exposed to both compounds alone and combined. As depicted in the data of Fig. 3, and in comparison to the control, dovitinib *per se* significantly increased the percentage of cells in SubG1-phase, which is associated with cell death. Accordingly, dovitinib reduced the percentage of cells in the G0/G1-phase, as compared to the control. Remarkably, the combination of dovitinib with calcitriol further increased the accumulation of cells in the SubG1 phase and reduced that of G0/G1 ($P < 0.05$). The treatments also augmented accumulation of cells in the S-phase. Of note, dovitinib slightly augmented the percentage of cells in G2/M phases of the cell cycle when compared to control cells, reaching statistical significance when combined with calcitriol (Fig. 3). This phenomenon is suggestive of mitotic catastrophe, a process preceding cell death [32] in which the uneven distribution of chromosomes between daughter nuclei, and the deficient separation of the nucleus during cytokinesis derive in multinucleation/micronucleation [33]. Therefore, we evaluated the proportion of these cells in our treated cell-cultures. We found that the treatment with dovitinib, either alone or in combination with calcitriol, significantly increased the proportion of multinucleated cells when compared to control cells $P < 0.001$ (Fig. 4).

### 3.5. In vivo co-administration of dovitinib and calcitriol significantly decreased tumor volume in a greater extent than each compound alone

Based on the effective antiproliferative action of calcitriol + dovitinib combination observed *in vitro*, we decided to evaluate the antitumor effect of this scheme in a murine model *in vivo*. As expected, and as previously shown for calcitriol [23], this compound and dovitinib *per se* slowed MBCDF-T tumor growth compared to the control group. However, the co-administration of these compounds significantly reduced tumor volume to a greater extent than each compound alone (Fig. 5A). Of note, there were no apparent side effects induced by the treatments, as judged by the absence of diarrhea and weight loss, suggesting no treatment-associated toxicity at the doses tested.

### 3.6. The in vivo antiangiogenic activity of dovitinib was not affected by calcitriol

In a representative mouse from each group, SPECT/CT images were acquired at the end of the experiment, showing decreased $^{99m}$Tc-RGD$_2$ tumor uptake in treated mice, with a greater reduction in dovitinib and Dov + Cal groups (Fig. 5B). Then, to quantitatively assess the effect of the treatments in tumor angiogenesis, vessel count was performed in Itgb3-immunostained slides. We knew from previous studies [23,34] that calcitriol does not modify tumor angiogenesis in breast tumor xenografts and that its administration may increase vascular endothelial growth factor (VEGF) and FGF levels [34–36]. Therefore, we expected

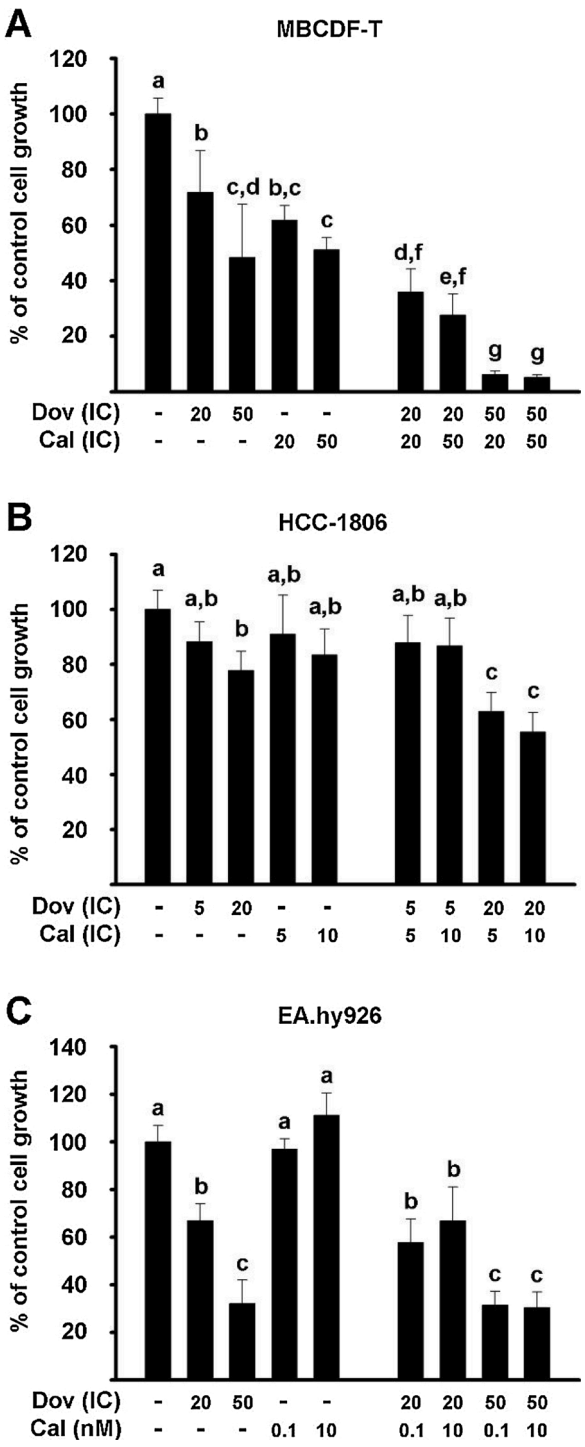


**Fig. 2.** Calcitriol increases dovitinib antiproliferative activity in TNBC cells. MBCDF-T cells (A), HCC-1806 (B) and EA.hy926 cells (C) were incubated in the presence of dovitinib (Dov), calcitriol (Cal) or their combination at their respective inhibitory concentration (IC) values at 5%, 10 %, 20 % or 50 %. For HCC-1806, the $IC_5$ value of dovitinib was 2.4 nM, while the $IC_5$ and $IC_{10}$ of calcitriol were 0.047 nM and 0.412 nM, respectively. For EA.hy926 cells, Dov $IC_{20}$ and $IC_{50}$ were combined with Cal 0.1 nM and 10 nM. Each bar represents the mean ± S.D. of at least three independent experiments by triplicate normalized *vs.* control values, which were set to 100 %. Different letters indicate statistical significance ($P < 0.05$).

**Table 2**
Combination index values and dose-reduction index for dovitinib/calcitriol treatment of TNBC cells.

| Cell line | Comb. Schemes Dov/Cal | Comb. index | Effect | DRI (folds) | |
|---|---|---|---|---|---|
| | | | | Dov | Cal |
| MBCDF-T | $IC_{20}/IC_{20}$ | 0.491 | Synergism | 4.58 | 3.66 |
| | $IC_{20}/IC_{50}$ | 0.564 | Synergism | 5.92 | 2.53 |
| | $IC_{50}/IC_{20}$ | 0.197 | Strong synergism | 6.18 | **28.62** |
| | $IC_{50}/IC_{50}$ | 0.203 | Strong synergism | **7.04** | 16.50 |
| HCC-1806 | $IC_{20}/IC_{5}$ | 0.543 | Synergism | 2.26 | 9.89 |
| | $IC_{20}/IC_{10}$ | 0.875 | Synergism | 3.32 | 1.74 |

that using calcitriol with an antiangiogenic factor such as dovitinib would improve their overall anticancer properties. However, it was necessary to ascertain that dovitinib antiangiogenic activity prevailed in the presence of calcitriol. As seen in Fig. 6, tumors in dovitinib-treated mice significantly had a fewer number of vessels as compared to controls and to calcitriol. This effect was preserved in the tumors of mice co-treated with Dov + Cal.

### 3.7. Dovitinib reduced tumor VEGFR2 expression in vivo

To further assess the effect of the treatments in tumor angiogenesis, we quantified by immunohistochemistry the tumor expression of VEGFR2, a primary responder to VEGF signal and a target of dovitinib. We found that, in agreement to vessel count results in Itgb3-stained slides, tumors in dovitinib-treated mice significantly showed less VEGFR2 protein expression than the control and calcitriol groups (Fig. 7).

Of note, we found lipid droplets-like structures in the tumors of dovitinib-treated mice (Fig. 7, Dov and Dov + Cal). This observation might relate to previous reports with similar findings using other RTKI [37] and deserve further studying.

## 4. Discussion

Due to the heterogeneous nature of TNBC, the poor prognosis, and the lack of targeted therapy, these tumors remain a clinical challenge nowadays. However, the high expression of diverse RTKs in most TNBC tumors makes these markers plausible oncological targets [38]. Drugs with multikinase inhibitory activity are a good option to treat TNBC patients since the concomitant targeting of different RTKs translates into increased efficacy and reduced resistance. Nevertheless, some adverse side effects may develop. Here, we evaluated the *in vivo* and *in vitro* pharmacological interaction of dovitinib and calcitriol with the objective to potentiate their anticancer effect while allowing for dose-reduction in TNBC. The analysis of our results using the combination index theorem of Chou-Talalay [28] showed that in TNBC-cells, the combination of calcitriol with dovitinib was highly synergic, reaching combination index values as low as 0.2 in the $IC_{50}/IC_{20}$ scheme in MBCDF-T cells. Remarkably, in all the combination schemes, the dose-reduction for each drug was favorable (DRI > 1) and was greater when the synergism was stronger. In this sense, the greatest dose-reduction was observed with the combination of dovitinib/calcitriol $IC_{50}/IC_{20}$ and $IC_{50}/IC_{50}$, where each compound concentration can be reduced by more than 7 and 28 folds, respectively in MBCDF-T cells. DRI was also favorable in HCC-1806 cells, although to a lesser extent. Overall, these results suggest the possibility to reduce the compounds' dose and therefore toxicity and resistance in therapeutic applications. To gain mechanistic insight into the drug synergism, we evaluated the effect of the combined treatment on cell cycle distribution and found that it strongly induced accumulation of MBCDF-T-cells in the Sub-G1 phase, suggesting cell death. Interestingly, we also found a significant accumulation of cells in the S-phase of the cell cycle in cells treated with all compounds alone and combined. Accumulation of cells in the S-phase may suggest DNA damage or inhibition of the DNA-replication machinery. Indeed, some RTKIs may directly interact with the DNA, inhibiting cancer cell proliferation [39]. Particularly in the case of dovitinib, its antiproliferative activity results not only from inhibiting multiple kinases, but also, in part, from its ability to block the ATP binding site of topoisomerases [40], which are DNA-interacting enzymes essential for proliferating cells [41]. Of note, calcitriol or its analogs have been shown to enhance the efficacy of topoisomerase-inhibitors in cancer cells, as well as to induce breast cancer cell apoptosis [42,43]. Moreover, the flow cytometric analysis of our data also indicated that the Dov + Cal combination significantly increased the percentage of G2/M-cells, which may suggest mitotic catastrophe, a process associated with cell death as a result of aberrant/failed mitosis, and which main

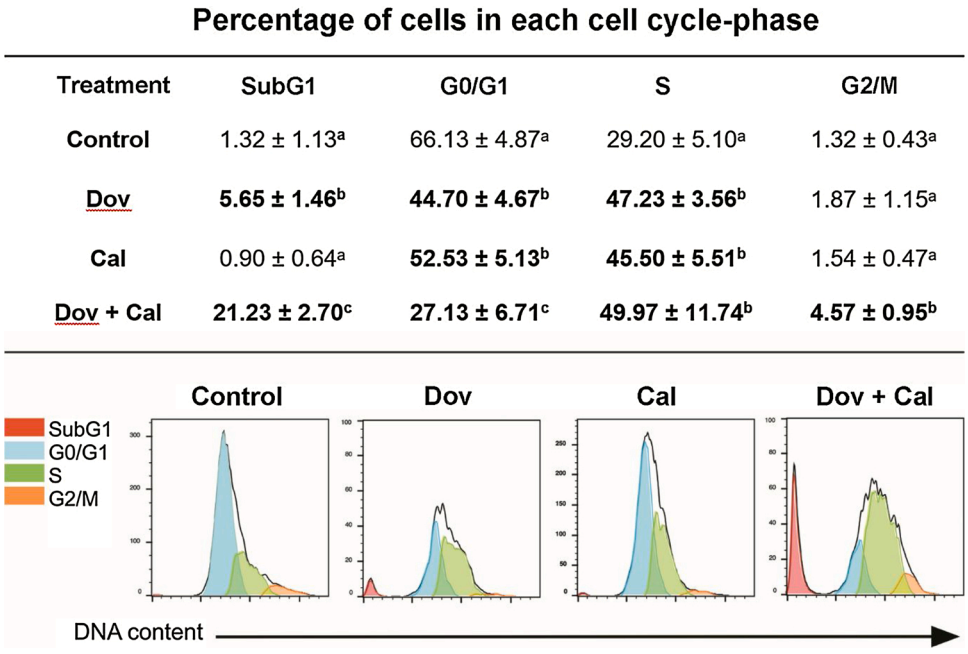


**Fig. 3.** Modification of cell cycle distribution by dovitinib, calcitriol, and their combination in TNBC MBCDF-T cells. The effects of dovitinib (Dov, $IC_{50}$), calcitriol (Cal, 10 nM), and their combination (Dov + Cal) on cell cycle distribution were evaluated in MBCDF-T cells. Results are shown as the mean ± S.D. of three independent experiments. Different letters indicate statistical significance ($P < 0.05$). Representative flow cytometry plots are shown in the lower panel. Cells in G1-peak are shown in blue, whereas S-region cells are shown in green and G2/M cells in orange. SubG1 subpopulation, corresponding to dead cells, is shown in red.

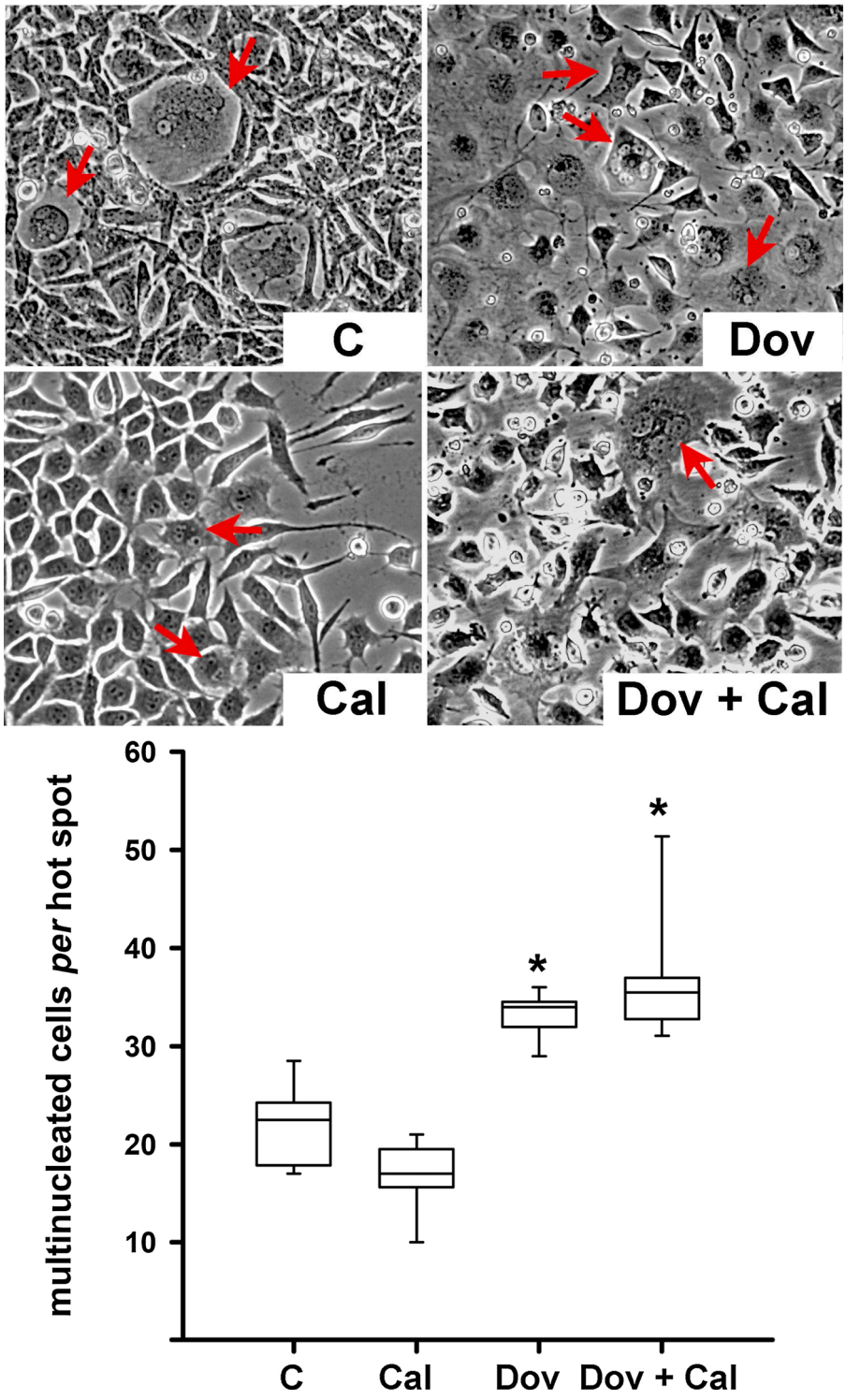


**Fig. 4.** Induction of multinucleated/micronucleated cells in TNBC MBCDF-T cells. The effects of dovitinib (Dov, $IC_{50}$), calcitriol (Cal, 10 nM), and their combination (Dov + Cal) on the induction of multinucleated cells in culture were evaluated in MBCDF-T cells. Box plots indicate 25, 50 and 75 percentiles. * $P < 0.001$ *vs.* control (C) and *vs.* calcitriol.

morphological marker is the production of giant, multinucleated aneuploid cells. Although we found these cells in all of our studied groups, their presence was significantly enhanced by the presence of dovitinib. Mitotic catastrophe has been previously demonstrated in diverse cancer cell lines, where dovitinib promoted a delay in mitotic exit, causing G2 arrest by activating the DNA damage checkpoint [44]. Interestingly, enriching the number of G2-phase cells has resulted in enhanced radiosensitivity [45]; therefore, future studies are warranted combining dovitinib and calcitriol with radiotherapy.

It is known from earlier studies that calcitriol may either favor or inhibit angiogenesis by stimulating proangiogenic factors or down-regulating some RTKs, including FGFR1 [23,34–36,46,47]. However, considering that this hormone inhibits breast cancer cell proliferation through different mechanisms [16,48], we hypothesized that its combination with a VEGFR/FGFR-targeting agent would improve overall anticancer effects. Our results showed that, while the antitumor effects

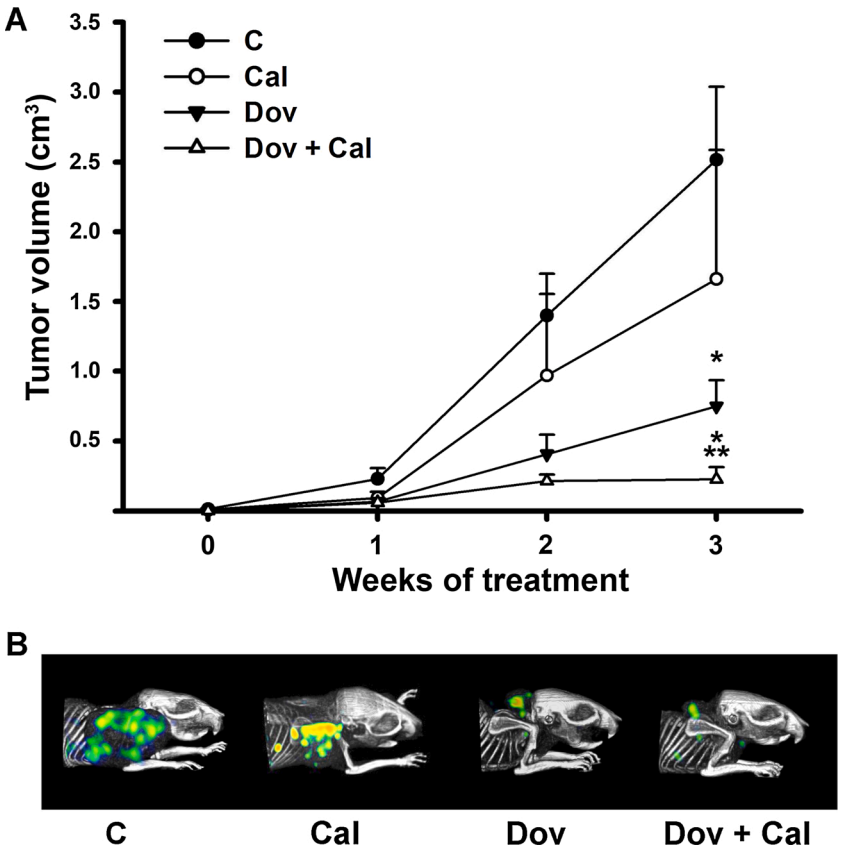


**Fig. 5.** *In vivo* antitumor and antiangiogenic effects of dovitinib in combination with calcitriol. MBCDF-T cells were xenografted in female nude mice, starting treatments the following day with saline solution (C), calcitriol (Cal), dovitinib (Dov), or their combination (Dov + Cal) during three weeks. During the experiment, tumor volume was calculated, and the results are depicted as the mean ± SEM (A). N = 4 mice *per* treatment. * $P < 0.05$ *vs.* C, ** $P < 0.05$ *vs.* Dov and *vs.* Cal. At the end of the treatments, $^{99m}$Tc-RGD$_2$ tumor uptake was evaluated in representative mice by SPECT/CT imaging (B).

of both compounds were synergistically enhanced in both *in vivo* and *in vitro* conditions, the antiangiogenic activity of dovitinib remained unchanged in the presence of calcitriol, as shown in endothelial cell proliferation, tumor vessel count, and $^{99m}$Tc-RGD$_2$ tumor uptake. This positive effect suggests the convergence of different antitumorigenic mechanisms of calcitriol and dovitinib, resulting in a beneficial anticancer outcome. Similarly, previous studies have shown that vitamin D derivatives exert synergistic effects when used in combination with other oncological drugs [18–21]. In particular, it has been demonstrated that the combination of calcitriol or its analogs with gefitinib, a synthetic RTKI, enhances global anticancer activity by inhibiting tumor growth and inducing apoptosis, and in cancer patients it does not result in serious undesirable side effects [17,20,49,50]. To the best of our knowledge, this is the first study addressing the antineoplastic effects of dovitinib in combination with calcitriol. Notably, the effective inhibitory concentrations of calcitriol determined herein and in other studies [23], which are in the nanomolar range, are significantly lower than the blood levels reached in calcitriol-treated cancer patients in which little toxicity has been reported [49,51], making it a safely achievable dose in the clinic. Likewise, the dovitinib $IC_{50}$ values calculated herein for breast cancer cells (< 60 nM, equivalent to ~24 ng/mL) were significantly lower than the previously reported serum levels in dovitinib-treated patients (60–100 ng/mL) [52]. Considering this, we believe that this is a promising drug combination for TNBC patients.

In this study, cancer cells resulted a more sensitive target to dovitinib compared to endothelial cells, which might be explained by the different RTKs present in each cell line, as well as their differential levels of expression. These results further support RTKs in TNBC tumors as plausible oncological targets. Regarding this, the observed ability of dovitinib to downregulate tumor VEGFR2 expression is of particular relevance.

Limitations of this study include the lack of evaluation of: 1) overall survival as an endpoint in the *in vivo* murine model, 2) the type of cell death induced by the co-treatment and 3) tumor regrowth and angiogenesis restoration after dovitinib withdrawal. All this remain the subject of future studies. The overall findings reported herein open new avenues for upcoming clinical research designed to assess the mechanisms by which TNBC-tumors respond to dovitinib and calcitriol in combination.

## 5. Conclusions

In summary, we demonstrated that at clinically achievable and safe concentrations, the combination of calcitriol with dovitinib is highly synergic in inhibiting tumorigenesis and breast cancer cell proliferation. Mechanistically, the combination regimen inhibited tumor angiogenesis and induced cancer cell death. The conclusions of this study suggest the feasibility of dose-reduction to avoid dose-related toxicity while retaining therapeutic efficacy in a combined treatment scheme for TNBC in the clinic. Further studies are warranted to explore dovitinib and calcitriol in combination with radiotherapy.

## Funding

This study was funded by Consejo Nacional de Ciencia y Tecnología (CONACyT), grant number A1-S-10749 to LD. The funders had no role in study design, analysis and interpretation of the data, writing of the manuscript or the decision to submit the article for publication.

## CRediT authorship contribution statement

**Janice García-Quiroz:** Conceptualization, Validation, Methodology, Investigation, Formal analysis, Writing - original draft, Visualization. **Nohemí Cárdenas-Ochoa:** Validation, Methodology, Investigation, Formal analysis, Visualization. **Rocío García-Becerra:** Writing - review & editing. **Gabriela Morales-Guadarrama:**

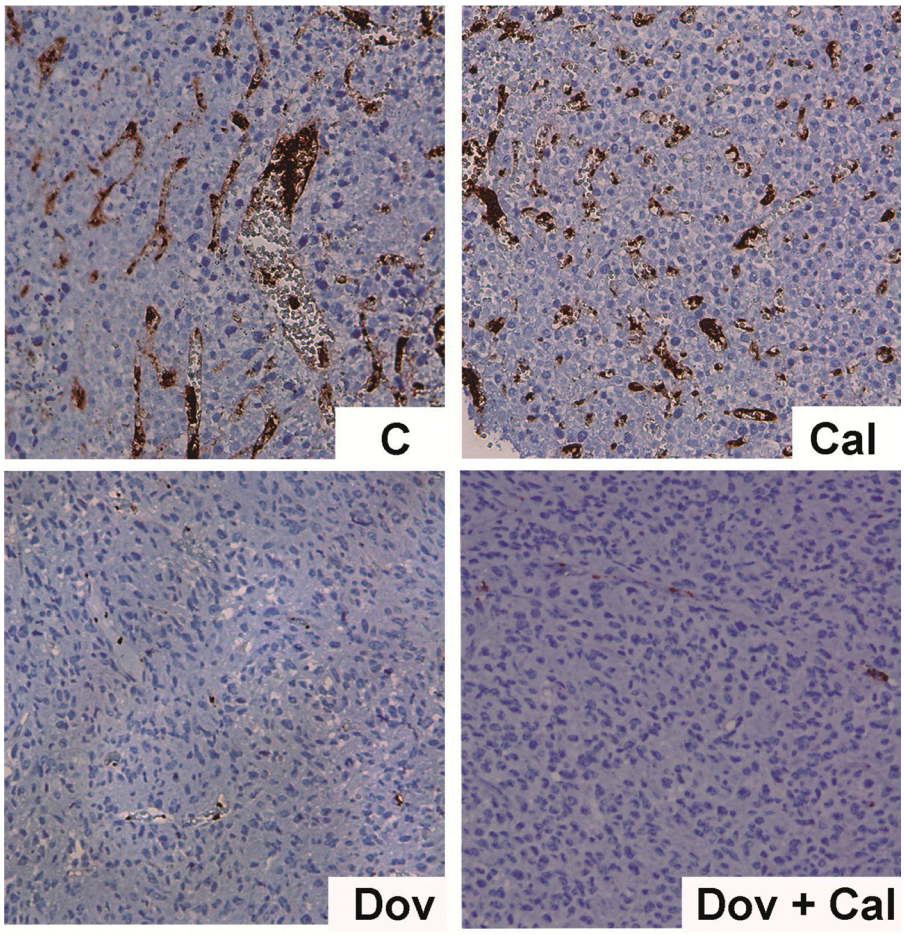


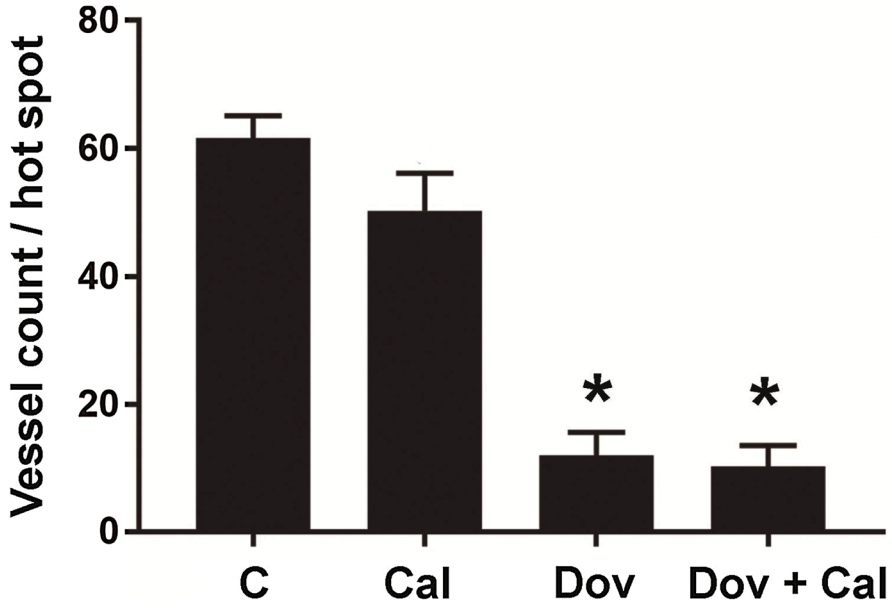


**Fig. 6.** Vessel density was analyzed in tumors from control mice (C), treated with calcitriol (Cal), dovitinib (Dov), or with the combination of dovitinib and calcitriol (Dov + Cal) by Itgb3 immunostaining. Immunohistochemistry representative images show Itgb3 in brown staining with 20 X magnification. Vessel count *per* hot spot is shown in the lower panel. Results are depicted as the mean ± SEM of the number of vessels in three different high-density fields *per* tumor (N = 4 different tumors/treatment), $P < 0.05$ *vs.* C.

Methodology, Investigation, Formal analysis, Visualization. **Edgar A. Méndez-Pérez:** Methodology, Investigation, Formal analysis. **Clara Santos-Cuevas:** Methodology, Investigation, Formal analysis, Visualization. **Gerardo J. Ramírez-Nava:** Methodology, Investigation, Formal analysis, Visualization. **Mariana Segovia-Mendoza:** Methodology, Investigation, Formal analysis, Visualization. **Heriberto Prado-García:** Methodology, Investigation, Formal analysis, Visualization. **Euclides Avila:** Writing - review & editing. **Fernando Larrea:** Writing - review & editing. **Lorenza Díaz:** Conceptualization, Validation, Methodology, Investigation, Formal analysis, Writing - original draft, Supervision, Project administration, Funding acquisition.

## Declaration of Competing Interest

None.

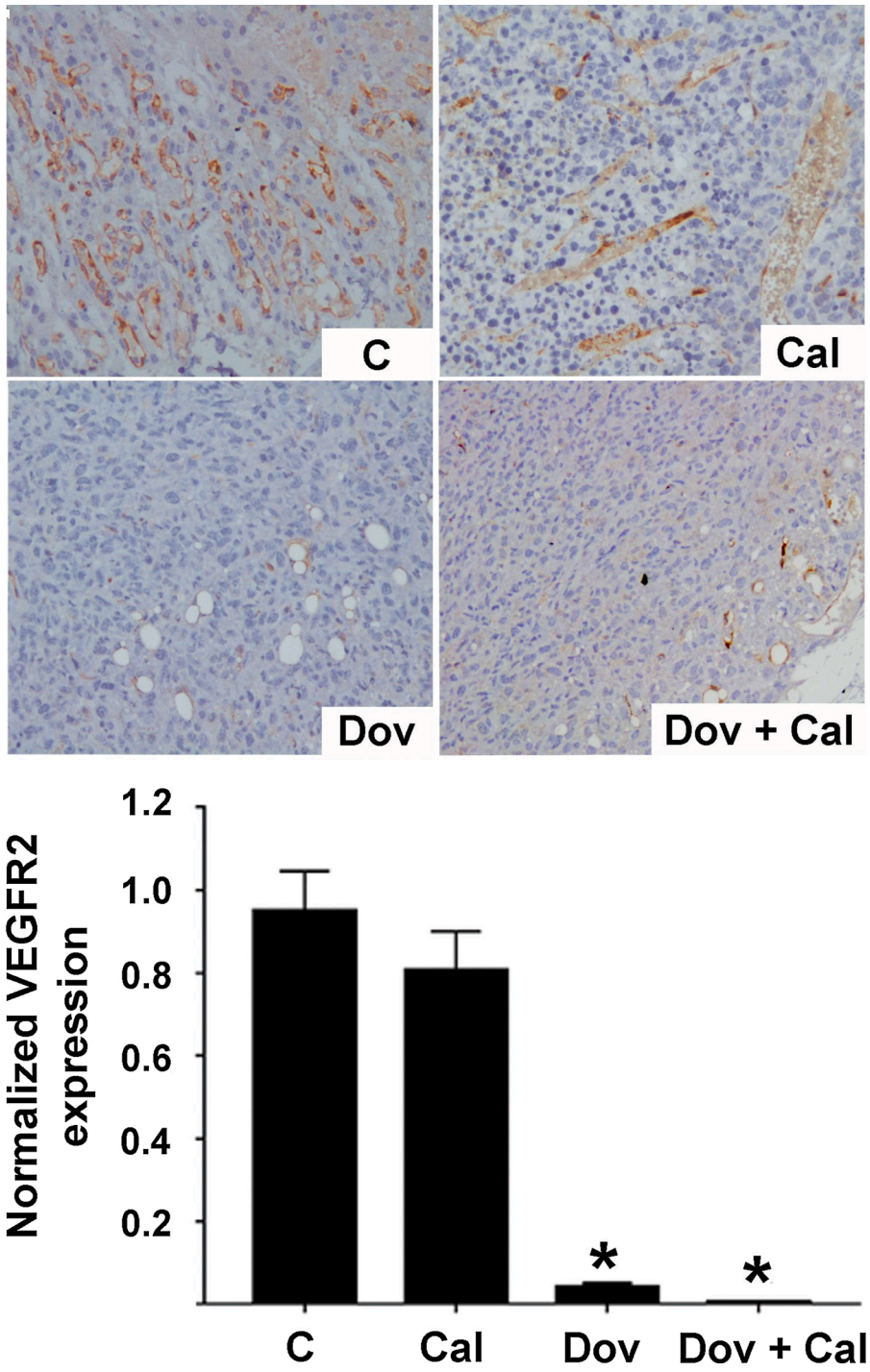


**Fig. 7.** Tumor VEGFR2 expression was inhibited by dovitinib. VEGFR2 immunohistochemistry was performed on tumor slides from control mice (C), calcitriol (Cal), dovitinib (Dov), or their combination (Dov + Cal). Slides were counterstained with hematoxylin. Representative images show VEGFR2 in brown color with 20 X magnification. VEGFR2-DAB staining was normalized against the total number of nucleus present in each picture, and is shown in the graphic as semi-quantitative analysis of VEGFR2 intensity. Results are depicted as mean normalized VEGFR2 intensity ± SEM considering 8 different photographs of each treatment, $P < 0.05$ *vs.* C and *vs.* Cal.

## Acknowledgments

We are grateful to María J Ibarra-Sánchez and José Esparza-López (Instituto Nacional de Ciencias Médicas y Nutrición Salvador Zubirán, Ciudad de México, México) for the donation of the parental cells that produced MBCDF-T cells, and to Alejandro Zentella-Dehesa (Instituto de Investigaciones Biomédicas, UNAM, México) for EA.hy926 cells donation. We thank the INCan / UNAM Biomedical Cancer Research Unit of the National Cancer Institute for the microPET / SPECT / CT studies. Some of this study was carried out as part of the activities of the "Laboratorio Nacional de Investigación y Desarrollo de Radiofármacos LANIDER-CONACyT". This study was part of the thesis work to obtain the bachelor's degree in Nutrition of NCO from Facultad de Ciencias de la Nutrición y Gastronomía de la Universidad Autónoma de Sinaloa, México.

## References

[1] F.J. Velloso, A.F. Bianco, J.O. Farias, N.E. Torres, P.Y. Ferruzo, V. Anschau, H. C. Jesus-Ferreira, T.H. Chang, M.C. Sogayar, L.F. Zerbini, R.G. Correa, The crossroads of breast cancer progression: insights into the modulation of major signaling pathways, Onco. Ther. 10 (2017) 5491–5524.

[2] C.M. Perou, T. Sorlie, M.B. Eisen, M. van de Rijn, S.S. Jeffrey, C.A. Rees, J. R. Pollack, D.T. Ross, H. Johnsen, L.A. Akslen, O. Fluge, A. Pergamenschikov, C. Williams, S.X. Zhu, P.E. Lonning, A.L. Borresen-Dale, P.O. Brown, D. Botstein, Molecular portraits of human breast tumours, Nature 406 (2000) 747–752.

[3] M.F. Santolla, M. Maggiolini, The FGF/FGFR system in breast Cancer: oncogenic features and therapeutic perspectives, Cancers 12 (2020).

[4] N.J. Chew, E.V. Nguyen, S.P. Su, K. Novy, H.C. Chan, L.K. Nguyen, J. Luu, K. J. Simpson, R.S. Lee, R.J. Daly, FGFR3 signaling and function in triple negative breast cancer, Cell Commun. Signal 18 (2020) 13.
[5] A. Pearson, E. Smyth, I.S. Babina, M.T. Herrera-Abreu, N. Tarazona, C. Peckitt, E. Kilgour, N.R. Smith, C. Geh, C. Rooney, R. Cutts, J. Campbell, J. Ning, K. Fenwick, A. Swain, G. Brown, S. Chua, A. Thomas, S.R.D. Johnston, M. Ajaz, K. Sumpter, A. Gillbanks, D. Watkins, I. Chau, S. Popat, D. Cunningham, N. C. Turner, High-level clonal FGFR amplification and response to FGFR inhibition in a translational clinical trial, Cancer Discov. 6 (2016) 838–851.
[6] N. Turner, M.B. Lambros, H.M. Horlings, A. Pearson, R. Sharpe, R. Natrajan, F. C. Geyer, M. van Kouwenhove, B. Kreike, A. Mackay, A. Ashworth, M.J. van de Vijver, J.S. Reis-Filho, Integrative molecular profiling of triple negative breast cancers identifies amplicon drivers and potential therapeutic targets, Oncogene 29 (2010) 2013–2023.
[7] T. Yamaoka, S. Kusumoto, K. Ando, M. Ohba, T. Ohmori, Receptor tyrosine kinase-targeted Cancer therapy, Int. J. Mol. Sci. 19 (2018).
[8] K. Golfmann, L. Meder, M. Koker, C. Volz, S. Borchmann, L. Tharun, F. Dietlein, F. Malchers, A. Florin, R. Buttner, N. Rosen, V. Rodrik-Outmezguine, M. Hallek, R. T. Ullrich, Synergistic anti-angiogenic treatment effects by dual FGFR1 and VEGFR1 inhibition in FGFR1-amplified breast cancer, Oncogene 37 (2018) 5682–5693.
[9] F. Andre, T. Bachelot, M. Campone, F. Dalenc, J.M. Perez-Garcia, S.A. Hurvitz, N. Turner, H. Rugo, J.W. Smith, S. Deudon, M. Shi, Y. Zhang, A. Kay, D.G. Porta, A. Yovine, J. Baselga, Targeting FGFR with dovitinib (TKI258): preclinical and clinical data in breast cancer, Clin. Cancer Res.: Off. J. Am. Assoc. Cancer Res. 19 (2013) 3693–3702.
[10] A. Issa, J.W. Gill, M.R. Heideman, O. Sahin, S. Wiemann, J.H. Dey, N.E. Hynes, Combinatorial targeting of FGF and ErbB receptors blocks growth and metastatic spread of breast cancer models, Breast Cancer Res. 15 (2013) R8.
[11] A. Musolino, M. Campone, P. Neven, N. Denduluri, C.H. Barrios, J. Cortes, K. Blackwell, H. Soliman, Z. Kahan, H. Bonnefoi, M. Squires, Y. Zhang, S. Deudon, M.M. Shi, F. Andre, Phase II, randomized, placebo-controlled study of dovitinib in combination with fulvestrant in postmenopausal patients with HR(+), HER2(-) breast cancer that had progressed during or after prior endocrine therapy, Breast Cancer Res. 19 (2017) 18.
[12] C. Corcoran, L. O'Driscoll, Receptor tyrosine kinases and drug resistance: development and characterization of in vitro models of resistance to RTK inhibitors, Methods Mol. Biol. 1233 (2015) 169–180.
[13] Y.W. Hsiao, Y.C. Lin, R.C. Hui, C.H. Yang, Fulminant acneiform eruptions after administration of dovitinib in a patient with renal cell carcinoma, J. Clin. Oncol. 29 (2011) e340–341.
[14] C. Porta, P. Giglione, W. Liguigli, C. Paglino, Dovitinib (CHIR258, TKI258): structure, development and preclinical and clinical activity, Future Oncol. 11 (2015) 39–50.
[15] T.H. Turner, M.A. Alzubi, J.C. Harrell, Identification of synergistic drug combinations using breast cancer patient-derived xenografts, Sci. Rep. 10 (2020) 1493.
[16] L. Diaz, M. Diaz-Munoz, A.C. Garcia-Gaytan, I. Mendez, Mechanistic effects of calcitriol in Cancer biology, Nutrients 7 (2015) 5020–5050.
[17] Z. Jia, Y. Zhang, A. Yan, M. Wang, Q. Han, K. Wang, J. Wang, C. Qiao, Z. Pan, C. Chen, D. Hu, X. Ding, 1,25-dihydroxyvitamin D3 signaling-induced decreases in IRX4 inhibits NANOG-mediated cancer stem-like properties and gefitinib resistance in NSCLC cells, Cell Death Dis. 11 (2020) 670.
[18] S.T. Lim, Y.W. Jeon, H. Gwak, S.Y. Kim, Y.J. Suh, Synergistic anticancer effects of ruxolitinib and calcitriol in estrogen receptorpositive, human epidermal growth factor receptor 2positive breast cancer cells, Mol. Med. Rep. 17 (2018) 5581–5588.
[19] E. Maj, B. Filip-Psurska, M. Milczarek, M. Psurski, A. Kutner, J. Wietrzyk, Vitamin D derivatives potentiate the anticancer and anti-angiogenic activity of tyrosine kinase inhibitors in combination with cytostatic drugs in an A549 non-small cell lung cancer model, Int. J. Oncol. 52 (2018) 337–366.
[20] M. Segovia-Mendoza, L. Diaz, M.E. Gonzalez-Gonzalez, I. Martinez-Reza, J. Garcia-Quiroz, H. Prado-Garcia, M.J. Ibarra-Sanchez, J. Esparza-Lopez, F. Larrea, R. Garcia-Becerra, Calcitriol and its analogues enhance the antiproliferative activity of gefitinib in breast cancer cells, J. Steroid Biochem. Mol. Biol. 148 (2015) 122–131.
[21] M. Segovia-Mendoza, L. Diaz, H. Prado-Garcia, M.J. Reginato, F. Larrea, R. Garcia-Becerra, The addition of calcitriol or its synthetic analog EB1089 to lapatinib and neratinib treatment inhibits cell growth and promotes apoptosis in breast cancer cells, Am. J. Cancer Res. 7 (2017) 1486–1500.
[22] N. Shaukat, F. Jaleel, F.A. Moosa, N.A. Qureshi, Association between vitamin d deficiency and breast Cancer, Pak. J. Med. Sci. 33 (2017) 645–649.
[23] J. Garcia-Quiroz, R. Garcia-Becerra, C. Santos-Cuevas, G.J. Ramirez-Nava, G. Morales-Guadarrama, N. Cardenas-Ochoa, M. Segovia-Mendoza, H. Prado-Garcia, D. Ordaz-Rosado, E. Avila, A. Olmos-Ortiz, S. Lopez-Cisneros, F. Larrea, L. Diaz, Synergistic antitumorigenic activity of calcitriol with curcumin or resveratrol is mediated by angiogenesis inhibition in triple negative breast Cancer xenografts, Cancers 11 (2019).
[24] J. Esparza-Lopez, H. Medina-Franco, E. Escobar-Arriaga, E. Leon-Rodriguez, A. Zentella-Dehesa, M.J. Ibarra-Sanchez, Doxorubicin induces atypical NF-kappaB activation through c-Abl kinase activity in breast cancer cells, J. Cancer Res. Clin. Oncol. 139 (2013) 1625–1635.
[25] J. Garcia-Quiroz, R. Garcia-Becerra, N. Santos-Martinez, E. Avila, F. Larrea, L. Diaz, Calcitriol stimulates gene expression of cathelicidin antimicrobial peptide in breast cancer cells with different phenotype, J. Biomed. Sci. 23 (2016) 78.
[26] V. Vichai, K. Kirtikara, Sulforhodamine B colorimetric assay for cytotoxicity screening, Nat. Protoc. 1 (2006) 1112–1116.
[27] T.C. Chou, Theoretical basis, experimental design, and computerized simulation of synergism and antagonism in drug combination studies, Pharmacol. Rev. 58 (2006) 621–681.
[28] T.C. Chou, Drug combination studies and their synergy quantification using the Chou-Talalay method, Cancer Res. 70 (2010) 440–446.
[29] T.C. Chou, The mass-action law based algorithm for cost-effective approach for cancer drug discovery and development, Am. J. Cancer Res. 1 (2011) 925–954.
[30] N. Weidner, J.P. Semple, W.R. Welch, J. Folkman, Tumor angiogenesis and metastasis–correlation in invasive breast carcinoma, N. Engl. J. Med. 324 (1991) 1–8.
[31] A.R. Crowe, W. Yue, Semi-quantitative determination of protein expression using immunohistochemistry staining and analysis: an integrated protocol, Bio Protoc 9 (2019).
[32] H. Vakifahmetoglu, M. Olsson, B. Zhivotovsky, Death through a tragedy: mitotic catastrophe, Cell Death Differ. 15 (2008) 1153–1162.
[33] R. Caruso, F. Fedele, R. Luciano, G. Branca, C. Parisi, D. Paparo, A. Parisi, Mitotic catastrophe in malignant epithelial tumors: the pathologist's viewpoint, Ultrastruct. Pathol. 35 (2011) 66–71.
[34] J. Garcia-Quiroz, M. Rivas-Suarez, R. Garcia-Becerra, D. Barrera, I. Martinez-Reza, D. Ordaz-Rosado, N. Santos-Martinez, O. Villanueva, C.L. Santos-Cuevas, E. Avila, A. Gamboa-Dominguez, A. Halhali, F. Larrea, L. Diaz, Calcitriol reduces thrombospondin-1 and increases vascular endothelial growth factor in breast cancer cells: implications for tumor angiogenesis, J. Steroid Biochem. Mol. Biol. 144 (Pt A) (2014) 215–222.
[35] L.A. Garcia, M.G. Ferrini, K.C. Norris, J.N. Artaza, 1,25(OH)(2)vitamin D(3) enhances myogenic differentiation by modulating the expression of key angiogenic growth factors and angiogenic inhibitors in C(2)C(12) skeletal muscle cells, J. Steroid Biochem. Mol. Biol. 133 (2013) 1–11.
[36] V. Trujillo, P. Marin-Luevano, I. Gonzalez-Curiel, A. Rodriguez-Carlos, M. Ramirez-Reyes, E. Layseca-Espinosa, J.A. Enciso-Moreno, L. Diaz, B. Rivas-Santiago, Calcitriol promotes proangiogenic molecules in keratinocytes in a diabetic foot ulcer model, J. Steroid Biochem. Mol. Biol. 174 (2017) 303–311.
[37] N.E. Sounni, J. Cimino, S. Blacher, I. Primac, A. Truong, G. Mazzucchelli, A. Paye, D. Calligaris, D. Debois, P. De Tullio, B. Mari, E. De Pauw, A. Noel, Blocking lipid synthesis overcomes tumor regrowth and metastasis after antiangiogenic therapy withdrawal, Cell Metab. 20 (2014) 280–294.
[38] S. Jansson, P.O. Bendahl, D.A. Grabau, A.K. Falck, M. Ferno, K. Aaltonen, L. Ryden, The three receptor tyrosine kinases c-KIT, VEGFR2 and PDGFRalpha, closely spaced at 4q12, show increased protein expression in triple-negative breast cancer, PLoS One 9 (2014), e102176.
[39] K.Y. Chen, K.L. Zhou, Y.Y. Lou, J.H. Shi, Exploring the binding interaction of calf thymus DNA with lapatinib, a tyrosine kinase inhibitor: multi-spectroscopic techniques combined with molecular docking, J. Biomol. Struct. Dyn. 37 (2019) 576–583.
[40] B.B. Hasinoff, X. Wu, J.L. Nitiss, R. Kanagasabai, J.C. Yalowich, The anticancer multi-kinase inhibitor dovitinib also targets topoisomerase I and topoisomerase II, Biochem. Pharmacol. 84 (2012) 1617–1626.
[41] Z. Skok, N. Zidar, D. Kikelj, J. Ilas, Dual inhibitors of human DNA topoisomerase II and other cancer-related targets, J. Med. Chem. 63 (2020) 884–904.
[42] S.Y. James, E. Mercer, M. Brady, L. Binderup, K.W. Colston, EB1089, a synthetic analogue of vitamin D, induces apoptosis in breast cancer cells in vivo and in vitro, Br. J. Pharmacol. 125 (1998) 953–962.
[43] M. Sun, Q. Zhang, X. Yang, S.Y. Qian, B. Guo, Vitamin d enhances the efficacy of irinotecan through miR-627-Mediated inhibition of intratumoral drug metabolism, Mol. Cancer Ther. 15 (2016) 2086–2095.
[44] W.Y. Man, J.P. Mak, R.Y. Poon, Dovitinib induces mitotic defects and activates the G2 DNA damage checkpoint, J. Cell. Mol. Med. 18 (2014) 143–155.
[45] S.A. Krueger, G.D. Wilson, E. Piasentin, M.C. Joiner, B. Marples, The effects of G2-phase enrichment and checkpoint abrogation on low-dose hyper-radiosensitivity, Int. J. Radiat. Oncol. Biol. Phys. 77 (2010) 1509–1517.
[46] T.W. Lee, T.I. Lee, Y.K. Lin, Y.H. Kao, Y.J. Chen, Calcitriol downregulates fibroblast growth factor receptor 1 through histone deacetylase activation in HL-1 atrial myocytes, J. Biomed. Sci. 25 (2018) 42.
[47] D.J. Mantell, P.E. Owens, N.J. Bundred, E.B. Mawer, A.E. Canfield, 1 alpha,25-dihydroxyvitamin D(3) inhibits angiogenesis in vitro and in vivo, Circ. Res. 87 (2000) 214–220.
[48] R. Garcia-Becerra, L. Diaz, J. Camacho, D. Barrera, D. Ordaz-Rosado, A. Morales, C. S. Ortiz, E. Avila, E. Bargallo, M. Arrecillas, A. Halhali, F. Larrea, Calcitriol inhibits Ether-a go-go potassium channel expression and cell proliferation in human breast cancer cells, Exp. Cell Res. 316 (2010) 433–442.
[49] M.G. Fakih, D.L. Trump, J.R. Muindi, J.D. Black, R.J. Bernardi, P.J. Creaven, J. Schwartz, M.G. Brattain, A. Hutson, R. French, C.S. Johnson, A phase I pharmacokinetic and pharmacodynamic study of intravenous calcitriol in combination with oral gefitinib in patients with advanced solid tumors, Clinical cancer research: an official journal of the American Association for Cancer Research 13 (2007) 1216–1223.
[50] J.R. Muindi, C.S. Johnson, D.L. Trump, R. Christy, K.L. Engler, M.G. Fakih, A phase I and pharmacokinetics study of intravenous calcitriol in combination with oral dexamethasone and gefitinib in patients with advanced solid tumors, Cancer Chemother. Pharmacol. 65 (2009) 33–40.
[51] T.M. Beer, Development of weekly high-dose calcitriol based therapy for prostate cancer, Urol. Oncol. 21 (2003) 399–405.
[52] X. Wang, A. Kay, O. Anak, E. Angevin, B. Escudier, W. Zhou, Y. Feng, M. Dugan, H. Schran, Population pharmacokinetic/pharmacodynamic modeling to assist dosing schedule selection for dovitinib, J. Clin. Pharmacol. 53 (2013) 14–20.

processes

MDPI

*Article*

# α-Mangostin Synergizes the Antineoplastic Effects of 5-Fluorouracil Allowing a Significant Dose Reduction in Breast Cancer Cells

**Galia Lara-Sotelo [1,†], Lorenza Díaz [1,†], Rocío García-Becerra [2], Euclides Avila [1], Heriberto Prado-Garcia [3], Gabriela Morales-Guadarrama [1], María de Jesús Ibarra-Sánchez [4], José Esparza-López [4], Fernando Larrea [1] and Janice García-Quiroz [1,*]**

[1] Departamento de Biología de la Reproducción, Instituto Nacional de Ciencias Médicas y Nutrición Salvador Zubirán, Ciudad de México 14080, Mexico; laragaso@gmail.com (G.L.-S.); lorenza.diazn@incmnsz.mx (L.D.); euclides.avilac@incmnsz.mx (E.A.); gabriela.mguadarrama@gmail.com (G.M.-G.); fernando.larreag@incmnsz.mx (F.L.)
[2] Departamento de Biología Molecular y Biotecnología, Instituto de Investigaciones Biomédicas, Universidad Nacional Autónoma de México, Ciudad de México 04510, Mexico; rocio.garciab@iibiomedicas.unam.mx
[3] Departamento de Enfermedades Crónico-Degenerativas, Instituto Nacional de Enfermedades Respiratorias Ismael Cosío Villegas, Ciudad de México 14080, Mexico; hpradog@yahoo.com
[4] Departamento de Bioquímica, Instituto Nacional de Ciencias Médicas y Nutrición Salvador Zubirán, Ciudad de México 14080, Mexico; maria.ibarras@incmnsz.mx (M.d.J.I.-S.); jose.esparzal@incmnsz.mx (J.E.-L.)
* Correspondence: janice.garciaq@incmnsz.mx
† These authors contributed equally as first author.

**Abstract:** Breast cancer is the most common neoplasm and the leading cause of cancer death in women worldwide. Although 5-fluorouracil is a conventional chemotherapeutic agent for breast cancer treatment, its use may result in severe side effects. Thus, there is widespread interest in lowering 5-fluorouracil drawbacks, without affecting its therapeutic efficacy by the concomitant use with natural products. Herein, we aimed at evaluating whether α-mangostin, a natural antineoplastic compound, could increase the anticancer effect of 5-fluorouracil in different breast cancer cell lines, allowing for dose reduction. Cell proliferation was evaluated by sulforhodamine-B assays, inhibitory concentrations and potency were calculated by dose-response curves, followed by analysis of their pharmacological interaction by the combination-index method and dose-reduction index. Cell cycle distribution was evaluated by flow cytometry. Each compound inhibited cell proliferation in a dose-dependent manner, the triple negative breast cancer cells being the most sensitive. When 5-fluorouracil and α-mangostin were used concomitantly, synergistic antiproliferative effect was observed. The calculated dose-reduction index suggested that this combination exhibits therapeutic potential for reducing 5-fluorouracil dosage in breast cancer. Mechanistically, the cotreatment induced cell death in a greater extent than each drug alone. Therefore, α-mangostin could be used as a potent co-adjuvant for 5-fluorouracil in breast cancer.

**Keywords:** α-mangostin; breast cancer; combination index; dose-reduction index; 5-fluorouracil



**Citation:** Lara-Sotelo, G.; Díaz, L.; García-Becerra, R.; Avila, E.; Prado-Garcia, H.; Morales-Guadarrama, G.; Ibarra-Sánchez, M.d.J.; Esparza-López, J.; Larrea, F.; García-Quiroz, J. α-Mangostin Synergizes the Antineoplastic Effects of 5-Fluorouracil Allowing a Significant Dose Reduction in Breast Cancer Cells. *Processes* **2021**, *9*, 458. https://doi.org/10.3390/pr9030458

Academic Editor: Bonglee Kim

Received: 11 February 2021
Accepted: 27 February 2021
Published: 3 March 2021



## 1. Introduction

Breast cancer is the most frequently diagnosed tumor and is the leading cause of oncological-related mortality among women worldwide [1]. Considering the molecular expression profile, breast cancer is generally classified into four different subtypes: luminal A, luminal B, human epidermal growth factor receptor 2 (HER-2) enriched and triple negative breast cancer (TNBC) [2–5]. Luminal tumors are estrogen receptor positive (ER+) [2–5], thus benefiting from hormonal therapy such as tamoxifen, fulvestrant and aromatase inhibitors [2,6], while HER-2 enriched breast tumors are mainly treated with monoclonal antibodies or tyrosine kinase inhibitors [7]. However, the TNBC are not candidates for

targeted therapy, and there are few existing therapeutic alternatives, including chemotherapeutic agents such as 5-fluorouracil (5-FU), a false nucleotide [6,8–10]. However, the well-known side effects of 5-FU limit its use [10–12]. A promising way for overcoming these drawbacks is to reduce 5-FU dose by its combination with less toxic agents with anti-neoplastic activity, such as natural compounds. In this regard, α-mangostin (AM), a xanthone obtained from the pericarp of mangosteen (*Garcinia Mangostana* Linn), exhibits a broad spectrum of anticancer effects including apoptosis, inhibition of cell proliferation and metastasis [13–15]. The antineoplastic mechanisms of AM have been widely studied in leukemia [16,17], prostate [18–20], pancreatic [21], colon [22–24], and breast cancer [25–30]. In the last, different outcomes have been reported regarding AM potency in non-hormone and hormone-dependent breast cancer [25,28,30]. On one hand, Li and colleagues showed that AM induces apoptosis with similar potency regardless of ER expression by inhibiting fatty acid synthase, which is required for cell proliferation [28]. On the other hand, Won and colleagues reported that only ER+ breast cancer cells are highly sensitive to AM [30]. Similarly, Balunas and colleagues showed that, in this phenotype, AM inhibits aromatase activity, blocking the main survival pathway of these cells [25]. Of note, the antineoplastic effect of AM has been evaluated in conjunction with chemotherapeutic agents in colon [31,32], melanoma [33], pancreatic [34], cervical [35] and gallbladder cancer cells [36], where the effect was greater than mono-treatments. The above suggests that the xanthone could act as an adjuvant agent of conventional chemotherapy. Regarding breast cancer, there are only two reports studying the effects of the ethanolic extract of mangosteen or AM combined with doxorubicin [37,38]. However, to our knowledge, there are no studies looking specifically at the combination of AM in combination with 5-FU in breast cancer cells with different phenotypes.

Therefore, in this study we investigated the effects of AM alone or combined with 5-FU on proliferation of breast cancer cell lines with a different phenotype. Additionally, we evaluated the nature of the pharmacological interaction between the chemotherapeutic agent and the natural compound, as well as the effect on cell cycle distribution in order to gain insight into the mechanisms involved.

## 2. Materials and Methods

### *2.1. Cell Culture*

In this study, we used breast cancer cell lines with different phenotypes (Table 1). The established human breast cancer cell lines SUM-229PE (Asterand, San Francisco, CA, USA), HCC-1806 and T-47D (ATCC, Manassas, VA, USA) were maintained following indications from suppliers. The M serial breast cancer ductal F primary cell culture (MBCDF) and MBCDF-D5 were kindly provided by Dr. María de Jesús Ibarra-Sánchez and Dr. José Esparza-López (Instituto Nacional de Ciencias Médicas y Nutrición Salvador Zubirán, México). All experimental procedures were performed in DMEM-F12 medium supplemented with 100 units/mL penicillin plus 100 µg/mL streptomycin and 5% charcoal-stripped-heat-inactivated fetal bovine serum (Gibco, Dublin, Ireland) under standard cell culture conditions.

**Table 1.** Breast cancer cells phenotype.

| Cell Line | Phenotype | References |
|---|---|---|
| **SUM-229PE** | TNBC | [39] |
| **MBCDF-D5** | TNBC | [40,41] |
| **HCC-1806** | TNBC | [39] |
| **MBCDF** | HER-2 enriched | [41] |
| **T-47D** | ER+ | [42] |

The SUM-229PE, MBCDF-D5 and HCC-1806 cells represent a triple negative breast cancer (TNBC) phenotype. MBCDF is human epidermal growth factor receptor 2 (HER-2) enriched, and T-47D cells are estrogen receptor positive (ER+).

### 2.2. Proliferation Studies

Cells were seeded in 96-well plates (1000 cells/well) and after 24 h they were incubated in the presence of different concentrations of 5-FU (0.01–6.0 μM, Sigma-Aldrich, St Louis, MO, USA), AM (0.1–8.0 μM, Sigma-Aldrich) or their vehicle (0.1% v/v DMSO) for 6 days. Afterward, cell proliferation was evaluated by the sulforhodamine B (SRB) colorimetric assay [43]. Briefly, cells were fixed in ice-cold trichloroacetic acid at 4 °C for 1 h and air-dried, then SRB (dissolved in acetic acid at 0.057%) was added to each well and incubated at room temperature for 1 h. The unbound dye was removed with acetic acid (1% v/v) and the protein-bound dye was extracted from viable cells with an alkaline solution (10 mM Tris base, pH 10.5) and shaking. The absorbance was read at 492 nm in a microplate reader (Synergy HT Multi Mode Microplate Reader, BioTek, VT, USA). The concentration values that caused 20% ($IC_{20}$) and 50% ($IC_{50}$) cell growth inhibition were calculated by the dose-response fitting function, using the scientific graphing software Origin 9.0 (OriginLab Corporation, Northampton, MA, USA).

### 2.3. Combination Index and Dose Reduction Index Determination

The $IC_{20}$ and $IC_{50}$ values of each compound were used to determine the pharmacological interaction between 5-FU and AM, by calculating the combination index and dose reduction index (DRI), as previously reported [44,45]. Combination index values < 1, =1 or >1 depict synergism, additive effect or antagonism, respectively, while DRI values < 1, =1 or >1 indicate not favorable dose-reduction, no dose-reduction or favorable dose reduction, respectively [44,45].

### 2.4. Cell Cycle Distribution

Cells were seeded in 6-well plates (30,000–70,000 cells per well, depending on the cell line). After 24 h, the cells were incubated with vehicle (DMSO 0.1%) or 5-FU ($IC_{20}$ or $IC_{50}$) in the presence or absence of AM ($IC_{50}$) during 72 h. After treatment, cells were collected, washed in PBS, fixed in ethanol (70% v/v) and kept at −20 °C. For cell cycle analyses, samples were washed twice with PBS pH 7.2 and incubated in a solution containing RNase (10 μg/mL), Triton X-100 (0.1% v/v) and 7-amino actinomycin D (7AAD, 1 μg/mL) in the dark at room temperature for 20 min. The DNA content was determined using the FACSCanto II flow cytometer (Becton Dickinson, CA, USA) and results were analyzed by FlowJo V10 software (Becton Dickinson, Ashland, OR, USA).

### 2.5. Statistical Analysis

Statistical differences were established by one-way ANOVA followed by appropriate post hoc tests for multiple comparisons. The comparisons between two treatments were analyzed by Student´s *t*-test using a specialized software package (SigmaStat 3.5, Jandel Scientific, CA, USA). Differences were considered statistically significant at $P < 0.05$.

## 3. Results

### 3.1. 5-FU and AM Alone Inhibited Breast Cancer Cell Proliferation in a Dose-Dependent Manner

The antiproliferative effects of 5-FU and AM were evaluated in a panel of breast cancer cell lines. Briefly, the cells were treated with different concentrations of 5-FU or AM for 6 days followed by the analysis of proliferation by the SRB assay. After analysis, both compounds significantly inhibited breast cancer cell proliferation in a dose-dependent manner (Figure 1). According to the dose-response curves, the greatest growth inhibitory effect of the compounds was observed in the TNBC cells. When using drug concentrations higher than 2 μM and 5 μM for 5-FU and AM, respectively, a complete inhibition of cell proliferation was observed.

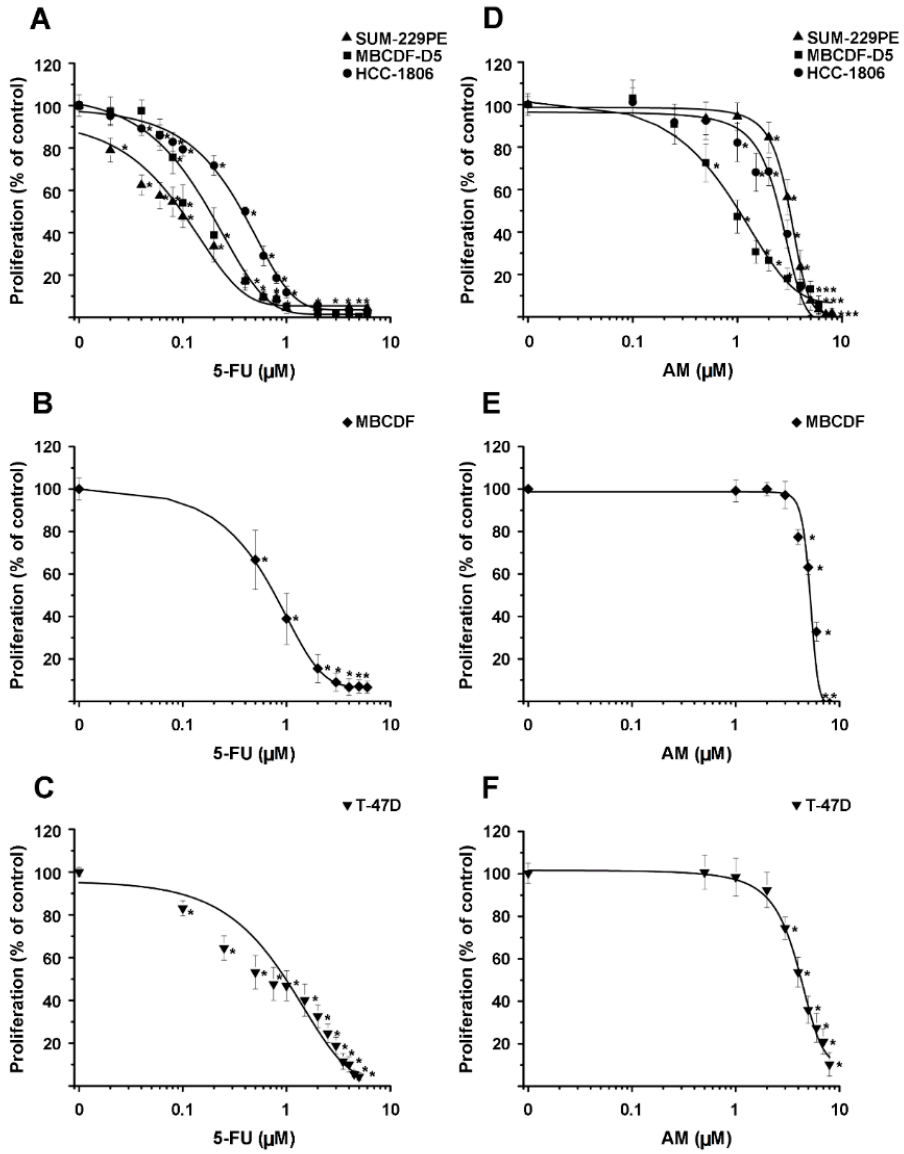


**Figure 1.** Antiproliferative effects of 5-fluorouracil and α-mangostin in a panel of breast cancer cells. The chemotherapeutic agent 5-fluorouracil (5-FU) and the xanthone α-mangostin (AM) dose-dependently inhibited cell proliferation with different potency, depending on the cell phenotype: triple negative (**A**,**D**), HER-2 enriched (**B**,**E**) and ER+ (**C**,**F**). The results are depicted as the mean ± SEM of six replicates in at least three independent experiments. Data from vehicle-treated cells were normalized to 100%. * $P < 0.001$ vs. control.

Based on the dose-response curves, the $IC_{20}$ and $IC_{50}$ values were calculated for both drugs (Table 2). These concentrations were taken into account for the combined treatments. Considering $IC_{50}$ values, the following scale of sensitivity was obtained among the cells studied, for 5-FU: SUM-229PE > MBCDF-D5 > HCC-1806 > T-47D > MBCDF, and for AM: MBCDF-D5 > HCC-1806 > SUM-229PE > T-47D > MBCDF. According to these results, TNBC cells were the most sensitive for 5-FU and AM, while the HER-2 enriched were the less sensitive cells. The mean values of $IC_{20}$ and $IC_{50}$ of 5-FU in TNBC cells are 0.105 ± 0.11 μM and 0.213 ± 0.192 μM, respectively; while mean values for AM are 1.47 ± 1.16 μM and 2.16 ± 1.236 μM, respectively.

**Table 2.** $IC_{20}$ and $IC_{50}$ values of 5-fluorouracil and α-mangostin.

| Cell line | 5-FU (μM) | | AM (μM) | |
|---|---|---|---|---|
| | $IC_{20}$ | $IC_{50}$ | $IC_{20}$ | $IC_{50}$ |
| **SUM-229PE** | 0.016 ± 0.01 | 0.061 ± 0.01 | 2.39 ± 0.12 | 3.13 ± 0.09 |
| **MBCDF-D5** | 0.07 ± 0.01 | 0.15 ± 0.01 | 0.16 ± 0.11 | 0.77 ± 0.22 |
| **HCC-1806** | 0.23 ± 0.02 | 0.43 ± 0.02 | 1.87 ± 0.20 | 2.59 ± 0.17 |
| **MBCDF** | 0.36 ± 0.03 | 0.70 ± 0.03 | 4.67 ± 0.24 | 5.23 ± 0.19 |
| **T-47D** | 0.18 ± 0.07 | 0.54 ± 0.13 | 2.70 ± 0.11 | 4.36 ± 0.17 |

Inhibitory concentrations at 20% ($IC_{20}$) and 50% ($IC_{50}$) were calculated based on the dose-response curves of 5-fluorouracil (5-FU) and α-mangostin (AM). Results are depicted as the mean ± SEM.

### *3.2. The Antiproliferative Activity of 5-FU Was Significanlty Enhanced by AM in Cultured Breast Cancer Cells*

To evaluate the antiproliferative effects of 5-FU combined with AM, the following combination schemes (5-FU/AM) were considered: $IC_{20}/IC_{20}$, $IC_{20}/IC_{50}$, $IC_{50}/IC_{20}$ and $IC_{50}/IC_{50}$. As shown in Figure 2, the combination of both drugs significantly reduced breast cancer cells proliferation in a greater extent than each compound alone. The $IC_{50}/IC_{50}$ combination inhibited cell growth up to ∼90% in SUM-229PE, 86% in HCC1806 and 80% in MBCDF-D5, MBCDF and T-47D (Figure 2). Although in the cell lines MBCDF-D5 (Figure 2B) and HCC-1806 cells (Figure 2C) all the combination schemes resulted in a similar growth inhibitory potency, in SUM-229PE, MBCDF and T-47D (Figure 2A, D and E, respectively), the scheme using higher doses of both compounds ($IC_{50}/IC_{50}$) was more potent as compared to the $IC_{20}/IC_{20}$ combination.

### *3.3. The Combination of 5-FU with AM Acted Synergistically to Inhibit Cell Growth in Most Cell Lines Tested, Allowing for a Significant 5-FU Dose-Reduction While Preserving Its Potency*

To discern the pharmacological interaction of 5-FU with AM, the combination index and DRI were calculated taking into account the combination schemes. In SUM-229PE, MBCDF-D5 and T-47D cells, all the co-treatment schemes showed combination index values < 1, reflecting synergism (Figure 3). A similar result was obtained in HCC-1806 cells with $IC_{20}/IC_{20}$ (5-FU/AM), while an additive effect was observed with $IC_{50}/IC_{20}$ and $IC_{50}/IC_{50}$. Regarding MBCDF cells, the drug combinations, although inhibitory, did not reflected synergistic effect (Figure 3). Of note, combination index values closer to zero reflect greater synergism than the values closer to one, while fraction affected values closer to one indicate greater inhibitory growth effect than the values closer to zero. In a general way and comparing the combination schemes per cell line, the greatest synergistic effect was observed with $IC_{20}/IC_{20}$ (Figure 3, circles) while the greatest fraction affected was observed with $IC_{50}/IC_{50}$ (Figure 3, diamonds).

With the aim to determine how many folds the dose of each drug in combination may be reduced, we calculated the DRI values on the combination schemes showing synergistic and additive antiproliferative effects (Table 3). Remarkably, in all cell lines tested, incubations in the presence of AM allowed to reduce 5-FU doses while maintaining the same efficacy as the drug alone. The cell lines in which 5-FU and AM doses could be significantly reduced were those where the compounds alone showed the highest antiproliferative effect (Table 2), as is the case of SUM-229PE and MBCDF-D5 (Table 3), where 5-FU and AM doses could be reduced up to 7- and 15-folds, respectively.

### *3.4. Breast Cancer Cell Death Was Promoted by AM, 5-FU and Their Combination*

To get mechanistic insights, we studied the cell cycle distribution effects of both compounds alone and combined in one cell line *per* breast tumor phenotype. Representative histograms depicting the cell cycle distribution of SUM-229PE cells treated with 5-FU, AM or their combinations are shown in Figure 4A. As seen, only 5-FU significantly induced cell death (Sub G1) in SUM-229PE cells, an effect that was further enhanced by its combination with AM (Figure 4A,B). Such effect was accompanied with a reduction in the G1 population

(Figure 4B). The opposite was observed in MBCDF and T-47D cells, where AM per se significantly promoted cell death, while 5-FU did not (Figure 4C,D). In these two cell lines, the drug combination did not further modify the effect of AM.

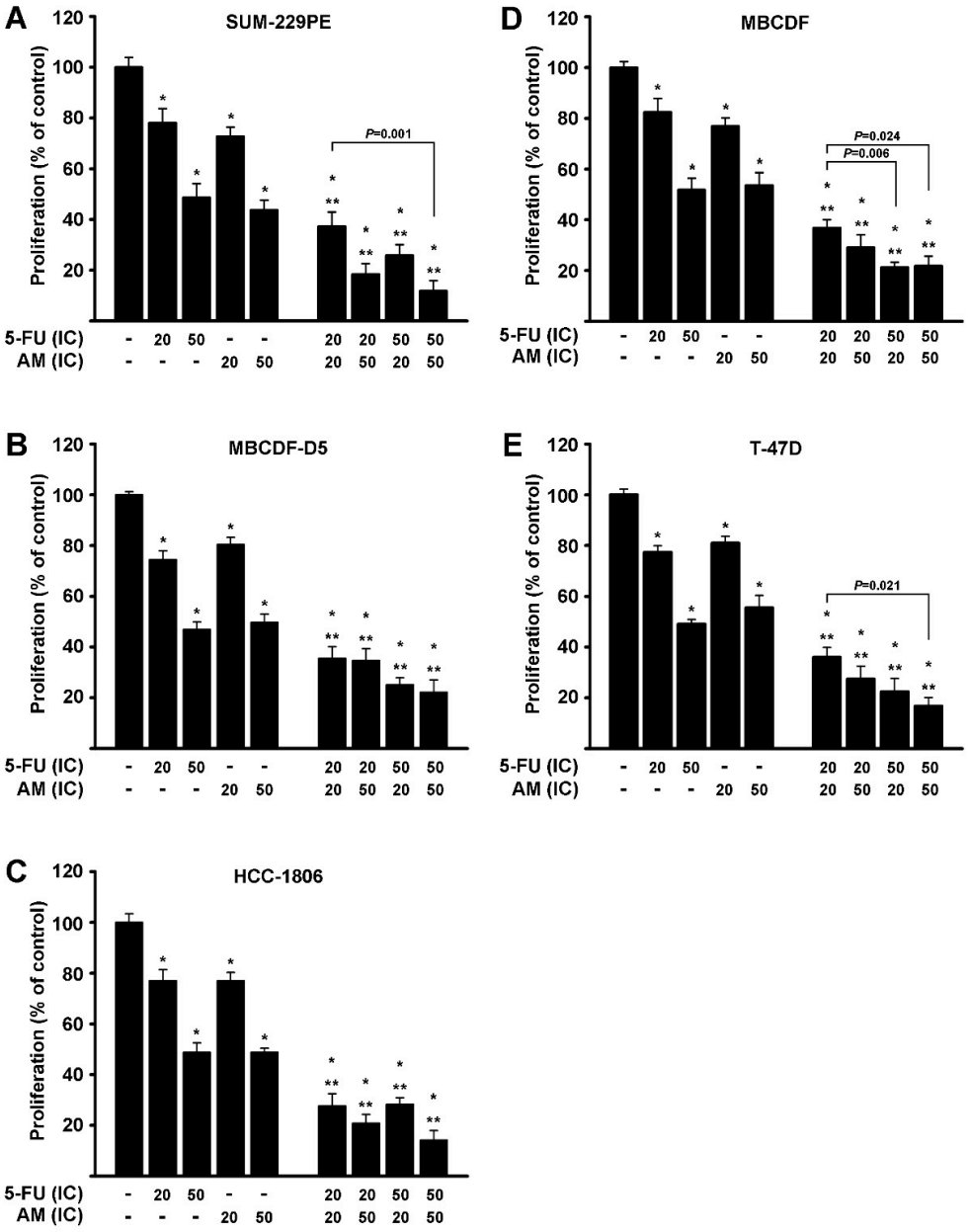


**Figure 2.** The combined treatment inhibited cell proliferation in a greater extent than each compound alone. The antiproliferative effect of the respective inhibitory concentrations (IC) at 20% and 50% of 5-fluorouracil (5-FU) and α-mangostin (AM) per se or in combination was evaluated in a panel of breast cancer cell lines. Results are depicted as the mean ± SEM of six replicates in at least three independent experiments. Data from vehicle-treated cells were normalized to 100%. * $P < 0.001$ vs. control, ** $P < 0.001$ vs. monotreatment (5-FU or AM alone).

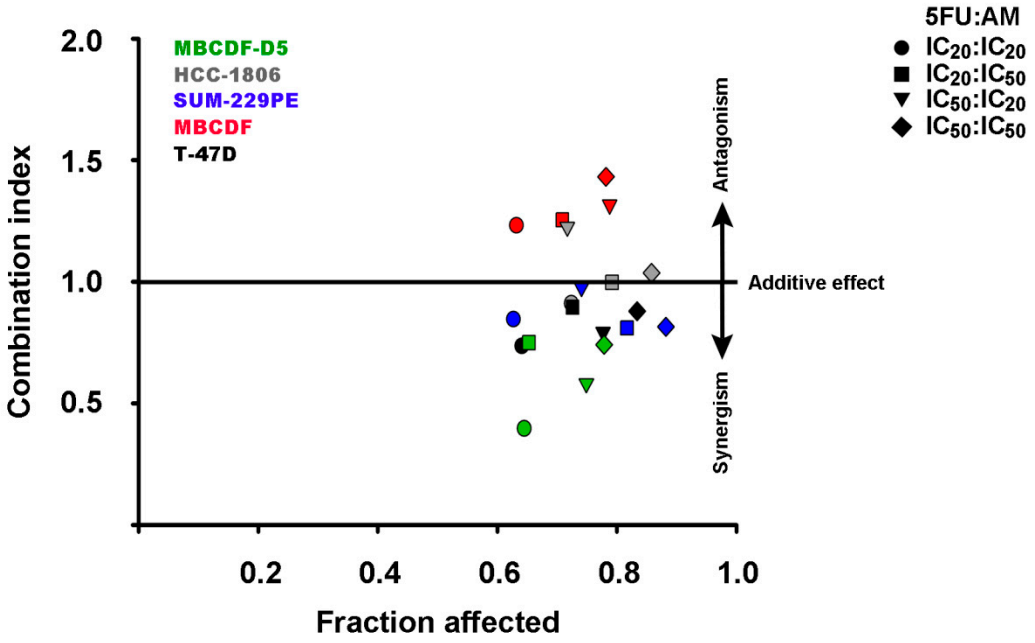


**Figure 3.** Combination index versus fraction affected in cells exposed to different combinations of 5-fluorouracil with α-mangostin. The combination index and the fraction affected were determined by co-incubating the cells in the presence of the inhibitory concentrations at 20% ($IC_{20}$) and/or 50% ($IC_{50}$) of 5-fluorouracil (5-FU) and α-mangostin (AM) in the breast cancer cell lines MBCDF-D5, HCC-1806, SUM-229PE, MBCDF and T-47D. The combination schemes evaluated (5-FU/AM) were $IC_{20}/IC_{20}$, $IC_{20}/IC_{50}$, $IC_{50}/IC_{20}$ and $IC_{50}/IC_{50}$. The symbols under, on or over the horizontal line depict synergism, addition or antagonism, respectively. Fraction affected values closer to 1 indicate greater inhibitory growth effect than values closer to 0. N ≥ 3 independent experiments with six replicates each.

**Table 3.** Dose reduction index of 5-fluorouracil and α-mangostin.

| Cell Line | Combination Schemes | DRI (Folds) | |
|---|---|---|---|
| | 5FU/AM | 5-FU | AM |
| MBCDF-D5 | $IC_{20}/IC_{20}$ | 3.32 | **10.38** |
| | $IC_{20}/IC_{50}$ | **3.40** | 2.20 |
| | $IC_{50}/IC_{20}$ | 1.94 | **15.45** |
| | $IC_{50}/IC_{50}$ | **2.11** | 1.24 |
| SUM-229PE | $IC_{20}/IC_{20}$ | **6.43** | 1.45 |
| | $IC_{20}/IC_{50}$ | **6.44** | 1.34 |
| | $IC_{50}/IC_{20}$ | **1.87** | 1.61 |
| | $IC_{50}/IC_{50}$ | **7.25** | 1.48 |
| T-47D | $IC_{20}/IC_{20}$ | **4.73** | 1.91 |
| | $IC_{20}/IC_{50}$ | **6.48** | 1.35 |
| | $IC_{50}/IC_{20}$ | **2.68** | 2.39 |
| | $IC_{50}/IC_{50}$ | **3.58** | 1.67 |
| HCC-1806 | $IC_{20}/IC_{20}$ | **3.00** | 1.73 |
| | $IC_{20}/IC_{50}$ | **3.76** | 1.37 |
| | $IC_{50}/IC_{50}$ | **2.63** | 1.52 |

The dose reduction index (DRI) calculation was based on the synergic or additive effect between 5-fluorouracil (5-FU) and α-mangostin (AM) using their inhibitory concentrations at 20% ($IC_{20}$) and 50% ($IC_{50}$). DRI values higher than one indicate a favorable dose reduction. DRI values highlighted in bold indicate the higher DRI value for each combination scheme.

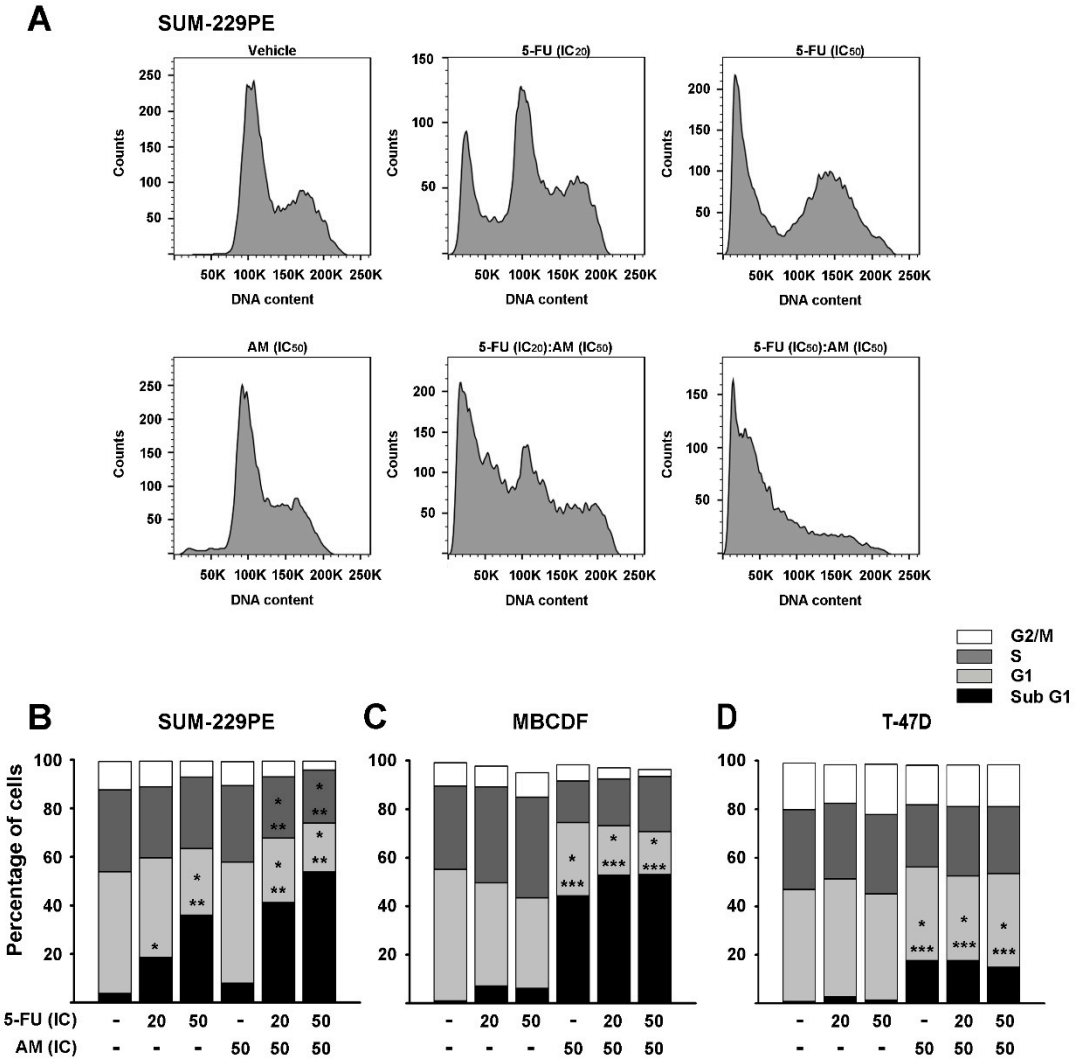


**Figure 4.** Effects of 5-fluorouracil, α-mangostin or their combination on the cell cycle distribution in neoplastic cells. The effects of the inhibitory concentrations at 20% ($IC_{20}$) and 50% ($IC_{50}$) of 5-fluorouracil (5-FU) and $IC_{50}$ of α-mangostin (AM) and/or 5-FU were evaluated in the cell cycle distribution of SUM-229PE (**A**,**B**), MBCDF (**C**), and T-47D (**D**) breast cancer cells. Results are depicted as the percentage of cells in each phase of the cell cycle from at least three independent experiments. * $P < 0.05$ vs. control, ** $P < 0.05$ vs. AM, *** $P < 0.05$ vs. 5-FU.

## 4. Discussion

One of the motivations of this study was to determine AM antiproliferative activity and potency in breast cancer cells with different phenotypes, given the discrepancy prevailing in the literature in this topic [25,28,30]. In addition, as chemotherapy is the main option for TNBC, we thought of importance to study if AM allowed for 5-FU dose reduction while maintaining a similar antiproliferative activity. Our results showed that AM consistently and significantly reduced proliferation in all breast cancer phenotypes, with TNBC being the most sensitive ($IC_{50}$ = 2.16 ± 1.24 μM), followed by ER+ cells ($IC_{50}$ = 4.36 ± 0.17 μM) and HER-2 enriched cells ($IC_{50}$ = 5.23 ± 0.19). These results support the idea that AM induces its antineoplastic effects regardless of ER expression. As expected, 5-FU also reduced proliferation in all breast cancer cells and the TNBC was the most sensitive. These results were consistent with other studies showing increased sensitivity to 5-FU in ER negative tumors [46,47]. A possible explanation for the increased effects of both compounds in TNBC cells may reside in their increased sensitivity to oxidative stress due to defects in the DNA damage response pathways, which can lead to mitotic catastrophe [48,49]. Regarding

this, both AM [18,32] and 5-FU [11] induce reactive oxygen species (ROS) accumulation, promoting oxidative stress and cell death.

Our results regarding the combination index strongly suggest that AM may function as an excellent adjuvant of 5-FU, given the synergic pharmacological activity observed in several breast cancer cell lines. The observed synergism may be the result of mutually exclusive antineoplastic mechanisms of both compounds [44]. While 5-FU targets cancer cells by blocking the synthesis of nucleic acids [8–10], AM exerts its antineoplastic effects by inhibiting cyclin-dependent kinases (CDK) involved in cell cycle progression [50,51], the expression and activity of fatty acid synthase [28], aromatase activity [25] and (4) the expression of ER in breast cancer [30].

Regarding the mechanisms of action of AM involved in the synergic effect observed herein, further studies are warranted; however, previous studies in other neoplasms such as leukemia and colon cancer have shown that AM induced apoptosis via the caspase-3 pathway or through the rupture of the mitochondrial membrane and the subsequent release of endonuclease-G [17,24].

One major aim for achieving synergy in drug combination studies is the dose-reduction of the cytotoxic agent while preserving the therapeutic effect [44]. Our results showed favorable dose reduction (DRI > 1), supporting the possibility to scale down the dose of 5-FU in breast cancer patients by combining it with AM. The combination of 5-FU and AM has been previously tested in colon cancer cells resistant to the chemotherapeutic agent, showing the sensitization of these cells to 5-FU–dependent apoptosis [32]. Similarly, other studies have shown an enhanced effect of chemotherapeutic agents when combined with AM in different tumors [31–36]. Particularly in breast cancer MCF-7 cells, the combination of doxorubicin with mangosteen derivatives has resulted in improved antineoplastic effects [38], including the reduction of stemness and the induction of cell death [37]. The above, together with our results, strongly support the concept that AM could act as an adjuvant of conventional chemotherapy. The current chemotherapeutic regimen to treat breast cancer includes 5-FU, commonly combined with other cytotoxic agents such as doxorubicin, epirubicin, cyclophosphamide and/or methotrexate [6]. The advantage to combine 5-FU with AM instead of these drugs would be the induction of synergism without increasing systemic toxicity. In line with this, in vivo studies have shown AM cardioprotective [52] and neuroprotective [53] properties, suggesting that the xanthone could counteract the adverse effects of 5-FU.

To our knowledge, this is the first report showing the combined effects of 5-FU with AM in breast cancer cells with different phenotypes. Interestingly, the synergic interaction between 5-FU and AM was not observed in MBCDF cells [54], which can satisfactorily be explained by the high cellular heterogeneity prevailing in this cell line [41,55].

Several studies have been carried out in order to elucidate AM anticancer mechanism. In TNBC, AM has been shown to promote apoptosis, cell cycle arrest [27], and spheroids-cell adhesion reduction [56]. Similarly, in ER+ cells, the xanthone induces apoptosis [26] and reduces metastasis [57]. The present study demonstrates that the combination of AM with 5-FU promoted greater accumulation of cells in Sub G1 phase, suggesting that death is part of the mechanisms involved. A limitation of this investigation is the lack of in vivo experiments, which remain the subject of future studies.

In summary, herein we describe the effects of combining 5-FU with AM on cell growth in various established and primary breast cancer cell lines. We determined the pharmacological interaction of the combined effect and the possibility to scale down the doses of both compounds, contributing to new knowledge in the field. Overall, our results provide scientific basis to test 5-FU with AM as a therapeutic option for patients whose only alternative is chemotherapy, specifically those with TNBC tumors.

## 5. Conclusions

The xanthone AM inhibited breast cancer cells proliferation independently of their phenotype, with greater potency in TNBC cells. AM allowed to significantly reduce 5-FU

dose while maintaining its efficacy to inhibit cell growth. Given the synergic interaction between 5-FU and AM, the use of this natural compound as co-adjuvant might result in less chemotherapy-derived adverse effects. We believe that our results may help to conceptualize further preclinical and clinical studies to provide TNBC-patients with an affordable and effective new therapeutic approach with reduced undesirable side effects.

**Author Contributions:** G.L.-S. performed the experiments and analysis of data. L.D. and J.G.-Q. performed analysis/interpretation of data and wrote the manuscript. R.G.-B. designed the figures. L.D., F.L., R.G.-B. and E.A. made substantive intellectual contributions to the study and helped to draft the manuscript. H.P.-G. carried out experimental flow cytometry analysis and interpretation of data, reviewed and edited the manuscript. M.d.J.I.-S. and J.E.-L. contributed with critical revision of the manuscript. G.M.-G. performed reviewed and edited the manuscript. J.G.-Q. conceived, designed and coordinated the study. All authors have read and agreed to the published version of the manuscript.

**Funding:** This study was supported by funds from Departamento de Biología de la Reproducción Carlos Gual Castro, Instituto Nacional de Ciencias Médicas y Nutrición Salvador Zubirán; by a grant from Instituto Científico Pfizer to RGB (INCMN/110/08/PI/86/15) and by a grant from the Consejo Nacional de Ciencia y Tecnología de México (CONACyT) to LD (A1-S-10749). The funders had no role in study design, analysis and interpretation of the data, writing of the manuscript or the decision to submit the article for publication.

**Institutional Review Board Statement:** This is an in vitro study approved by the Institutional Research Committee and the Research Ethics Committee (protocol number BRE-2606-18-21-1) of the Instituto Nacional de Ciencias Médicas y Nutrición Salvador Zubirán. This article does not contain any studies with animal or human participants.

**Informed Consent Statement:** Not applicable.

**Data Availability Statement:** Not applicable. All data generated or analyzed during this study are included in this article.

**Acknowledgments:** This study was part of the thesis work to obtain the M.Sc. degree of GL-S from El Programa de Ciencias Biológicas, Universidad Nacional Autónoma de México (UNAM) under a fellowship program from CONACyT. The graphical abstract was created with BioRender.com (accessed on 1 December 2020).

**Conflicts of Interest:** The authors declare no conflict of interest.

## References

1. Torre, L.A.; Islami, F.; Siegel, R.L.; Ward, E.M.; Jemal, A. Global Cancer in Women: Burden and Trends. *Cancer Epidemiol. Biomark. Prev.* **2017**, *26*, 444–457. [CrossRef]
2. Fragomeni, S.M.; Sciallis, A.; Jeruss, J.S. Molecular Subtypes and Local-Regional Control of Breast Cancer. *Surg. Oncol. Clin. N. Am.* **2018**, *27*, 95–120. [CrossRef]
3. Søkilde, R.; Persson, H.; Ehinger, A.; Pirona, A.C.; Fernö, M.; Hegardt, C.; Larsson, C.; Loman, N.; Malmberg, M.; Rydén, L.; et al. Refinement of breast cancer molecular classification by miRNA expression profiles. *BMC Genom.* **2019**, *20*, 1–12. [CrossRef]
4. Sorlie, T.; Perou, C.M.; Tibshirani, R.; Aas, T.; Geisler, S.; Johnsen, H.; Hastie, T.; Eisen, M.B.; van de Rijn, M.; Jeffrey, S.S.; et al. Gene expression patterns of breast carcinomas distinguish tumor subclasses with clinical implications. *Proc. Natl. Acad. Sci. USA* **2001**, *98*, 10869–10874. [CrossRef]
5. Zepeda-Castilla, E.J.; Recinos-Money, E.; Cuellar-Hubbe, M.; Robles-Vidal, C.D.; Maafs-Molina, E. Molecular classification of breast cancer. *Cir. Cir.* **2008**, *76*, 87–93.
6. Chávarri-Guerra, Y.; Villarreal-Garza, C.; Liedke, P.E.R.; Knaul, F.; Mohar, A.; Finkelstein, D.M.; Goss, P.E. Breast cancer in Mexico: A growing challenge to health and the health system. *Lancet Oncol.* **2012**, *13*, e335–e343. [CrossRef]
7. Wang, J.; Xu, B. Targeted therapeutic options and future perspectives for HER2-positive breast cancer. *Signal Transduct. Target. Ther.* **2019**, *4*, 1–22. [CrossRef]
8. Cameron, D.A.; Gabra, H.; Leonard, R.C. Continuous 5-fluorouracil in the treatment of breast cancer. *Br. J. Cancer* **1994**, *70*, 120–124. [CrossRef]
9. Parker, W.B. Enzymology of Purine and Pyrimidine Antimetabolites Used in the Treatment of Cancer. *Chem. Rev.* **2009**, *109*, 2880–2893. [CrossRef]
10. Wigmore, P.M.; Mustafa, S.; El-Beltagy, M.; Lyons, L.; Umka, J.; Bennett, G. Effects of 5-FU. *Adv. Exp. Med. Biol.* **2010**, *678*, 157–164. [CrossRef]

11. Focaccetti, C.; Bruno, A.; Magnani, E.; Bartolini, D.; Principi, E.; Dallaglio, K.; Bucci, E.O.; Finzi, G.; Sessa, F.; Noonan, D.M.; et al. Effects of 5-Fluorouracil on Morphology, Cell Cycle, Proliferation, Apoptosis, Autophagy and ROS Production in Endothelial Cells and Cardiomyocytes. *PLoS ONE* **2015**, *10*, e0115686. [CrossRef]
12. Lazar, A.; Jetter, A. Pharmakogenetik in der Onkologie: 5-Fluorouracil und die Dihydropyrimidin-Dehydrogenase. *DMW Dtsch. Med. Wochenschr.* **2008**, *133*, 1501–1504. [CrossRef]
13. Akao, Y.; Nakagawa, Y.; Nozawa, Y. Anti-Cancer Effects of Xanthones from Pericarps of Mangosteen. *Int. J. Mol. Sci.* **2008**, *9*, 355–370. [CrossRef]
14. Ibrahim, M.Y.; Hashim, N.M.; Mariod, A.A.; Mohan, S.; Abdulla, M.A.; Abdelwahab, S.I.; Arbab, I.A. α-Mangostin from *Garcinia mangostana* Linn: An updated review of its pharmacological properties. *Arab. J. Chem.* **2016**, *9*, 317–329. [CrossRef]
15. Shan, T.; Ma, Q.; Guo, K.; Liu, J.; Li, W.; Wang, F.; Wu, E. Xanthones from Mangosteen Extracts as Natural Chemopreventive Agents: Potential Anticancer Drugs. *Curr. Mol. Med.* **2011**, *11*, 666–677. [CrossRef]
16. Matsumoto, K.; Akao, Y.; Kobayashi, E.; Ohguchi, K.; Ito, T.; Tanaka, T.; Iinuma, A.M.; Nozawa, Y. Induction of Apoptosis by Xanthones from Mangosteen in Human Leukemia Cell Lines. *J. Nat. Prod.* **2003**, *66*, 1124–1127. [CrossRef]
17. Matsumoto, K.; Akao, Y.; Yi, H.; Ohguchi, K.; Ito, T.; Tanaka, T.; Kobayashi, E.; Iinuma, M.; Nozawa, Y. Preferential target is mitochondria in α-mangostin-induced apoptosis in human leukemia HL60 cells. *Bioorg. Med. Chem.* **2004**, *12*, 5799–5806. [CrossRef]
18. Johnson, J.J.; Petiwala, S.M.; Syed, D.N.; Rasmussen, J.T.; Adhami, V.M.; Siddiqui, I.A.; Kohl, A.M.; Mukhtar, H. alpha-Mangostin, a xanthone from mangosteen fruit, promotes cell cycle arrest in prostate cancer and decreases xenograft tumor growth. *Carcinogenesis* **2011**, *33*, 413–419. [CrossRef]
19. Hung, S.-H.; Shen, K.-H.; Wu, C.-H.; Liu, C.-L.; Shih, Y.-W. α-Mangostin Suppresses PC-3 Human Prostate Carcinoma Cell Metastasis by Inhibiting Matrix Metalloproteinase-2/9 and Urokinase-Plasminogen Expression through the JNK Signaling Pathway. *J. Agric. Food Chem.* **2009**, *57*, 1291–1298. [CrossRef]
20. Li, G.; Petiwala, S.M.; Nonn, L.; Johnson, J.J. Inhibition of CHOP accentuates the apoptotic effect of α-mangostin from the mangosteen fruit (*Garcinia mangostana*) in 22Rv1 prostate cancer cells. *Biochem. Biophys. Res. Commun.* **2014**, *453*, 75–80. [CrossRef]
21. Ma, Y.; Yu, W.; Shrivastava, A.; Srivastava, R.K.; Shankar, S. Inhibition of pancreatic cancer stem cell characteristics by α-Mangostin: Molecular mechanisms involving Sonic hedgehog and Nanog. *J. Cell. Mol. Med.* **2019**, *23*, 2719–2730. [CrossRef]
22. Matsumoto, K.; Akao, Y.; Ohguchi, K.; Ito, T.; Tanaka, T.; Iinuma, M.; Nozawa, Y. Xanthones induce cell-cycle arrest and apoptosis in human colon cancer DLD-1 cells. *Bioorg. Med. Chem.* **2005**, *13*, 6064–6069. [CrossRef]
23. Nabandith, V.; Suzui, M.; Morioka, T.; Kaneshiro, T.; Kinjo, T.; Matsumoto, K.; Akao, Y.; Iinuma, M.; Yoshimi, N. Inhibitory effects of crude alpha-mangostin, a xanthone derivative, on two different categories of colon preneoplastic lesions induced by 1, 2-dimethylhydrazine in the rat. *Asian Pac. J. Cancer Prev.* **2004**, *5*, 433–438.
24. Nakagawa, Y.; Iinuma, M.; Naoe, T.; Nozawa, Y.; Akao, Y. Characterized mechanism of α-mangostin-induced cell death: Caspase-independent apoptosis with release of endonuclease-G from mitochondria and increased miR-143 expression in human colorectal cancer DLD-1 cells. *Bioorg. Med. Chem.* **2007**, *15*, 5620–5628. [CrossRef]
25. Balunas, M.J.; Su, B.; Brueggemeier, R.W.; Kinghorn, A.D. Xanthones from the Botanical Dietary Supplement Mangosteen (*Garcinia mangostana*) with Aromatase Inhibitory Activity. *J. Nat. Prod.* **2008**, *71*, 1161–1166. [CrossRef]
26. Kritsanawong, S.; Innajak, S.; Imoto, M.; Watanapokasin, R. Antiproliferative and apoptosis induction of α-mangostin in T47D breast cancer cells. *Int. J. Oncol.* **2016**, *48*, 2155–2165. [CrossRef]
27. Kurose, H.; Shibata, M.-A.; Iinuma, M.; Otsuki, Y. Alterations in Cell Cycle and Induction of Apoptotic Cell Death in Breast Cancer Cells Treated withα-Mangostin Extracted from Mangosteen Pericarp. *J. Biomed. Biotechnol.* **2012**, *2012*, 1–9. [CrossRef]
28. Li, P.; Tian, W.; Ma, X. Alpha-mangostin inhibits intracellular fatty acid synthase and induces apoptosis in breast cancer cells. *Mol. Cancer* **2014**, *13*, 138. [CrossRef]
29. Moongkarndi, P.; Kosem, N.; Kaslungka, S.; Luanratana, O.; Pongpan, N.; Neungton, N. Antiproliferation, antioxidation and induction of apoptosis by *Garcinia mangostana* (mangosteen) on SKBR3 human breast cancer cell line. *J. Ethnopharmacol.* **2004**, *90*, 161–166. [CrossRef]
30. Won, Y.-S.; Lee, J.-H.; Kwon, S.-J.; Kim, J.-Y.; Park, K.-H.; Lee, M.-K.; Seo, K.-I. α-Mangostin-induced apoptosis is mediated by estrogen receptor α in human breast cancer cells. *Food Chem. Toxicol.* **2014**, *66*, 158–165. [CrossRef]
31. Aisha, A.F.A.; Abu-Salah, K.M.; Ismail, Z.; Majid, A.M.S.A. α-Mangostin Enhances Betulinic Acid Cytotoxicity and Inhibits Cisplatin Cytotoxicity on HCT 116 Colorectal Carcinoma Cells. *Molecules* **2012**, *17*, 2939–2954. [CrossRef]
32. Lee, J.; Kang, J.-S.; Choi, B.-Y.; Keum, Y.-S. Sensitization of 5-Fluorouracil-Resistant SNUC5 Colon Cancer Cells to Apoptosis by α-Mangostin. *Biomol. Ther.* **2016**, *24*, 604–609. [CrossRef]
33. Xia, Y.; Li, Y.; Westover, K.D.; Sun, J.; Chen, H.; Zhang, J.; Fisher, D.E. Inhibition of Cell Proliferation in an NRAS Mutant Melanoma Cell Line by Combining Sorafenib and α-Mangostin. *PLoS ONE* **2016**, *11*, e0155217. [CrossRef]
34. Kim, M.; Chin, Y.-W.; Lee, E.J. α, γ-Mangostins Induce Autophagy and Show Synergistic Effect with Gemcitabine in Pancreatic Cancer Cell Lines. *Biomol. Ther.* **2017**, *25*, 609–617. [CrossRef]
35. Pérez-Rojas, J.M.; González-Macías, R.; González-Cortes, J.; Jurado, R.; Pedraza-Chaverri, J.; García-López, P. Synergic Effect of α-Mangostin on the Cytotoxicity of Cisplatin in a Cervical Cancer Model. *Oxidative Med. Cell. Longev.* **2016**, *2016*, 1–13. [CrossRef]

36. Shi, Y.; Fan, Y.; Hu, Y.; Jing, J.; Wang, C.; Wu, Y.; Geng, Q.; Dong, X.; Li, E.; Dong, D. α-Mangostin suppresses the de novo lipogenesis and enhances the chemotherapeutic response to gemcitabine in gallbladder carcinoma cells via targeting the AMPK/SREBP1 cascades. *J. Cell. Mol. Med.* **2020**, *24*, 760–771. [CrossRef]
37. Bissoli, I.; Muscari, C. Doxorubicin and α-Mangostin oppositely affect luminal breast cancer cell stemness evaluated by a new retinaldehyde-dependent ALDH assay in MCF-7 tumor spheroids. *Biomed. Pharmacother.* **2020**, *124*, 109927. [CrossRef]
38. Laksmiani, N.P.L. Ethanolic extract of mangosteen (*Garcinia mangostana*) pericarp as sensitivity enhancer of doxorubicin on MCF-7 cells by inhibiting P-glycoprotein. *Nusant. Biosci.* **2019**, *11*, 49–55. [CrossRef]
39. García-Quiroz, J.; García-Becerra, R.; Santos-Martínez, N.; Avila, E.; Larrea, F.; Díaz, L. Calcitriol stimulates gene expression of cathelicidin antimicrobial peptide in breast cancer cells with different phenotype. *J. Biomed. Sci.* **2016**, *23*, 1–7. [CrossRef]
40. García-Quiroz, J.; García-Becerra, R.; Lara-Sotelo, G.; Avila, E.; López, S.; Santos-Martínez, N.; Halhali, A.; Ordaz-Rosado, D.; Barrera, D.; Olmos-Ortiz, A.; et al. Chronic moderate ethanol intake differentially regulates vitamin D hydroxylases gene expression in kidneys and xenografted breast cancer cells in female mice. *J. Steroid Biochem. Mol. Biol.* **2017**, *173*, 148–156. [CrossRef]
41. Esparza-López, J.; Ramos-Elías, P.A.; Castro-Sánchez, A.; Rocha-Zavaleta, L.; Escobar-Arriaga, E.; Zentella-Dehesa, A.; León-Rodríguez, E.; Medina-Franco, H.; Ibarra-Sánchez, M.D.J. Primary breast cancer cell culture yields intra-tumor heterogeneous subpopulations expressing exclusive patterns of receptor tyrosine kinases. *BMC Cancer* **2016**, *16*, 740. [CrossRef]
42. García-Quiroz, J.; García-Becerra, R.; Barrera, D.; Santos, N.; Avila, E.; Ordaz-Rosado, D.; Rivas-Suárez, M.; Halhali, A.; Rodríguez, P.; Gamboa-Domínguez, A.; et al. Astemizole Synergizes Calcitriol Antiproliferative Activity by Inhibiting CYP24A1 and Upregulating VDR: A Novel Approach for Breast Cancer Therapy. *PLoS ONE* **2012**, *7*, e45063. [CrossRef]
43. Vichai, V.; Kirtikara, K. Sulforhodamine B colorimetric assay for cytotoxicity screening. *Nat. Protoc.* **2006**, *1*, 1112–1116. [CrossRef]
44. Chou, T.-C. Theoretical Basis, Experimental Design, and Computerized Simulation of Synergism and Antagonism in Drug Combination Studies. *Pharmacol. Rev.* **2006**, *58*, 621–681. [CrossRef]
45. Zhang, N.; Fu, J.-N.; Chou, T.-C. Synergistic combination of microtubule targeting anticancer fludelone with cytoprotective panaxytriol derived from panax ginseng against MX-1 cells in vitro: Experimental design and data analysis using the combination index method. *Am. J. Cancer Res.* **2015**, *6*, 97–104.
46. Ring, A.E.; Smith, I.E.; Ashley, S.; Fulford, L.G.; Lakhani, S.R. Oestrogen receptor status, pathological complete response and prognosis in patients receiving neoadjuvant chemotherapy for early breast cancer. *Br. J. Cancer* **2004**, *91*, 2012–2017. [CrossRef]
47. Rosner, D.; Lane, W.W.; Nemoto, T. Differential response to chemotherapy in metastatic breast cancer in relation to estrogen receptor level. Results of a prospective randomized study. *Cancer* **1989**, *64*, 6–15. [CrossRef]
48. Alli, E.; Sharma, V.B.; Sunderesakumar, P.; Ford, J.M. Defective Repair of Oxidative DNA Damage in Triple-Negative Breast Cancer Confers Sensitivity to Inhibition of Poly(ADP-Ribose) Polymerase. *Cancer Res.* **2009**, *69*, 3589–3596. [CrossRef]
49. Castedo, M.; Perfettini, J.-L.; Roumier, T.; Andreau, K.; Medema, R.H.; Kroemer, G. Cell death by mitotic catastrophe: A molecular definition. *Oncogene* **2004**, *23*, 2825–2837. [CrossRef]
50. Nauman, M.C.; Tocmo, R.; Vemu, B.; Veenstra, J.P.; Johnson, J.J. Inhibition of CDK2/CyclinE1 by xanthones from the mangosteen (*Garcinia mangostana*): A structure-activity relationship study. *Nat. Prod. Res.* **2020**, *10*, 1–5. [CrossRef]
51. Vemu, B.; Nauman, M.C.; Veenstra, J.P.; Johnson, J.J. Structure Activity Relationship of Xanthones for Inhibition of Cyclin Dependent Kinase 4 from Mangosteen (*Garcinia mangostana* L.). *Int. J. Nutr.* **2019**, *4*, 38–45. [CrossRef]
52. Sampath, P.D.; Kannan, V. Mitigation of mitochondrial dysfunction and regulation of eNOS expression during experimental myocardial necrosis by alpha-mangostin, a xanthonic derivative from *Garcinia mangostana*. *Drug Chem. Toxicol.* **2009**, *32*, 344–352. [CrossRef]
53. Weecharangsan, W.; Opanasopit, P.; Sukma, M.; Ngawhirunpat, T.; Sotanaphun, U.; Siripong, P. Antioxidative and Neuroprotective Activities of Extracts from the Fruit Hull of Mangosteen (*Garcinia mangostana* Linn). *Med. Princ. Pr.* **2006**, *15*, 281–287. [CrossRef]
54. Segovia-Mendoza, M.; Díaz, L.; González-González, M.E.; Martínez-Reza, I.; García-Quiroz, J.; Prado-Garcia, H.; Ibarra-Sánchez, M.J.; Esparza-López, J.; Larrea, F.; García-Becerra, R. Calcitriol and its analogues enhance the antiproliferative activity of gefitinib in breast cancer cells. *J. Steroid Biochem. Mol. Biol.* **2015**, *148*, 122–131. [CrossRef]
55. Esparza-López, J.; Medina-Franco, H.; Escobar-Arriaga, E.; León-Rodríguez, E.; Zentella-Dehesa, A.; Ibarra-Sánchez, M.J. Doxorubicin induces atypical NF-κB activation through c-Abl kinase activity in breast cancer cells. *J. Cancer Res. Clin. Oncol.* **2013**, *139*, 1625–1635. [CrossRef]
56. Scolamiero, G.; Pazzini, C.; Bonafè, F.; Guarnieri, C.; Muscari, C. Effects of α-Mangostin on Viability, Growth and Cohesion of Multicellular Spheroids Derived from Human Breast Cancer Cell Lines. *Int. J. Med. Sci.* **2018**, *15*, 23–30. [CrossRef]
57. Lee, Y.-B.; Ko, K.-C.; Shi, M.-D.; Liao, Y.-C.; Chiang, T.-A.; Wu, P.-F.; Shih, Y.-X.; Shih, Y.-W. α-Mangostin, A Novel Dietary Xanthone, Suppresses TPA-Mediated MMP-2 and MMP-9 Expressions through the ERK Signaling Pathway in MCF-7 Human Breast Adenocarcinoma Cells. *J. Food Sci.* **2010**, *75*, H13–H23. [CrossRef]